Interferon-stimulated genes implicated in the BK polyomavirus life cycle

Michelle Antoni

Submitted in accordance with the requirements for the degree of Doctor of Philosophy

The University of Leeds

School of Molecular and Cellular Biology

September, 2020

The candidate confirms that the work submitted is her own and that appropriate credit has been given where reference has been made to the work of others.

Acknowledgements

This work would not be possible without the continuous support and invaluable guidance of my supervisors Dr Andrew Macdonald and Dr Stephen Griffin. I would like to thank Dr Marietta Müller for carrying out the initial work of this project and for performing the BSL3 work required for the CHIKV infections in this study. Dr Margarita-Maria Panou provided me with key training, helpful advice and supported me throughout my studies as a true friend.

I am very grateful for working alongside many talented individuals in the Macdonald lab over the years. Their useful critiques and constructive suggestions have been instrumental in improving my work and myself as a scientist. I would like to offer my special thanks to Dr Christopher Wasson, Dr Ethan Morgan, who also performed the IF imaging in this study, Dr Daniel Hurdiss, Dr Yigen Li, Dr Eleni-Anna Loundras, Dr David Kealy, Dr Gemma Swinscoe, Molly Patterson, Corinna Brockhaus, James Scarth, Diego Barba Moreno and Aniek Meijers for encouraging me throughout my project.

I wish to thank Kidney Research UK (KRUK) for funding my PhD studies and Dr Sam Wilson for providing the ISG-encoding plasmids for our screen.

I would like to express my gratitude to my parents Maria and Andy, my sister Elena and my partner Andreas for their patience, encouragement and constant support. Thank you to my family and close friends for always being there for me.

Αυτό το γράφω για σένα γιαγιά μου και σου το αφιερώνω. Σ’ευχαριστώ που με υποστηρίζεις σε ό,τι κάνω. Θα σε αγαπώ για πάντα.

Abstract

BK polyomavirus (BKPyV) is a small, non-enveloped virus with double-stranded DNA. It is a widespread infectious agent among the general population, where it establishes a life-long persistent infection in the kidneys and urinary tract. Rampant BKPyV replication can take place upon immunosuppression, typically following kidney transplantation, and can lead to polyomavirus-associated nephropathy (PVAN) which results in kidney rejection in up to 90% of cases. Due to the lack of effective treatment, PVAN management relies on reducing immunosuppression which, ultimately, threatens the viability of the transplanted organ. To address the associated clinical outcomes, it is imperative to understand how BKPyV interacts with the host immune response to allow infection and persistence to take place.

Cells respond to viral infections by producing interferon and upregulating interferon-stimulated genes (ISGs), which intervene in the viral life cycle to prevent viral spread. BKPyV is susceptible to the action of interferon, thus, we investigated which ISGs may act against BKPyV infection. To this end, this study adapted a gain-of-function screening strategy to identify ISGs implicated in the BKPyV life cycle. Virion binding assays and molecular-based techniques further characterised the role of each ISG in inhibiting infection.

Herein, we report the first ‘ISG-overexpression screen’ against a polyomavirus, where interferon regulatory factor 1 (IRF1) and heparanase (HPSE) were identified as restriction factors against BKPyV infection. Some of these antiviral functions are conserved in a physiologically relevant cell culture model and against the related polyomaviruses, SV40 and JCPyV. Further investigation is required to fully elucidate the mechanism through which each ISG is targeting BKPyV. By clarifying how individual components of innate immunity interact with BKPyV infection, we can generate insights into how different types of cells respond to infection and persistence. Furthermore, therapeutic targets may be identified through such studies, which can improve the management of associated diseases.

Table of Contents

List of Tables

List of Figures

Abbreviations

°C	Degree Celsius
$5HT_{2A}R$	5-hydroxytryptamine 2A receptor
Å	Ångström
aa	amino acid
AIM2	Absent in melanoma 2
APC	Antigen presenting cells
ATM	Ataxia telangiectasia mutated
ATP	Adenosine triphosphate
ATR	Ataxia telangiectasia and Rad-3-related
BCA	Bicinchoninic acid
BFA	Brefeldin A
BKPyV	BK polyomavirus
BMDM	Bone marrow-derived macrophages
bp	base pair
BSA	Bovine serum albumin
Ca^{2+}	Calcium cation
Cav-1	Caveolin-1
CDV	Cidofovir
CFTR	Cystic fibrosis transmembrane conductance regulator
cGAS	Cyclic GMP-AMP synthase
CH25H	Cholesterol-25-hydroxylase
CHIKV	Chikungunya virus
CLR	C-type lectin receptor
CMV	Cytomegalovirus
CPE	Cytopathic effect
CsCl	Caesium chloride

CTL	Cytotoxic T lymphocyte
DAI	DNA-dependent activator of interferon-regulatory factors
DAMP	Danger-associated molecular pattern
DBD	DNA-binding domain
dCMP	Deoxycytidine monophosphate
DDR	DNA damage response
DIDS	4,4’-diisothiocyano-2,2’-stilbenedisulfonic acid
DMSO	Dimethyl sulphoxide
DsDNA	Double-stranded DNA
ECM	Extracellular matrix
EerI	Eeyarestatin I
ELISA	Enzyme-linked immunosorbent assay
ER	Endoplasmic reticulum
ERAD	ER-associated protein degradation
ERK	Extracellular signal-regulated kinase
EV	Extracellular vesicle
FAK	Focal adhesion kinase
FFA	Fluorescent focus assay
GAF	Interferon-gamma-activated factor
GAG	Glycosaminoglycan
GAS	Gamma-activated sequence
GlcNAc	N-acetylated glucosamine
GlcNS	N-sulphated glucosamine
GlcUA	Glucuronic acid
GUV	Giant unilamellar vesicle
h	Hour
HA	Haemagglutination assay

HAART	Highly active antiretroviral therapy
HC	Haemorrhagic cystitis
HCDC	Human cortical collecting duct epithelial cell
HCV	Hepatitis C virus
HEK	Human embryonic kidney
HI	Haemagglutination inhibition
HIV	Human immunodeficiency virus
HK	Human keratinocyte
HNSCC	Head and neck squamous cell carcinoma
HP1-α	Heterochromatin protein 1 alpha
hpi	Hours post-infection
HPSE	Heparanase
hpt	Hours post-transfection
HPyVs	Human polyomaviruses
HS	Heparan sulphate
Hsc70	Heat shock cognate 70
HSCT	Haematopoietic stem cell transplant
HSPG	Heparan sulphate proteoglycan
HSV-1	Herpes simplex virus type-1
hTERT	Human telomerase reverse transcriptase
IAD	IRF-association domain
IARC	International Agency for Research on Cancer
IdoUA	Iduronic acid
IFI16	Interferon-gamma-inducible protein 16
IFIT	Interferon induced protein with tetratricopeptide repeats
IFITM	Interferon-inducible transmembrane protein
IFN	Interferon

IFNAR	Interferon-α/β receptor
IFNGR	Interferon-gamma receptor
IKK	IkappaB kinase
IL	Interleukin
IRF	Interferon regulatory factor
ISG	Interferon-stimulated gene
ISGF3	Interferon-stimulated gene factor 3
ISRE	Interferon-stimulated response element
IU	Infectious units
JAK	Janus kinase
JCPyV	JC polyomavirus
K^+	Potassium ion
KA	Keratoacanthoma
kbp	Kilobase pair
KIPyV	KI polyomavirus
KSHV	Kaposi’s sarcoma-associated herpesvirus
LBR	Lamin B receptor
LIPyV	Lyon IARC polyomavirus
LSTc	Lactoseries tetrasaccharide c
LT-Ag	Large tumour antigen
LVEC	Lung vascular endothelial cell
m	Milli
M	Molar concentration
MAPK	Mitogen-activated protein kinase
MCC	Merkel cell carcinoma
MCPyV	Merkel cell polyomavirus
MDA5	Melanoma differentiation-associated protein 5

MEF	Mouse embryonic fibroblasts
MF1	Maturation factor 1
MFI	Mean fluorescence intensity
MHC	Major histocompatibility complex
MHV68	Murine gammaherpesvirus 68
miRNA	MicroRNA
mL	Millilitre
MMF	Mycophenolate mofetil
MMP	Matrix metalloproteinases
MOI	Multiplicity of infection
MPyV	Mouse polyomavirus
mTOR	Mammalian target of rapamycin
MWPyV	Malawi polyomavirus
MxA	Myxovirus resistance 1
MXPyV	Mexico polyomavirus
NAG	Neuroblastoma amplified gene
NCCR	Non-coding control region
NDV	Newcastle disease virus
NF-κB	Nuclear factor-κB
NH_4Cl	Ammonium chloride
NIKS	Naturally immortalised keratinocytes
NJPyV	New Jersey polyomavirus
NK	Natural killer
NLR	Nucleotide-binding oligomerisation domain-like receptors
NLS	Nuclear localisation signal
NPC	Nuclear pore complex
nsP3	Non-structural protein 3

OAS	2’5’-oligoadenylate synthetase
ODN	Oligodeoxynucleotide
PAMP	Pathogen-associated molecular pattern
PBS	Phosphate-buffered saline
PCNA	Proliferating cell nuclear antigen
PDI	Protein disulphide isomerase
PEI	Polyethylenimine
PHFG	Primary human foetal glial
PI3K	Phosphoinositide 3-kinase
PKC	Protein kinase C
PKR	Protein kinase R
PML	Progressive multifocal leukoencephalopathy
PML-NB	Promyelocytic leukemia nuclear body
poly(I:C)	Polyinosinic-polycytidylic acid
PP2A	Protein phosphatase 2A
PRR	Pattern recognition receptor
pSTAT	Phosphorylated STAT
PVAN	Polyomavirus-associated nephropathy
qPCR	Quantitative polymerase chain reaction
RAD	Renal tubule cell assist device
Rb	Retinoblastoma susceptibility protein
RIG-I	Retinoic acid-inducible gene-I
RINT1	RAD50 interactor 1
RLR	Retinoic acid-inducible gene-I-like receptor
RPA	Replication protein A
RPTE	Renal proximal tubular epithelial
RT-qPCR	Quantitative reverse transcription polymerase chain reaction

SDS	Sodium dodecyl sulphate
SDS-PAGE	Sodium dodecyl sulphate polyacrylamide gel electrophoresis
siRNA	Small interfering RNA
SOT	Solid organ transplant
ssRNA	Single-stranded RNA
sT-Ag	Small tumour antigen
STAT	Signal transducer and activator of transcription
STING	Stimulator of interferon genes
STLPyV	Saint Louis polyomavirus
SV40	Simian vacuolating virus 40
TBK1	TANK Binding Kinase 1
TBP	TATA-binding protein
TBS	Tris-buffered saline
TBS/T	Tris-buffered saline with Tween-20
TF	Transcription factor
TLR	Toll-like receptor
TRIM56	Tripartite motif-56
TruncTAg	Truncated large tumour antigen
TSPyV	Trichodysplasia spinulosa-associated polyomavirus
UGCG	UDP-glucose ceramide glucosyltransferase
V	Volts
v/v	Volume per volume
VEC	Microvascular endothelial cells
VEEV	Venezuelan equine encephalitis virus
vIRF	Viral interferon regulatory factor
VLP	Virus-like particle
VSV	Vesicular stomatitis virus

VV	Vaccinia virus
w/v	Weight per volume
WUPyV	WU polyomavirus
YFV	Yellow fever virus
ZC3HAV1	Zinc-finger CCCH-type, antiviral 1
ZRE	ZC3HAV responsive element
ZW10	ZW10 kinetochore protein
α-SNAP	α-soluble N-ethylmaleimide-sensitive fusion attachment protein
ΔAgno	Agnoprotein-deficient
µg	Microgram

Chapter 1
Introduction

1.1 Discovery and taxonomy of *Polyomaviridae*

The *Polyomaviridae* is a virus family encompassing small, non-enveloped, double-stranded DNA (dsDNA) viruses. Members of the *Polyomaviridae* are characterised by a 40-45 nm icosahedral capsid assembled around the circular dsDNA genome of approximately 5.0 kilobase pairs (kbp) (Table 1.1) (Moens, Calvignac-Spencer, *et al.*, 2017). Mammals, birds and, recently, fish have been identified as hosts for polyomavirus infections (Buck *et al.*, 2016). Each family member exhibits restricted host specificity. Some polyomaviruses are of medical or veterinary importance, being the etiological cause of symptomatic infection or cancer in their respective host (Moens, Krumbholz, *et al.*, 2017).

Polyomaviruses were initially grouped with papillomaviruses in a genus within the *Papovaviridae*. Ultimately, differences in genomic organisation and size, and replication strategies, established the *Polyomaviridae* and *Papillomaviridae* as distinct virus families (Acheson, 2011). The ever expanding *Polyomaviridae* currently consists of 102 recognised species, while additional polyomaviruses remain unclassified (Moens, Calvignac-Spencer, *et al.*, 2017). Four genera, which are recognised by the International Committee on Taxonomy of Viruses (ICTV), compose the polyomavirus family; Alphapolyomavirus, Betapolyomavirus, Gammapolyomavirus and Deltapolyomavirus (Figure 1.1). Alpha-, Beta- and Deltapolyomavirus are comprised of mammalian species, while the genus Gammapolyomavirus encompasses only avian polyomaviruses (Moens, Krumbholz, *et al.*, 2017). The recent delineation of the four genera is based upon the amino acid (aa) sequence of the viral large tumour antigen (LT-Ag) protein, which represents a recombination cold-spot and exhibits less polytomies than the major capsid protein, VP1 (Carr *et al.*, 2017). The evolution of polyomaviruses has likely occurred through a gradual co-divergence with individual host animal lineages, as is suggested by the recent discovery of polyomavirus-like sequences in fish and arthropods (Buck *et al.*, 2016).

Table 1.1 Characteristics of *Polyomaviridae* members. Adapted from Moens, Calvignac-Spencer, *et al.* (2017).

Virion	Non-enveloped, 40-45 nm, icosahedral
Genome	Approximately 5 kbp circular dsDNA
Replication	Bidirectional from a unique origin of replication
Translation	Early and late transcripts, alternative splicing, alternative ORFs
Host range	Mammals, birds and fish
Taxonomy	Four genera, more than 100 species

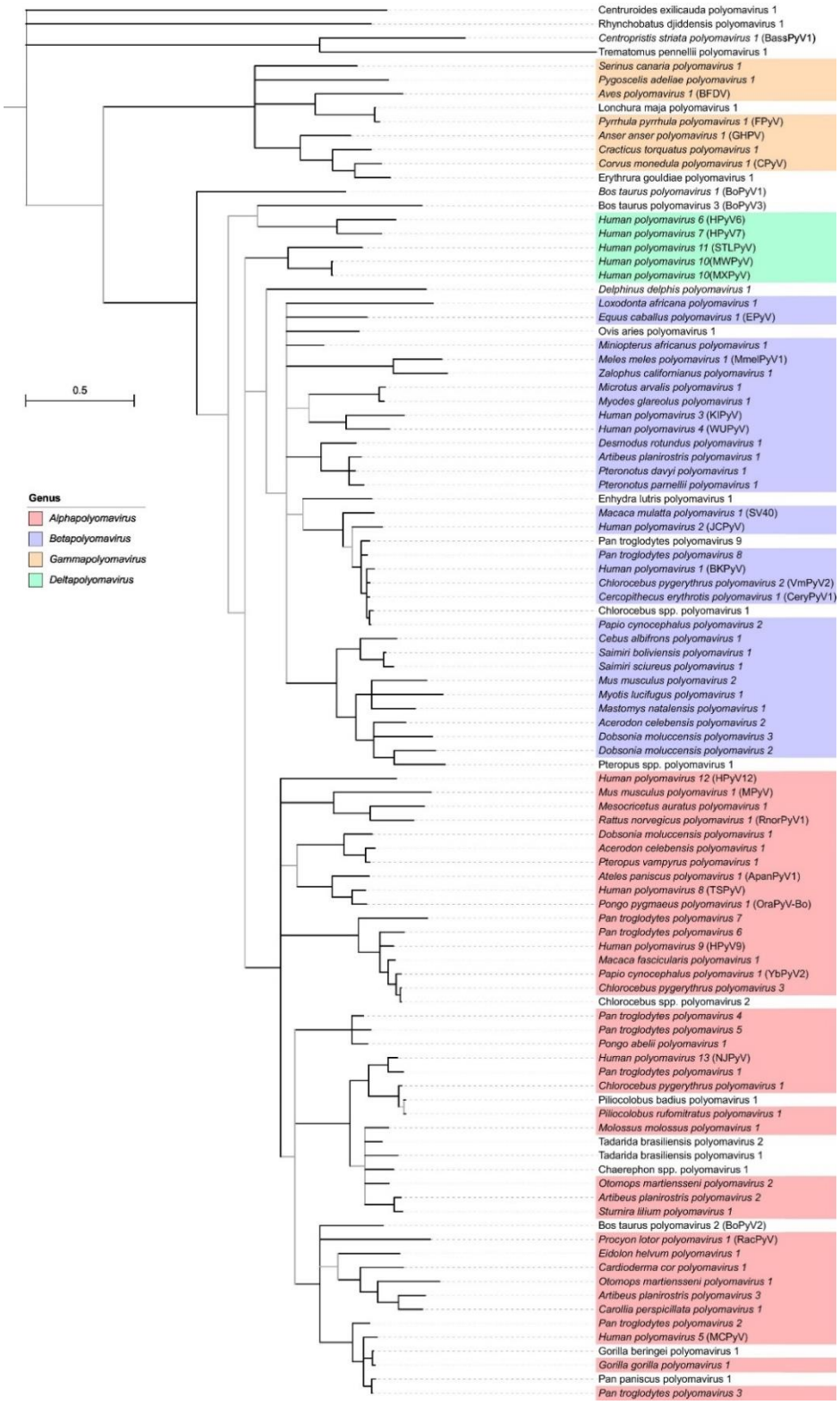

Figure 1.1 Phylogenetic tree for polyomaviruses based on their LT-Ag protein sequence. The scale is in amino acid substitution per site. Italicised species names represent those recognised by ICTV. Polyomaviruses which have been or might be proposed as species have not been italicised. The four genera are represented by different colours. The phylogenetic tree was obtained from Moens, Krumbholz, *et al.* (2017).

1.1.1 Discovery of mouse polyomavirus as a tumour-inducing agent

The founder of the polyomavirus family, mouse polyomavirus (MPyV), was discovered in laboratory mice in the 1950s. Newborn or suckling mice were injected with filtered extracts of tumours from Ak leukemic mice. Some of the mice developed epitheliomas in the salivary glands (Gross, 1953). The carcinogenic potential of the filterable agent from Gross' studies was further investigated by Stewart *et al.* (1957). Stewart and colleagues exposed mice to the supernatants of tissue cultures derived from leukaemia cells and salivary gland tumour cells. They observed many inoculated mice developing neoplasms in multiple tissues. Due to its demonstrated ability to cause different types of tumours in various experimental animals, this infectious agent was promptly named 'polyomavirus' (Greek *poly* for many and *-oma* for tumour) (Buck *et al.*, 2016).

1.1.2 Discovery of SV40 as a contaminant in poliovirus vaccines

Simian vacuolating virus 40 (SV40) was the first primate polyomavirus to be discovered. The cytoplasmic vacuolation observed in infected cell cultures gave the virus its name (Sweet and Hilleman, 1960). SV40 was detected in normal monkey kidney cells, in all 3 types of live poliovirus vaccines and in an adenovirus vaccine during the course of vaccine safety testing. Primary rhesus monkey kidney cell cultures, used in early vaccine preparation, were the source for SV40 contamination in the tested vaccine stocks (Sweet and Hilleman, 1960). The inactivated poliovirus vaccine was also found to contain SV40, generating great concern for the millions of people already administered contaminated batches of the vaccine between 1955 and 1963 (Garcea and Imperiale, 2003). Towards the end of this vaccination period, studies began to demonstrate the oncogenic potential of SV40, as it was able to induce tumours in hamsters and to transform human renal cells *in vitro* (Girardi *et al.*, 1962; Shein and Enders, 1962). These findings have raised the question of whether SV40 could cause cancer in people who received contaminated vaccines or have otherwise been exposed to SV40. Numerous studies have reported the presence of SV40 DNA sequences in human cancer specimens, including brain tumours, osteosarcomas and mesotheliomas. Equally, many researches failed to detect SV40 upon analysis of the same tumour types (Rotondo *et al.*, 2019). Thus far, there is no conclusive evidence of deleterious consequences arising

from SV40 exposure or of productive SV40 transmission within the human population (Shah and Nathanson, 1976; Buck *et al.*, 2016).

1.1.3 Discovery of human polyomaviruses

To date, 14 human polyomaviruses (HPyVs) have been identified (Moens and Macdonald, 2019). The first human polyomaviruses to be discovered, BK and JC polyomaviruses (BKPyV and JCPyV), were simultaneously reported in *The Lancet* in 1971 and named after the index case patient (Knowles, 2002). Gardner *et al.* (1971) isolated BKPyV as what appeared to be a new papovavirus from a Sudanese patient suffering from ureteric obstruction, following renal transplantation. Inclusion-bearing cells and a large number of virus particles were observed in the patient's urine deposit. The viral morphology was identical to that of members of the then polyoma subgroup of the papovavirus family. Intranuclear virus particles were also observed by electron microscopy in epithelial cells lining the lumen of the donor-derived ureter. Both donor and recipient appeared to have been infected with this viral agent prior to transplantation, as evidenced by serological data (Gardner *et al.*, 1971). The original isolate of BKPyV is known as the Gardner strain (Knowles, 2002).

In the same year a second 'papova-like' virus was isolated, this time from the brain of a patient with progressive multifocal leukoencephalopathy (PML), a rare demyelinating disease first described by Åström *et al.* (1958). The patient developed PML as a complication of Hodgkin's disease. Papovavirus-like virions were observed inside the nucleus, cytoplasm or both, of human foetal glial cells inoculated with the patient's brain extract. These virus particles were similar in size and structure to those observed in electron micrographs of glial cells from brain tissue with PML (Padgett *et al.*, 1971). Padgett and associates established that the etiological agent of PML was distinct from SV40 and MPyV, and proposed the new polyomavirus be named JC polyomavirus (Walker, 2002).

More than 35 years after the independent discoveries of BKPyV and JCPyV, technological developments in high-throughput sequencing resulted in a rapid, sudden expansion of the human polyomavirus subfamily. In 2007, KI polyomavirus (KIPyV) and WU polyomavirus (WUPyV) were identified in

respiratory tract samples at Karolinska Institute and Washington University, respectively (Allander *et al.*, 2007; Gaynor *et al.*, 2007). Merkel cell polyomavirus (MCPyV) was detected in Merkel cell carcinoma (MCC), a rare and aggressive form of skin cancer (Feng *et al.*, 2008). HPyV6 and HPyV7 were discovered in forehead samples of healthy volunteers (Schowalter *et al.*, 2010). Trichodysplasia spinulosa-associated polyomavirus (TSPyV) was identified in facial lesions from a heart transplant patient with the rare skin disease, trichodysplasia spinulosa (van der Meijden *et al.*, 2010). In 2011, serum analysis of an immunosuppressed kidney transplant recipient led to the discovery of HPyV9 (Scuda *et al.*, 2011). HPyV10, also known as Malawi polyomavirus (MWPyV) or Mexico polyomavirus (MXPyV), was detected in condyloma and faecal specimens (Buck *et al.*, 2012; Siebrasse *et al.*, 2012; Yu *et al.*, 2012). Saint Louis polyomavirus (STLPyV) was identified in a paediatric stool sample (Lim *et al.*, 2013), HPyV12 in liver tissue (Korup *et al.*, 2013) and New Jersey polyomavirus (NJPyV) in a muscle biopsy from a pancreatic transplant patient (Mishra *et al.*, 2014). More recently, Lyon IARC polyomavirus (LIPyV) was proposed as the fourteenth human polyomavirus upon its discovery in skin swabs, oral gargles and eyebrow hair follicles (Gheit *et al.*, 2017). LIPyV has yet to be assigned as a polyomavirus species.

1.2 Human polyomaviruses (HPyVs)

1.2.1 Seroprevalence

HPyV infections are widespread in the human population and antibodies against HPyVs have even been detected in remote, tribal populations (Brown *et al.*, 1975; Major and Neel, 1998). Primary infection is acquired during childhood and seroprevalence increases with age (Gardner, 1973); both common characteristics of all HPyVs as indicated by seroepidemiological studies thus far (Moens, Krumbholz, *et al.*, 2017). Seroprevalences are comparable between studies performed in adults, although the use of different detection assays, and sociodemographic and biological characteristics may explain observed variations in seroprevalence (Decaprio and Garcea, 2013; van der Meijden *et al.*, 2013; Gossai *et al.*, 2016; Šroller *et al.*, 2016).

The seroprevalence of different HPyV species varies. A comprehensive study of 1,050 Dutch blood donors indicated high seroprevalence for the majority of HPyVs (60-100%), but low seroprevalence for HPyV12 (4.0%), NJPyV (5.2%) and LIPyV (5.9%) (Kamminga *et al.*, 2018). The authors proposed that a low HPyV12 seroprevalence supports the notion of this virus being a shrew-derived virus (Gedvilaite *et al.*, 2017). Contradictory findings were presented by Gaboriaud *et al.* (2018) investigating an Italian general population in the Ferrara region where seroprevalence for HPyV12 and NJPyV peaked at 97.3% and 57.5%, respectively. The seroprevalences of NJPyV and LIPyV are not fully settled due to the existence of conflicting literature in the case of the former or because of their very recent discovery in the case of the latter. Table 1.2 presents HPyV seroprevalences in healthy adulthood.

Seropositivity for multiple polyomaviruses is also common (Gossai *et al.*, 2016). In the study of Dutch blood donor seroreactivity, Kamminga *et al.* (2018) revealed that, on average, an individual was infected with nine different human polyomaviruses. Most HPyV serological studies have been conducted using haemagglutination inhibition (HI), virus-like particle (VLP)-based or VP1 capsomere-based enzyme immunoassays for determining serum reactivity against the immunodominant major capsid protein, VP1 (Kean *et al.*, 2009). Serological studies are subject to bias through cross-reactivity of IgG antibodies against related polyomavirus capsid proteins, for example BKPyV, JCPyV and

SV40 VP1 proteins (Viscidi and Clayman, 2006). In conclusion, interpretation of serological data must be done with caution (Moens *et al.*, 2013).

Table 1.2 Human polyomaviruses (HPyVs). The seroprevalence of human polyomaviruses in healthy adults is listed as in Moens, Krumbholz, *et al.* (2017) (section 1.2.1). Proven and probable disease association is listed for each HPyV and references are in-text (section 1.2.2). HPyV9-13 and LIPyV are of unknown pathogenic potential.

Genus	Virus	Seroprevalence (%)	References	Disease
Betapolyomavirus	HPyV1/BKPyV	55-90	(Knowles *et al.*, 2003; Moens *et al.*, 2013)	Polyomavirus-associated nephropathy (PVAN) Haemorrhagic cystitis (HC)
Betapolyomavirus	HPyV2/JCPyV	44-90	(Carter *et al.*, 2009; Moens *et al.*, 2013)	Progressive multifocal leukoencephalopathy (PML)
Betapolyomavirus	HPyV3/KIPyV	55-91	(Kean *et al.*, 2009; Kamminga *et al.*, 2018)	Respiratory disease
Betapolyomavirus	HPyV4/WUPyV	69-98	(Kean *et al.*, 2009; Kamminga *et al.*, 2018)	Respiratory disease
Alphapolyomavirus	HPyV5/MCPyV	58-96	(Carter *et al.*, 2009; Pastrana *et al.*, 2009)	Merkel cell carcinoma (MCC)
Deltapolyomavirus	HPyV6	67-98	(Schowalter *et al.*, 2010; Nicol *et al.*, 2013)	Keratoacanthoma Kimura disease Pruritic and dyskeratotic dermatosis

Genus	Virus	Seroprevalence (%)	References	Disease
Deltapolyomavirus	HPyV7	35-86	(Schowalter *et al.*, 2010; Nicol *et al.*, 2013)	Thymomas Pruritic and dyskeratotic dermatosis
Alphapolyomavirus	HPyV8/TSPyV	70-84	(van der Meijden *et al.*, 2013; Gossai *et al.*, 2016)	Trichodysplasia spinulosa
Alphapolyomavirus	HPyV9	20-70	(Nicol *et al.*, 2012; Kamminga *et al.*, 2018)	Unknown
Deltapolyomavirus	HPyV10/MWPyV/ MXPyV	42-99	(Berrios *et al.*, 2015; Kamminga *et al.*, 2018)	Unknown
Deltapolyomavirus	HPyV11/STLPyV	68-70	(Lim *et al.*, 2014)	Unknown
Alphapolyomavirus	HPyV12	23-33	(Korup *et al.*, 2013)	Unknown
Alphapolyomavirus	HPyV13/NJPyV	Unknown*	(Gaboriaud *et al.*, 2018; Kamminga *et al.*, 2018)	Unknown
-	LIPyV	Unknown*	(Kamminga *et al.*, 2018)	Unknown

* = not examined extensively

1.2.2 Associated diseases

HPyVs are likely transmitted via direct person-to-person contact or indirectly through contaminated food, water, biological products and fomites (Dalianis and Hirsch, 2013). The respective mode of transmission has not been definitively resolved for any HPyV as the clinical manifestations of primary infection have not been identified. This is due to primary HPyV infections taking a subclinical course or symptoms being non-specific (Hirsch *et al.*, 2014). Following primary infection, polyomaviruses generally establish a life-long persistent infection in the healthy host (Imperiale and Jiang, 2016) (section 1.3.1). Clinical manifestations of HPyV infection arise primarily in hosts with suppressed immune systems, either by natural means or iatrogenic interventions (Bennett *et al.*, 2012). A summary of proven and probable HPyV-associated diseases is presented in Table 1.2.

Twenty years after the discovery of BKPyV, researchers recognised BKPyV as the causative agent of polyomavirus-associated nephropathy (PVAN) in renal transplant patients (Purighalla *et al.*, 1995; Randhawa *et al.*, 1999). In haematopoietic stem cell transplant (HSCT) recipients, BKPyV replication is significantly associated with post-engraftment haemorrhagic cystitis (HC) (Erard *et al.*, 2004). Albeit rarely observed, BKPyV-related meningoencephalitis, native kidney nephritis and fatal viral pneumonia have been reported in severely immunocompromised individuals (Vallbracht *et al.*, 1993; Haririan *et al.*, 2002; Galan *et al.*, 2005). Ophthalmological manifestations, which may be linked to BKPyV infection, have also been observed in the form of retinitis in a patient with AIDS (Hedquist *et al.*, 1999). Jeffers *et al.* (2009) investigating salivary shedding of BKPyV in immunosuppressed human immunodeficiency virus (HIV) positive patients, suggested a potential role for BKPyV in HIV-associated salivary gland disease (Jeffers and Webster-Cyriaque, 2011).

JCPyV is established as the etiological agent of PML; a rare and, often, fatal neurological disease. JCPyV reactivates in immunosuppressed patients, replicating in their oligodendrocytes and ultimately leading to cell destruction (Barth *et al.*, 2016). Subsequently, demyelinated lesions are formed in the brain, which correspond to the devastating neurologic sequalae of PML; mainly visual deficits, cognitive impairment and motor dysfunction (Bhattacharjee and Chattaraj, 2017). PML became a significant problem in the late 1980s following

the AIDS epidemic (Berger and Concha, 1995). The introduction of highly active antiretroviral therapy (HAART) for AIDS patients was accompanied by an improvement in survival rates. While PML is consistently observed in 3-5% of HIV-infected individuals, additional predisposing conditions to PML are becoming more common (Major, 2010). Patients undergoing immunomodulatory therapy, such as natalizumab, for multiple sclerosis are at risk of developing PML (Williamson and Berger, 2017). Furthermore, systemic lupus erythematosus is also associated with increased risk for PML, regardless of whether the patient is receiving treatment at the time of onset (Molloy and Calabrese, 2009). Interestingly, some studies report an association between BKPyV and PML development (Reploeg *et al.*, 2001). JCPyV is now recognised to cause additional pathologies in the central nervous system, including granule cell neuronopathy, encephalopathy and meningitis (Koralnik *et al.*, 2005; Wüthrich *et al.*, 2009; Agnihotri *et al.*, 2014).

A possible role has been proposed for both KIPyV and WUPyV in respiratory diseases. Both HPyVs were first identified in paediatric respiratory specimens and are readily detected in such samples from immunocompromised patients presenting with respiratory symptoms (Mourez *et al.*, 2009). No causative link has been established between respiratory disease and KIPyV or WUPyV, mainly due to occurrence of co-infection with other respiratory viruses (Rao *et al.*, 2011; Babakir-Mina *et al.*, 2013).

Beckervordersandforth *et al.* (2016) detected HPyV6 DNA in 42.3% of keratoacanthomas (KA) upon analysing a large number of non-melanoma skin cancer specimens, suggesting a role for HPyV6 in KA etiopathogenesis. HPyV6 has also been implicated in Kimura disease, a rare chronic inflammatory disorder. Shotgun metagenomic sequencing conducted by Rascovan *et al.* (2016) on lymph node specimens detected HPyV6 in the internal tissues of a patient with an angiolymphoid hyperplasia with eosinophilia, or Kimura disease. Further examination is required to demonstrate a causal link between HPyV6 and the development of Kimura disease. Although mainly detected on the skin surface of healthy individuals, HPyV6 and HPyV7 may also be involved in the pathogenesis of skin rashes, specifically pruritic and dyskeratotic dermatosis, in immunosuppressed patients (Nguyen *et al.*, 2017). An additional role has been proposed for HPyV7 in thymic epithelial tumours, where HPyV7 DNA and large

tumour antigen expression were detected in 54% and 46% of thymomas, respectively (Rennspiess *et al.*, 2015).

TSPyV is associated with the rare skin condition, *Trichodysplasia spinulosa*, characterised by an eruption of follicular papules and keratin spines, and often alopecia of the eyebrows and eyelashes. *Trichodysplasia spinulosa* is primarily seen in solid organ transplant (SOT) recipients, particularly kidney and heart transplant recipients, and patients receiving chemotherapy for haematologic malignancies (Kirchhof *et al.*, 2014). Some of the newly discovered polyomaviruses, HPyV9-13 and LIPyV, have not yet been associated with a specific disease phenotype.

1.2.2.1 Oncogenic potential of HPyVs

Interest in studying the role of polyomaviruses in cancer has been generated due to the cell-cycle altering functions of their regulatory proteins. The oncogenic properties of specific viral antigens are discussed in section 1.4.

MCPyV is the only human polyomavirus to date with a likely causal relationship to a form of cancer. MCPyV is strongly associated with the development of MCC and, thus, The International Agency for Research on Cancer (IARC) assigned MCPyV to Group 2A as an agent probably carcinogenic to humans (IARC, 2014; Prado *et al.*, 2018). While the viral genome of most HPyVs remains episomal in human cells, MCPyV sequences were detected in 80% of MCC tumours and found integrated in the genome of six out of eight MCPyV-positive MCCs (Feng *et al.*, 2008). Importantly, Shuda *et al.* (2008) discovered mutations in nine MCC tumours which truncated MCPyV LT-Ag. The origin binding and helicase domains were removed, eliminating the viral DNA replication capacity of the integrated virus which would threaten cell survival. The main epidemiologic risk factors for MCC are immunosuppression, exposure to ultraviolet light and advanced age. Current treatment options for localised MCC rely on surgical excision and/or radiotherapy, while chemotherapy and immunotherapy are employed to manage metastatic disease (Banks *et al.*, 2016).

The role of BKPyV and JCPyV in human cancer, however, is still debated. Thus far, IARC classifies both BKPyV and JCPyV in Group 2B as possibly carcinogenic to humans (IARC, 2014). The tumourigenic properties of BKPyV

and JCPyV have been demonstrated in animal models, particularly in rodents (Tognon *et al.*, 2003; Maginnis and Atwood, 2009). Hamster kidney cells were transformed by BKPyV and then injected into newborn and adult hamsters, where they caused tumours 20 days after inoculation (Portolani *et al.*, 1975). The presence of BKPyV genomic material in tumours, including prostate, colorectal and renal cancers, proposed a role for BKPyV in human malignancy while other studies report no causal association (Abend *et al.*, 2009; Levican *et al.*, 2018). Recently, Starrett and Buck (2019) have presented their argument in favour of BKPyV playing a causal role in bladder carcinomas. Although BKPyV DNA is rarely seen integrated in muscle-invasive bladder tumours in the general population, several studies implicated BKPyV in increasing the risk of bladder cancer in immunosuppressed kidney transplant patients (Robertson *et al.*, 2017; Gupta *et al.*, 2018). In a review of JCPyV and its role in oncogenesis, Del Valle and Piña-Oviedo (2019), concluded JCPyV should not be considered a cause of, but rather a contributing factor in the pathogenesis of brain tumours, colon cancer or other malignancies. Advancements in deep sequencing and epidemiological studies could establish or refute the role of BKPyV and JCPyV in human malignancy (Prado *et al.*, 2018).

1.3 BK polyomavirus (BKPyV)

1.3.1 Transmission and epidemiology

With primary BKPyV infection occurring during early childhood, 70% of children were found to be seroconverted by the age of 10 (Ambalathingal *et al.*, 2017). As with all other HPyVs, the mode of transmission for BKPyV has yet to be defined. Many authors speculate that the respiratory route is how BKPyV is mainly acquired. Serological studies in children have suggested that tonsillitis and upper respiratory infections accompany seroconversion to BKPyV (Goudsmit *et al.*, 1982). Initial infection of tonsillar tissue may allow entry of BKPyV into the bloodstream. Subsequent infection of monocytes would facilitate dissemination to tissues and organs, including the urinary tract where BKPyV persists for the lifetime of its host (Helle *et al.*, 2017; Bennett *et al.*, 2012). Respiratory inhalation may be a common route of primary infection for both BKPyV and JCPyV, as JCPyV genome has also been detected in tonsil tissue (Goudsmit *et al.*, 1982; Monaco *et al.*, 1998).

There is also evidence for other possible routes of infection. Following analysis of nasopharyngeal aspirates from children with respiratory illness, BKPyV DNA was only detected in approximately 1% of specimens tested (Sundsfjord *et al.*, 1994). Furthermore, there was no BKPyV or JCPyV DNA in saliva samples collected from immunodeficient and healthy adults in the same study. Therefore, Sundsfjord *et al.* (1994) proposed that the gastrointestinal tract should be considered as a route of entry for BKPyV and JCPyV. While a more recent study has detected BKPyV in the saliva of healthy volunteers and patients with HIV-associated salivary gland disease, other evidence supports the faecal-oral transmission of BKPyV (Jeffers *et al.*, 2009). In fact, both BKPyV and JCPyV have been detected by a nested PCR assay in sewage samples collected in Spain, Greece, Egypt and the USA (Bofill-Mas *et al.*, 2001).

An alternative proposed mechanism for transmission is the transplacental passage of BKPyV. BKPyV DNA was present in a high percentage of both foetal and placental tissue, as analysed by PCR (Pietropaolo *et al.*, 1998; Boldorini *et al.*, 2010). In addition to vertical transmission, BKPyV may also be transmitted through sexual contact. BKPyV sequences were detected in genital tissues and sperm samples with a frequency of 57-95% (Monini *et al.*, 1996).

BKPyV may also spread via blood transfusion or organ transplantation, particularly from renal allografts (Dolei *et al.*, 2000; Andrews *et al.*, 1988).

1.3.2 Persistence and reactivation

Primary infection with BKPyV is often asymptomatic or may be experienced as a mild respiratory illness (Ambalathingal *et al.*, 2017). Following primary infection, the virus persists for the lifetime of its host at different sites. Persistence enables a viral genome to exist in a host cell without causing cell destruction which would otherwise alert the immune system to its presence and lead to virus clearance (Imperiale and Jiang, 2016). BKPyV has been detected in the kidney, bladder, ureter and to a much lesser extent in B cells, leukocytes, lymph nodes, brain and spleen (Reploeg *et al.*, 2001). Therefore, while the haematopoietic system, the central nervous system and the genital tract are all considered sites of persistence, the primary site of BKPyV persistence remains the renourinary tract, particularly the kidney where JCPyV also persists (Imperiale and Jiang, 2016). BKPyV persistent infection is not disseminated throughout the kidneys of healthy individuals. Instead, Southern blotting and real-time PCR have detected episomal BKPyV DNA in a fraction of kidney specimens obtained from the same non-immunosuppressed organ, indicating a focal distribution of BKPyV in the kidneys (Heritage *et al.*, 1981; Randhawa *et al.*, 2005).

Periodical reactivation from sites of persistence may manifest as asymptomatic viruria, characterised by the presence of exfoliated epithelial cells (decoy cells) in the urine (Ramos *et al.*, 2002). BKPyV is shed in the urine of 0-62% of immunocompetent individuals and in up to 25% of pregnant women (Dörries, 2001; Jin *et al.*, 1993). Viruria is more commonly observed in immunocompromised patients, including kidney and non-kidney SOT patients, than in healthy individuals indicating that BKPyV viruria is influenced by immune status (Imperiale and Jiang, 2016). Nearly all bone marrow transplant recipients have detectable BKPyV in their urine, with 10-25% developing haemorrhagic cystitis (Bogdanovic *et al.*, 2004; Dropulic and Jones, 2008). It is generally believed that polyomavirus viruria results from persistent virus reactivation as opposed to re-infection. Amongst renal transplant patients, reactivation of BKPyV can lead to PVAN development, which often manifests as viremia and

endangers graft survival due to lytic replication in renal tubular epithelial cells (Randhawa *et al.*, 1999). Contrary to the notion of virus reactivation resulting in disease, analysis of 108 sera from renal transplant patients revealed that different serotypes of BKPyV may be acquired during transplantation, suggesting that PVAN may in fact be the result of *de novo* BKPyV infection (Pastrana *et al.*, 2012).

The mechanisms allowing establishment of viral persistence and subsequent reactivation of human polyomaviruses are still unclear. Studies have yet to define whether BKPyV remains latent in host cells or if low level gene expression is maintained during persistent infection (Ambalathingal *et al.*, 2017). Epigenetic regulation, viral microRNA (miRNA) and immune regulation appear to be involved in the switch between persistence and reactivation of polyomavirus infection. Polyomavirus DNA is associated with cellular histones and the use of histone deacetylase inhibitors has been shown to stimulate JCPyV transcription (Wollebo *et al.*, 2013). Moreover, BKPyV encodes a miRNA responsible for controlling viral replication by targeting early viral mRNAs, suggesting that this miRNA may also contribute to persistence (Broekema and Imperiale, 2013). The mechanism through which the immune system may be involved in the establishment of polyomavirus persistence and the changes required for reactivation are also poorly elucidated. It is speculated that high levels of monocytes may suppress the immune response in pregnant women, leading to BKPyV reactivation observed as viruria or a rise in anti-BKPyV antibody titres (Coleman *et al.*, 1983). In addition, it is likely that polyomaviruses have developed immune evasion strategies to avoid detection by the innate immune system and enable the virus to persist inside host cells. For example, early viral genes of both BKPyV and MCPyV potently inhibit TLR9 gene expression possibly to evade detection of their viral genomes (Shahzad *et al.*, 2013).

Figure 1.2 presents an overview of what may occur during polyomavirus persistence and reactivation using evidence gathered from animal models of MPyV persistence. Robust MPyV replication was demonstrated by *in situ* autoradiography of differentiated cells, as opposed to actively dividing cells which showed no viral DNA replication (Atencio and Villarreal, 1994). Furthermore, chemical or ischemic damage to kidneys resulted in reactivation of

MPyV replication by promoting cellular differentiation (Atencio *et al.*, 1993). In fact, Coleman *et al.* (1978) postulated that BKPyV may reactivate as a result of immunosuppression and trauma to the kidney during the transplantation process which contributed to the narrowing, or stenosis, of the donor ureter. The contribution of trauma to reactivation, often manifesting as PVAN in kidney transplant patients, is still debated. PVAN presents itself months after transplantation when injury to the allograft is expected to have been resolved by then (Hirsch *et al.*, 2006).

On a cellular level, renal proximal tubular epithelial (RPTE) cells have been identified as the primary viral reservoir for BKPyV and as major sites of reactivation in kidney transplant patients (Popik *et al.*, 2019). RPTE cells form the lining of renal proximal tubules which are part of the nephron, the functional unit of the renal system (Carroll, 2007). Proximal tubule cells have several functions, enabling the kidney to remove waste products from the blood and to form urine. These include recovering non-waste blood products and returning them to circulation, producing vitamin precursors and maintaining blood pressure and volume (Briggs *et al.*, 2014) (Figure 1.3). Furthermore, proximal tubule cells release cytokines and chemokines, such IL-6, IL-8, IL-15, TNF-α, MCP-1, RANTES and TGF-β, to communicate with the host immune response in the event of infections or toxicity (Daha and Van Kooten, 2000).

RPTE cells represent a useful *in vitro* tool in studying various aspects of human pathology and biology, such as kidney diseases. Using RPTE cells, Humes *et al.* (2002) engineered a renal tubule cell assist device (RAD) for nutrient recovery, blood pressure and blood volume functions which would benefit patients with kidney failure. RPTE cells maintained their differentiated state *in vitro* and were capable of being passaged in cell culture up to six times. Following the development of RAD, RPTE cells were used to establish a physiologically relevant cell culture model of BKPyV infection as they are natural targets for the virus (Low *et al.*, 2004). This work was based on histopathologic findings and electron micrographs demonstrating lytic infection of RPTE cells by BKPyV in PVAN patient biopsies (Randhawa *et al.*, 1999). Numerous studies have since used RPTE cells to characterise various aspects of the viral life cycle, including the interaction between BKPyV and host factors.

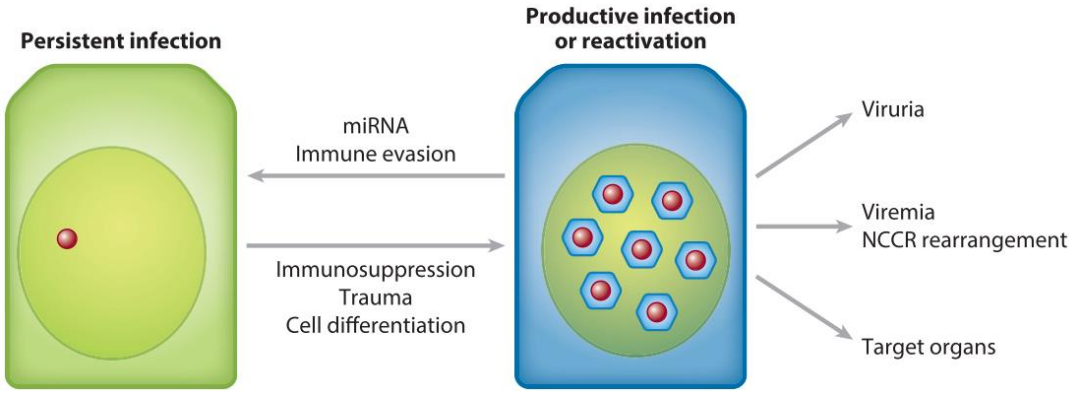

Figure 1.2 Polyomavirus persistence and reactivation. In healthy hosts, polyomaviruses persist as episomal DNA inside the nucleus of host cells. Persistence is thought to be facilitated by viral microRNA (miRNA) and immune evasion strategies. Polyomaviruses reactivate and undergo productive replication under immunosuppression, trauma or cell differentiation. Polyomavirus reactivation can lead to viruria, viremia, non-coding control region (NCCR) rearrangement and viral dissemination from the sites of persistence to other target organs. Obtained from Imperiale and Jiang (2016).

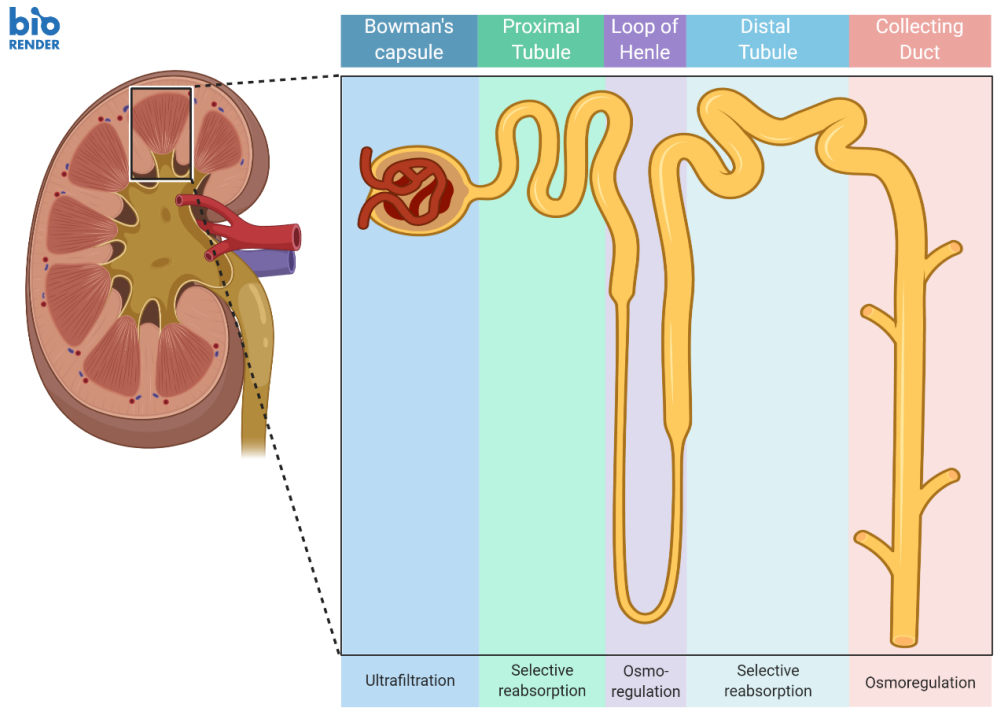

Figure 1.3 The nephron is the functional unit of the kidney. Schematic of a nephron in a cross-section of the kidney showing the relationship between nephron structures and functions. Created with BioRender.com.

1.3.3 Clinical disease and diagnosis

Following reactivation, lytic infection of BKPyV induces diverse complications in circumstances involving prolonged immune impairment where viral replication is no longer controlled. The major BKPyV-associated diseases are haemorrhagic cystitis (HC) and polyomavirus-associated nephropathy (PVAN) observed in bone marrow transplant recipients and kidney transplant patients, respectively (Bennett *et al.*, 2012).

In haematopoietic stem cell transplant (HSCT) recipients, HC can occur pre- or post-engraftment resulting from chemotherapeutic agents or viral infection, respectively. Cytomegalovirus (CMV), adenovirus and BKPyV are all capable of causing HC in these patients. However, the majority of post-engraftment HC cases observed in 10-25% HSCT patients are attributed to BKPyV (Dropulic and Jones, 2008). HC is characterised by dysuria, urinary frequency, lower abdominal pain and haematuria, and usually presents two weeks post-transplantation (Ambalathingal *et al.*, 2017). BKPyV-associated HC is diagnosed through urine examination by detection of decoy cells which have enlarged nuclei and a large basophilic intranuclear inclusion (Fogazzi *et al.*, 2001) (Figure 1.4). As the presence of decoy cells is not specific for BKPyV infection, detection of viral DNA in urine or serum samples by PCR is more specific for the diagnosis of BKPyV-associated diseases (Viscount *et al.*, 2007).

Albeit being a rare BKPyV-associated disease in non-renal SOT patients, PVAN is documented in 1-10% of renal transplantation cases (Costa and Cavallo, 2012; Hirsch *et al.*, 2006). The level of immunosuppression and trauma at the main site of persistence may explain why PVAN develops more frequently in renal transplant patients compared to other immunosuppressed patients (Bennett *et al.*, 2012). PVAN usually presents 10-13 months following renal transplantation and is a form of interstitial nephritis, characterised by intranuclear inclusions in tubular, collecting duct and glomerular epithelial cells (Boothpur and Brennan, 2010) (Figure 1.5). The American Society of Transplantation has recently updated the morphologic classification of PVAN to include the degree of viral cytopathic changes as well as the degree of inflammation and tubular atrophy (Nickeleit *et al.*, 2018). PVAN often leads to impairment of kidney function and eventual allograft rejection in up to 90% of cases (Huang *et al.*, 2015).

The first long-term successful kidney transplant was performed in 1954 between identical twins without any immunosuppressive medication (Hatzinger *et al.*, 2016). Due to complications arising from immunological recognition of the transplanted organ in other patients, the transplantation field underwent immense improvements with better donor-recipient matching and, crucially, with the use of potent immunosuppressive medication (Barker and Markmann, 2013). With increasing use of potent iatrogenic intervention persistent infections are resurging. Thus, BKPyV is becoming a major concern for the transplant population in a setting where immunosuppression is routinely implemented to prolong graft survival (Bohl and Brennan, 2007). Calcineurin inhibitors, mammalian target of rapamycin (mTOR) inhibitors, antimetabolites and corticosteroids commonly comprise the post-transplant regimen for allograft recipients. Immunosuppressants, such as cyclosporine and tacrolimus, suppress T lymphocyte activation. Azathioprine and mycophenolate mofetil (MMF) inhibit cell proliferation, while corticosteroids have anti-inflammatory properties (Kalluri and Hardinger, 2012). While these drugs work synergistically to prevent graft rejection, they also contribute to viral reactivation. To date, no specific immunosuppressant has being implicated in increasing the risk of polyomavirus-related illnesses (Weikert and Blumberg, 2008).

No single risk factor has been significantly associated with PVAN development in renal transplant patients and data from ethnically diverse populations is lacking. Instead, a variety of risk factors have been reported which are related with transplantation, immunosuppression and immunity (Chong *et al.*, 2019). Male sex, HLA-mismatching, recipient age under 18 or over 60, depleting antibody induction therapy and acute rejection are all factors associated with increased risk for BKPyV-associated disease as determined by a large retrospective study of paired kidneys (Thangaraju *et al.*, 2016). New evidence is emerging of donor factors influencing the outcome of a kidney transplant which may challenge the long-standing view of PVAN developing mainly due to BKPyV reactivation in the recipient following the loss of cellular immunity (Pastrana, 2020). Schmitt *et al.* (2014) analysed the BKPyV sequences of 249 living donor/recipient pairs, concluding that sequences isolated from recipients following transplantation were identical to the donor-derived sequence. A different study assessed development of viruria, viremia and PVAN in 168 renal

transplant recipients and 69 donors (Solis *et al.*, 2018). The authors demonstrated that weak antibody neutralising responses from the recipient increased the risk of developing PVAN. The culmination of data from both studies suggests that a subpopulation might exist which is more vulnerable to PVAN development due to the inability to initiate a potent immune response against the donor's viral genotype (Pastrana, 2020). In a cohort of 23 renal transplant patients, BKPyV genotype Ia was found to be associated with increased urine viral load compared to genotype Ib1 (Varella *et al.*, 2018). It is unclear whether it is the virulence of incoming virus or the mismatch between transmitted and recipient viruses that is important in determining whether disease occurs (Chong *et al.*, 2019).

At present time, there is no reliable non-invasive method to diagnose PVAN. As with BKPyV-associated HC, urine cytology examines the presence of decoy cells in the urine of patients with suspected PVAN but offers poor specificity compared to other methods (Viscount *et al.*, 2007). Detection of BKPyV viral load by PCR is routinely used for serum examination, however, diagnosing concurrent PVAN presents a challenge (Chong *et al.*, 2019). The gold standard for diagnosing PVAN is a renal biopsy, which is a time-consuming and invasive procedure (Sawinski and Goral, 2015). Moreover, PVAN and acute cellular rejection have overlapping histological findings making it challenging for a definitive PVAN diagnosis (Drachenberg *et al.*, 2004). Due to the focal nature of the infection, PVAN can be under-diagnosed by obtaining a false negative biopsy (Drachenberg and Papadimitriou, 2006). The development of novel biomarkers, such as CXCL9, CXCL10 and BKPyV genotype-specific neutralising antibody titres are promising for their potential use in screening and monitoring of PVAN as early diagnosis is linked to better prognosis (Jackson *et al.*, 2011; Solis *et al.*, 2018).

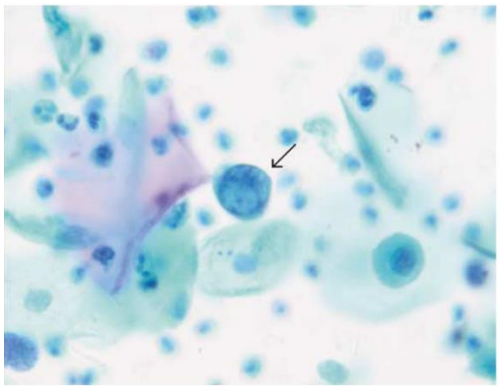

Figure 1.4 Cytologic preparation of urine epithelial cells. Cytology detects decoy cells which are characteristic polyomavirus-infected cells containing an enlarged nucleus with a single large basophilic intranuclear inclusion (arrow). × 60 magnification. Obtained from Dropulic and Jones (2008).

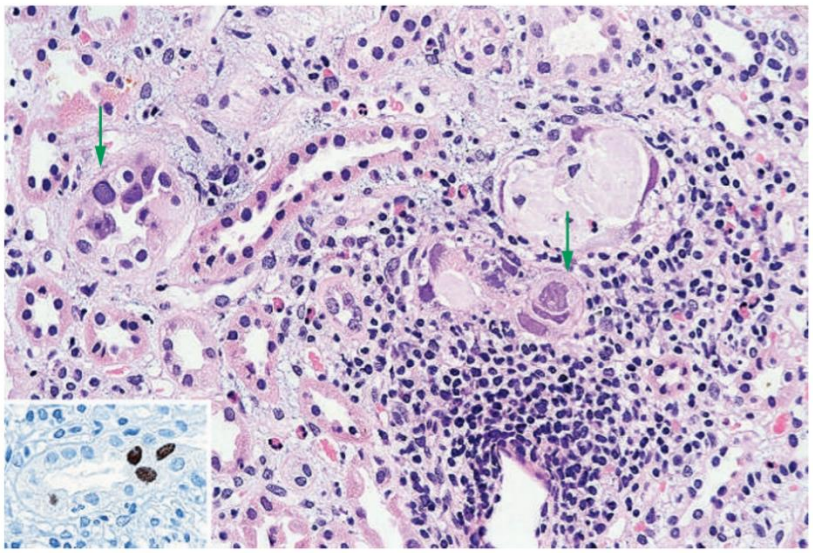

Figure 1.5 Cytopathic changes detected in a renal allograft biopsy. Protocol biopsy was taken 20 months after transplantation, whereupon large, pleomorphic tubular epithelial cells (green arrows) and associated mixed interstitial inflammation were observed. Haematoxylin and eosin stain; original magnification ×200. Inset: immunohistochemistry for the SV40 antigen demonstrated strong nuclear staining in infected cells. Obtained from Liptak *et al.* 2006).

1.3.4 Therapeutic interventions

Clinicians face an undisputed challenge in treating BKPyV-associated sequelae due to the lack of effective, non-nephrotoxic antiviral agents. As a result, there is no accepted standard protocol for the treatment of BKPyV infection. Supportive care in the form of pain management, hyperhydration, bladder irrigation and diuresis is provided for patients to relieve symptoms of painful HC. Mild cases of HC can resolve spontaneously with supportive care within two weeks (Dropulic and Jones, 2008). The management of PVAN centres primarily on reducing immunosuppressive medication, an approach which ultimately risks graft loss (Beimler *et al.*, 2007).

The lack of FDA-approved drugs for specifically treating BKPyV infection has led researchers to test drugs which target other DNA viruses. Cidofovir, fluoroquinolones, leflunomide and mTOR inhibitors are amongst the drugs that have been tested for their *in vitro* efficacy against BKPyV. Cidofovir is an intravenous nucleotide phosphonate analogue of deoxycytidine monophosphate (dCMP) which competitively inhibits the DNA synthesis by viral DNA polymerase (Lea and Bryson, 1996). The underlying mechanism of action against BKPyV infection is presently unclear as polyomaviruses do not encode a viral DNA polymerase which can be targeted by the drug. Cidofovir was originally developed for treating CMV infections and is licensed to treat CMV retinitis in HIV/AIDS patients (De Clercq, 2007). The *in vitro* activity of cidofovir was first evaluated against mouse and non-human primate polyomaviruses as part of a screen of several antiviral compounds (Andrei *et al.*, 1997). Furthermore, BKPyV DNA replication was inhibited in cell culture upon cidofovir treatment of human embryonic lung fibroblast cells (WI-38) and RPTE cells (Farasati *et al.*, 2005; Bernhoff *et al.*, 2008).

Weekly treatments with low-dose cidofovir were proven to be a safe treatment option for BKPyV-associated HC in HSCT patients, where cidofovir reduced viraemia and viruria in 47% and 84% of cases, respectively (Savona *et al.*, 2007). There are variable and conflicting clinical cases or retrospective studies regarding the use of cidofovir for PVAN treatment. Recently, Mühlbacher *et al.* (2019) demonstrated the efficacy of a dual therapeutic approach using low-dose cidofovir and conversion to mTOR-based immunosuppression for treating patients with biopsy-proven PVAN. However, there still exists a clear need for

randomised controlled studies to better define the role of cidofivir in treating PVAN patients. A randomised, placebo-controlled, dose-escalation clinical trial was undertaken to assess the effect of cidofovir in PVAN-diagnosed renal transplant recipients (ClinicalTrials.gov; NCT00138424).

Nephrotoxicity is a severe adverse effect of cidofovir as the drug accumulates in renal tubules due to an organic anion transporter, hOAT1 (Ho *et al.*, 2000). As shown *in vitro*, cidofovir causes apoptosis of RPTE cells by decreasing both host cellular DNA replication and metabolic activity (Ortiz *et al.*, 2005; Bernhoff *et al.*, 2008). Co-administration of probenecid with cidofovir reduces cidofovir-induced nephrotoxicity and is now a requirement by the FDA for cidofovir-based treatment (Morrissey *et al.*, 2013). An additional caveat of cidofovir is the intravenous method of administration requiring patients to be hospitalised (Rinaldo *et al.*, 2010).

A lipid ester prodrug of cidofovir, brincidofovir (CMX001), was recently evaluated in a post-organ transplant study of patients with BKPyV viruira (ClinicalTrials.gov; NCT00793598). The results from this Phase Ib/IIa clinical trial have yet to become available. CMX001 is orally bioavailable with broad spectrum antiviral activity against polyomaviruses, herpesviruses and adenoviruses demonstrated in cell culture and *in vivo* (Camargo *et al.*, 2016). CMX001 inhibits BKPyV replication in RPTE cells in a similar way to cidofovir, albeit having a more rapid and enduring antiviral effect (Rinaldo *et al.*, 2010). In fact, CMX001 was active against BKPyV at a 400-fold lower concentration than that of cidofovir. No significant drug-associated nephrotoxicity has been observed compared to its parent drug as CMX001 is not an hOAT1 substrate (Tippin *et al.*, 2016).

Leflunomide is an immunomodulatory agent which inhibits BKPyV mainly at the level of DNA synthesis and, to a lesser extent, interferes with virion assembly and progeny release (Bernhoff *et al.*, 2010). The anti-BKPyV mechanism of leflunomide seems to be dependent on pyrimidine depletion. Similar to cidofovir, the *in vivo* efficacy of leflunomide is disputed. A systematic review of *in vitro* studies, case reports, retrospective and prospective cohort studies suggested a potential benefit of using leflunomide for PVAN treatment (Wu and Harris, 2008). A derivative of the active metabolite of leflunomide (FK778) was evaluated in 46 renal transplant patients with newly diagnosed or untreated

PVAN (Guasch *et al.*, 2010). Despite resulting in a significant reduction of viraemia, the Phase II clinical trial determined that FK778 therapy had no benefit. The drug was associated with higher incidence of acute rejection and unimproved renal function compared to reduction of immunosuppression alone.

Fluoroquinolones are antibiotics which inhibit bacterial DNA replication and are thought to target the helicase activity of LT-Ag to suppress viral replication (Song *et al.*, 2016). Several fluoroquinolones, such as ciprofloxacin, gatifloxacin or levofloxacin, have been assessed *in vitro* and *in vivo* in the prophylaxis or treatment of BKPyV infection and were initially reported to be efficacious (Khalil *et al.*, 2018). Leung *et al.* (2005) observed a decrease in HC incidence when HSCT patients were treated with ciprofloxacin as a prophylactic measure. Gatifloxacin treatment of renal transplant patients resulted in reduced viraemia or viruria in 60% of cases (Bennett *et al.*, 2012). In contrast, a systematic review of randomised controlled trials and observational studies with a total of 1,477 participants concluded that there was no benefit of fluoroquinolone prophylaxis in preventing BKPyV infection following kidney transplantation (Song *et al.*, 2016). Fluoroquinolones were not associated with reduced BKPyV viraemia or a lower risk of graft failure due to PVAN.

The mTOR inhibitors, sirolimus and torin-1, inhibit BKPyV replication in RPTE cells, suggesting an mTOR-dependent replication pathway (Hirsch *et al.*, 2016). The success of mTOR inhibitors in treating BKPyV infection has yet to be reproduced in large studies (Jouve *et al.*, 2015). Analysis of data from the Scientific Registry of Transplant Recipients on 42,838 kidney transplant patients revealed that the outcomes of BKPyV infection within the first year of transplantation were similar in sirolimus-treated and tacrolimus/cyclosporine-treated patients (Schold *et al.*, 2009). However, comparison of the mTOR inhibitor everolimus to MMF administration in 296 renal transplant patients indicated a lower risk of viraemia, lower viral load and no graft loss with everolimus treatment (Moscarelli *et al.*, 2013). An issue arising from interpreting such data is that mTOR inhibitors also act as immunosuppressants. Thus, the efficacy of mTOR inhibition during BKPyV infection may be confounded by their immunosuppressive activities (Chong *et al.*, 2019). Nonetheless, conversion to everolimus is under evaluation in a clinical trial for outcomes on severe BKPyV

infection, as everolimus may be beneficial in cases where immunosuppression cannot be lifted (ClinicalTrials.gov; NCT03216967).

Intravenous immunoglobulins (IVIG) are used as empiric therapy in BKPyV-associated diseases upon immunosuppression reduction because of its immunomodulatory and potential anti-BKPyV properties (Bohl and Brennan, 2007). Randhawa *et al.* (2010) assessed various commercially available human IVIG preparations and concluded that these contain BKPyV antibodies with neutralising activities. Vu *et al.* (2015) examined the effect of intravenous IVIG in PVAN-diagnosed renal transplant patients with inadequate response to immunosuppression reduction and leflunomide therapy. A significant decrease in viral load was observed following 1 month of IVIG therapy and 90% of the 30 IVIG-treated patients had cleared viraemia within the 1 year follow-up. In addition, IVIG therapy promoted graft survival in 96.7% of cases arguing for its protective effect against BKPyV infection. Others report of BKPyV neutralising antibodies not contributing to viral control in immunosuppressed patients or even IVIG therapy resulting in enhanced viral load in a single case study (Comoli *et al.*, 2004; Bohl *et al.*, 2008; Maggiore *et al.*, 2010). Multi-centre trials are warranted to determine the efficacy of therapeutic IVIG in BKPyV infection.

Another approach in treating BKPyV may involve the adoptive transfer of cytotoxic T lymphocytes (CTLs). CTLs improved active BKPyV infection in six of seven HSCT patients who experienced BKPyV viraemia (Papadopoulou *et al.*, 2014). Furthermore, a single case report of a HSCT patient who developed HC following transplantation, showed full resolution of symptoms and viraemia with BKPyV-specific CTL treatment (Pello *et al.*, 2017). Randomised controlled clinical trials should be undertaken to define the effect of CTL treatment in treating pathological forms of BKPyV replication.

Prophylactic therapies are also being considered for preventing disease in candidate organ transplant recipients. A multivalent VLP-based BKPyV vaccine against all four known serotypes is currently in a pre-clinical development stage (Rodriguez, 2019). Pastrana *et al.* (2012) proposed that this vaccine may offer protection against BKPyV-associated diseases in transplant recipients who are initially naïve against specific serotypes. Moreover, a DNA vaccine is being developed by SL VaxiGen to simultaneously target CMV and BKPyV infections. The vaccine is based on three DNA plasmids encoding the antigens and

adjuvant. It is currently under evaluation in Phase I clinical trials in patients scheduled to receive kidney transplants from living donors (ClinicalTrials.gov; NCT03576014).

1.4 Molecular biology of BKPyV

1.4.1 Structure and genomic organisation

The 45-50 nm non-enveloped polyomavirus virion encapsidates an approximately 5.2 kb covalently-closed, circular dsDNA genome (Jeffers *et al.*, 2009). Host cell H2A, H2B, H3 and H4 histone proteins facilitate packaging of the viral genome into a 'mini-chromosome' within the virion (Fang *et al.*, 2015).

The BKPyV particle is comprised only of a protein capsid and DNA, with the major structural protein VP1 and less abundant minor capsid proteins VP2 and VP3 serving as building blocks for its structure. Structural studies on MPyV and SV40 revealed that the exterior surface of the polyomavirus capsids is entirely composed of 360 copies of VP1 (Rayment *et al.*, 1982; Liddington *et al.*, 1991; Stehle *et al.*, 1996). The VP1 molecules form 72 pentameric capsomeres, each consisting of a ring of five β-barrell-containing VP1 monomers (Figure 1.6A). Pentamers form a T=7d icosahedral lattice, with a C-terminal arm from each VP1 interacting with neighbouring pentamers for capsid stabilisation (Stehle *et al.*, 1994; Nilsson *et al.*, 2005). Furthermore, calcium cations (Ca^{2+}) and an extensive network of intra- and inter-pentameric disulphide bonds stabilise the viral capsid. Polyomavirus virions demonstrate a high degree of capsid stability as SV40 infectivity is influenced significantly upon heating to 95°C for 1 hour (Sauerbrei and Wutzler, 2008; Nims and Plavsic, 2013). A single copy of either the VP2 or VP3 minor capsid protein is incorporated within the inward-facing cavity of each pentamer (Chen *et al.*, 1998; Hurdiss *et al.*, 2016) (Figure 1.6B).

In 2016, Hurdiss *et al.* published the first sub-nanometre-resolution of a cryo-EM structure of a native BKPyV particle at 7.6 Å. High-resolution structural information enabled discrete bridges of density connecting VP1 and the encapsidated genome to be visualised for the first time. The authors proposed that there may be a direct interaction between the viral mini-chromosome and the capsid to aid genome packaging (Hurdiss *et al.*, 2016) (Figure 1.6C). Further refinement of the cryo-EM structure revealed the location of disulphide bonds and Ca^{2+} binding, as well as determined the interaction of BKPyV with a fragment of one of its major receptors, GT1b ganglioside (Hurdiss *et al.*, 2018).

The viral genome is arranged into three functional sections; the regulatory, early and late regions (Figure 1.7**;** bottom). The regulatory region is a non-coding

control region (NCCR) of approximately 400 base pairs (bp) and harbours the origin of DNA replication, along with promoters to drive the transcription of early and late viral genes (Helle *et al.*, 2017). There are two forms of the viral genome, termed archetypal and rearranged, depending on the sequence of the regulatory region. The archetypal NCCR is divided into five blocks of sequence designated O (origin of replication) followed arbitrarily by P, Q, R and S (Figure 1.7; top). Point mutations, deletions, duplications, and rearrangements within the NCCR give rise to rearranged variants (Moens and Van Ghelue, 2005). Archetype virus is thought to be the transmissible form capable of establishing persistent infection as it gives rise to all known NCCR rearrangements. Furthermore, archetype virus is isolated from both healthy and immunosuppressed individuals (Bennett *et al.*, 2012). In contrast, rearranged variants tend to be associated with disease (Broekema and Imperiale, 2012). Gosert *et al.* (2008) reported that BKPyV variants with rearranged NCCRs replaced archetype virus *in vivo* in 50% of patients with PVAN and were associated with 20-fold higher plasma viral loads. Notably, rearranged NCCR BKPyV variants grow more readily in cell culture and are thus more frequently used for *in vitro* studies (Broekema and Imperiale, 2012).

The early and late genes are transcribed from opposite strands of the circular viral genome (Gu *et al.*, 2009). Following infection of a host cell, transcription from the early region of the genome gives rise to alternatively spliced mRNAs coding for large tumour antigen (LT-Ag), small tumour antigen (sT-Ag) and the truncated form of large tumour antigen (truncTAg). The three structural proteins, VP1, VP2 and VP3, and agnoprotein are encoded by the late region of the genome and are expressed following initiation of genomic replication (Bethge *et al.*, 2015). In addition, the BKPyV genome encodes two viral miRNAs, named 5p-miRNA and 3p-miRNA (Tian *et al.*, 2014).

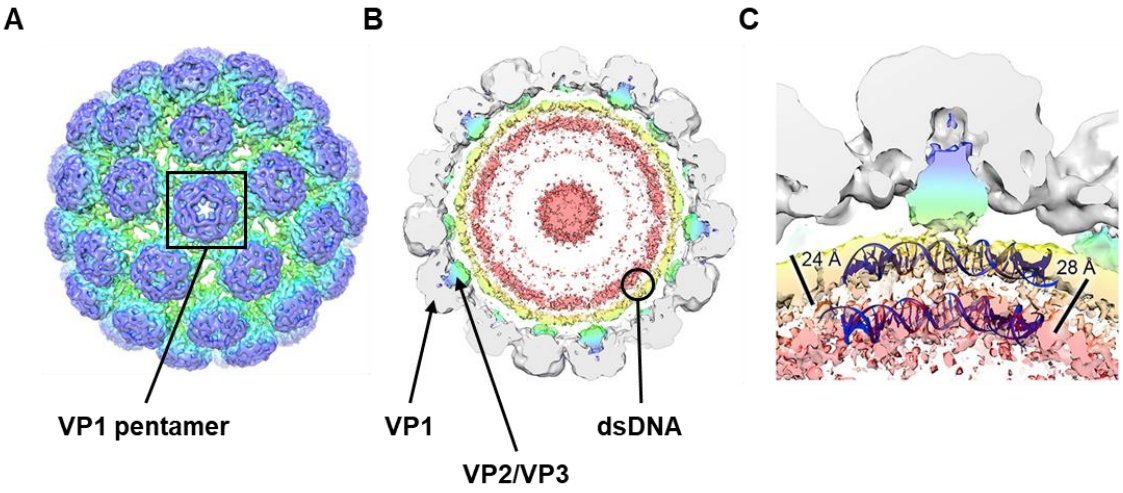

Figure 1.6 Cryo-electron microscopy structure of infectious BKPyV virion. A) An external view of the BKPyV virion shown at a contour level of 0.022. A pentamer of VP1 molecules is highlighted. B) View of a 40-Å-thick slab through the unsharpened/unmasked virion map shown at a contour level of 0.0034. Major capsid proteins (VP1; grey), minor capsid proteins (VP2 or VP3; blue/green) and genome organisation (dsDNA; yellow/pink) are visualised. C) Enlarged view of the pyramidal density beneath a single VP1 penton of the virion shown at a contour level of 0.0032. Strands of dsDNA wrapped around a human histone octamer are also visualised. Scale bars shown. Adapted from Hurdiss *et al.* (2016).

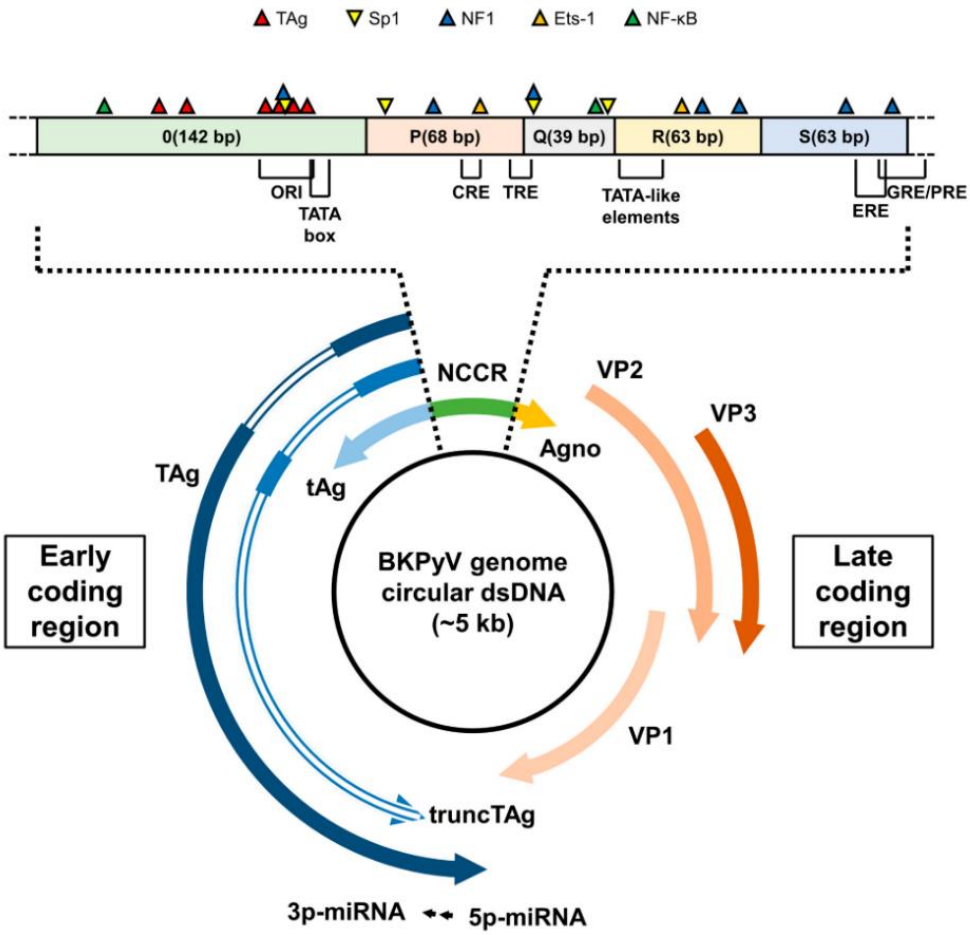

Figure 1.7 Map of the BKPyV genome. The BKPyV genome (bottom) is a closed circular, double-stranded DNA (dsDNA) molecule of approximately 5.2 kilobase pairs (kb). The noncoding control region (NCCR), early and late coding regions comprise the three functional regions of the polyomavirus genome. The NCCR is a hyper-variable region containing the origin of DNA replication (ORI), along with promoters to drive the bidirectional transcription of early and late viral genes. Large tumour antigen (LT-Ag), small tumour antigen (sT-Ag) and the truncated form of large tumour antigen (truncTAg) are produced from different alternatively spliced mRNAs which are expressed from the early coding region of the genome. Double lines represent the introns in the early coding region. The late coding region encodes the structural proteins VP1, VP2, and VP3, and the non-structural protein, agnoprotein. The late proteins are translated from two classes of late RNAs, 16S and 19S, that are generated by alternative splicing from a common pre-mRNA. The 19S RNA is translated to yield both VP2 and VP3 while the 16S RNA species is translated to yield agnoprotein and VP1. The BKPyV genome also encodes two miRNAs, 5p-miRNA and 3p-miRNA, produced after processing of a common pre-miRNA hairpin and are

perfectly complementary to the TAg encoding mRNAs. The schematic organisation (top) of the BKPyV archetype NCCR is represented. The NCCR is divided into five sequence blocks (O, P, Q, R and S) and includes the ORI, TATA box and TATA-like elements. Binding sites important for LT-Ag and transcription factors including Sp1, nuclear factor κB (NF-κB) and cAMP-responsive-element (CRE) are also mentioned. CRE: cAMP responsive-element; TRE: phorbol ester responsive-element; GRE/PRE: glucocorticoid/progesterone responsive-element; ERE: oestrogen responsive-element. Obtained from Helle *et al.* (2017).

1.4.2 Regulatory proteins

The early promoter found within the BKPyV NCCR drives the expression of a single mRNA transcript which is alternatively spliced, giving rise to the three early proteins; LT-Ag (695 aa; 80 kDa), sT-Ag (172 aa; 20 kDa) and truncTAg (136 aa; 17 kDa) (Helle *et al.*, 2017). LT-Ag is translated when the first exon and the next exon are included in the mature mRNA following splicing of the early pre-mRNA. Alternatively, retention of the first intron gives rise to sT-Ag as a termination codon is reached within this intron during translation. Therefore, the first 82 amino acids of sT-Ag and LT-Ag are identical. Furthermore, Abend, Joseph *et al.* (2009) demonstrated that LT-Ag and truncTAg share the first 133 amino acids. TruncTAg is expressed from an alternatively spliced mRNA of the early pre-mRNA which is derived through the excision of two introns. One of these two introns is also removed during the generation of the LT-Ag-encoding mRNA (Abend, Joseph *et al.*, 2009). BKPyV LT-Ag is mainly localised to the nucleus as it contains a nuclear localisation signal (NLS; ^{129}KKKRK^{133}) which is similar to that of SV40 LT-Ag (Kalderon *et al.*, 1984; Abend, Joseph *et al.*, 2009). TruncTAg, is also found in the nucleus as it contains the entire NLS with the exception of the last valine residue, like SV40 17KT.

All polyomavirus LT-Ag proteins contain four well-conserved domains; J domain, DNA-binding domain (DBD), zinc (Zn)-binding domain and ATPase domain (An *et al.*, 2012) (Figure 1.8A). The J domain is found at the N-terminus of all three early proteins and is homologous to the amino acid sequence of molecular chaperones which are members of the DnaJ family (Decaprio and Garcea, 2013; Kelley and Georgopoulos, 1997). Through the J domain, polyomaviruses interact with the co-chaperone heat shock cognate 70 (Hsc70) to promote efficient viral replication (Campbell *et al.*, 1997) (Figure 1.8B). The sT-Ag also carries out the same functions mediated by domains located in the N-terminus, such as the J-domain, which it shares with LT-Ag (Harris *et al.*, 1998). The DBD, Zn-binding domain and ATPase domain confer a DNA helicase activity to LT-Ag, while the region encompassing these domains is truncated in truncTAg (An *et al.*, 2012). Any unique functions of truncTAg remain to be determined and it is likely that the role of truncTAg in carrying out LT-Ag functions is redundant (Abend, Joseph *et al.*, 2009; Bennett *et al.*, 2012).

LT-Ag is a multifunctional regulatory protein and, during productive replication, it carries out two critical functions. Firstly, LT-Ag inactivates the retinoblastoma susceptibility protein (Rb) through a conserved ^{105}LXCXE^{109} motif in the LT-Ag amino acid sequence (Harris *et al.*, 1996). Interaction with Rb and its family members, p107 and p130, alleviates the E2F-mediated inhibition of transcription (Harris *et al.*, 1998). In addition, LT-Ag binds to a second tumour suppressor protein, p53, and impairs transcription of downstream tumour suppressor targets to counteract apoptosis (Harris *et al.*, 1996). Together, these interactions promote entry into the S phase of the cell cycle (An *et al.*, 2012). Due to their limited coding capacity polyomaviruses cannot synthesise their own replication machinery (Verhalen *et al.*, 2015). Therefore, entry into S phase grants access to the cellular DNA synthetic machinery which supports viral replication. The second function of LT-Ag is to initiate viral genome replication by binding the origin of DNA replication through its DBD. The DBD recognises the GAGGC sequence present in four repeats within the origin of replication in the NCCR (Deb *et al.*, 1987). Subsequently, LT-Ag utilises its helicase activity to unwind viral DNA and recruits the host DNA polymerase α primase complex to replicate the viral genome (Stahl *et al.*, 1986; Dornreiter *et al.*, 1992). The role of LT-Ag in viral genome replication is discussed further in section 1.5.5.

While LT-Ag and truncTAg are located primarily in the nucleus, sT-Ag is found both in the nucleus and cytoplasm (Ellman *et al.*, 1984). A C-terminal unique region within sT-Ag contains two zinc-binding motifs which flank the shared N-terminal domain (Cho *et al.*, 2007) (Figure 1.8C). To facilitate progression through the cell cycle, the zinc-binding motifs bind to the A and C subunits of protein phosphatase 2A (PP2A) resulting in its inactivation.

The cell cycle-altering functions of both LT-Ag and sT-Ag confer oncogenic potential to PyVs and are, thus, often referred to as viral oncogenes (Ahuja *et al.*, 2005). BKPyV causes malignant cell transformation of BHK-21 clone 13 cells *in vitro* which grow as tumours when inoculated into adult hamsters (Major and Di Mayorca, 1973). In fact, injecting rodents with BKPyV results in the formation of multiple tumours (Tognon *et al.*, 2003). In contrast to its episomal form in human cells following infection, the viral genome integrates into the host genome of rodent cells (Cubitt, 2006). Recently, BKPyV has been proposed as a potential co-factor in the development of prostate cancer and in having a

causal role in bladder carcinomas developing in transplant patients (Tognon and Provenzano, 2015; Starrett and Buck, 2019). Furthermore, examination of a renal allograft carcinoma demonstrated that BKPyV had integrated into the BRE gene of human chromosomal DNA (Kenan *et al.*, 2017). The authors did not detect any BKPyV integration in normal kidney cells. However, there still remains a lack of conclusive causal evidence in support of BKPyV oncogenicity in humans (Prado *et al.*, 2018).

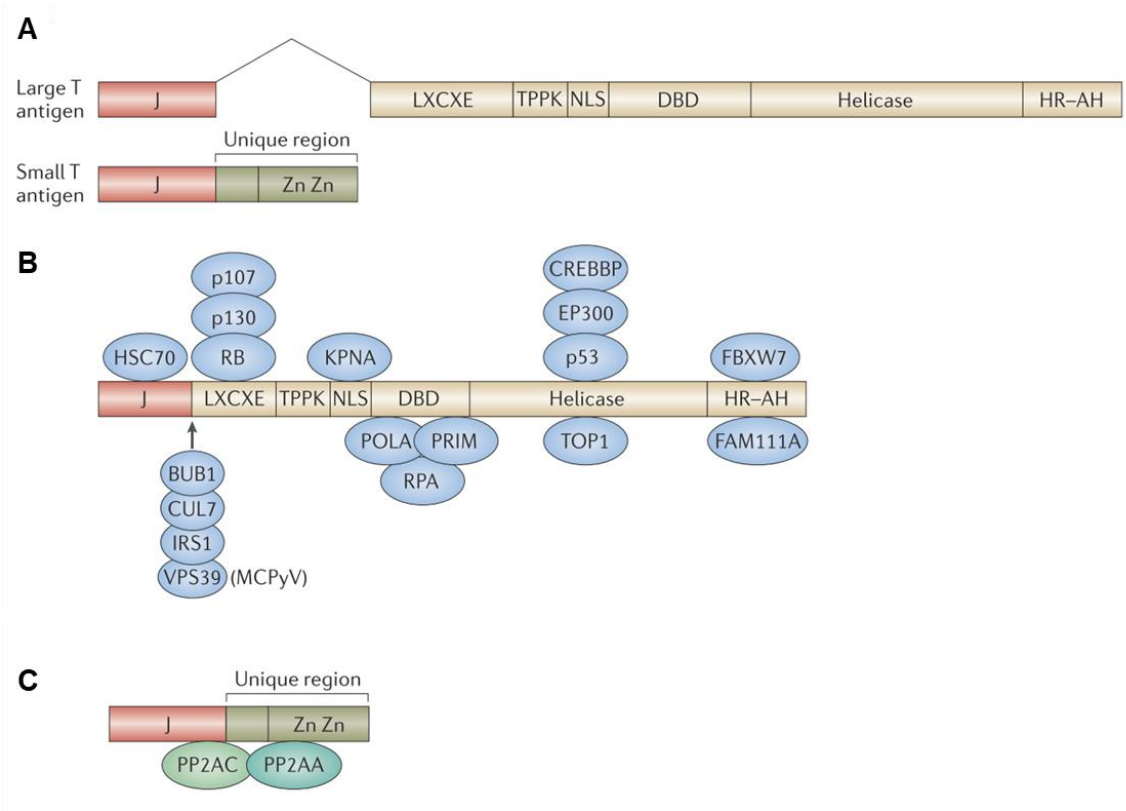

Figure 1.8 The functional domains of large and small T-antigens. A) The N-terminal DnaJ (J) domain is shared between small (sT-Ag) and large (LT-Ag) T-antigens. LT-Ag contains a retinoblastoma-associated protein (Rb) -binding LXCXE motif, a threonine-proline-proline-lysine (TPPK) motif, a nuclear-localisation sequence (NLS), a DNA-binding domain (DBD), a helicase domain and a host range and adenovirus helper function (HR–AH) domain. Small T-antigen shares the J domain with LT-Ag, which is followed by a unique region containing two zinc-binding motifs. B) LT-Ag binds to many cellular proteins, including interacting with the heat shock cognate 71 kDa protein (HSC70) homologues through the J domain. Rb and the related proteins, p107 and p103, associate with LT-Ag through the LXCXE domain. To replicate the viral genome, the DBD recruits DNA polymerase-α catalytic subunit (POLA), the replication protein A complex (RPA) and the DNA primase complex (PRIM), while the helicase domain binds EP300, CREBBP, p53 and DNA topoisomerase 1 (TOP1). C) The interaction between sT-Ag and the A and C subunits of protein phosphatase 2A (PP2A) is mediated by the unique domain of sT-Ag. Adapted from Decaprio and Garcea (2013).

1.4.3 Capsid proteins

During the late phases of infection and following initiation of DNA replication, the structural proteins VP1, VP2 and VP3 are expressed along with agnoprotein from the late coding region in the viral genome (Bennett *et al.*, 2012). Transcription form the late region yields a pre-mRNA which is alternatively spliced into polycistronic 16S and 19S late RNAs (Good, Welch, Ryu, *et al.*, 1988). VP1 and agnoprotein are produced from the 16S RNA, while VP2 and VP3 are translated from the 19S RNA (Grass and Manley, 1987; Good, Welch, Barkan, *et al.*, 1988). The structural proteins are particularly important during the entry step of the viral life cycle and in forming capsomeres, which assemble around newly synthesised viral genomes to give rise to stable viral particles (Dugan *et al.*, 2007).

VP1 is a 42 kDa (362 aa) protein which is divided into five loops; BC, DE, EF and HI are the surface-exposed loops with GH as an interior loop (Teunissen *et al.*, 2013). By mutating charged amino acids within surface-exposed loops, Dugan *et al.* (2007) showed that VP1 loops are important for virus proliferation and virion production as they mediate capsid assembly. As discussed previously, VP1 pentamers compose the external portion of the capsid. The N-terminal region of VP1 found on the inside of the particle is involved in DNA binding (Hurdiss *et al.*, 2016). The C-terminus of each VP1 monomer brings together neighbouring capsomeres to form virions via extended arms. Expression of VP1 alone in a eukaryotic baculovirus expression system allows its self-assembly into virus-like particles (VLPs), which package histone-associated dsDNA similar in size to that of the polyomavirus genome (Salunke *et al.*, 1986; Gillock *et al.*, 1997). Truncations in the VP1 C-terminus renders the capsomeres incapable of forming these VLPs, emphasising the role of this region during virion assembly (Garcea *et al.*, 1987; Yokoyama *et al.*, 2007).

VP1 plays a crucial role in entry by mediating virion attachment to susceptible cells. The work of Neu *et al.* (2013) identified lysine 68 as a determinant of cellular receptor specificity (section 1.5.1). Mutation of this residue enables BKPyV to switch to a different class of gangliosides as the receptor, allowing the virus to bind the SV40 receptor GM1. The shallow groove formed by the VP1 BC and HI loops likely represents the receptor-binding pocket based on molecular modelling of BKPyV VP1 (Dugan *et al.*, 2007). Residues 61-83 of the

BC loop constitute the epitope responsible for serotype differences between BKPyV isolates (Jin, Gibson, Knowles, *et al.*, 1993). Variations within this 69 bp region, termed ‘VP1 subtyping region’, also determines the genotype of BKPyV (Jin, Gibson, Booth, *et al.*, 1993). There are four distinct genotypes (I-IV) which correspond to serotypes BK, SB, AS and IV respectively, as determined by HI assays (Knowles *et al.*, 1989). Tremolada *et al.* (2010) investigated the importance of the BC loop in the viral life cycle and revealed that different BKPyV isolates representing the four genotypes, replicated at different rates in Vero cells. VLP-based neutralising assays have demonstrated that VP1 proteins from each of the four BKPyV genotypes can evade neutralising antibodies which have been raised against the other genotypes (Pastrana *et al.*, 2013). These findings implied that BKPyV genotypes may exhibit different cellular entry tropisms and virulence potentials *in vivo*. Furthermore, the authors provided evidence of the BKPyV sub-genotypes Ib1 and Ib2 also representing distinct serotypes. Two amino acid differences within the BC2 surface loop seem to be responsible for this difference between these two sub-genotypes.

On the internal face of each VP1 pentamer, there is a single copy of either VP2 (351 aa; 38 kDa) or VP3 (232 aa; 27 kDa) (Hurdiss *et al.*, 2016). VP2/VP3 inserts into the central cavity of a VP1 pentamer and binds to it through hydrophobic interactions (Chen *et al.*, 1998). The stoichiometric ratio of VP2 to VP3 is not equal, the underlying reason remaining unknown, and they exhibit uneven distribution (Bennett *et al.*, 2012). Both minor capsid proteins are expressed from the same late mRNA and VP3 is translated from the second in-frame initiation codon of VP2 (Fang *et al.*, 2010). Therefore, two-thirds of the C-terminal sequence of VP2 is identical to the VP3 sequence. In addition, VP2 has a unique N-terminal sequence which contains a putative myristoylation site at Gly-2 (Streuli and Griffin, 1987). However, Fang *et al.* (2010) were unable to detect this modification in BKPyV VP2 by mass spectrometry. The C-terminal region of VP2 and VP3 contains the VP1-binding region, a DNA-binding region and an NLS (Henriksen *et al.*, 2016) (Figure 1.9). A previously uncharacterised VP1-VP2/3 binding interface has also been explored by Kane *et al.* (2020) during studies which identified a potent antiviral VP2/VP3-derived peptide capable of binding within the upper pore of VP1 pentamers. The minor capsid proteins are not required for viral assembly nor does their removal influence

virion stability, however, they are essential in producing infectious progeny (Daniels *et al.*, 2006; Teunissen *et al.*, 2013). In fact, VP2-, VP3- or VP2/VP3-deficient BKPyV mutants resulting from start codon substitutions display over 99% reduction in their infectivity compared to wild-type virus (Henriksen *et al.*, 2016). An additional feature suggested as a requirement for *in vitro* BKPyV propagation is phosphorylation of VP2 at Ser-254 (Chen *et al.*, 2011). Upon site-directed mutagenesis of this phosphorylation site, LT-Ag expression was barely detected following transfection of the VP2-S254A mutant. Notably, the same study showed that phosphorylation of VP1 Ser-80 was also essential for virus growth.

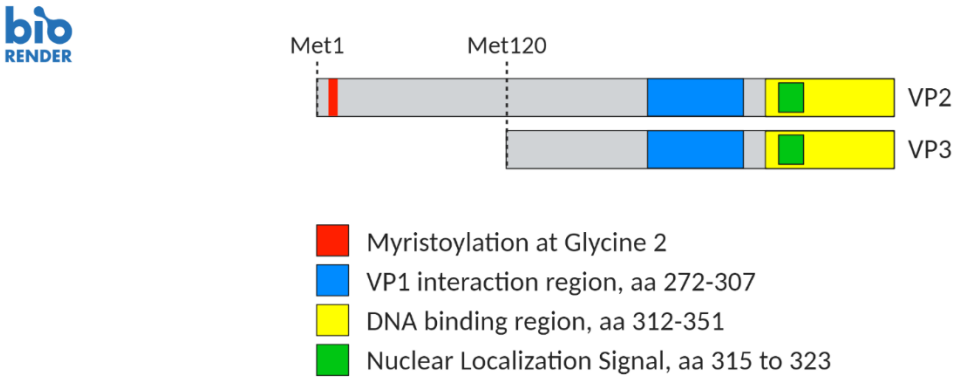

Figure 1.9 The BKPyV minor capsid proteins. Schematic overview of the BKPyV minor capsid protein VP2 and its truncated variant, VP3. Regions and motifs are annotated according to the UniProtKB database, accession number P03094**.**

1.4.4 Agnoprotein

BKPyV agnoprotein is an 8 kDa non-structural, basic protein and its amino acid sequence is >50% homologous with that of JCPyV and SV40 (Gerits and Moens, 2012). Following its expression during the late phase of the BKPyV life cycle, agnoprotein mainly localises in the perinuclear area as evidenced by immunoperoxidase staining (Rinaldo *et al.*, 1998). Unterstab *et al.* (2010) investigated the subcellular localisation of agnoprotein in more detail using confocal laser scanning microscopy to screen cellular markers. The authors found that agnoprotein interacts with lipid droplets through an amphipathic helix

formed by amino acids 20 to 42. The helix-containing region from JCPyV, BKPyV and SV40 agnoproteins is a Leu/Ile/Phe-rich domain which is involved in forming highly stable dimers and oligomers, the functions of which have yet to be elucidated (Saribas *et al.*, 2016) (Figure 1.10).

BKPyV agnoprotein is phosphorylated by Protein Kinase C (PKC), PKA and PKD as demonstrated *in vitro* by Johannessen *et al.* (2008). Both PKC and PKD can phosphorylate agnoprotein at Ser-7, Ser-11 and Thr-21, while Ser-11 is the only phosphor-acceptor site for PKA. Furthermore, PKC was implicated in the phosphorylation of Ser-11 *in vivo*. The phosphorylation levels of Ser-11 fluctuated during viral propagation, leading the authors to suggest a critical role for the phosphorylation pattern at this site. While mutating Ser-11 to alanine or aspartate impedes viral propagation and destabilises agnoprotein, it has no effect on the co-localisation with lipid droplets (Johannessen *et al.*, 2008; Unterstab *et al.*, 2010).

Agnoprotein has been implicated in various stages of the polyomavirus life cycle, including acting as a viroporin, facilitating virion assembly or as an egress factor from the nucleus (Ng *et al.*, 1985; Suzuki *et al.*, 2010; Panou *et al.*, 2018). There is evidence in support of agnoprotein playing an important, yet not critical, role in the BKPyV life cycle. An agnoprotein-deficient (ΔAgno) BKPyV generated through a point mutation in the gene start codon was found to still be infectious in Vero and RPTE cells, albeit to a lower degree compared to wild-type virus (Johannessen *et al.*, 2008; Panou *et al.*, 2018). Similar to what has been shown for ΔAgno BKPyV, some BKPyV strains with an NCCR deletion including the 5’ end of the agnoprotein sequence cannot release progeny virions into the extracellular environment (Myhre *et al.*, 2010). The authors proved that virion production and release could be rescued through reconstruction of the agnogene in cis or by providing agnoprotein in trans through co-infection with rearranged BKPyV. Together these findings suggested that agnoprotein could play a role in assembly, maturation and/or release of infectious virions.

It has been shown that JCPyV agnoprotein promotes translocation of virions out of the nucleus by binding heterochromatin protein 1 alpha (HP1-α) (Okada *et al.*, 2005). This results in dissociation of HP1-α from the lamin B receptor (LBR) in the inner nuclear membrane, which in turn perturbs the nuclear envelope.

The N-terminal 24 amino acids involved in disrupting the interaction between HP1-α and LBR are highly homologous to that of BKPyV agnoprotein. Therefore, Okada *et al.* (2005) speculated that BKPyV agnoprotein may also be involved in destabilising the nuclear membrane to facilitate progeny release from the nucleus. Myhre *et al.* (2010), however, did not observe co-localisation of BKPyV agnoprotein with either HP1-α or lamin A/C in RPTE cells. In infected cells, lamin A/C and HP1-α staining was nuclear while the agnoprotein was localised exclusively in the cytoplasm. The authors concluded that the role of the agnoprotein as a nuclear egress factor in the BKPyV life cycle does not depend on interactions with lamin A/C or HP1-α in the nuclear membrane.

A subset of host cellular proteins co-immunoprecipitate with agnoprotein (Rinaldo *et al.*, 1998). Through a yeast two-hybrid assay, α-soluble N-ethylmaleimide-sensitive fusion attachment protein (α-SNAP) was identified as an interacting partner of BKPyV agnoprotein and the N-terminal 38 amino acids of the viral protein are predominantly required for this interaction (Johannessen *et al.*, 2011). The interaction between α-SNAP and agnoprotein is essential in shuttling BKPyV virions out of the nucleus (Panou *et al.*, 2018). In addition, BKPyV agnoprotein interacts with proliferating cell nuclear antigen (PCNA) to prevent DNA replication (Gerits *et al.*, 2011). Therefore, agnoprotein may serve to switch off viral replication during the late stages of infection in order to allow for virion assembly to take place. BKPyV agnoprotein may also be involved in impairing DNA repair activity following DNA damage as has been shown for JCPyV agnoprotein (Darbinyan *et al.*, 2004). Furthermore, Gosert *et al.* (2008) demonstrated that the agnoprotein negatively regulates early and late viral gene expression through use of a bi-directional reporter vector controlled by the NCCR of BKPyV. In agreement with their results, ΔAgno BKPyV expresses increased levels of VP1 and LT-Ag compared to wild-type infection (Johannessen *et al.*, 2008; Panou *et al.*, 2018).

More recently, agnoprotein has been implicated in the evasion of innate immune sensing during BKPyV infection of RPTE cells (Manzetti *et al.*, 2020). Agnoprotein was seen co-localising with mitochondria, which play a key role in innate immunity, to induce mitochondrial fragmentation during the late phase of infection (Koshiba *et al.*, 2011; Manzetti *et al.*, 2020). Importantly, agnoprotein-disrupted mitochondria were targeted for mitophagy. Moreover, nuclear

translocation of interferon regulatory factor 3 (IRF3) and interferon-β (IFN-β) expression was prevented in the presence of agnoprotein, thereby, supporting that agnoprotein expression impairs cytosolic innate immune sensing. Disruption of the mitochondrial network also occurs for JCPyV and SV40, suggesting this is an evolutionary conserved function for agnoproteins.

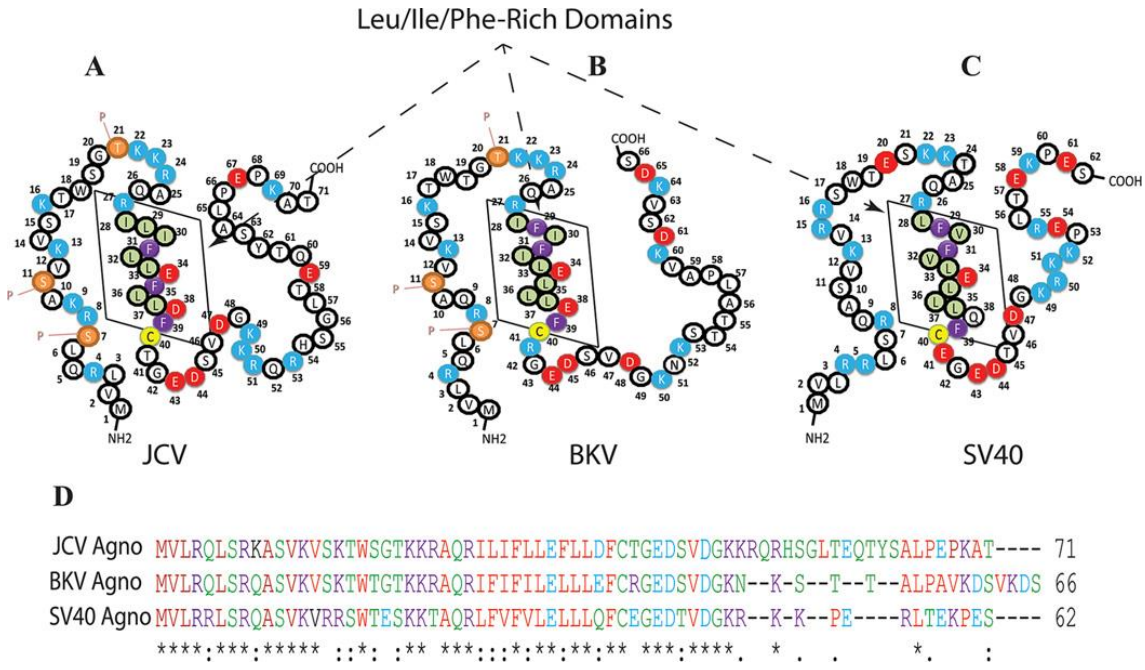

Figure 1.10 JCPyV, BKPyV and SV40 agnoproteins. A-C) The primary structures of JCPyV, BKPyV and SV40 agnoproteins, respectively. The Leu/Ile/Phe-rich domain of each protein is indicated by a box. Sites of phosphorylation are designated by the red letter 'P'. D) Alignment of the amino acid sequence of the three agnoproteins. Obtained from Saribas *et al.* (2016).

1.4.5 Viral microRNA (miRNA)

BKPyV and JCPyV encode a pre-miRNA hairpin molecule, which is processed into two mature miRNAs; 5p-miRNA and 3p-miRNA (Seo *et al.*, 2008). Both BKPyV and JCPyV miRNAs are homologous to SV40 miRNAs and all are perfectly complementary to their respective early viral mRNAs. Sullivan *et al.* (2005) first defined a function for SV40 miRNAs, by showing accumulation of miRNAs at late stages of infection and cleavage of SV40 early mRNA by Northern blot analysis. The authors proposed that the two miRNAs, processed

from each arm of the pre-miRNA hairpin, were active against the same target to result in cleavage of the early viral transcripts. In turn, downregulation of T-antigens could potentially promote CTL evasion by infected cells. SV40 miRNAs share this conserved autoregulatory function with BKPyV and JCPyV miRNAs (Seo *et al.*, 2008). In their study, Seo *et al.* (2008) demonstrated that miRNAs encoded by these HPyVs also direct the cleavage of the early viral transcripts and JCPyV miRNAs were shown to downregulate LT-Ag expression during the late stages of infection. Furthermore, JCPyV miRNAs were detected in PML lesions from deceased patients, indicating that these miRNAs are expressed *in vivo*.

Later studies evaluated the functional role of miRNA from archetype BKPyV in RPTE cells. By creating a flipped NCCR structure mutant, Broekema and Imperiale (2013) showed that miRNA expression is dictated by the balance of NCCR regulatory elements. Viral miRNAs regulated early mRNA targets and, in fact, limited viral replication in RPTE cells. Tian *et al.* (2014) further demonstrated that suppression of viral replication by miRNA is through inhibition of LT-Ag-mediated autoregulation. Furthermore, these findings implicate viral miRNAs in the mechanism of BKPyV persistence. In archetype virus, miRNAs are robustly expressed to limit DNA replication. In contrast, miRNA expression from rearranged variants is low and, thus, cannot regulate early mRNAs sufficiently (Broekema and Imperiale, 2013).

Importantly, BKPyV and JCPyV miRNAs can target cellular genes. In particular, 3p-miRNA – which is identical in sequence between JCPyV and BKPyV – targets the stress-induced ligand ULBP3 (Bauman *et al.*, 2011). ULBP3 is a ligand of the activating receptor, NKG2D, expressed on immune cells such as natural killer (NK) cells and various T cell subsets (Sutherland *et al.*, 2006; Wensveen *et al.*, 2018). By downregulating ULBP3, viral miRNAs contribute to a reduction in NKG2D-mediated elimination of infected cells by immune cells. Hence, the authors postulated that by preventing NKG2D-mediated detection, JCPyV and BKPyV can evade both innate and adaptive immune responses. Therefore, miRNAs may have a critical role in achieving and maintaining viral persistence (Broekema and Imperiale, 2013).

1.5 The BKPyV life cycle

Understanding the viral life cycle within natural cell targets of BKPyV is essential to improve the management of BKPyV-associated diseases. Moreover, it may expand our knowledge of innate immune components which may be involved in BKPyV infection and may offer potential intervention targets. A number of different cell types and organs throughout the body are permissive to BKPyV infection (section 1.3.2). However, the most commonly used cell types to study the viral life cycle are of renal epithelial origin, as the virus mainly reactivates and replicates within the kidneys and urinary tract.

For successful infection to take place, a virion must first attach to the host cell surface, interact with a functional receptor to become internalised and, for DNA viruses, the viral genome must be delivered to the nucleus. Each stage in the BKPyV life cycle is discussed in more detail below.

1.5.1 Receptor binding

Polyomavirus infections are generally dependent on interactions between VP1 and cell surface glycans carrying sialic acid residues (Bhattacharjee and Chattaraj, 2017). Gangliosides are glycosphingolipids containing one or more sialic acid residue(s), such as N-acetylneuraminic acid or N-glycolylneuraminic acid, in their carbohydrate moiety (Figure 1.11). Glycosphingolipids are composed of one or more carbohydrate residues linked to either a sphingoid or a ceramide hydrophobic lipid moiety through a glycosidic linkage (Yu *et al.*, 2011). Stehle and Harrison (1996) determined the crystal structure of a recombinant MPyV VP1 pentamer with a branched-chain receptor fragment. The high resolution work revealed that there are two surface grooves on MPyV which are critical for recognising α2,3-linked sialic acid on the surface of susceptible cells (pockets 1 and 2). In addition, some MPyV strains could also bind branched oligosaccharides bearing α2,6-linked sialic acid through a third pocket (Stehle and Harrison, 1996, 1997). Flotation studies later defined the specific gangliosides acting as receptors; GD1a and GT1b for MPyV and GM1 for the structurally related SV40 (Tsai *et al.*, 2003). Antibodies directed at α4β1 integrin inhibit a post-attachment step in MPyV infection, demonstrating that this integrin dimer acts as a co-receptor for MPyV, while SV40 utilises major

histocompatibility complex (MHC) class I molecules to facilitate its attachment (Caruso *et al.*, 2003; Atwood and Norkin, 1989).

Combined with knowledge about MPyV and SV40 receptor usage, one of the first observations to indicate a role for gangliosides in BKPyV infection, was that haemagglutination of human erythrocytes by BKPyV is sensitive to neuraminidase treatment (Mantyjarvi *et al.*, 1972). Furthermore, haemagglutination by BKPyV can be attenuated through pre-incubation with soluble gangliosides (Sinibaldi *et al.*, 1987). Initial studies to define the receptors for BKPyV were performed in the monkey-derived kidney cell line, Vero cells. Neuraminidase- and sialidase S-treated Vero cells were challenged with virus and BKPyV infection was scored at 48 hours post-infection (Dugan *et al.*, 2005). Sialidase S removes α2,3-linked sialic acid from glycoproteins and complex carbohydrates, while neuraminidase cleaves both α2,3- and α2,6-linked sialic acid from glycoproteins, gangliosides and complex carbohydrates. Selective cleavage of α2,3-linked sialic acids by either enzyme inhibited infection, suggesting a role for α2,3-linked sialic acids during BKPyV infection. Subsequently, Low *et al.* (2006) identified the specific ganglioside receptors through sucrose floatation assays using ganglioside-containing liposomes and purified BKPyV. Interactions between BKPyV and liposomes containing ganglioside GD1b or GT1b, were strong enough to enable flotation of the virus. Importantly, exogenous addition of GD1b and GT1b allows for infection of LNCaP cells which are naturally non-permissive to BKPyV (Low *et al.*, 2006). Many of these observations have been repeated in the more relevant cell culture model of RPTE cells. Using small interfering RNA (siRNA) to silence UDP-glucose ceramide glucosyltransferase (UGCG), which catalyses the first step in ganglioside synthesis, Zhao *et al.* (2016) confirmed previous findings of BKPyV requiring GD1b and GT1b as receptors for entering RPTE cells.

A terminal α2,8-linked disialic acid motif present in GD1b and GT1b gangliosides has been suggested to be important for the interaction between the virus and its receptors (Low *et al.*, 2006). By determining the structure of BKPyV bound to the oligosaccharide moiety of ganglioside GT1b at 3.4 Å resolution, Hurdiss *et al.* (2018) were able to resolve the disialic acid motif located on the GT1b right arm (Figure 1.12A). Importantly, there was no detectable conformational change in VP1, indicating that the receptor functions

to increase the avidity of virus attachment to the cell surface. Furthermore, N-linked glycoproteins consisting of α2,3-linked sialic acid may act as host co-receptors for BKPyV infection, however, further investigation is required to define specific co-receptors for BKPyV (Dugan *et al.*, 2005; Ambalathingal *et al.*, 2017).

The use of gangliosides as receptors for entering a target cell is a common feature of most polyomaviruses (Table 1.3). JCPyV engages multiple sialic acid-containing structures, including GT1b, GD1b and GD2 as identified by enzyme-linked immunosorbent assay (ELISA) (O'Hara *et al.*, 2014). In addition, JCPyV interacts with the linear sialylated pentasaccharide lactoseries tetrasaccharide c (LSTc) as determined through a glycan array screening (Neu *et al.*, 2010). The serotonin 5-hydroxytryptamine 2A receptor ($5HT_{2A}R$) facilitates JCPyV infectious entry as indicated in inhibitor and overexpression studies (Maginnis *et al.*, 2010; Assetta *et al.*, 2013). In contrast, cellular entry of JCPyV in human brain microvascular endothelial cells (VEC) appears to be independent of $5HT_{2A}R$ (Chapagain *et al.*, 2007).

Crystal structures of recombinantly expressed VP1 proteins of HPyV6 and HPyV7 indicated that these two viruses may engage non-sialylated cellular receptors for host cell recognition. This is likely due to an obstruction of the groove normally involved in binding sialic acid-bearing glycan receptors (Stroh *et al.*, 2014). Erickson *et al.* (2009) identified GT1b as a putative host cell receptor for MCPyV using VP1 pentameric capsomeres in a flotation assay and determined that the sialic acids on both arms of the ganglioside are required for binding VP1. Further work revealed that sialylated glycans are, in fact, not required for the initial interaction of MCPyV virions with cultured cells but may be required as co-receptors in a post-attachment entry step (Schowalter *et al.*, 2011). Instead, the authors presented compelling evidence of the requirement for sulphated glycosaminoglycans (GAGs), particularly heparan sulphate, in mediating the interaction of MCPyV with the host cell surface. Interestingly, heparin or heparan sulphate-blocking antibodies prevent cellular entry of PML-mutant JCPyV and of a sialic acid non-binding mutant BKPyV, hinting that sialylated glycan-independent infectious entry pathways may also exist for JCPyV and BKPyV, as shown for MCPyV infection (Schowalter *et al.*, 2011; Bhattacharjee and Chattaraj, 2017). In fact, during the investigation of Hurdiss

et al. (2018) into non-sialylated GAGs acting as receptors for BKPyV infection, density – ascribed to heparin – was observed between the capsomeres and above each capsomere pore (Figure 1.12B). This observation suggests a GAG interaction with the BKPyV capsid.

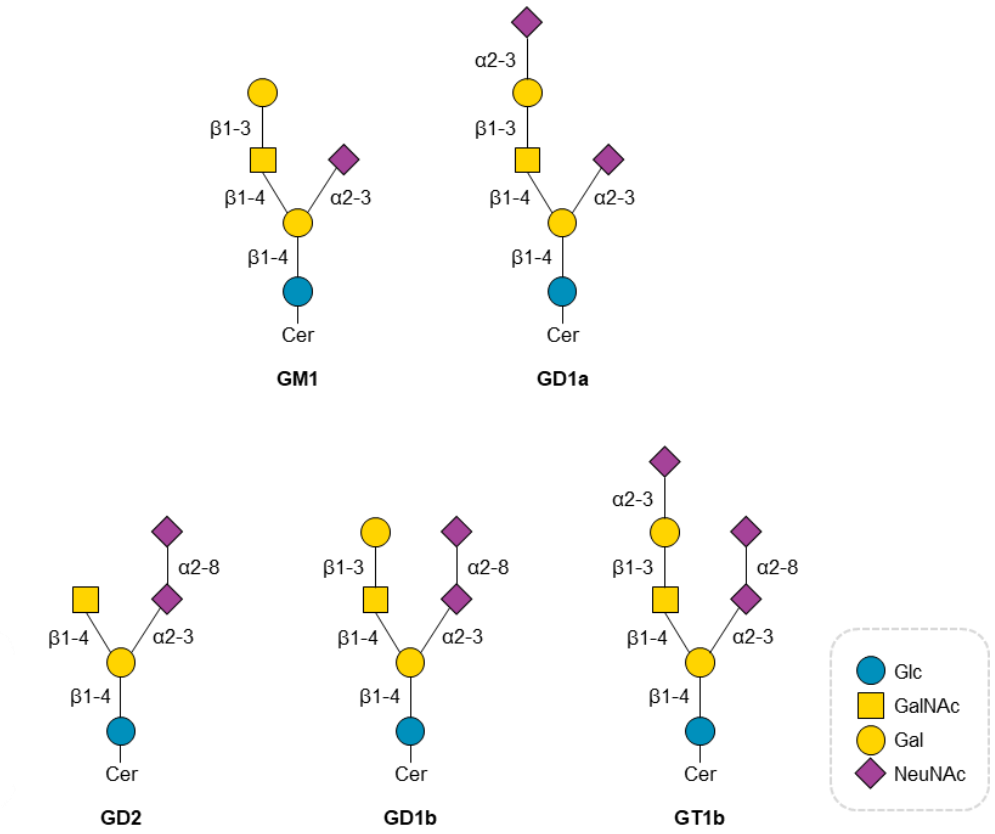

Figure 1.11 Gangliosides involved in polyomavirus binding. Symbol Nomenclature for Glycans (SNFG)-representation of oligosaccharides used as receptors by polyomaviruses (Varki *et al.*, 2015). Host glycans are anchored to the cell membrane through linkage to glycosphingolipids (Cer: ceramide). Glc: Glucose, GalNAc: N-acetylgalactosamine, NeuNAc: N-acetylneuraminic acid, Gal: Galactose.

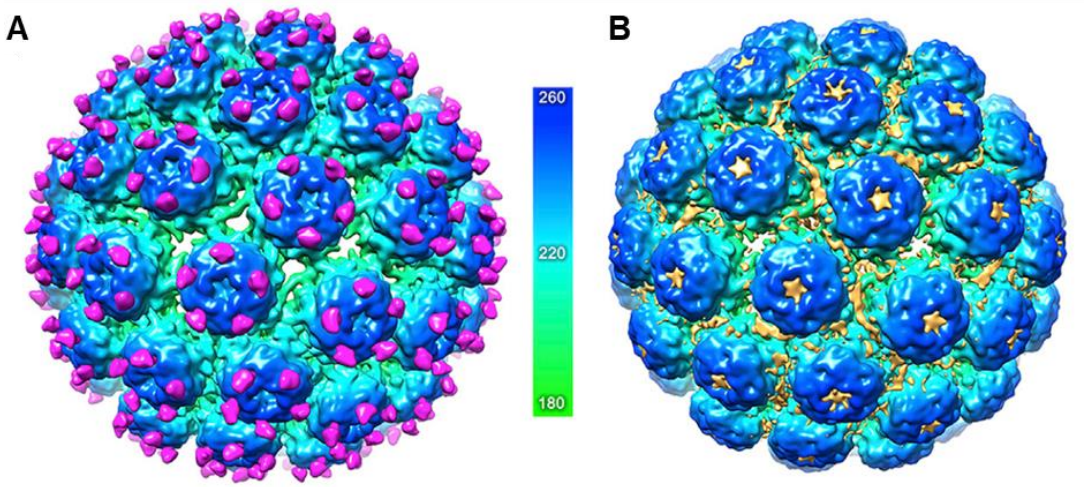

Figure 1.12 Interaction of BKPyV with GT1b and Heparin. The unsharpened and 8 Å low-pass-filtered representations of the BKPyV-GT1b (A) and BKPyV-heparin (B) maps. Structures are coloured according to the radial colouring scheme shown (Å). A) The GT1b difference density (3.4 σ) is coloured in magenta. B) The putative heparin difference density (3.4 σ) is shown in orange. Obtained from Hurdiss *et al.* (2018).

Table 1.3 Receptor and co-receptor usage of polyomaviruses. Adapted from O'Hara *et al.* (2014).

Virus	Receptor	Co-receptor
MPyV	GD1a, GT1b	α4β1-Integrin
SV40	GM1	MHC-I
BKPyV	GD1b, GT1b	Unknown
JCPyV	LSTc, GD1b, GT1b, GD2	$5HT_{2A}R$
MCPyV	Glucosaminoglycans (GAGs)	Unknown

1.5.2 Internalisation

Viruses exploit the various pinocytic mechanisms of endocytosis to become internalised into the cell. Clathrin-mediated endocytosis, macropinocytosis and caveolae/lipid raft-mediated endocytosis are the main well-characterised pathways of internalisation (Mercer *et al.*, 2010). Both clathrin-mediated and caveolae-mediated endocytosis involve the formation of plasma membrane invaginations termed clathrin-coated pits or caveolae, respectively. Clathrin is the main structural component of clathrin-coated pits and is a trimer of three heavy chains, each with an associated light chain (Ungewickell and Branton, 1981). Clathrin proteins are recruited around membrane invaginations by adaptor proteins, while dynamin self-assembles around the neck of these coated pits to catalyse membrane fission giving rise to clathrin-coated vesicles (Mettlen *et al.*, 2009). The caveolin family of integral membrane proteins is associated with caveolae and is comprised of caveolin-1 (Cav-1), -2 and -3. Caveolin-1 and -2 are present in most non-muscle cell types, excluding neurons and leukocytes, while caveolin-3 is muscle cell-specific (Doherty and Mcmahon, 2009). Cav-1 is the only caveolin required for caveolae formation as disruption of its gene in mice leads to loss of caveolae amongst other defects (Drab *et al.*, 2001).

Following adsorption to the cell surface via the b-series gangliosides, the BKPyV virion enters the host cell through a partially elucidated internalisation pathway involving caveolin-dependent or caveolin-independent endocytosis. By investigating the ability of the virus to escape antibody-mediated neutralisation, Eash *et al.* (2004) showed that the majority of BKPyV enters Vero cells between 2 and 4 hours after infection. Blocking clathrin-mediated endocytosis using dominant-negative Eps15 constructs had no effect on BKPyV infection. In contrast, cells transfected with a Cav-1 mutant were less susceptible to infection. Moreover, depletion of cholesterol resulted in inhibition of infection, demonstrating a role for caveola-mediated endocytosis for BKPyV uptake in Vero cells. BKPyV was shown to co-localise with the caveola-mediated endocytosis marker, cholera toxin subunit B, but not with the clathrin-dependent endocytosis marker, transferrin. Internalisation depends upon an intact microtubule network since nocodazole-induced disassembly of tubulin polymers impeded normal virus trafficking (Eash and Atwood, 2005).

Evidence exists for both caveolae-dependent and caveolae- and clathrin-independent pathways for BKPyV internalization into RPTE cells. Moriyama *et al.* (2007) were able to recapitulate previous findings from Vero cells in RPTE cells and used labelled BKPyV to show co-localisation with Cav-1. Depletion of either Cav-1 or clathrin by siRNA revealed that only Cav-1 siRNA inhibited BKPyV infection. The authors concluded that in RPTE cells, BKPyV internalisation occurs via caveolin-mediated endocytosis and not through clathrin-coated pits. Both MPyV and SV40 reportedly use caveolae-mediated endocytosis to enter host cells, while JCPyV enters glial cells through clathrin-dependent receptor-mediated endocytosis (Richterová *et al.*, 2001; Pelkmans *et al.*, 2001; Pho *et al.*, 2000). Subsequent studies showed that SV40 can also utilise caveolae-independent entry pathways in cells devoid of Cav-1 (Damm *et al.*, 2005).

More recent work from Zhao *et al.* (2016), proposed that viral entry in RPTE cells may involve a caveolin- and clathrin-independent endocytosis. Silencing either process by siRNA knockdown of Cav-1, Cav-2 or clathrin heavy chain did not affect BKPyV infection of RPTE cells. The authors postulate that BKPyV gains entry into its natural host cells via an unknown endocytic pathway. ARF6-, RhoA/Rac1-, flotillin- and Cdc42-mediated endocytosis could potentially assist BKPyV in gaining entry into RPTE cells (Radhakrishna and Donaldson, 1997; Lamaze *et al.*, 2001; Glebov *et al.*, 2006; Chadda *et al.*, 2007). However, most of these endocytic pathways have been associated with actin polymerisation, which is not required for BKPyV entry (Doherty and Mcmahon, 2009; Eash and Atwood, 2005). Therefore, Zhao *et al.* (2016) hypothesised that BKPyV is more likely to enter RPTE cells via a yet uncharacterised endocytic pathway.

BKPyV entry may rely on protein-independent endocytic pathways, such as lipid-mediated endocytosis. Bacia *et al.* (2005) used artificial liposomes containing cholesterol and GM1, termed giant unilamellar vesicles (GUVs), to demonstrate formation of caveolae-like vesicles which do not require addition of host proteins. Furthermore, SV40 was shown to induce membrane curvature on GUVs and the extracellular side of cells through multivalent binding of its VP1 pentamers to cell surface GM1 (Ewers *et al.*, 2010). BKPyV may enter cells in a similar manner by engaging gangliosides with its VP1 proteins to induce vesicle membrane invaginations which are stabilised by cholesterol (Zhao *et al.*, 2016).

Due to discrepant observations regarding the entry of BKPyV, further investigation is required to define its mode of internalisation.

1.5.3 Intracellular trafficking

Following endocytosis, BKPyV particles remain associated with caveolae at the cell surface up to 4 hours post-infection, as observed in co-localisation studies with Cav-1 (Moriyama *et al.*, 2007). While BKPyV infection of RPTE cells proceeds relatively slowly, SV40 and MPyV co-localise with Cav-1 at 0.5 hours after infection of CV-1 and C6 rat glioma cells, respectively (Gilbert and Benjamin, 2004; Engel *et al.*, 2011). Ultrastructural analysis of renal transplant biopsies indicated association of BKPyV with caveosome-like structures (Drachenberg *et al.*, 2003). However, caveosomes are endosomal compartments with neutral pH, whereas BKPyV infection is pH-dependent, indicating that BKPyV may enter an acidic compartment during intracellular trafficking (Jiang *et al.*, 2009).

BKPyV infection was assessed in Vero cells in the presence of lysosomotropic agents, such as chloroquine and ammonium chloride (NH_4Cl), which disrupt the acidification of intracellular organelles (Eash *et al.*, 2004). Treatment with either lysosomotropic agent inhibited infection, indicating that BKPyV entry in Vero cells requires a low pH step during its life cycle. A parallel experiment with SV40 demonstrated that these compounds had no effect on infection of Vero cells, concurring with previous findings of SV40 trafficking from caveolae through caveosomes to the ER and that its infection does not rely on an acidification step (Pelkmans *et al.*, 2001; Ashok and Atwood, 2003). The model of SV40 entry has since been revised to include the endosomal entry of SV40 in CV-1 cells (Engel *et al.*, 2011). Using NH_4Cl to elevate the pH of acidic cellular compartments in RPTE cells, Jiang *et al.* (2009) provided further evidence of BKPyV requiring an acidic environment during the first 2 hours of infection. Therefore, similar to MPyV, JCPyV and SV40, BKPyV likely enters endosomes following endocytosis (Liebl *et al.*, 2006; Querbes *et al.*, 2006; Engel *et al.*, 2011).

Based on transmission electron microscopy of infected tissue samples, BKPyV virions traffic to smooth tubular structures which communicate with the rough endoplasmic reticulum (ER) and are continuous with the Golgi system

(Drachenberg *et al.*, 2003). Brefeldin A (BFA) and retro-2^{cycl} which inhibit retrograde transport to the ER, block BKPyV infection in RPTE cells suggesting that BKPyV virions move to the ER compartment on their way to the nucleus (Low *et al.*, 2006; Jiang *et al.*, 2009; Nelson *et al.*, 2013). Furthermore, the use of ER and Golgi apparatus markers in co-localisation studies indicated that BKPyV reached the ER of RPTE cells between 6 to 12 hours post-infection (Moriyama and Sorokin, 2008). In the same study, BKPyV could not be detected in the Golgi apparatus, suggesting that it either bypasses this organelle or passes through too rapidly to be detected. Trafficking to the ER is not a unique requirement by BKPyV as SV40 and MPyV, which use the same class of receptor molecules for entry, also transit to the ER before entering the nucleus (Norkin *et al.*, 2002; Gilbert and Benjamin, 2004).

Several studies have demonstrated that BKPyV relies on being transported along microtubules to reach the ER. Nocodazole-induced disassembly of the microtubule network in Vero and RPTE cells results in decreased levels of BKPyV infection (Eash and Atwood, 2005; Moriyama and Sorokin, 2008; Jiang *et al.*, 2009). To the contrary, an intact actin cytoskeleton is not required for BKPyV intracellular transport, as disruption of actin filaments with latrunculin A did not impede infection of Vero cells (Eash and Atwood, 2005). While BKPyV movement is independent of microtubule motor protein dynein activity, conflicting results exist regarding the role of microtubule dynamics following internalisation (Eash and Atwood, 2005; Moriyama and Sorokin, 2008). Following paclitaxel treatment of RPTE cells to disrupt microtubules dynamics, Moriyama and Sorokin (2008) observed a significant decrease in the percentage of BKPyV-infected cells compared to control cells. Therefore, the dynamics of microtubules have an important role in transporting BKPyV in RPTE cells, but not in Vero cells (Eash and Atwood, 2005).

Recent efforts have focused on the identification of key components involved in BKPyV trafficking from the late endosome to the ER. Zhao and Imperiale (2017) implemented a whole human genome small interfering RNA (siRNA) screen on BKPyV-infected RPTE cells to reveal the importance of Rab18, syntaxin 18 and the NRZ complex in the endosome-ER trafficking of BKPyV. Ras-related protein Rab-18 is involved in lipid droplet homeostasis and has a role in retrograde vesicle-mediated transport from the Golgi apparatus to the ER (Dejgaard *et al.*,

2008). The majority of Rab-18 localises in the membranes of cis-Golgi and ER, however, it is also recruited to endosomes, lysosomes and lipid droplets (Dejgaard *et al.*, 2008; Zhang *et al.*, 2016). In addition to syntaxin 18, Rab18 interacts with ZW10 kinetochore protein and RAD50 interactor 1 (RINT1) as identified by Gillingham *et al.* (2014) using affinity chromatography followed by mass spectrometry. ZW10 and RINT1 interact with each other via their N termini and, together with neuroblastoma amplified gene (NAG), compose the NRZ complex (Arasaki *et al.*, 2006). Syntaxin 18 is an ER-localised t-SNARE protein which interacts with the NRZ complex indirectly to form a protrusion from the surface of the ER membrane (Aoki *et al.*, 2009; Zhao and Imperiale, 2017). Importantly, syntaxin 18 mediates vesicle fusion with the ER membrane upon interaction of ZW10 with GTP-activated Rab18 on the surface of vesicles (Iinuma *et al.*, 2009).

Silencing of Rab18 or syntaxin 18 decreased LT-Ag expression, providing evidence of both host proteins playing a critical role in BKPyV infection (Zhao and Imperiale, 2017). Furthermore, the disruption of the NRZ complex through siRNA knockdown of RINT1 and ZW10 also interfered with BKPyV infection. The role of Rab18 in targeting vesicles to the ER led to the authors to assess co-localisation of Rab18 and BKPyV-containing vesicles. Between 6 and 8 hours post-infection, VP1 was seen co-localised with Rab18 by confocal microscopy, indicating that Rab18 co-localises with the viral capsid during virus intracellular trafficking. In the absence of Rab18, BKPyV accumulated in late endosomes. These findings suggest that, upon sorting through endosomes, BKPyV travels in Rab18-positive vesicles to the ER along microtubules. The NRZ complex captures and tethers BKPyV-containing vesicles to the ER surface, with syntaxin 18 mediating vesicle fusion with the ER membrane through an unidentified v-SNARE. Thus, BKPyV is able to enter the ER lumen via this late-endosome-to-ER trafficking step (Helle *et al.*, 2017; Zhao and Imperiale, 2017) (Figure 1.13).

While the details of Rab18-mediated retrograde transport of BKPyV to the ER have yet to be fully elucidated, other pathways may also be involved in BKPyV intracellular trafficking. Autophagy inhibitors or siRNA knockdown of autophagy genes, ATG7 and Beclin-1, impede BKPyV infection early in the viral life cycle (Bouley *et al.*, 2014). Together, these findings suggested that induction of

autophagy promotes BKPyV infection. In contrast, autophagy acts an anti-viral process during JCPyV infection (Sariyer *et al.*, 2012). Recently, the role of the chloride ion channel, cystic fibrosis transmembrane conductance regulator (CFTR), has been explored during the early stages of infection (Panou *et al.*, 2020). CFTR is likely involved in the trafficking of BKPyV to the ER as evidenced by time-of-addition assays using pharmacological inhibitors.

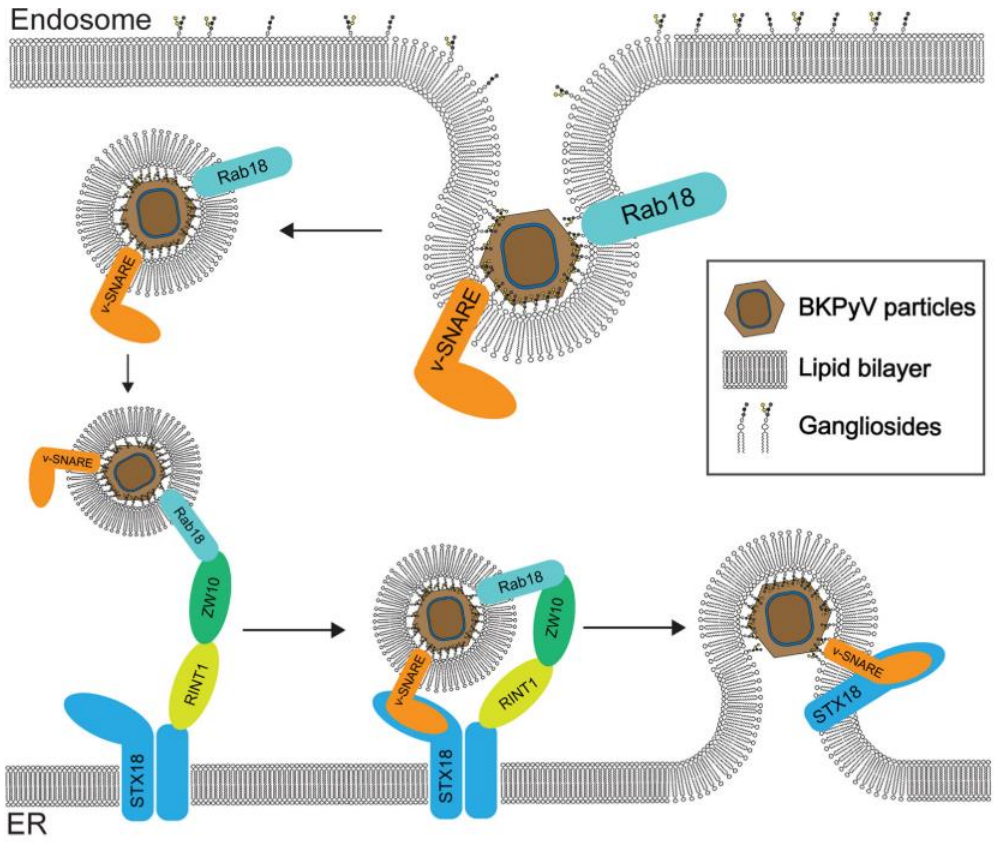

Figure 1.13 Schematic of model for BKPyV vesicular trafficking. BKPyV enters a vesicle from the membrane of the endosome. GTP-bound Rab18 interacts with the ZW10 component of the NRZ complex. Syntaxin 18 on the ER membrane interacts with v-SNARE on the transport vesicle to mediate vesicle fusion. BKPyV enters the ER lumen. Obtained from Zhao and Imperiale (2017).

1.5.4 Capsid uncoating and nuclear entry

Trafficking through the ER prior to reaching the cytosol is unique to DNA viruses and is a requirement by all polyomaviruses (Bennett *et al.*, 2012). The ER contains chaperones, disulphide isomerases and reductases creating a favourable environment for capsid disassembly to take place to enable nuclear entry of the viral genome (Ellgaard *et al.*, 2018). Disintegration of the extensive disulphide bond network in the BKPyV capsid begins at about 8 to 12 hours post-infection (Jiang *et al.*, 2009). Disruption of transport to the ER affects disulphide bond isomerization and VP1 cleavage pattern, suggesting that BKPyV capsid rearrangement may occur prior to trafficking to the ER.

More recently, Inoue *et al.* (2015) identified ERdj5 as an ER reductase which promotes BKPyV infection. By cooperating with Protein Disulphide Isomerase (PDI), ERdj5 reduces BKPyV disulphide bonds to facilitate BKPyV infection. In the same study, ERdj5 was shown to regulate SV40 ER-to-cytosol transport. ERdj5 disrupts the disulphide bonds, while PDI likely unfolds SV40. These two events induce structural changes rendering the viral particle hydrophobic and enabling its interaction with the ER membrane protein BAP31. Upon binding to BAP31, SV40 can penetrate the ER membrane to enter the cytosol.

Polyomaviruses exploit the ER-associated protein degradation (ERAD) machinery to penetrate the ER membrane and reach the cytosol before nuclear entry (Lilley *et al.*, 2006; Schelhaas *et al.*, 2007; Geiger *et al.*, 2011; Goodwin *et al.*, 2011). The ERAD machinery is a mechanism of ER quality control through which misfolded proteins in the ER are retro-translocated into the cytosol to be degraded by the ubiquitin-proteasome system (Smith *et al.*, 2011). Several proteins of the Hsp70, Hsp110, membrane J-protein or Derlin families are involved in the ERAD pathway. Through experiments with dominant negative constructs or siRNA knockdowns, the Derlin family of proteins was found to participate in the transportation of MPyV, SV40 and BKPyV out of the ER (Lilley *et al.*, 2006; Schelhaas *et al.*, 2007; Jiang *et al.*, 2009). Furthermore, the ERAD and proteasome inhibitors, Eeyarestatin I (EerI) and epoxomicin, prevent productive infection from occurring and result in accumulation of partially uncoated BKPyV virions with exposed VP2/VP3 in the ER (Bennett *et al.*, 2013). EerI targets the AAA-ATPase, p97, which functions upstream of the proteasome as a cytosolic component of the ERAD pathway, while epoxomicin

inhibits primarily the chymotrypsin-like activity, as well as the trypsin-like and peptidyl-glutamyl peptide hydrolysing activities of the proteasome (Wang *et al.*, 2008; Meng *et al.*, 1999). BKPyV infection remains sensitive to both inhibitors until 18 hours post-infection, which agrees with previous observations of BKPyV trafficking through the ER between 8 and 16 hours post-infection (Jiang *et al.*, 2009). These findings implicate the ERAD pathway along with the proteasome in facilitating BKPyV trafficking from the ER into the cytosol. However, neither inhibitor prevented BKPyV entry in the cytosol, as measured by the appearance of VP1 monomers in cytosolic fractions. Upon observation of a decrease in BKPyV genomes present in the cytosol following epoxomicin treatment to inhibit the proteasome, the authors proposed that some infectious particles may remain trapped in the ER, while VP1 protein reaches the cytosol. Furthermore, partial uncoating in the ER exposes VP2/VP3 to bind and likely integrate in the ER membrane to enable the release of partially disassembled virus into the cytosol (Rainey-Barger *et al.*, 2007; Goodwin *et al.*, 2011).

Prior to membrane penetration, the ER-resident Hsp70 family member, BiP, maintains hydrophobic BKPyV in a soluble state (Goodwin *et al.*, 2011; Inoue and Tsai, 2015). Knockdown studies showed that the release of the ER-localised BKPyV from BiP is triggered by Grp170, which converts ADP-BiP to ATP-BiP (Inoue and Tsai, 2015). Jiang *et al.* (2009) performed a pull-down assay to demonstrate that Derlin-1 interacts with VP1 to mediate the ER-to-cytosol transit of BKPyV. Subsequently, a cytosolic complex composed of Hsp105 and SGTA proteins is likely recruited to extract BKPyV from the ER into the cytosol (Walczak *et al.*, 2014; Ravindran *et al.*, 2015).

From the cytosol, the viral genome must be transported into the nucleus to gain access to the cellular DNA replication and DNA damage repair machinery, as polyomaviruses do not encode a DNA polymerase to replicate their genome. In investigating how BKPyV enters the nucleus, Bennett *et al.*, (2015) revealed that the NLS located on the minor capsid proteins VP2 and VP3 is essential in this process. Through the use of the inhibitor ivermectin and silencing of importin β1, the importin α/β canonical nuclear import pathway was found to be required for BKPyV nuclear entry. Therefore, these findings support a model whereby the exposed NLS of VP2/VP3 is bound by importin α/β to actively

transport the viral genome into the nucleus through the nuclear pore complex (Bennett *et al.*, 2015).

An alternative nuclear entry pathway has been proposed to exist along with the model involving import through the nuclear pore, as mutagenesis of the NLS only results in attenuation of infection (Bennett *et al.*, 2015). Furthermore, inhibition of the importin α/β nuclear import pathway leads to a 50% knockdown of infection. Therefore, it has been proposed that an alternative NLS sequence to the one studied by Bennett *et al.* (2015) may be used by BKPyV, as VP1 contains an NLS buried within the partially uncoated virion (Moreland and Garcea, 1991; Ishii *et al.*, 1996). Supporting the use of another viral NLS to still exploit the canonical import pathway, is the observation of ivermectin inhibiting the NLS-mutant virus to a similar extent as wild-type BKPyV (Bennett *et al.*, 2015). Alternatively, the viral particle may gain entry into the nucleus during mitosis when the nuclear envelope begins to break down, as shown for SV40 (Butin-Israeli *et al.*, 2011). In the same study, Butin-Israeli *et al.* (2011) provided evidence of SV40 nuclear entry in non-dividing cells through the induction of nuclear envelope deformation. Caspase-6 was required for the cleavage of lamin A/C fractions to trigger nuclear envelope breakdown. Through virus-induced alterations to the nuclear envelope, SV40 gains direct entry from the ER into the nucleus (Figure 1.14). The authors suggested that the similarity of BKPyV to SV40 may allow for the same nuclear entry pathway to be exploited by the former.

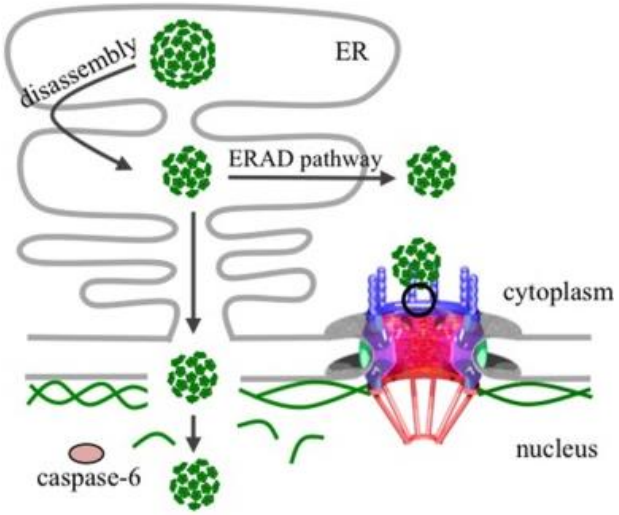

Figure 1.14 Strategies used by SV40 for nuclear entry of its genome. SV40 partially disassembles inside the endoplasmic reticulum (ER). To deliver the viral genome into the nucleus, the uncoated particles can exit the ER and enter the cytosol through the cellular ERAD pathway and the help of cellular chaperones. From the cytosol, further disassembly at the nuclear pore complex (NPC) allows the import of the uncoated genome through the NPC. Alternatively, SV40 may enter directly from the ER to the nucleus by inducing the breakdown of the nuclear envelope; a process involving caspase-6. Adapted from Fay and Panté (2015).

1.5.5 Viral gene expression and replication

Following nuclear entry of the viral genome, BKPyV hijacks cellular enzymes for the temporal expression of its viral genes and DNA replication (Acheson, 2011). In cells of human origin, the BKPyV genome is found in an episomal state following particle disassembly and nuclear entry (Cubitt, 2006). Early viral gene expression in the nucleus begins by 24 hours post-infection, with expression levels increasing up to 72 hours post-infection (Low *et al.*, 2004). Following early viral protein production in the cytoplasm, LT-Ag is translocated from the cytoplasm into the nucleus via its NLS, where it auto-regulates its own transcription (Kalderon *et al.*, 1984; Deyerle *et al.*, 1989). At low concentrations, the LT-Ag of mammalian polyomaviruses occupies conserved LTAg-binding motifs (5′-GRGGC-3′) within the NCCR to stimulate transcription from the early region (Moens, Krumbholz, *et al.*, 2017).

LT-Ag binds to Rb and p53 in order to promote cell cycle progression and block apoptosis, thereby, guaranteeing access to the host DNA synthetic machinery required for replicating the viral genome (Ahuja *et al.*, 2005). In addition, Seamone *et al.* (2010) showed that activation of the mitogen-activated protein kinase (MAPK), ERK1/2, enhances BKPyV replication in HEL-299 and Vero cells. ERK1/2 signalling mediates cell proliferation and its activation results in S-phase entry through cyclin D1 upregulation (Seamone *et al.*, 2010; Lavoie *et al.*, 1996). The findings of Seamone *et al.* (2010) suggested that the ERK1/2 signalling pathway may act in synergy with LT-Ag to promote G1/S-phase transition and enhance viral replication. Furthermore, key components of the translation pathway, Akt and mTORC-1, become activated early during infection of RPTE cells by BKPyV (Liacini *et al.*, 2010). It has also been shown that SV40 infection activates the Akt/mTOR pathway through its LT-Ag and sT-Ag (Yu and Alwine, 2002; Ugi *et al.*, 2004). Akt, also known as protein kinase B, is a key serine/threonine kinase controlling cell growth and survival. Akt is activated by the upstream phosphoinositide 3-kinase (PI3K) pathway (Yu and Alwine, 2008). The mTOR pathway is downstream of Akt and controls protein synthesis, whereby mTORC1 specifically controls the initiation of translation. The active metabolite of leflunomide (A77 1726) and sirolimus target Akt and mTORC-1, respectively. In addition to repressing BKPyV LT-Ag expression, leflunomide (A77 1726) and sirolimus have immunosuppressive activity and, thus, may

represent a potential combination treatment for PVAN without the need to reduce immunosuppression (Liacini *et al.*, 2010). Together, these findings demonstrate that conditions promoting cell growth and division favour BKPyV replication *in vitro*.

Small T-Ag also contributes to BKPyV replication by forming a complex with the catalytic and regulatory subunits of PP2A, thereby inhibiting its enzymatic activity. This is a unique function of sT-Ag which results in increased cyclins D1 and A, and downregulation of p27 to promote cell cycle progression (Skoczylas *et al.*, 2004).

SV40 has been extensively studied to provide insights into a variety of cellular processes, thus, the mechanisms of BKPyV replication have been extrapolated from what is known about SV40 DNA replication. Due to its small coding capacity, BKPyV does not encode a viral DNA polymerase and all replication factors are supplied by the host cell (Verhalen *et al.*, 2015). The multifunctional LT-Ag is the only viral protein necessary for viral genome replication (Pipas, 2001; Bennett *et al.*, 2012). Viral genome replication is initiated upon binding of LT-Ag to GAGGC motifs in the origin of replication to form two hexamers (Vanloock *et al.*, 2002; Helle *et al.*, 2017). The two LT-Ag hexamers unwind the dsDNA in a bidirectional manner with their helicase activity (An *et al.*, 2012) (Figure 1.15). Another important function of LT-Ag is to facilitate the assembly of the replication complex. Replication protein A (RPA) is recruited by the LT-Ag DBD to bind stretches of single stranded DNA, while topoisomerase I relaxes viral DNA. Next, DNA polymerase α primase is recruited to synthesise short RNA primers which serve as a starting point of DNA synthesis by the polymerase function of the enzyme complex. To complete leading and lagging strand synthesis, DNA polymerase δ, PCNA and replication factor C are also recruited to the enzyme complex (Tikhanovich and Nasheuer, 2010; Tikhanovich *et al.*, 2011). The primer is removed during the termination stage by RNase H and maturation factor 1 (MF1). Lastly, DNA ligase joins together the gaps of the newly synthesised strands to complete viral genome replication (An *et al.*, 2012).

BKPyV modulates the expression of numerous cellular genes, as evidenced by transcriptomic and proteomic analyses of RPTE and human endothelial cells (Grinde *et al.*, 2007; Abend *et al.*, 2010; An *et al.*, 2019; Caller *et al.*, 2019). As

several genes involved in DNA damage repair are upregulated in BKPyV infection, Jiang *et al.* (2012) investigated the role of the cellular DNA damage response (DDR) during BKPyV infection (Abend *et al.*, 2010). Both ataxia telangiectasia mutated (ATM)- and ataxia telangiectasia and Rad-3-related (ATR)-mediated DDR were activated to minimise the DNA damage which occurs during BKPyV infection of RPTE cells (Jiang *et al.*, 2012). Upon silencing either ATM or ATR kinase, there was accumulation of severe DNA damage during infection. The authors concluded that BKPyV replication activates the DDR through ATM and ATR in order to protect cells from virus-induced host DNA damage.

BKPyV DNA replication also causes alterations in the number and size of promyelocytic leukemia nuclear bodies (PML-NBs) (Jiang *et al.*, 2011). During early infection, PML-NBs co-localised with LT-Ag. In contrast, PML-NBs were found adjacent to BKPyV DNA during the late stages of infection. This dramatic reorganisation of PML-NBs by BKPyV may represent a mechanism through which the virus inactivates and evades their intrinsic antiviral functions.

Upon initiation of genomic replication at approximately 36 hours post-infection, late protein expression ensues to produce the structural proteins VP1, VP2 and VP3, and agnoprotein (Low *et al.*, 2004). Late gene transcription is permitted by the increase of DNA templates and is controlled by LT-Ag (Gruda *et al.*, 1993; Moens, Krumbholz, *et al.*, 2017). LT-Ag binds to transcription factors TATA-binding protein (TBP), AP-1, Sp1 and TEF-1 to stimulate transcription from the viral late promoter (Moens *et al.*, 1997).

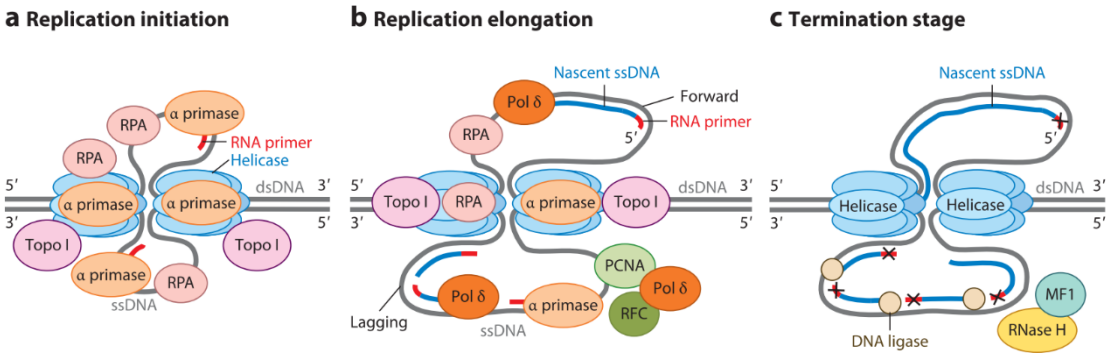

Figure 1.15 Large T antigen (LT-Ag) is the master molecule directing viral DNA replication. A) During the initiation process of polyomavirus DNA replication, the LT-Ag DNA-binding domain binds to the origin of replication. Two hexamers of LT-Ag form and their helicase activity unwinds the double-stranded DNA (dsDNA) template. Replication proceeds in a bi-directional manner. The cellular factors which interact with LT-Ag at this stage are replication protein A (RPA), DNA polymerase α primase and topoisomerase I (Topo I). RPA facilitates unwinding of dsDNA by binding to single-stranded DNA (ssDNA). DNA polymerase α primase synthesises RNA primers (red lines) which serve as a starting point of DNA synthesis. Topo I functions to relieve strain in DNA caused by unwinding. B) More cellular replicative factors are involved in the DNA elongation process. Replication factor C (RFC) and proliferating cell nuclear antigen (PCNA) facilitate the switch from α primase to DNA polymerase (Pol) δ. Pol δ extends the nascent ssDNA (blue lines) from the primer, while the α primase produces primers repeatedly for synthesis of the lagging strand. C) The primer is removed during the termination stage of viral DNA replication by RNase H and maturation factor 1 (MF1), a 5' to 3' nuclease. Lastly, the gaps between the DNA fragments are covalently closed by DNA ligase to complete viral genome replication. Obtained from An *et al.* (2012).

1.5.6 Assembly and egress

Following translation in the cytoplasm from differently spliced late mRNAs, the capsid proteins VP1, VP2 and VP3 are translocated into the nucleus for virion assembly. It has been reported that only the NLS of VP1 is required to import VP1-VP2 and VP1-VP3 complexes into the nucleus as the transport of nuclear localisation-defective minor capsid proteins is not affected (Bennett *et al.*, 2015). The nucleus offers a favourable environment for virion assembly due to its high calcium concentration which promotes encapsidation of newly synthesised viral genomes (Teunissen *et al.*, 2013). To prevent premature assembly in the cytosol, the 72 kDa cellular chaperone protein Hsc70 binds the C-terminal of VP1 following translation (Chromy *et al.*, 2003). To generate each BKPyV virion, VP1 molecules form pentamers with each pentamer having one molecule of VP2 or VP3 associated with it (Hurdiss *et al.*, 2016). Progeny virions are detectable in RPTE cells by FFU assay starting at 2 days post-infection (Low *et al.*, 2004). Randhawa *et al.* (2002) estimated that there is a mean of 6000 BKPyV virions per infected cell in renal allograft tissue biopsies of patients with PVAN. Viral particles can be seen in dense crystalline arrays by transmission electron microscopy (Drachenberg *et al.*, 2003).

BKPyV virions are released from the infected cell via an incompletely understood mechanism. Non-enveloped viruses, such as BKPyV, are believed to be passively released from infected cells through host cell lysis. However, usage of the lytic pathway counteracts the notion of establishing persistence *in vivo* in the presence of an intact immune system (Helle *et al.*, 2017). Indeed, the lytic replication cycle of BKPyV has been characterised in RPTE cells, where morphologic changes similar to those in PVAN were observed (Low *et al.*, 2004). However, strong cytopathic effects are rarely observed in BKPyV infection compared to SV40 infection (Henriksen *et al.*, 2016).

Emerging evidence supports the active secretion of BKPyV virions instead of passive lysis of the infected cell. Firstly, Evans *et al.* (2015) provided evidence of an active route of egress by treating RPTE cells with the anion channel inhibitor 4,4’-diisothiocyano-2,2’-stilbenedisulfonic acid (DIDS), known to block cellular secretion pathways (Pamenter *et al.*, 2012). Quantification of cell-free virus at 48 hours post-infection revealed that 1% of infectious progeny was released in the extracellular environment and that this route of egress was

sensitive to DIDS (Evans *et al.*, 2015). In addition, newly formed virions accumulated in acidic compartments of lysosomal or late endosomal origin following treatment. These findings supported previous work by Clayson *et al.* (1989) indicating that the release of SV40 may occur without cell lysis. Knockout and knockdown studies elucidated a critical role of agnoprotein and its binding partner, α-SNAP, in shuttling progeny virions from the nucleus to the cytoplasm of RPTE cells to actively release BKPyV (Panou *et al.*, 2018). Interestingly, DIDS treatment further decreased the release of infectious virions from cells infected with virus lacking agnoprotein. This observation demonstrated that the egress pathway, in which the cellular target of DIDS lies, is independent of agnoprotein. More recently, Handala *et al.* (2020) identified two populations of infectious particles released from both Vero and RPTE cells. One population co-sedimented with extracellular vesicles (EVs), leading the authors to conclude that BKPyV may be released in EVs through a non-lytic pathway. Further investigation is required to fully decipher the mechanism of lytic and/or non-lytic release of BKPyV. A schematic representation of the BKPyV life cycle is shown in Figure 1.16 to summarise the most important stages.

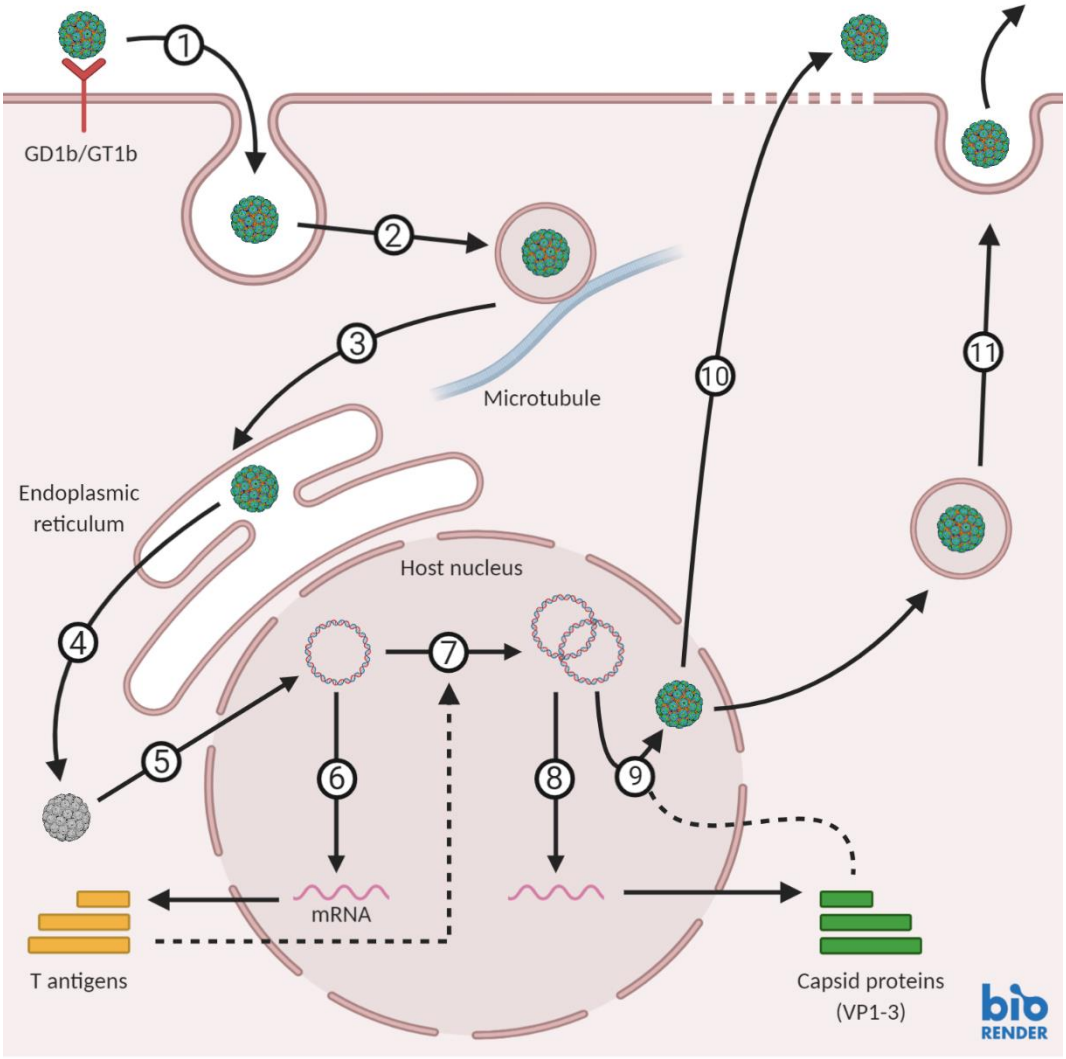

Figure 1.16 Model of the BKPyV life cycle. VP1 mediates cell adsorption via the b-series ganglioside receptors, GD1b and GT1b (1). BKPyV virion attachment is believed to form deep invaginations on the host plasma membrane. Virions are internalised through a ganglioside-dependent, caveolin- and clathrin-independent endocytosis step (2). BKPyV traffics along microtubules from the late endosomes to the endoplasmic reticulum (ER); a process mediated by Rab18 (3). Virions arrive in the ER approximately 10 hours post-infection (hpi), where they benefit from chaperones, disulphide isomerases and reductases to assist in partial capsid disassembly. VP2/VP3 become exposed to integrate into the ER membrane and, along with the ER-associated protein degradation (ERAD) machinery, facilitate the release of partially uncoated viruses into the cytosol (4). The genome is imported through the nuclear pore complex after importin α/β1 binds to the NLS of VP2/VP3 (5).

Early gene expression occurs approximately 24 hpi (6). The early viral proteins are then translocated into the nucleus to initiate viral DNA replication (7). Late viral genes are expressed (8) and capsid proteins move back to the nucleus where they self-assemble around newly synthesised viral genomes (9). Progeny virions can be released through lytic or non-lytic egress pathways (10, 11). Created with Biorender.com.

1.6 Antiviral immunity

To ensure successful propagation, viruses rely on host cellular machinery and are, therefore, characterised as ‘obligate intracellular parasites’ (Maginnis, 2018). Inevitably, each step of the viral life cycle can become a target for antiviral action to prevent damage or death of host cells following infection. To protect themselves from viral pathogens, host organisms have acquired immune defences which are historically categorised into innate and adaptive immunity (Janeway, Jr *et al.*, 2001). The early barriers to infection are formed by innate mechanisms, which ensure a rapid response against invading pathogens and do not rely on the clonal expansion of antigen-specific immune cells. Adaptive immune responses are engaged through the use of antigen-specific receptors and cells mediating adaptive immunity can be long-lived. The cross-talk between the various arms of the immune system is fundamental in developing potent and lasting immune responses (Chaplin, 2010).

1.6.1 The innate immune response to BKPyV

1.6.1.1 Pattern recognition receptors (PRRs)

The innate immune response is a crucial defence against viral infections and the first step in this process is pathogen recognition. Immune and non-immune cells express germ-line encoded pattern recognition receptors (PRRs) which recognise pathogen-associated molecular patterns (PAMPs) and danger-associated molecular patterns (DAMPs) derived from pathogens (Moens and Macdonald, 2019). Four different classes of PRR families have been identified, including the transmembrane Toll-like receptors (TLRs) and C-type lectin receptors (CLRs), and cytoplasmic proteins such as the retinoic acid-inducible gene-I (RIG-I)-like receptors (RLRs) and NOD-like receptors (NLRs) (Takeuchi and Akira, 2010). The well-studied TLR family comprises of 10 members in humans. TLR1, TLR2, TLR4, TLR5, TLR6, and TLR10 are localised to the cell surface, while TLR3, TLR7, TLR8 and TLR9 are expressed in intracellular vesicles such as the ER, endosomes, lysosomes and endo-lysosomes (Kawai and Akira, 2010) (Figure 1.17). Several structural components of the virus can be specifically recognised by TLRs. TLR2 and TLR4 detect surface glycoproteins decorating the virion (Akira *et al.*, 2006). Viral single-stranded RNA (ssRNA) is sensed by TLR7 and TLR8, while TLR3 recognises viral

dsRNA; a by-product of both RNA and DNA viruses (Weber *et al.*, 2006). TLR9 binds viral dsDNA which harbours unmethylated CpG motifs (Hemmi *et al.*, 2000). TLR-induced responses are mediated by three major signalling pathways, including NF-κB, MAPKs and IRFs (Mogensen, 2009). Activation of NF-κB and MAPK signalling pathways results in the induction of a pro-inflammatory response, while IRFs are essential for stimulating IFN production (Akira and Takeda, 2004).

TLR9 expression is downregulated following early region expression of BKPyV, JCPyV, KIPyV, WUPyV, MCPyV and SV40 in RPMI-8226 cells (Shahzad *et al.*, 2013). BKPyV, SV40 and MCPyV were the most potent inhibitors of TLR9 promoter luciferase activity. Further work on MCPyV ascribed TLR9 inhibition to LT-Ag which downregulates the transcription factor C/EBPβ. Accordingly, silencing of LT-Ag by siRNA rescues TLR9 expression in naturally immortalised keratinocytes (NIKS) stably expressing MCPyV LT-Ag. Furthermore, TLR9 inhibition seems to be cell-specific as SV40 and WUPyV early region expression do not reduce TLR9 mRNA levels in NIKS cells, as opposed to the effect exerted in RPMI-8226 cells. Additionally, repression of TLR9 transcription was also achieved by sT-Ag but to a lesser extent, and through an unknown mechanism. The authors proposed that sT-Ag may act directly through a distinct mechanism to that of LT-Ag or indirectly by promoting LT-Ag stabilisation (Shahzad *et al.*, 2013). Furthermore, a decrease in TLR9 expression was found to correlate strongly with an MCPyV-positive status in MCC biopsies (Jouhi *et al.*, 2015). The reason for TLR9 downregulation by HPyVs is not yet known, however, it may benefit viral infection and may allow virus-induced tumours to escape an immune response (Moens and Macdonald, 2019).

Basal expression of TLRs was investigated in immortalised human cortical collecting duct epithelial cells (HCDCs) by Ribeiro *et al.* (2012). Robust expression was observed by quantitative reverse transcription PCR (RT-qPCR) for TLR1-6 and TLR9. Following infection of HCDCs with BKPyV, a significant increase was observed in both TLR3 and RIG-I expression at 12 hours post-infection and was followed by a decrease in mRNA levels for both PRRs. Interestingly, only TLR3 and not RIG-I mRNA expression was significantly induced in the tubulointerstitial compartment of renal allograft biopsies with

PVAN compared to biopsies with ongoing acute rejection. The authors proposed that the discrepancy between *in vitro* and *in vivo* observations could be reconciled as different DNA- and RNA-sensing pathways may be triggered simultaneously in HCDCs, resulting in the induction of several receptors. Different innate immunity pathways could, therefore, cross-talk with each other to initiate an antiviral response to infection.

RPTE cells also express TLR3, along with melanoma differentiation–associated gene 5 (MDA5) and RIG-I (Heutinck, Rowshani, *et al.*, 2012). Activation of these viral dsRNA sensors with either polyinosinic-polycytidylic acid (poly(I:C)) or 3pRNA led to the induction of a potent antiviral, pro-inflammatory and pro-apoptotic response in RPTE cells. Further investigation into cytosolic DNA sensors and RNA sensors by de Kort *et al.* (2017) revealed that RPTE cells express TLR9, DNA-dependent activator of interferon-regulatory factors (DAI) and AIM2 (absent in melanoma 2) at low levels under basal conditions. Upon stimulation of RPTE cells with CpG oligodeoxynucleotides (ODNs), TLR9 expression was upregulated. Using dsDNA and poly(I:C) to mimic viral infection, the authors also observed induction of cytosolic DNA sensors DAI, AIM2 and IFI16 (interferon-gamma-inducible protein 16) expression. Moreover, stimulation by poly (I:C) also enhanced the expression of cytosolic sensor cyclic GMP-AMP synthase (cGAS) and its downstream signalling effector stimulator of interferon genes (STING). As a DNA virus, BKPyV may trigger cytosolic DNA sensors upon trafficking of the partially uncoated viral particle from the ER through the cytoplasm into the nucleus. However, the cytosolic DNA sensor DAI was not upregulated upon BKPyV infection of RPTE cells and this observation remained unchanged over time. This finding was indicative of BKPyV not eliciting an antiviral response in RPTE cells as assessed through DAI expression (de Kort *et al.*, 2017).

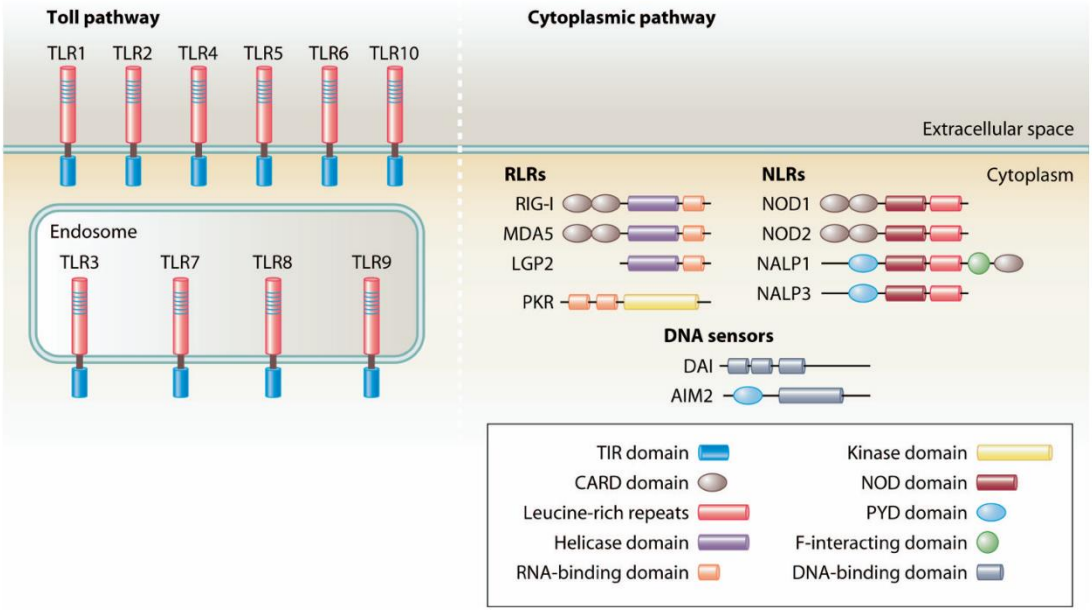

Figure 1.17 Pattern recognition receptor (PRRs). Membrane-bound Toll-like receptors (TLRs) are found in cellular or endosomal membranes. TLRs recognise PAMPs through their leucine-rich repeat (LRR) motif, while the Toll/Interleukin-1 Receptor (TIR) domain transduces the signal to the intracellular environment. Retinoic acid-inducible gene (RIG-I)-like receptors (RLRs) contain an RNA-binding domain at the C-terminus and relay the signal to downstream effectors through a caspase activation and recruitment domain (CARD). NOD-like receptors (NLRs) are intracellular proteins characterised by a central NOD domain and a C-terminal LRR domain. The latter domain recognises PAMPs and the cytoplasmic NLR transduces the signal through N-terminal domains, including CARD and pyrin (PYD) domains. Obtained from Mogensen (2009).

1.6.1.2 The interferon (IFN) signalling pathway

The interferon (IFN) response is considered the first line of defence encountered by invading pathogens and is triggered by signalling cascades initiated upon PRR activation (Platanias, 2005). IFN was first discovered by Isaacs and Lindenmann (1957) as a substance which 'interfered' with the growth of influenza virus. Since then, IFNs have been extensively studied for their antiviral effects and are classed as cytokines with pleiotropic effects (Lee and Ashkar, 2018). Interferons are typically divided into three classes, type I, II and III, which are related by signalling pathways and function (Pestka *et al.*, 2004). Type I IFNs include several subtypes of IFN-α and IFN-β, IFN-ε, IFN-κ, IFN-ω, IFN-δ, IFN-ζ and IFN-τ. Type I IFNs play a critical role in innate immunity against viruses as they are typically produced and secreted by almost all cell types early on during a viral infection (Liu *et al.*, 2012). The type III interferon group, also termed IFN-λ, is composed of IFN-λ1 (IL-29), IFN-λ2 (IL-28a), IFN-λ3 (IL-28b) and IFN-λ4 (Zhou *et al.*, 2018). IFN-γ is the only member of the type II class of IFNs and is produced by immune cells such as NK cells as an innate immune mediator or by activated T lymphocytes, antigen presenting cells (APCs) and B cells as an adaptive immune mediator (Schroder *et al.*, 2004).

Upon PRR activation in response to viral infection, signalling pathways are triggered which converge on the activation of IRF3, IRF7 and NF-κB transcription factors (Akira *et al.*, 2006). Notably, the IRF transcription factors were first characterised as modulators of both type I IFNs and IFN-stimulated genes (ISGs), and have since been regarded as master regulators of IFN response pathways (Tamura *et al.*, 2008; Ikushima *et al.*, 2013). IRF3 and IRF7 are phosphorylated by the serine/threonine kinases TBK1 and IκB kinase (IKK) ε (IKKε), while NF-κB is liberated from IκB through IKK complex activation (Yanai *et al.*, 2012; Akira *et al.*, 2006). Subsequently, nuclear translocation of IRF3/7 and NF-κB leads to production of IFN and pro-inflammatory cytokines, respectively (Heutinck, Rowshani, *et al.*, 2012).

IFN proteins are then secreted to exert both autocrine and paracrine functions (Samuel, 2001). Signal transduction by type I and II IFNs is mediated through the formation of multiprotein complexes consisting of IRF and signal transducer and activator of transcription (STAT) family proteins. Typically, IFN-α/β secreted by somatic cells protects infected and neighbouring, uninfected cells by binding

to the interferon-α/β receptor (IFNAR) and activating the Janus kinase (JAK)-dependent phosphorylation of STAT1 and STAT2. STAT1 is phosphorylated at Tyr701, Ser708 and Ser727, while STAT2 is activated upon Tyr690 phosphorylation (Wang *et al.*, 2017). Phosphorylated STAT1 (pSTAT1) and pSTAT2 assemble with IRF9 into the interferon-stimulated gene factor 3 (ISGF3) complex (Platanias, 2005). ISGF3 translocation into the nucleus promotes the transcription of hundreds of ISGs from the interferon-sensitive response element (ISRE) sequence (Cheon *et al.*, 2013). Some of these gene products possess antiviral functions which allow cells to enter an antiviral state (Ivashkiv and Donlin, 2014). In contrast, IFN-γ signalling through the IFN-γ receptor (IFNGR) requires pSTAT1 homodimer formation, also known as IFN-γ-activated factor (GAF), to induce ISG transcription from the γ-activated sequence (GAS) (Varinou *et al.*, 2003; Michalska *et al.*, 2018).

Upon BKPyV infection of endothelial cells (VEC), IRF3 translocates to the nucleus and leads to a low level production of IFN-β as indicated by immunofluorescent studies and ELISA assays, respectively (An *et al.*, 2019). Furthermore, pSTAT1 localises to the nuclei of infected VEC independently of VP1 expression which is suggestive of paracrine signalling taking place. In contrast, neither IRF3 activation nor IFN-β production was observed in RPTE cells following BKPyV infection (An *et al.*, 2019; de Kort *et al.*, 2017). Interestingly, another study provided evidence in support of BKPyV, along with JCPyV, inducing IFN-β production in RPTE cells (Assetta *et al.*, 2016). Moreover, An *et al.* (2019) could not detect any nuclear translocation of pSTAT1 in BKPyV-inoculated RPTE cells and, similarly, Assetta *et al.* (2016) observed low levels of IRF9 and no pSTAT1 in the nucleus of RPTE cells. In contrast, pSTAT1 and IRF9 co-localised in JCPyV-infected nuclei indicating recognition of JCPyV by PRRs in RPTE cells. Nuclear translocation of transcription factors was succeeded by upregulation of various ISGs (Assetta *et al.*, 2016). Notably, BKPyV replication is susceptible to both type I and type II IFNs as measured by viral gene expression and progeny production (Abend *et al.*, 2007; Assetta *et al.*, 2016). Interestingly, IFN-γ protects RPTE cells against apoptosis and attenuates the effects of cisplatin in inducing renal injury as demonstrated in mice (Kimura *et al.*, 2012). Furthermore, IFN-γ was reported to have an inhibitory effect on SV40 promoters (Harms and Splitter, 1995). However, the

contribution of type I IFN in viral nephropathies remains unclear (Anders *et al.*, 2010).

1.6.1.3 Interferon-stimulated genes (ISGs)

An ISG can be simply defined as any gene which is induced during the IFN response or, more specifically defined, as any gene which is a direct target of ISGF3 or GAF (Schoggins, 2019). Many ISGs are also directly targeted by IRFs (IRF1, IRF3, IRF7), NF-κB or IL-1 signalling and can even be induced independently of IFN signalling (Rubio *et al.*, 2013; Schneider *et al.*, 2014; Michalska *et al.*, 2018; Orzalli *et al.*, 2018). Furthermore, expression of ISG-inducing factors, including IRF1 and IRF7, is also upregulated upon stimulation by IFN (Harada *et al.*, 1989; Marié *et al.*, 1998). Therefore, this leads to multiple pathways through which an ISG can be induced. In addition to being induced by the IFN response, some ISGs are basally expressed while others are only induced during IFN signalling (Mostafavi *et al.*, 2016). Since the discovery of the first ISGs, the number of known ISGs has expanded with the application of high throughput screening methods in the last 20 years (Knight and Korant, 1979; Larner *et al.*, 1984; Schoggins and Rice, 2011). Microarray studies and RNA sequencing analyses revealed that there may be more than 1,000 ISGs (de Veer *et al.*, 2001; Lanford *et al.*, 2006; Shaw *et al.*, 2017).

ISGs operate alone or in a concerted manner to promote antiviral defences, have anti-proliferative effects or stimulate adaptive immunity (Schoggins, 2019). To exert their antiviral functions, ISGs interfere with various stages of the viral life cycle. For example, the enzyme heparanase (HPSE) prevents viral attachment of alphaviruses, flaviviruses and paramyxoviruses following its ectopic expression (Schoggins *et al.*, 2011, 2014). Interferon-inducible transmembrane proteins (IFITMs) impair viral entry for enveloped viruses, while TRIM5α inhibits trafficking of retroviral particles (Spence *et al.*, 2019; Wu *et al.*, 2006). Viral gene expression can be targeted by IFI16 as shown for the human cytomegalovirus DNA polymerase gene (UL54) (Gariano *et al.*, 2008). Protein Kinase R (PKR), IFN-induced proteins with tetratricopeptide repeats (IFITs) and ZC3HAV1 all target viral protein translation, while genome amplification can be inhibited by APOBEC enzymes and RSAD2 (Viperin) (Zhang *et al.*, 2003; Li *et al.*, 2015; Gizzi *et al.*, 2018). ISGs can also prevent later stages of the replication cycle, such as the well-characterised tetherin which inhibits retrovirus

egress (Neil *et al.*, 2008). Therefore, an ISG-mediated antiviral state is established within infected and nearby, uninfected cells in response to viral infection which leads to attenuation of replication and limitation of viral spread (Randall and Goodbourn, 2008).

ISG induction by BKPyV and JCPyV appears to occur in a cell-specific and virus-specific manner, with several studies noting an increase in ISG expression following JCPyV infection. Verma *et al.* (2006) performed microarray analysis of primary human foetal glial cells (PHFG) following transfection of JCPyV. Amongst the 410 cellular genes which were differentially expressed, there were 15 ISGs with a 2-fold increase in expression. Upregulated ISGs included STAT1, ISG56, myxovirus resistance 1 (MxA), 2’5’-oligoadenylate synthetase (OAS) and *cig5* (Viperin). Importantly, the induction of these ISGs was further confirmed in JCPyV-infected PHFG and the human glioblastoma cell line U87MG by RT-qPCR. In addition, transcriptome profiling of JCPyV-infected RPTE cells further demonstrated that the virus induces a strong antiviral response (Assetta *et al.*, 2016). As infection progressed, an exponential increase was observed in the number of ISGs which were differentially expressed. While JCPyV infection of RPTE cells resulted in ISG upregulation, primary human astrocyte cells showed no alteration in ISG expression following infection (Radhakrishnan *et al.*, 2003; Moens and Macdonald, 2019).

ISG upregulation in response to BKPyV infection was overall limited to four genes (IFI6, IRF7, OAS3 and HERC5) in RPTE cells (Assetta *et al.*, 2016). A quantitative temporal proteomics study by Caller *et al.* (2019) found no change in ISG product levels upon BKPyV infection of RPTE cells. MX1, ISG15, IFIT1, IFIT2, IFIT3, IRF3, IFI16, and BST2 (tetherin) protein levels remained unchanged throughout the three days of infection. More recent studies have highlighted the importance of studying various aspects of BKPyV infection, including the interaction with innate immunity, in different cell types of natural infection. An *et al.* (2019) showed activation of the IFN signalling pathway by BKPyV infection in pulmonary VEC. The authors observed induction of multiple ISGs and additional genes involved in immunity in VEC, including antiviral effectors (MX1, RSAD2, BST2, ISG15, HERC5, EIF2AK2 (PKR), OAS1-3, OASL), pathogen sensors (DDX60, RIG-I, cGAS) and positive regulators of IFN signalling (STAT1, STAT2, IRF7, IRF9). Increased mRNA levels were also

detected for genes involved in antigen presentation (HLA-F, MICA and MICB, LMP2, TAP1 and TAP2). In contrast, the majority of ISGs were not enhanced in BKPyV-inoculated RPTE cells. In support of the work in endothelial cells, an earlier study found ISG induction upon BKPyV infection of human umbilical vein endothelial cells as ISG15 and IFIT3 expression was enhanced (Grinde *et al.*, 2007).

Thus, it is evident that some cells respond to BKPyV infection by activating IFN signalling and, subsequently, inducing ISG expression, while others show an apparent lack of an innate immune response. The reason for the discrepancy between cell types is yet unknown, although the induction of an antiviral state may serve in allowing persistence to take place by restricting viral replication (Imperiale and Jiang, 2016; An *et al.*, 2019). One possibility as to why some types of cells may not be able to mount an antiviral response against BKPyV is the inability to sense the virus. Alternatively, BKPyV may counteract cellular defences through immune evasion, either by blocking the function of antiviral effectors or targeting them for degradation (An *et al.*, 2019).

1.6.1.4 Cytokines and chemokines

Viral infection also induces the production of additional cytokines, including chemokines, which have pro-inflammatory effects and help induce immune responses in the host (Mogensen, 2009). Renal epithelial cells, particularly cells originating from collecting tubules, have the ability to behave as inflammatory cells and secrete cytokines or chemokines (Ribeiro *et al.*, 2012). Pro-inflammatory mediators are often associated with renal disruption due to cytokine-induced changes in potassium ion (K^+) channel activity (Nakamura *et al.*, 2015).

Numerous studies have detected enhanced cytokine/chemokine expression *in vitro* upon HPyV infection. MCPyV T antigens expressed by immortalised BJ human foreskin fibroblast cells exhibit increased expression of inflammatory cytokine and chemokine genes, including IL-1β, IL-6, IL-8 and CXCL1 (Richards *et al.*, 2015). JCPyV infection also modulates cytokine and chemokine expression. Human embryonic neural progenitor cells upregulate mRNA expression and secretion of RANTES, GRO, CXCL1, CXCL16, IL-8, CXCL5, CXCL10 and the chemokine receptor CXCR2 in response to JCPyV infection

(Darbinyan *et al.*, 2013). Likewise, BKPyV-inoculated HCDCs show a small, albeit significant, increase in IL-6, IL-8, RANTES, CCL2 and CXCL10 production as indicated by RT-qPCR and ELISA assays (Ribeiro *et al.*, 2012, 2016). While TNFα expression is downregulated, TNF receptors 1 and 2, TLR3 and RIG-I mRNA levels are enhanced (Ribeiro *et al.*, 2012, 2016). In contrast, RPTE cells do not alter dramatically their cytokine expression levels in response to BKPyV infection as determined through assessment of up to 85 cytokine genes at 4 hours post-infection (Abend *et al.*, 2010). While RPTE cells respond to dsDNA stimulation by upregulating several cytokines (CXCL10, IFN-β, IL-6) and cytosolic DNA sensors, de Kort *et al.* (2017) provided evidence suggesting that BKPyV evades innate immunity and does not induce a pro-inflammatory response in this cell type. Escaping the antiviral response is, however, limited to RPTE cells as leukocytes elicit a potent innate immune response against BKPyV. Furthermore, analysis of microarray data from renal transplant patients highlighted CXCL10 and STAT1 as significant genes contributing to PVAN (Jia *et al.*, 2018). Thus, BKPyV infection may result in kidney damage by promoting inflammation and prohibiting tissue repair.

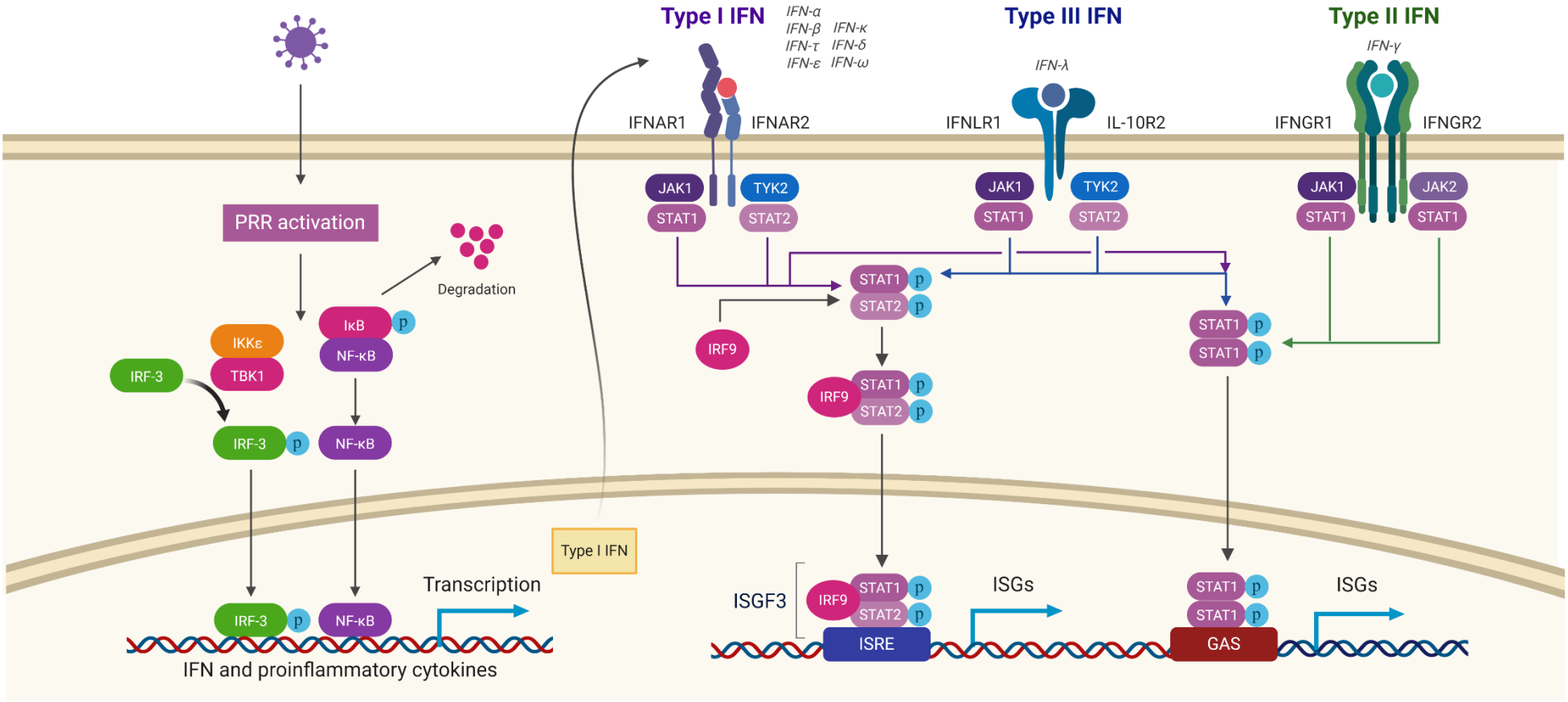

Figure 1.18 Simplified schematic of the interferon (IFN) response to viral pathogens. Upon detection of a virus, pattern-recognition receptors (PRRs) initiate signalling pathways which activate the transcription factors interferon regulatory factor 3 (IRF3), IRF7 and/or nuclear factor-κB (NF-κB). IRF3 and IRF7 are phosphorylated by TANK Binding Kinase 1 (TBK1) and IκB kinase (IKK) ε (IKKε), while

NF-κB is liberated from IκB, which is subsequently degraded by the proteasome. Nuclear translocation of IRF3/7 and NF-κB leads to production of type I IFN and pro-inflammatory cytokines. IFN is secreted from the infected cell to act in autocrine and paracrine manners. Binding of type I IFN to the interferon-α/β receptor (IFNAR) triggers the JAK/STAT signalling pathway which leads to STAT1/STAT2 phosphorylation. Phosphorylated STAT1 (pSTAT1) and pSTAT2 combine with IRF9 to form the interferon-stimulated gene factor 3 (ISGF3) complex. ISGF3 promotes the transcription of hundreds of interferon-stimulated genes (ISGs) from the interferon-sensitive response element (ISRE) sequence. Type III IFN signalling occurs through the IFN-γ receptor (IFNGR) but requires pSTAT1 homodimer formation to induce ISG transcription from the γ-activated sequence (GAS). Some of the ISG products have antiviral functions which allow cells to enter an antiviral state in order to limit viral spread. Created with BioRender.com.

1.6.2 The adaptive immune response to BKPyV

1.6.2.1 Humoral immunity

Neutralising antibodies, produced during infection, can participate in preventing viral spread. Up to 90% of the adult population has BKPyV-specific antibodies, however, having a seropositive status prior to transplantation does not protect renal transplant recipients from developing PVAN as determined by a prospective study of 78 subjects (Hirsch *et al.*, 2002; Hirsch and Steiger, 2003; Comoli *et al.*, 2004). On the other hand, a study examining BKPyV-specific antibodies in 20 renal transplant subjects experiencing different stages of PVAN, found that revocery from PVAN and elimination of BKPyV infection was associated with developing an IgG antibody response as opposed to IgM antibodies (Hariharan *et al.*, 2005). Furthermore, negative BKPyV antibody status of the recipient correlates with a greater risk of virus replication and progression to PVAN in pediatric kidney transplant patients (Ginevri *et al.*, 2003; Smith *et al.*, 2004).

Antibody titre levels were assessed by Bohl *et al.* (2008) in plasma samples obtained over a 1-year period from 70 kidney transplant recipients with active BKPyV infection and 17 control patients without active infection. Mean antibody titre increased as infection progressed from no infection, to transient viruria, sustained viruria, transient viremia and sustained viremia. However, the humoral response offered incomplete protection and did not clear viruria or viremia. The role of humoral immunity in regulating BKPyV infection remains uncertain, however, VLP-based preventative vaccines have been suggested for use in immunocompromised patients to generate a BKPyV-specific humoral response (Comoli *et al.*, 2013; IARC, 2014).

1.6.2.2 Cell-mediated immunity

Virus-specific cell-mediated immunity is fundamental in controlling viral replication during infection and persistence (Dekeyser *et al.*, 2015). This antiviral effect is mediated by virus-specific $CD4^+$ and $CD8^+$ T cells which secrete cytokines and are involved in the elimination of virus-infected target cells (Harari *et al.*, 2006). $CD8^+$ T cells, also known as cytotoxic T lymphocytes (CTLs), recognise cell-associated viral epitopes and trigger cell lysis. Both healthy individuals and kidney transplant patients mount T cell responses

against BKPyV LT-Ag, sT-Ag, VP1, VP2 and VP3 proteins, however, no immunodominant antigen has been identified (Mueller *et al.*, 2011; Comoli *et al.*, 2013). Conversely, no cellular immune response was directed against agnoprotein, suggesting that this viral antigen is largely immunologically ignored (Leuenberger *et al.*, 2007). A response against LT-Ag is more likely to invovle $CD8^+$ T cells, whereas VP1 stimulates a $CD4^+$ T cell response (Binggeli *et al.*, 2007). Cellular immunity to BKPyV peaks in immunocompetent individuals aged 20 and 30 years, whereupon it begins to decline (Schmidt *et al.*, 2014). This cellular immune response was found to be dominated by $CD4^+$ T cells expressing IFN-γ, IL-2 and TNF-α. However, further investigation is required to determine precisely which subset has a protective role in regulating the infection (Trydzenskaya *et al.*, 2011).

A strong CTL response and low antibody titres in PVAN patients is associated with decreased viruria and viremia, suggesting that a BKPyV-specific cellular immune response is more important in containing BKPyV replication compared to the humoral response (Chen *et al.*, 2006). Moreover, BKPyV-specific IFN-γ secreting T cells could not be detected in kidney transplant patients treated with immunosuppressors for PVAN, whereas reduction of immunosuppression in these patients was linked to emergence of IFN-γ secreting T cells to levels comparable to that of healthy controls (Comoli *et al.*, 2004; Ginevri *et al.*, 2007). Furthermore, an increase in virus-specific T cells coincided with a decrease in serum creatinine levels; an indicator of stable renal allograft function (Ginevri *et al.*, 2007). The importance of BKPyV-specific T cells in controlling BKPyV replication and PVAN was confirmed in a more recent study where renal transplant recipients with self-limited virus reactivation developed virus-specific cellular immunity without the need for therapeutic interventions (Schachtner *et al.*, 2011). It is evident that host immunity plays a critical role in determining viral infection and persistence, thus, further investigation into various aspects of the immune response may provide valuable insights into specific components which may modulate BKPyV infection.

1.7 Aims and objectives

Published data propose the susceptibility of BKPyV infection to interferon. The main aim of this research project is to investigate host intrinsic factors which may be acting in the interferon pathway to modulate BKPyV infection and provide further data regarding the interaction of BKPyV and innate immunity. To this end, the objectives of this project are:

1. To demonstrate susceptibility of BKPyV infection to the action of interferon.

2. To adapt and perform an ISG-overexpression screening assay for BKPyV infection.

3. To validate and characterise potential candidates with enhancing or inhibitory activity for BKPyV infection.

4. To identify the stage in the BKPyV life cycle where ISG candidates potently carry out their activity.

5. To assess the requirement of ISG candidates for their effect during BKPyV infection in a primary renal proximal epithelial cell culture model.

6. To investigate whether the role of ISG candidates is conserved in other polyomavirus infections.

Chapter 2
Materials and Methods

2.1 Mammalian cell culture

2.1.1 Culturing and passaging mammalian cells

Vero cells (The Pirbright Institute), SVG-A cells (Walter Atwood, Brown University, USA) and HEK-293TT (Christopher Buck, National Cancer Institute, USA) were cultured in Dulbecco's Modified Eagle Medium-high glucose (DMEM; Sigma-Aldrich) supplemented with 10% foetal bovine serum (FBS; Gibco™, Thermo Fisher Scientific) and 100 U/mL penicillin/streptomycin (Gibco™, Thermo Fisher Scientific) to form the complete growth medium. Continuous cell lines were cultured at 37°C in a humidified cell culture incubator supplied with 5% CO_2.

Primary human renal proximal tubule epithelial (RPTE) cells (ATCC® PCS-400-010™) were cultivated with Renal Epithelial Cell Basal Medium 2 (PromoCell) supplemented with 5% fetal calf serum, 10 ng/mL epidermal growth factor, 5 µg/mL insulin, 36 ng/mL hydrocortisone, 0.5 µg/mL epinephrine, 4 pg/mL triiodo-L-thyronine and 5 µg/mL transferrin (PromoCell). The addition of serum and selected growth factors to the basal medium formed the complete growth medium for primary RPTE cells. Primary cells were cultured at 37°C with 5% CO_2 in a humidified incubator, designated for primary cell cultures only. Their growth medium was replenished every 2-3 days until the next passage. RPTE cells maintain their differentiated state up to passage 6, thus, were not used in experiments past the indicated passage number (Humes *et al.*, 2002).

Prior to passaging cells, the growth medium was decanted and the cell monolayer was washed with 1X Phosphate-Buffered Saline (PBS; Corning). To enzymatically dissociate cells from the culturing surface, 1X Trypsin-Versene® (Lonza) was incubated with cells at 37°C. Upon cell detachment, trypsin was neutralised with the appropriate growth medium to form a cell suspension. A 1:10 dilution of the cell suspension was seeded in a new tissue culture flask (Thermo Scientific) with fresh media and incubated at 37°C.

2.1.2 Cell counting

To determine the number of cells per mL, the cell monolayer was detached from the cell culture substrate with 1X Trypsin-Versene®, as described previously. Upon re-suspension in complete growth medium, a 1:1 dilution of the cell suspension was made with Trypan Blue solution (Sigma-Aldrich). Ten µL of the dilution was loaded onto a haemocytometer and cells were counted in the four large corner squares under the 10x objective of an AE2000 inverted microscope (Motic). The average number of cells per mL was calculated as follows:

$$\frac{\text{Number of cells counted}}{\text{Number of large squares counted}} \times \text{dilution factor} \times 10^4 = \text{Cells per mL}$$

2.1.3 Cryopreservation and thawing of mammalian cells

Cryopreservation of cells was performed to maintain stocks of mammalian cells. Cells were detached gently and the viable cell count per mL was determined as described previously (2.1.2). Cells were centrifuged for 5 minutes at 82.2 x g at 4°C to obtain a pellet. The supernatant was carefully removed and cells were re-suspended at a concentration of 10^6 cells/mL in 10% dimethyl sulphoxide (DMSO; Thermo Scientific) dissolved in complete growth medium. The suspension was aliquoted into cryogenic vials, which were stored overnight in a -80°C freezer within a Mr. Frosty freezing container (Nalgene®, Sigma-Aldrich) to achieve a 1°C/min cooling rate. Cryogenic vials were then transferred to liquid nitrogen for long-term storage.

Upon retrieving frozen cryovials from storage, cells were quickly thawed (<1 minute) in a 37°C water bath and diluted immediately in pre-warmed growth medium. Following an overnight incubation at 37°C, the medium was replaced to remove traces of cryoprotectant.

2.1.4 MTT cytotoxicity assay

To assess cell viability, 10^4 cells were seeded per well of a 96-well plate. At 48 hours post-seeding, cells were incubated with MTT reagent (1 mg/mL; Invitrogen™, Thermo Fisher Scientific) dissolved in Opti-MEM™ I Reduced Serum Medium (Gibco™, Thermo Fisher Scientific) for 30 minutes at 37°C. As a control for the induction of cell death, cells were incubated with 1 µM staurosporine (Sigma-Aldrich) for 18 hours prior to determining cell viability.

2.2 Bacterial cell culture

2.2.1 DNA transformation into competent bacterial cells

DH5α *Escherichia coli* cells (NEB) were grown in SOB-media (10 mM NaCl, 0.5% yeast extract, 2% peptone, 2.5 mM KCl, pH 7.5) at 18°C until cultures reached an optical density of ~ 0.6 at 600 nm. Bacterial cells were pelleted by centrifugation at 2,500 x g for 10 minutes. Cells were made chemically competent through re-suspension in transformation buffer (15 mM $CaCl_2$, 10 mM PIPES, 55 mM $MnCl_2$, 250 mM KCl, pH 6.7). Following a second centrifugation step, bacterial cells were transferred in cold transformation buffer with 7% DMSO and aliquoted for long-term storage at -80°C.

For plasmid DNA amplification, 50 µL competent cells were thawed on ice and 5 µL DNA was introduced into cells. The mixture was incubated on ice for 10 minutes, heat shocked at 42°C for 45 seconds, and returned on ice for 2 minutes. Transformed cells were cultured in 450 µL antibiotic-free LB medium (200 mM NaCl, 1% tryptone, 0.5% yeast extract) at 37°C for 1 hour at 180 RPM. Cells were then plated on LB agar plates containing the appropriate antibiotic at 100 µg/mL and incubated at 37°C overnight.

Single colonies were then incubated with 5-10 mL antibiotic-containing LB media. Small scale bacterial cultures were incubated at 37°C at 180 RPM for 4 hours or overnight, depending on the DNA purification method. Large scale bacterial cultures were set up with 100 mL antibiotic-containing LB media and 5 mL of a small scale bacterial culture. Flasks were incubated overnight at 37°C at 180 RPM.

2.2.2 Plasmid DNA purification from bacterial cells

2.2.2.1 Mini-prep

Ten mL of overnight small scale bacterial cultures were harvested by centrifugation at 3,028 x g for 15 minutes at 4°C. Plasmid DNA was isolated and purified according to the manufacturer's protocol using Wizard® Plus SV Minipreps DNA Purification System (Promega). DNA was eluted in 100 µL nuclease-free water and quantified with the NanoDrop™ One microvolume spectrophotometer (Thermo Fisher Scientific).

2.2.2.2 Maxi-prep

Hundred mL of overnight large scale bacterial cultures were harvested by centrifugation at 3,028 x g for 45 minutes at 4°C. Plasmid DNA was purified by following the manufacturer's instructions using the QIAGEN Plasmid Maxi kit (QIAGEN). DNA was eluted in 400 µL nuclease-free water and quantified using the NanoDrop™ One.

2.3 Preparation of viral genomes

2.3.1 BKPyV and SV40 genome preparation

Ten µg of plasmids (Michael Imperiale, University of Michigan, USA) were digested in a 50 µL reaction with 20 units of restriction enzyme (NEB) to excise the respective polyomavirus genome (Table 2.1). The reaction mixture was incubated at 37°C for 1 hour and was followed by addition of another 20 units of enzyme for a total digestion time of 2 hours. Linear genomes were circularised overnight at 16°C with 400 units of T4 DNA ligase (NEB) in a total volume of 1 mL.

Table 2.1 Viral genomes used for viral stock propagation are listed below. The plasmid containing the viral genome and the restriction enzyme required for initial digestion are given below.

Plasmid	Restriction enzyme
pGEM7-BKPyV-Dunlop	BamHI-HF®
pUC-SV40	KpnI-HF®

2.3.2 DNA purification and quantification

Following ligation, DNA was purified using Monarch® PCR & DNA Cleanup Kit (NEB), with a 2:1 ratio of Binding Buffer:Sample. Ligated DNA was eluted in 20 µL of elution buffer and analysed by agarose gel electrophoresis, together with digestion products.

2.3.3 Agarose gel electrophoresis

Samples of the digestion and ligation reactions were prepared with 500 ng DNA and 6X Purple Loading Dye (NEB) in 6 µL total volume. DNA was analysed on 0.7% agarose gels, which contained 1X SYBR Safe DNA Gel Stain (Invitrogen™), and run at 100 Volts (V) for 40 minutes using 1X TAE buffer (40

mM Tris, 20 mM acetic acid, 1 mM EDTA). One kb Plus DNA Ladder (100 bp to 10 kb; NEB) served as the molecular weight marker and DNA bands were visualised with the InGenius gel documentation system (Syngene Bio Imaging), following exposure to UV for 1-2 seconds.

2.4 Propagation of polyomavirus stocks in mammalian cells

2.4.1 BKPyV DNA transfections and infections of primary RPTE cells

Two 75 cm^2 flasks were seeded with approximately $1x10^6$ RPTE cells and left to adhere overnight. The following day, and immediately before transfection, 4 µg re-ligated DNA genome were mixed with 400 µL Opti-MEM™ I Reduced Serum Medium for each flask. The diluted DNA was then mixed with 12 µL TransIT®-LT1 Transfection Reagent (Mirus Bio). Following a 30 minute incubation period to allow for the formation of TransIT®-LT1 Reagent: DNA complexes, the mixtures were added to the flasks in complete growth medium. Transfection complexes were not removed due to low toxicity exhibited by the transfection reagent used. Cells were incubated for two weeks at 37°C, at the end of which cells were scrapped into their growth media for harvest.

Viral lysates were prepared by three cycles of freeze(-196°C)-thaw(40°C). Six 175 cm^2 flasks of RPTE cells were infected with approximately 5 mL viral lysate at 70% cell confluency for 2 h at 37°C. The virus inoculum was then removed and replaced with growth medium. Flasks were incubated for two weeks before harvesting with a cell scrapper. The resulting cell suspension was subjected to three freeze-thaw cycles and stored at -80°C to be used for crude viral infections or virus purification.

2.4.2 Purification of BKPyV viral lysate

To perform infections at the desired multiplicity of infection (MOI) in a small-scale format, BKPyV was purified following its propagation in cell culture. Virus purification also facilitates the removal of non-BKPyV proteins from viral stocks, which may act as contaminants.

Viral lysates were centrifuged at 671.1 x g for 30 minutes at 4°C and the resulting supernatant was stored on ice until required. The cell pellet was re-suspended in 10 mL Buffer A (10 mM HEPES pH 7.9, 1 mM $CaCl_2$, 1 mM $MgCl_2$, 5 mM KCl) and sonicated for 5 minutes in an ultrasonic bath (Ultrawave). The pH was then lowered to 6.0 by addition of 12 M HCl. Ten units of neuraminidase (sialidase) from *Clostridium perfringens* (Sigma-Aldrich) were added to the suspension, to cleave the sialic acid residues from glycoproteins

on the host cell surface. After 1 hour incubation at 37°C, the pH of the solution was adjusted to 7.4 with 1 M NaOH and the sample was heated to 40°C for 5 minutes. The solution was centrifuged at 16,000 x g for 5 minutes, the supernatant was stored on ice and the pellet was re-suspended in 10 mL Buffer A. The suspension was incubated with 0.1% deoxycholic acid (Sigma) for 15 minutes at 37°C, with occasional vortexing. Following a second centrifugation step at 16,000 x g for 5 minutes, the pellet was discarded while the supernatant was combined with the previous two supernatants. The virus-containing supernatants were centrifuged through a 20% sucrose layer at 85,500 x g for 3 hours at 20°C in an Optima XPN-80 Ultracentrifuge (Beckman Coulter). The virus-containing pellets were re-suspended in 1 mL Buffer A per pellet, sonicated for 5 minutes and centrifuged at 1,073 x g for 5 minutes. The supernatant was then overlaid onto a caesium chloride (CsCl) gradient, formed by 1.5 mL low (1.2 g/cm^3) and 1.5 mL high (1.4 g/cm^3) density CsCl solution. After centrifugation at 155,000 x g at 15°C for 16 hours, the bottom viral fraction was extracted with a 21 gauge needle inserted into a 1 mL syringe. The collected fraction was dialysed using Pur-A-Lyzer™ Midi 6000 Dialysis kit (Sigma-Aldrich) against 2 L Buffer A at 4°C overnight. The resulting purified virus was aliquoted and stored at -80°C. Sucrose and CsCl solutions were prepared in Buffer A. Figure 2.1 summarises the process undertaken for BKPyV propagation and subsequent purification.

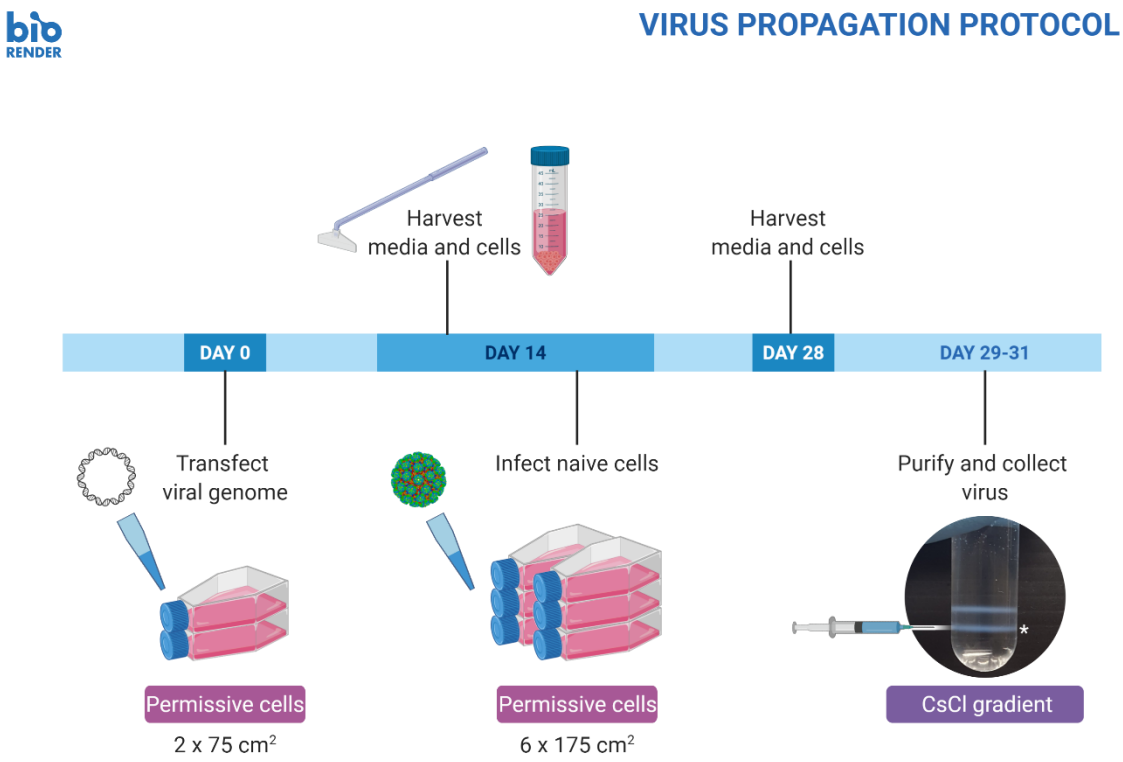

Figure 2.1 BKPyV propagation and purification. Cells in two 75 cm^2 flasks are transfected with the circular BK polyomavirus (BKPyV) genome. After 14 days, intracellular and extracellular virus is collected in the form of a cell suspension. Cells are forced to burst open in order to release intracellular virus and this resulting viral lysate is used to infect naïve cells. After 14 days of infections, the virus-containing media and cells are again collected and viral lysate is prepared. Infection is monitored through sample collection on days 14 and 28. The virus can be purified through a sucrose cushion and, subsequently, through a caesium chloride (CsCl) gradient. The bottom viral fraction (asterisk) is collected from the CsCl gradient, dialysed, titrated and used for infections. Created with BioRender.com.

2.4.3 Labelling purified BKPyV

To investigate the ability of BKPyV to bind to the host cell surface, 450 µg of purified BKPyV were mixed gently by inversion with one vial Alexa Fluor® 488 reactive dye from the Molecular Probes Alexa Fluor® 488 Protein Labelling Kit (Invitrogen™). The reaction mixture was stirred for 1 hour at room temperature in the dark. The virus was then dialysed against 4 L of 10 mM Tris pH 8.0, 50 mM NaCl and 10 µM $CaCl_2$ overnight at 4°C in the dark. The virus was aliquoted and frozen at -80°C. Labelled purified BKPyV is, henceforth, termed AF488-BKPyV.

2.4.4 SV40 generation

Vero cells were seeded into two 75 cm^2 tissue culture flasks and left to adhere overnight. The circular DNA of SV40 polyomavirus was transfected into Vero cells at 50% confluency using TransIT®-LT1 Transfection Reagent, as previously described. Following a 7-day incubation period at 37°C, transfected cells were harvested in their media through scrapping. Following 5 minutes of sonication, the cell suspension was centrifuged at 671.1 x g for 30 minutes. The SV40-containing supernatant was aliquoted and stored at -80°C to be used directly in infection assays.

2.4.5 JCPyV generation

JC polyomavirus Mad-4 (ATCC) was propagated in SV40-transformed human foetal astroglial cells, SVG-A cells (Major et al., 1985). Two 75 cm^2 tissue culture flasks with 50% confluent SVG-A cells, were infected with 0.1 mL JCPyV each. Infected cells were incubated, without removing the virus, at 37°C for 2 weeks when cells were scrapped into their media for harvesting. Viral lysate was prepared through three cycles of freeze-thaw, aliquoted and stored at -80°C to be used directly in infection assays.

2.5 Virus titration by fluorescent focus assay (FFA)

2.5.1 Virus titration

To determine the titre of viral stocks, a fluorescent focus assay (FFA) was setup in a 96-well plate format. Cells were seeded as 2 x 10^3 cells per well and left to adhere overnight. Purified or crude virus was serially diluted two-fold into Opti-MEM™ I Reduced Serum Medium across 6 wells of the plate in a final volume of 50 µL. Ten µL were used as the input volume for purified virus, while 50 µL was used for crude virus. Infections were performed for 2 hours at 37°C, with gentle rocking of the plate every 30 minutes. The virus-containing inoculum was then removed, cells were gently washed in 1X PBS and fresh medium was added. At 48 hours post-infection, the plate was fixed in 4% paraformaldehyde for 10 minutes and viral antigen was detected by indirect immunofluorescence.

2.5.2 Immunofluorescence for IncuCyte® ZOOM imaging

The following immunofluorescence staining method was adapted from Stewart *et al.* (2015). Fixed cells were washed in 1X PBS and permeabilised with 0.1% Triton™ X-100 (Sigma-Aldrich) in PBS for 10 minutes. Following one wash in 1X PBS, non-specific antibody binding was reduced by incubation with 1% bovine serum albumin (BSA; Sigma-Aldrich) in PBS for 30 minutes. Cells were then incubated overnight at 4°C with anti-VP1 mouse antibody (PAB597) diluted 1:250 in 1% BSA in PBS. The following day, the plate was washed three times with 1X PBS and incubated for 1 hour at room temperature with Alexa Fluor® 488 chicken anti-mouse IgG (Invitrogen™) diluted 1:250 in 1% BSA in PBS. Cells were then washed four times with 1X PBS and left in 100 µL PBS for imaging by the IncuCyte® ZOOM instrument (Essen BioScience) with a 10x objective.

2.5.3 IncuCyte® ZOOM imaging and analysis

To quantify polyomavirus-infected cells, the IncuCyte® ZOOM analysis software version 2018A (Essen BioScience) was used to enumerate green cells in each well. Green cells exhibited distinct, nuclear VP1 staining and, therefore, represented infected cells. The default processing definition for image analysis was modified for the green channel to optimise detection of infected cells (Table 2.2).

Three non-overlapping fluorescent images were used to calculate the mean number of green cells per image and the software extrapolated this value to predict the total number of infected cells per well (Stewart *et al.*, 2015). The number of infected cells per well was then multiplied by the reciprocal of each dilution factor. The resulting value was then corrected for input volume, calculating the viral titre which was given as infectious units per mL (IU/mL).

Table 2.2 Modifications to the default processing definition used for image analysis on the IncuCyte® ZOOM software. The following changes were made to the default processing definition used to analyse the number of infected cells per image, in order to optimise the algorithm used for green cell detection.

Parameters	Top-Hat
Radius (μm)	100.00
Threshold (GCU)	2.0000
Edge Split	On
Filters	
Area (μm^2)	Min: 120.00, Max: 1000.0
Mean Intensity	Min: 3.0000

2.6 Generation of interferon-stimulated gene (ISG)-expressing lentiviruses

Lentiviral pseudoparticles expressing individual ISGs were generated by co-transfection of ISG-encoding SCRPSY, HIV-1 gag–pol and VSV-G plasmids (Sam Wilson, Centre for Virus Research, UK) in a ratio of 5:5:1, respectively. For 10 cm dishes, 11 µg total DNA was combined with 500 µL Opti-MEM™ I Reduced Serum Medium and mixed by vortexing. Polyethylenimine (PEI) was added to the diluted DNA with 4 µL of PEI per µg of DNA being used. The DNA/PEI mixture was incubated 30 minutes at room temperature, followed by dropwise addition onto 80% confluent HEK-293TT cells. Transfections were carried out overnight, upon which the medium containing transfection complexes was removed and replaced with fresh DMEM. Supernatants were collected at 72 hours post-transfection and clarified by filtration using 0.45 µm filters (Minisart™, Sartorius Stedim Biotech). Aliquots were rapidly frozen on dry ice and transferred at -80°C for long-term storage.

2.6.1 Lentiviral transductions of cells

For transduction assays, cells were seeded in 6-well (10^5 cells/well) or 96-well (10^3 cells/well) plates. Target cell lines were incubated overnight with ISG-expressing lentiviruses diluted in a 1:3 ratio in transduction medium, consisting of 25 mM HEPES and 4 µg/ml polybrene in DMEM. The following day, lentivirus-containing medium was removed, cells were washed in 1X PBS and returned to normal growth medium. TagRFP, which is encoded within the SCRPSY lentiviral plasmid, was confirmed to be expressed on ECLIPSE TS100 (Nikon) configured with the epi-fluorescence attachment and was used as a marker for transduction. Cells were then infected with viral stocks as detailed in section 2.7.1.

2.6.2 Generation of ISG-expressing stable cell lines

Stable cell lines expressing individual ISGs were generated using Vero cells. Cells were seeded as 3 x 10^5 per well in 6-well plates. The following day, cells were transduced with 500 µL ISG-expressing lentiviruses in 1.5 mL transduction media and incubated overnight. Lentivirus-containing medium was then replaced with growth medium and at 48 hours post-transduction, cells were detached with trypsin and re-suspended in growth medium. A 1:3 dilution series

was performed across all wells of a 6-well plate and cells were left to adhere overnight. Media was replaced with 2 µg/mL puromycin (InvivoGen) in growth medium and cells were incubated for 2-3 days before the next antibiotic-containing medium change. This process continued until all mock-transduced cells in wells of higher dilutions were no longer viable. ‘Selected’ cells were trypsinized and re-seeded into 25 cm^2 tissue culture flasks. Polycloncal cell lines were then expanded in 75 cm^2 tissue culture flasks with antibiotic selection and cryopreserved as previously described (section 2.1.3).

2.7 Infections

2.7.1 Cell infections with polyomavirus stocks

Cells were infected with BKPyV, JCPyV or SV40 at the indicated MOI for 2 hours at 37°C. Virus was diluted in Opti-MEM™ I Reduced Serum Medium in a total volume of 500 µL (6-well plate) or 50µL (96-well plate) per well. The plate was gently rocked every 30 minutes during the 2 hour incubation period. The virus was then removed, cells were washed with 1X PBS and returned to their growth medium. Cells were collected through trypsin-mediated cell dissociation or scrapping, and processed for analysis at the indicated time post-infection.

For time-course experiments, cells were cooled at 4°C for 15 minutes prior to infection. Cells were infected with virus in cold Opti-MEM™ I Reduced Serum Medium at the indicated MOI and infections were synchronised for 1 hour at 4°C with gentle rocking every 15 minutes. The virus was removed through two washes in 1X PBS and infections were initiated by addition of growth media and a temperature shift to 37°C. Cells were harvested for processing as described above at the indicated time-point of infection.

2.7.2 Cell infections with Chikungunya virus

Chikungunya virus (CHIKV) infections were performed by Dr Marietta Müller under Biosafety Level 3 containment. Cells were seeded as 1.4×10^5 per well in a 12-well plate format and transduced as previously described (section 2.6.1). Transduced cells were infected with CHIKV-ICRES-nsP3-ZsGreen at MOI 10 for 24 hours. Cells were then fixed with 4% paraformaldehyde for 10 minutes and analysed by flow cytometry.

2.7.3 Cell infections with polyomavirus-containing media

Vero or RPTE cells were seeded as 2 x 10^3 cells per well in a 96-well plate and left to attach overnight. Cells were infected the following day with 100 µL of virus-containing media for 2 hours at 37°C. Following removal of the virus inoculum, cells were incubated for a total of 48 hours post-infection and infected cells were fixed and processed for IncuCyte® ZOOM imaging and analysis (Figure 2.2).

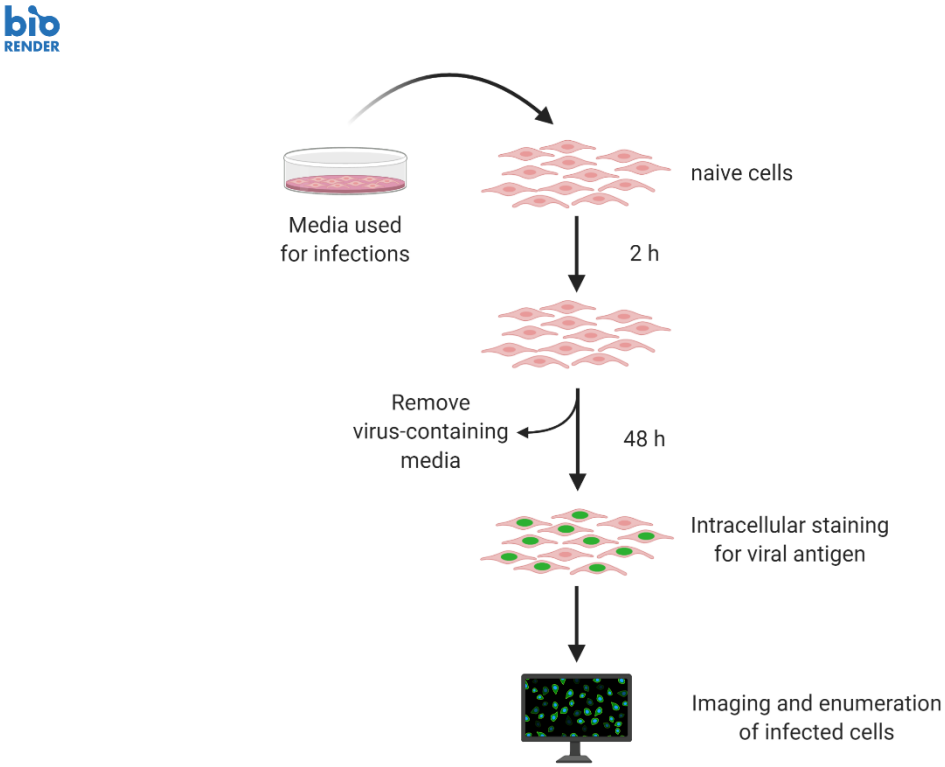

Figure 2.2 The virion release assay. Naïve cells are infected for 2 hours with virus-containing media, previously collected from infected cells. Following the removal of virus-containing inoculum, cells are incubated for 48 hours prior to fixation. Cells are labelled green for viral antigen through indirect immunofluorescence staining and imaged by the IncuCyte® ZOOM instrument. Green cells are enumerated to determine the number of infected cells per well. Created with BioRender.com.

2.8 Cell treatments with cytokines and chemical inhibitors

Recombinant human interferon alpha 2a (IFN-α) protein (Novus Biologicals) was dissolved in sterile water for a 1 mg/mL solution. Recombinant interferon gamma (IFN-γ) protein (PeproTech) was reconstituted in 0.1% BSA in 1X PBS to give a solution of 10^7 U/mL. RPTE cells were treated with various concentrations of IFN-α or IFN-γ in complete growth medium at 4 hours post-infection.

A 2 mg/mL cidofovir (Cayman Chemicals) solution was prepared in PBS and cells were treated at 2 hours post-infection with 40 µg/mL cidofovir, added directly to the growth medium (Bernhoff *et al.*, 2008). OGT 2115 (Tocris Bioscience) powder was dissolved in DMSO to prepare a 10 mM stock solution. Treatment of cells with 10 µM OGT 2115 in DMEM was performed 24 hours prior to infection and for the duration of the assay.

2.9 Precipitation of anti-VP1 antibody from hybridoma cell supernatant

Hybridoma cells secreting anti-VP1 antibody PAB597 (Christopher Buck, NCI, USA) were cultured in suspension in RPMI-1640 Medium (25 mM HEPES and $NaHCO_3$; Sigma-Aldrich) supplemented with Hybridoma Fusion and Cloning Supplement (HFCS; Roche), 10% FBS, non-essential amino acids, Glutamax-1 and penicillin/streptomycin. The antibody is released in the media of these cells which is subsequently subjected to ammonium sulphate precipitation. An equal volume of saturated ammonium sulphate (4.32 M) was added gently to the hybridoma supernatant and precipitation occurred for 30 minutes at room temperature. The mixture was centrifuged at 3,000 x g for 20 minutes and the precipitate was re-suspended in 5 mL 1X PBS. To remove any remaining ammonium sulphate, the antibody sample was dialysed in PBS at 4°C for 16 h using the Slide-A-Lyzer™ Dialysis cassette (Extra Strength; 10,000 MWCO) (Life Sciences). PAB597 is cross-reactive against the VP1 proteins of SV40, BK and JC polyomaviruses.

2.10 SDS-PAGE and Western blotting

2.10.1 Cells lysis for protein extraction

Cells were collected through enzymatic dissociation with trypsin or scrapping, and pelleted at 2,000 x g for 5 minutes. Cells were washed in 1X PBS and re-suspended in 100 µL RIPA lysis buffer (50 mM Tris pH 7.5, 150 mM NaCl, 1 mM EDTA, 10 mM NaF, 1% Triton X-100, 0.1% SDS, 0.5% sodium deoxycholate) supplemented with 1X cOmplete EDTA-free protease inhibitor cocktail (Roche). Lysis occurred on ice for 45 minutes and the resulting lysate was clarified at 13,870 x g for 10 minutes at 4°C. The supernatant containing the cell lysate was then used in a bicinchoninic acid (BCA) assay to determine protein concentration.

2.10.2 Bicinchoninic acid (BCA) assay for total protein quantitation

A serial dilution of protein standards were prepared from 2 mg/mL BSA, according to the Pierce™ BCA Protein assay kit (Thermo Scientific). Following the microplate procedure detailed in the instructions of this kit, 5 µL of each standard or unknown sample were mixed with 100 µL working reagent (1:20 ratio) into a well of a 96-well plate. The plate was mixed thoroughly on a rocker for 30 seconds, followed by a 30 minute incubation at 37°C in the dark. The plate was then cooled to room temperature and the absorbance was measured in a PowerWave XS2 Microplate Spectrophotometer (BioTek Instruments) at a wavelength of 562 nm. Data was extracted from Gen5™ version 1.11 (BioTek) and a standard curve was plotted in Microsoft Excel (2013) for the absorbance values of samples with known concentrations. A linear curve was fitted to these standard points and the protein concentration of unknown samples was then calculated in µg/mL, using a linear equation.

2.10.3 Preparation of samples

Protein-containing samples were prepared for sodium dodecyl sulphate-polyacrylamide gel electrophoresis (SDS-PAGE) through mixing of 4X NuPAGE™ LDS Sample Buffer (Invitrogen™) containing 0.1% β-mercaptoethanol, with 10-30 µg protein from lysates. Samples were heated to 95°C for 10 minutes and loaded directly onto a polyacrylamide gel.

2.10.4 Protein separation by SDS-PAGE

Polyacrylamide resolving gels were prepared with 8%, 10% or 12.5% Acrylamide/Bis-acrylamide (30%, 37.5:1; Severn Biotech), 375 mM Tris pH 8.8, 0.1% SDS, 0.1% APS and 0.1% TEMED. Stacking gel solution, containing 4% Acrylamide/Bis-acrylamide, 125 mM Tris pH 6.8, 0.1% SDS, 0.1% APS and 0.1% TEMED, was allowed to polymerise above a resolving gel, with a 10- or 15-well comb inserted. The thickness of the gels was 1.0 or 1.5 mm, depending on the final sample volume loaded. Gels were assembled in a Mini-PROTEAN® Tetra cell (Bio-Rad) and electrophoresis occurred for 80 minutes at 120 V. A 1X SDS running buffer (25 mM Tris base, 250 mM glycine, 3.5 mM SDS) was used during electrophoresis to separate the proteins according to molecular weight in the discontinuous buffer system. Two µL of BLUeye Pre-Stained Protein Ladder (10-245 kDa; Geneflow) were used as a marker to determine the molecular weight of proteins.

2.10.5 Protein detection by Western blotting

Proteins separated by SDS-PAGE were then transferred from the gel onto an Amersham Protran 0.45 NC nitrocellulose membrane (GE Healthcare) soaked in 1X Transfer buffer (192 mM glycine, 25 mM Tris base, 20% (v/v) methanol). The gel, membrane and stacks of filter paper were assembled in a transfer cassette and loaded into the Trans-Blot® Turbo™ Instrument (Bio-Rad). Semi-dry transfer was performed at 25 V for 30 minutes. Non-specific antibody binding was reduced by incubating the membrane in 5% (w/v) dry skimmed milk dissolved in 1X Tris-Buffered Saline/Tween-20 buffer (TBS/T; 20 mM Tris pH 7.5, 137 mM NaCl, 0.1% Tween-20). Membrane blocking was performed for 1 hour at room temperature with rocking. Primary antibodies were diluted in 5% milk in 1X TBS/T and incubated with the membrane for 1 hour at room temperature or overnight at 4°C with gentle rocking (Table 2.3). Excess primary antibody was removed with three washes for 5 minutes in 1X TBS/T. HRP-conjugated secondary antibody was diluted in 5% milk in 1X TBS/T and added to the membrane for 1 hour at room temperature (Table 2.4). To remove excess secondary antibody, the membrane was washed four times in 1X TBS/T for 5 minutes each time.

The membrane was briefly incubated with Amersham™ ECL Western Blotting Detection Reagent (GE Healthcare), Amersham™ ECL Select Western Blotting Detection Reagent or alternative luminol and peroxide solutions at room temperature. Chemiluminescent signal was detected in an Amersham™ Hypercassette™ Autoradiography Cassette (GE Healthcare) by exposing CL-Xposure™ X-ray film (Thermo Scientific) to the membrane. The exposure time of the film to the membrane depended on the protein of interest to be detected. The film was processed automatically in a Compact X4 X-ray Film Processor (Xograph Imaging Systems).

Membranes were prepared for re-probing by removing antibodies from their antigens using 1X Re-blot Plus Strong Antibody Stripping Solution (Millipore). The membrane was submerged in stripping solution for 15 minutes at room temperature with gentle rocking. Following a brief wash in 1X TBS/T, the membrane was ready for re-probing with primary antibody.

Table 2.3 A list of targets for primary antibodies used in Western blotting. The host species, dilution for Western blot and the source for each antibody are also provided.

Immunogen	Host species	Dilution	Source
Agnoprotein (A81038P)	rabbit	1:10000	Ugo Moens, University of Tromsø, Norway
Large T-antigen (PAB108)	mouse	1:250	Daniel DiMaio, Yale University, USA
VP1 (PAB597)	mouse	1:250	Christopher Buck, NCI, USA
VP2/VP3 (ab53983)	rabbit	1:1000	Abcam
GAPDH (sc-365062)	mouse	1:5000	Santa Cruz Biotechnology

Table 2.4 The HRP-conjugated secondary antibodies used for chemiluminescent Western blotting.

HRP-conjugated secondary antibody	Dilution	Source
Goat anti-mouse IgG	1:5000	Sigma-Aldrich
Goat anti-rabbit IgG	1:4000	Sigma-Aldrich

2.10.6 Densitometry analysis

ImageJ 1.50i software (National Institutes of Health) was used to perform densitometry analysis of protein bands obtained through Western blotting. Scanned images of X-ray films were converted to 8-bit images, prior to obtaining the relative density of each protein band and quantifying it relative to a standard. This procedure was performed for both the protein of interest and GAPDH, which was used as a loading control. The density value was then calculated for the protein of interest relative to its corresponding GAPDH band. Data was analysed on Microsoft Excel (2013).

2.11 Virion binding assay

The virion binding assay was carried out on cells in suspension (Dugan *et al.*, 2008). Using Gibco® Cell Dissociation Buffer (enzyme-free; Thermo Fisher Scientific), 2.5 x 10^4 cells were collected per tube and pelleted. Each pellet was re-suspended in ice-cold Opti-MEM™ I Reduced Serum Medium and kept at 4°C for 15 minutes. Cells were then infected with AF488-BKPyV at MOI 0.2 and chilled at 4°C for 1 hour. The virus-containing inoculum was removed through two washes in ice-cold 1X PBS and cells were fixed in 4% paraformaldehyde for 10 minutes. Upon re-suspension in 250 µL 1X PBS, cells were immediately analysed by flow cytometry.

2.12 Flow cytometry

2.12.1 Indirect intracellular staining

Cells requiring indirect immunostaining for the detection of intracellular viral antigens were pelleted at 377.5 x g for 5 minutes. Following one wash in 1X PBS, fixation was performed for 10 minutes in 4% paraformaldehyde. To facilitate antibody binding to targets, cells were permeabilised with 0.1% Triton™ X-100 in 1X PBS for 10 minutes. Intracellular immunofluorescent staining for viral antigen was performed as described in 2.5.2. During all incubation periods cells were kept in suspension through gentle agitation on a rocker or inversion on a tube revolver. After the final wash, the cell pellet was re-suspended in 200-300 µL PBS, cells were placed on ice and immediately analysed by flow cytometry.

2.12.2 Data acquisition parameters

Flow cytometry of cells was conducted on a CytoFLEX S Flow Cytometer (Beckman Coulter). Data was acquired using the 488 nm and 561 nm laser lines, with a configuration of 525/40 and 585/42 band pass filters, respectively. The gains used for different assays are listed on Table 2.5. Compensation was assessed and determined not to be required for these assays.

Table 2.5 Acquisition parameters for flow cytometry of different assays.

	Configuration			
	488_525-40	**561_585-42**	**Assay**	**Live cells/sample**
Gain	115	167	BKPyV infection	20,000
	80	80	AF488-BKPyV binding	5,000

2.12.3 Gating strategy

Cell populations were gated to include live cells only. A gate was then applied onto the live cell population to select the TagRFP-expressing red cell population, representing ISG expression, and was facilitated by a red-only control sample. Using infected cells which did not express TagRFP as a green-only control, a second gate was applied onto the live cell population to select all infected cells. The green (infected) cells within the red population were enumerated and presented as a percentage of the red parent population (yellow circles; Figure 2.3). Data was analysed on CytExpert Software version 2.1 (Beckman Coulter), with further analysis conducted on Microsoft Excel (2013).

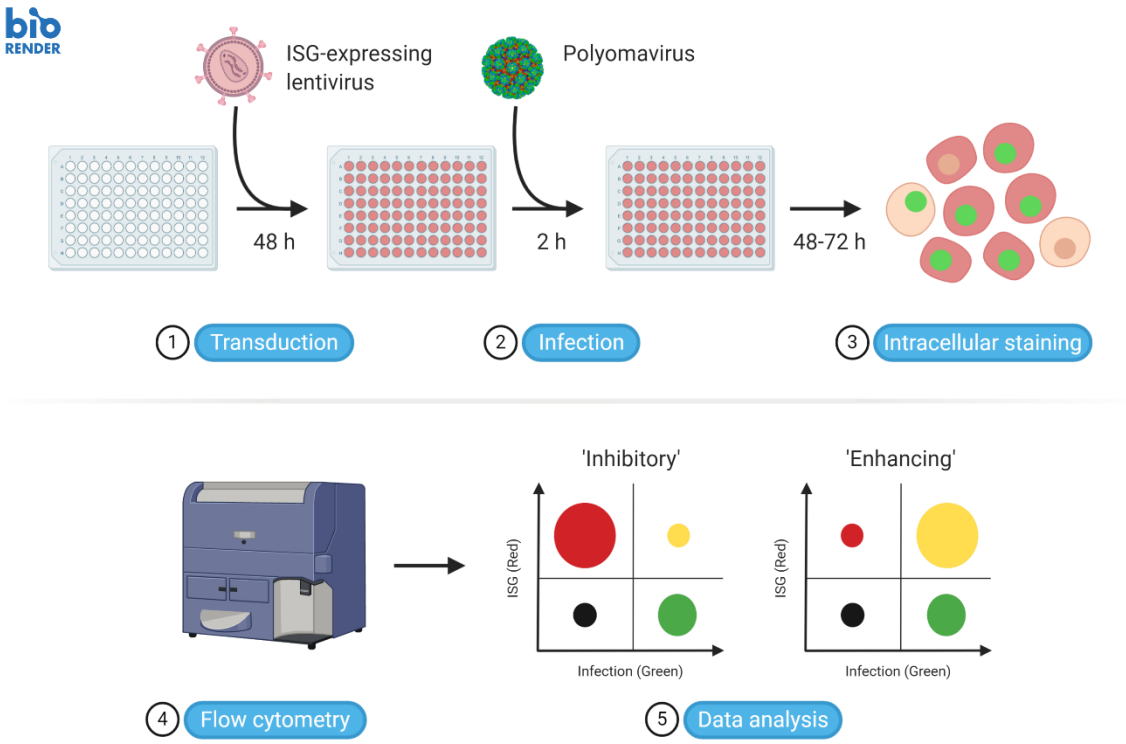

Figure 2.3 Workflow of the flow cytometry-based ISG overexpression assay. Cells are transduced by ISG-expressing lentiviral particles, which co-express a red fluorescent protein (1). At 48 hours post-transduction, cells are infected with virus (2) for 2 hours, whereupon cells are washed and returned to their normal growth medium. At 48-72 hours post-infection, cells are fixed and stained green with antibody against the viral antigen (3). Samples are then analysed by flow cytometry (4) to determine the percentage of double positive cells (red and green) within the red cell population (5). Created with BioRender.com.

2.13 VP2/VP3 exposure assay

Cells were seeded on 13 mm diameter coverslips (VWR) placed in 24-well plates and infected at 90% confluency with MOI 0.5. Infections were synchronised as previously described (2.7.1). Upon washing away the virus, cells were either returned to normal growth medium or treated with 25 mM NH_4Cl (Sigma-Aldrich) diluted in growth medium for the duration of the experiment. NH_4Cl treatment served as a control for the prevention of BKPyV intracellular trafficking (Eash, Querbes and Atwood, 2004). To assess VP2/VP3 exposure, cells were fixed with 4% paraformaldehyde at 10 hours post-infection and processed for immunofluorescent staining and confocal imaging (section 2.14).

2.14 Immunofluorescence staining for confocal imaging

The membranes of fixed cells were disrupted with 0.1% Triton in 1X PBS for 15 minutes and non-specific targets were blocked by incubating cells with 1% BSA in 1X PBS for 45 minutes at room temperature. Primary antibodies (Table 2.6) were diluted in 1% BSA in 1X PBS and left to bind their antigen overnight at 4°C. Following four washes with 1X PBS, cells were incubated with secondary antibody (Table 2.7) diluted in 1% BSA in 1X PBS for 2 hours at room temperature. Excess secondary antibody was removed with four washes in 1X PBS and coverslips were mounted onto microscope slides with 4 µL ProLong™ Gold Antifade Mountant with DAPI (Invitrogen™). Samples were imaged with the LSM 700 laser scanning confocal microscope (Carl Zeiss) under a 63x/1.4 oil-immersion objective lens. Images were exported from ZEN Black 2.3 (Carl Zeiss) and mean fluorescence intensity from VP2/VP3 puncta was quantified using ImageJ software.

Table 2.6 Primary antibodies used for immunofluorescence staining.

Immunogen	Host species	Dilution	Source
Protein Disulphide Isomerase (PDI) (MA3-019)	mouse	1:100	Thermo Fisher
VP2/VP3 (ab53983)	rabbit	1:500	Abcam

Table 2.7 Alexa Fluor®-conjugated secondary antibodies used for immunofluorescence staining.

Fluorochrome-conjugated secondary antibody	Dilution	Source
Alexa Fluor® 488 chicken anti-rabbit IgG	1:1000	Invitrogen™, Thermo Fisher Scientific
Alexa Fluor® 633 goat anti-mouse IgG	1:400	Invitrogen™, Thermo Fisher Scientific

2.15 Quantitative Polymerase Chain Reaction (qPCR)

To quantify viral DNA load from cells, DNA was extracted and purified from cultured cells using the E.Z.N.A® Tissue DNA Kit (Omega Bio-tek). RNA was removed by incubation with 4 µL of an RNAse A/T1 (2 mg/mL and 5000 U/mL) mix (Thermo Scientific) for 2 minutes at room temperature. The quantitative Polymerase Chain Reaction (qPCR) was performed on a CFX-Connect Real-Time PCR Detection System (Bio-Rad) and 10 ng DNA was amplified with the SsoAdvanced™ Universal SYBR Green® Supermix (Bio-Rad). The qPCR conditions used are listed on Table 2.8 and the specific primers used for the BK Dunlop viral genome are given on Table 2.9. A standard curve was generated in CFX Maestro™ Software (Bio-Rad) by determining the genome copy number of six serial dilutions of the GEM7-BKPyV-Dunlop plasmid. The genome copy number per µg was calculated for each unknown sample using the genome copy number values produced by the software.

Table 2.8 Cycling conditions implemented for quantitative Polymerase Chain Reaction (qPCR).

Temperature (°C)	Time	
95.0	3 minutes	
95.0	10 seconds	40 cycles
60.0	10 seconds	
72.0	30 seconds	
95.0	10 seconds	
65.0-95.0 at 0.5°C increments	5 seconds per step	Melt curve

Table 2.9 Primers used for the amplification of 152- and 164-base-pair fragments of the large T-antigen to quantify viral DNA load. 'F' and 'R' represent the forward and reverse primers, respectively.

Primer sequence	Literature
F: 5'-AAGGAAAGGCTGGATTCTGA-3'	Jiang *et al.* (2011)
R: 5'-TGTGATTGGGATTCAGTGCT-3'	

2.16 Quantitative reverse transcription PCR (RT-qPCR)

Total RNA was extracted from cultured cells using the E.Z.N.A.® Total RNA Kit I (Omega Bio-tek). RNA was treated with DNAse I (QIAGEN), as per the manufacturer's instructions, and 1 µg of total RNA was reverse transcribed in a T100™ Thermal Cycler (Bio-Rad) using the iScript™ cDNA Synthesis Kit (Bio-Rad). Quantitative PCR was performed using the SsoAdvanced™ Universal SYBR Green® Supermix (Bio-Rad) and the primers reported on Table 2.10. Cycling conditions used for the qPCR are detailed on Table 2.8 and the reaction was carried out on the CFX-Connect Real-Time PCR Detection System (Bio-Rad). The comparative C_T ($2^{-\Delta\Delta C_T}$) method was used to determine the fold change in the gene of interest, normalised to U6 mRNA (Livak and Schmittgen, 2001).

Table 2.10 A list of primers used for gene expression analysis. 'F' denotes the forward primer, while 'R' corresponds to the reverse primer.

Gene	Primer sequence	Literature
BK large T-antigen	F: 5'-GAGTAGCTCAGAGGTGCCAACC-3' R: 5'-CATCACTGGCAAACATATCTTCATGGC-3'	An *et al.* (2019)
BK VP1	F: 5'-CCAGATGAAAACCTTAGGGGCTT-3' R: 5'-AGATTTCCACAGGTTAGGTCCTCATT-3'	Gambarino *et al.* (2011)
HPSE	F: 5'-TACCTTCATTGCACAAACACTG-3' R: 5'-ACTTGGTGACATTATGGAGGTT-3'	Zcharia *et al.* (2009)
IRF1	F: 5'-GAGGAGGTGAAAGACCAGAGCA-3' R: 5'-TAGCATCTCGGCTGGACTTCGA-3'	Kooreman *et al.* (2017)
U6	F: 5'-CTGGCTTCGGCAGCACA-3' R: 5'-AACGCTTCACGAATTTGCGT-3'	Zhao *et al.* (2018)

2.17 Statistical analysis

Unpaired t test, with Welch's correction where appropriate, was performed using GraphPad Prism version 8.4.2 for Windows, GraphPad Software, La Jolla California USA, www.graphpad.com.

Chapter 3

Identification of antiviral genes against BKPyV infection

3.1 Introduction

3.1.1 Requirement for an ISG screen in BKPyV infection

To-date, the innate immune response to BKPyV remains poorly understood. Characterising the relationship between components of innate immunity and BKPyV may prove beneficial in understanding how the virus is able to infect, replicate and establish persistence within its host, while circumventing immune defences. From the perspective of the immunosuppressed host, studies into the interaction between the virus and innate immunity may also provide insights into how the virus is able to replicate without being controlled during reduction of immunosuppressive medication. Expanding our knowledge regarding the immune response to BKPyV infection may help in better management of BKPyV-associated diseases.

Approaches in investigating innate immune responses against BKPyV infection have focused on transcriptome profiling, multiplex cytokine assays and immune factor localisation experiments in human renal proximal tubule epithelial (RPTE) cells (Assetta *et al.*, 2016; de Kort *et al.*, 2017; An *et al.*, 2019). Evidence stemming from these studies support little or even complete absence of immune surveillance in RPTE cells – the main site of infection and persistence. However, findings indicate that BKPyV maintains sensitivity to the actions of interferon (Abend *et al.*, 2007). Thus, to further understand the extent to which BKPyV may be engaging an antiviral response, we focused on the effectors of interferon, the ISGs. We investigated the effect of individuals ISGs on polyomavirus infection through an overexpression assay.

The gain-of-function screening assay, adapted and conducted herein, was first described for a large-scale screen performed against diverse viral species; mostly RNA and some DNA viruses (Schoggins *et al.*, 2011). To construct the ISG library used in their screen, Schoggins *et al.* (2011) analysed microarray data of IFN-treated cells or tissues and established inclusion criteria. The genes compiled were derived only from type I IFN-treated cells or tissues, had a fold change greater than 2 or 4, and originated from early time-points (4, 6, 8 h). A

selection from this large ISG library was provided for this study. Adaptation of the gain-of-function screening assay was aimed at delivering a suitable flow cytometry-based method for polyomaviruses, which has yet to be reported in literature.

3.1.2 Chapter aims

The aims of this chapter are to demonstrate the propagation and titration of polyomavirus stocks, including BKPyV and SV40, for performing infection assays throughout this study. Then, susceptibility to the actions of interferons is investigated. Furthermore, the screening procedure is optimised using SV40 infection, prior to conducting the screen with BKPyV infection. Finally, this chapter aims to provide the basis for the following two chapters by identifying ISG ‘hits’ with potential anti-BKPyV activity to be studied in more detail.

3.2 Results

3.2.1 Generation of BK viral stock

3.2.1.1 BKPyV genome preparation through digestion and ligation

To address the first aim of propagating BKPyV stock, the viral genome was prepared for DNA transfection. The BKPyV Dunlop genome was enzymatically excised from pGEM7 plasmid DNA using the restriction enzyme BamHI-HF. Ten µg of pGEM7-BKPyV-Dunlop were used as starting material and the digestion reactions were performed in duplicate.

To enable successful gene expression and bi-directional replication from the genome, the digested, linear DNA was circularised in a ligation reaction with T4 DNA ligase occurring overnight. Ligation reactions were performed in duplicate and samples from both digestions and ligations were analysed on a 0.7% agarose gel at 100 V for 40 minutes. DNA bands were visualised for 2 seconds under UV illumination.

In Figure 3.1, lanes 3 and 4 depict two distinct bands representing the successful separation of the BKPyV genome (upper) and plasmid backbone (lower). Un-digested, pGEM7-BKPyV-Dunlop was also analysed on the same gel as a control for enzymatic digestion (lane 2). Lanes 5 and 6 indicate the presence of ligated products with approximate molecular weights of 3.0 and 5.0 kilobase pairs (kb). The latter represented the ligated form of BKPyV-Dunlop genome which consists of 5,153 base pairs (Seif, Khoury and Dhar, 1979), while the 3.0 kb band corresponds to plasmid DNA. Additional ligation products were generated during the reaction and, albeit, a purification step prior to DNA electrophoresis, were still observed on the gel.

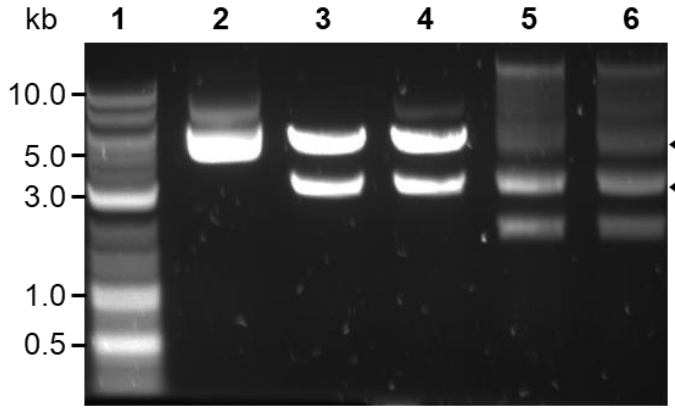

Lane	
1	1 kb Plus DNA Ladder (0.1-10 kb)
2	pGEM7-BKPyV-Dunlop
3-4	Digestion products
5-6	Ligation products

Figure 3.1 BKPyV genome preparation for transfections. Products generated following two independent digestion and ligation reactions were analysed on a 0.7% agarose gel run for 40 minutes at 100 V. Each lane was loaded with 500 ng DNA. Lane 2 represents un-digested pGEM7-BKPyV-Dunlop as a control for the digestion reaction. The image was obtained through UV illumination of the gel for 2 seconds and is representative of at least three independent experiments.

3.2.1.2 Transfection of BKPyV genome into primary RPTE cells

Following successful generation of circular BKPyV genome, virus propagation was initiated in permissive cells to produce BKPyV stocks for infection assays. This process, comprised of multiple steps (Figure 2.1), is simplified in Figure 3.2A.

Initially, the viral genome was transfected into RPTE cells to allow for virus production. At the end of a 14-day incubation period, samples were collected from RPTE cells and their media prior to harvesting cellular suspensions. Total protein content of cells and their media was analysed by SDS-PAGE and Western blot to detect viral antigens, which would suggest the presence of replicating and released BKPyV. Blots of media and lysates were both probed with an antibody raised against the major capsid protein of polyomavirus, VP1 (Figure 3.2B). Detection of the approximately 37 kDa GAPDH protein served as a loading control, to confirm an equal amount of total protein had been loaded.

VP1 was detected in the lysates (intracellular) and media (extracellular) of two independent cell cultures transfected with BKPyV genome (lanes 1-2), with double bands appearing in each lane. These protein bands corresponded to the expected molecular weight of VP1, which is approximately 42 kDa. Mock-transfected (M) cells lacked VP1-corresponding bands.

The detection of VP1 within lysates indicated late viral protein production and, hence, acted as a marker for intracellular BKPyV. VP1 detection in the culture medium served as a marker for released BKPyV virions.

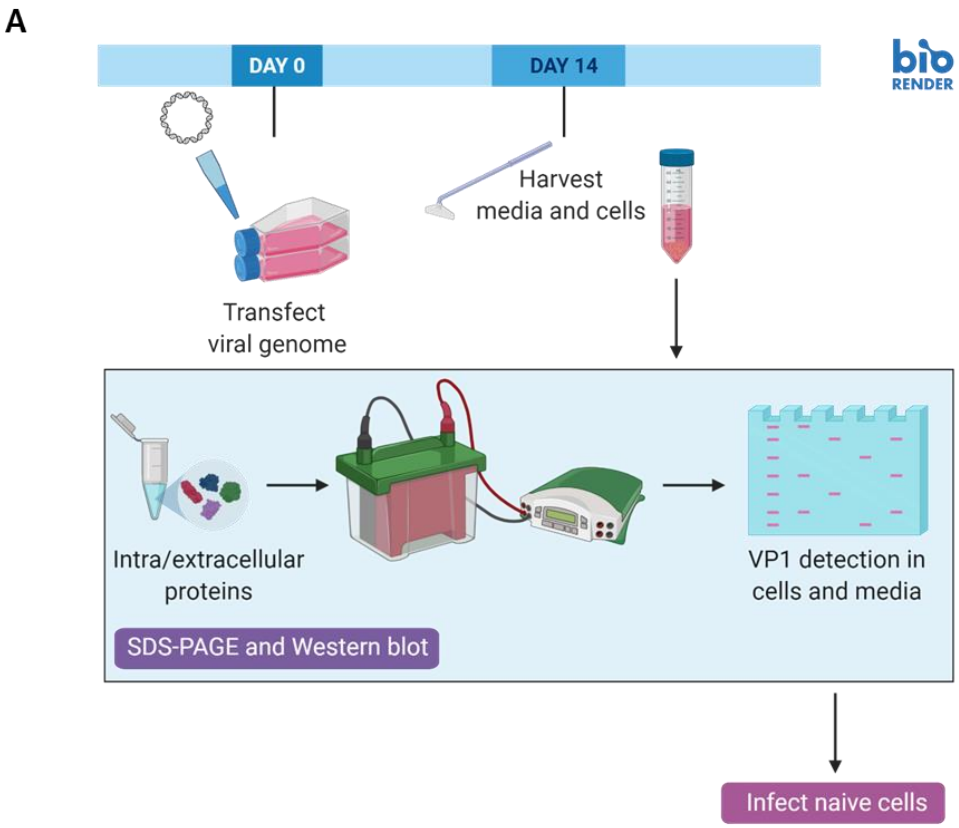

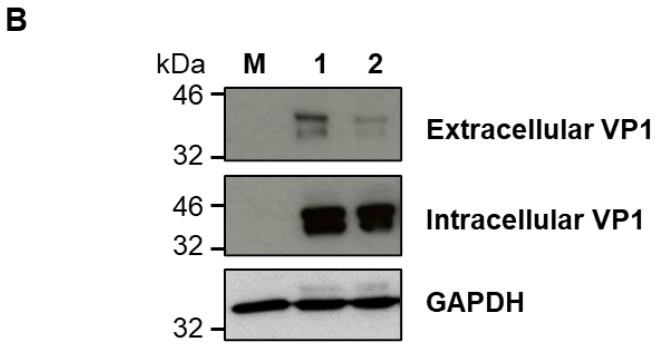

Figure 3.2 Transfection of BKPyV genome into RPTE cells. A) Simplified schematic of the multi-step process required for BKPyV stock generation. The process begins with viral genome transfection into RPTE cells. Transfected cells and media are harvested after 14 days as cell suspensions. This is followed by viral antigen detection through SDS-PAGE and Western blot. Created with BioRender.com. B) Cell lysates and media were collected from two RPTE cell culture flasks and their protein content was separated by SDS-PAGE. Thirty µL of media were loaded per lane. Western blot analysis was conducted for the presence of the major capsid protein, VP1. GAPDH served as a loading control. Blots are representative of at least three independent experiments. M: Mock-transfected cells/media, 1-2: BKPyV-transfected cells/media.

3.2.1.3 Infections of primary RPTE cells with viral lysate

Confirming the presence of cell-associated and released virus at the end of the transfection stage, led to BKPyV-containing cell suspensions being used for infections of naïve RPTE cells. This second round of cell infections was undertaken to generate sufficient quantities of BKPyV (Figure 3.3A).

After 14 days of incubation, samples of infected cells and their media were analysed by SDS-PAGE and Western blot. Cell lysates were probed for late viral proteins as a marker for intracellular BKPyV. Figure 3.3B depicts bands at 42 kDa, 38/26 kDa and 11 kDa, indicating the presence of VP1, VP2/3 and the agnoprotein, respectively, in infected cell lysates. This suggested that there was intracellular BKPyV following infections with BKPyV-containing cell suspensions. The presence of the major (VP1) and minor (VP2/3) capsid proteins in the culture media of infected cells also suggested that BKPyV was successfully secreted in the extracellular environment (Figure 3.3C).

Following viral antigen detection within the cellular lysate and medium, virus was purified from crude cell suspensions through two ultracentrifugation steps. The viral sample was first passed through a sucrose cushion and then overlaid onto a CsCl gradient, prior to extraction and dialysis. Purification served to concentrate virus stocks in smaller volumes and remove any non-BKPyV proteins from the preparation. Viral purification is also reported to remove other viruses and bacteria which may act as contaminants (Moriyama and Sorokin, 2009).

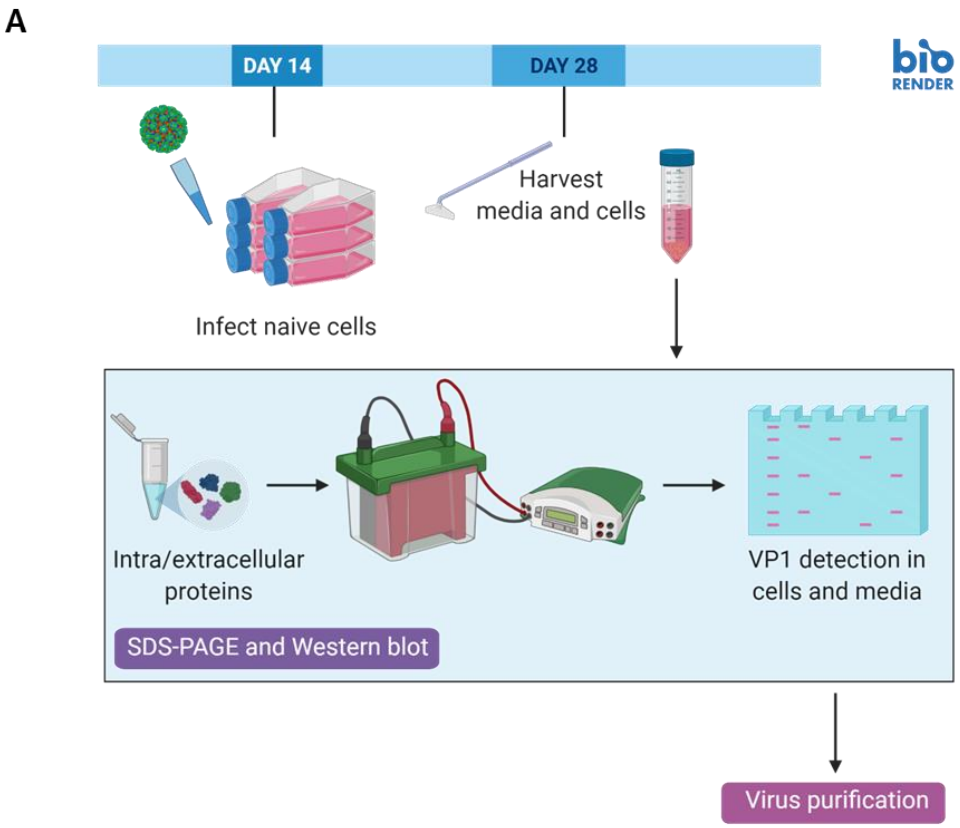

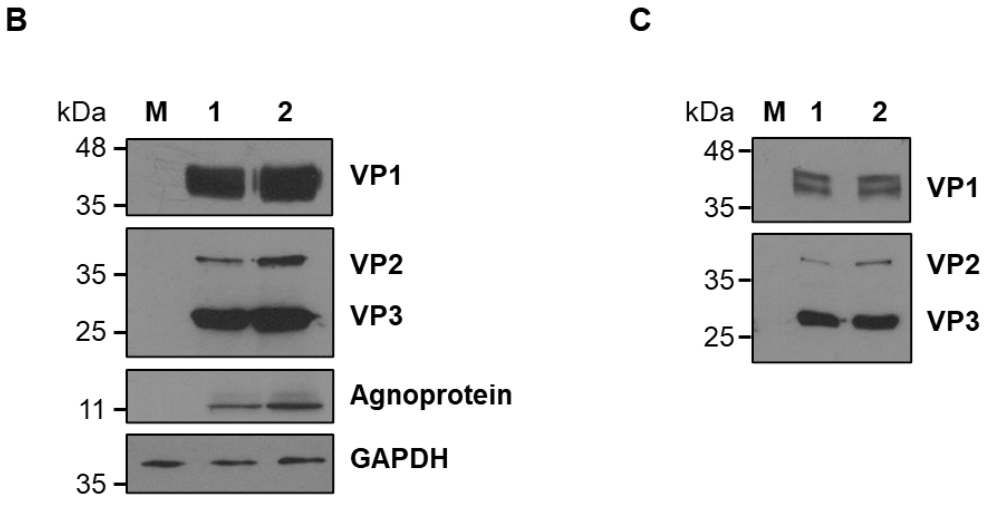

Figure 3.3 Infections of RPTE cells with BKPyV-containing cell suspensions. A) Simplified schematic of the multi-step process required for BKPyV stock generation. BKPyV-containing cell suspensions from transfected RPTE cell cultures are used to infect naïve RPTE cells for 14 days. Infected cells and media are then harvested as cell suspensions. This is followed by viral antigen detection in lysates and media samples through SDS-PAGE and Western blot. Created with BioRender.com. B) Infected RPTE cell lysates were probed for the presence of capsid proteins – VP1, VP2, VP3 – and the

agnoprotein. GAPDH acted as a loading control. M: Mock-infected cells, 1-2: BKPyV-infected cells. C) 30 µL of media samples were analysed for the presence of capsid proteins, VP1, VP2 and VP3. M: Mock-infected media, 1-2: BKPyV-infected media. Blots shown are representative of at least three independent experiments.

3.2.1.4 Titration of purified BKPyV stocks

To perform each experiment in this study under identical conditions, it was necessary to establish the amount of infectious particles within the resulting purified virus. Thus, the next experimental objective was to determine the titre of virus stock.

The plaque assay is a widely used approach to titre viruses, however, it can be time-consuming. Our method for determining the quantity of infectious virus relies on a fluorescent focus assay (FFA) followed by IncuCyte® ZOOM imaging. Serial two-fold dilutions were performed in 96-well plates seeded with RPTE cells. At 48 hours post-infection (hpi), the RPTE cell monolayer was fixed and indirectly labelled with green fluorescence for VP1. Cells emitting green fluorescence were determined to be VP1-positive and, thus, infected. The viral titre was calculated using the average number of infected cells from each well multiplied by the reciprocal of the dilution factor and the reciprocal of the sample volume added to the well (Moriyama and Sorokin, 2009; Stewart *et al.*, 2015).

Nuclear accumulation of VP1 was demonstrated in all wells, with the exception of mock-infected wells (Figure 3.4A). The number of infected RPTE cells decreased as the viral sample was diluted across the 96-well plate (Figure 3.4B). The infectious virus titre, given in infectious units per mL (IU/mL), was calculated for each dilution (Figure 3.4C) and averaged to 3×10^5 IU/mL for this specific BKPyV stock. Data presented here was obtained by titrating a sample from one batch of purified BKPyV and is representative of other FFAs performed during this study.

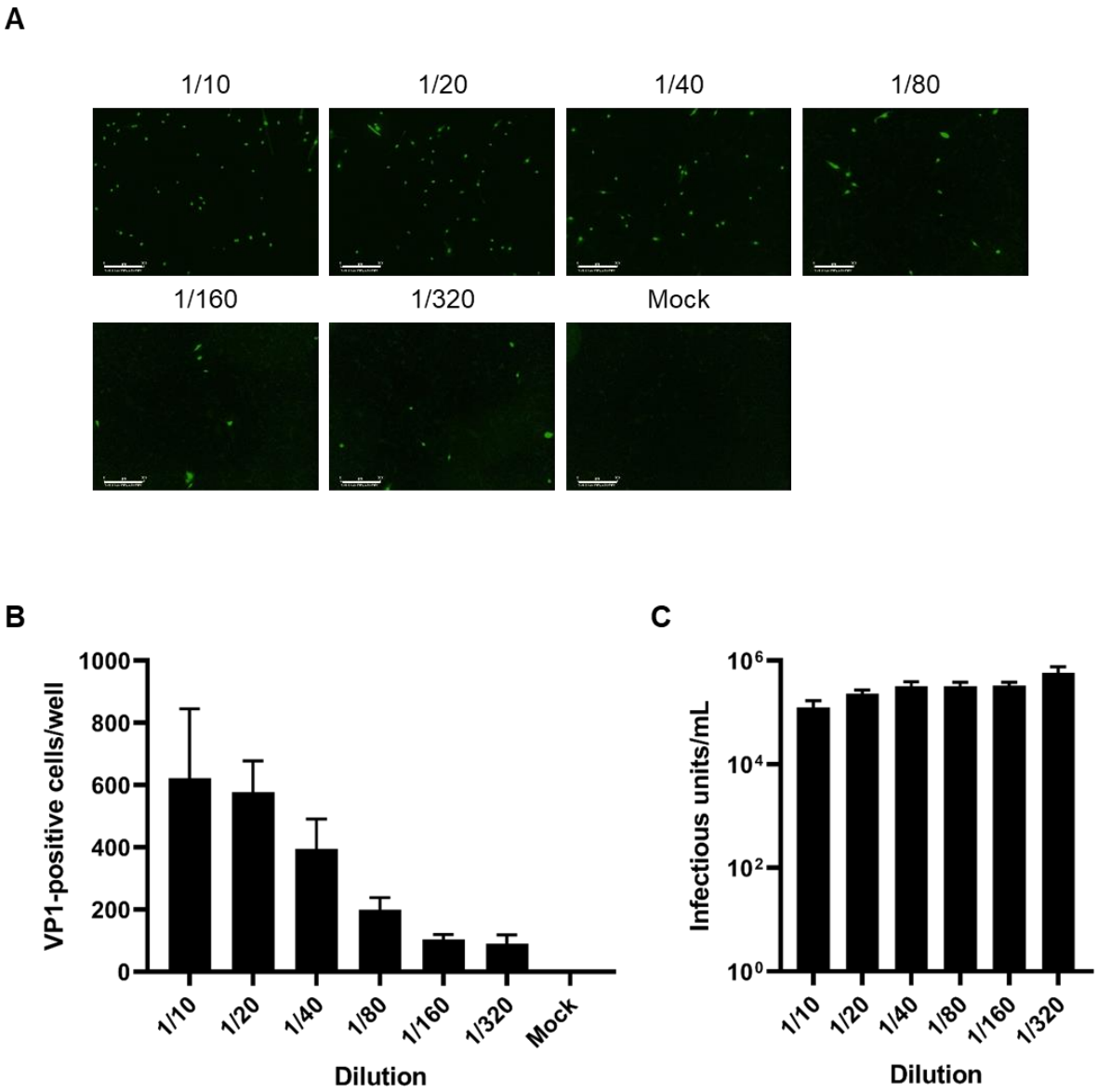

Figure 3.4 Titration of purified BKPyV stock. RPTE cells were infected with serially-diluted purified BKPyV for 2 h. At 48 hpi cells were labelled green for VP1 protein and imaged using IncuCyte® ZOOM. A) Green fluorescence images extracted from IncuCyte® ZOOM software. Numbers above images represent the dilution occurring in that specific well. Green dots represent VP1 and indicate localisation of VP1 in the nucleus of infected cells. Scale bar: 300 µm. B) The number of VP1-positive, infected cells per well was extrapolated by the software for each dilution performed. Mock: Mock-infected cells. C) The virus titre was determined by averaging the infectious units per mL calculated for each dilution. Error bars represent the mean ± the standard deviation (SD) of three technical repeats from a single representative experiment.

3.2.2 Generation of SV40 viral stock

3.2.2.1 Digestion and ligation of SV40 genome

Viral stocks of the non-human primate polyomavirus, SV40, were required during this investigation for optimisation and comparison studies.

In the first step of SV40 stock generation, the viral genome was prepared for cell transfections. The KpnI-HF restriction enzyme was allowed to digest 10 µg of pUC-SV40 for 2 hours and digested products were ligated with T4 DNA ligase in an overnight reaction.

Samples from two independent digestion reactions, followed each by a ligation reaction, were analysed on a 0.7% agarose gel at 100 V for 40 minutes. The resulting DNA bands were imaged for 2 seconds under UV illumination (Figure 3.5). Two distinct bands were present in lanes 3 and 4 loaded with digestion products. This observation suggested a separation of the viral genome ‘insert’ and plasmid DNA had taken place, when compared to the un-digested control of approximately 8.0 kb in lane 2. Furthermore, lanes 5 and 6 containing the ligation products show a distinct band where the SV40 genome is expected, at approximately 5.0 kb, suggesting successful ligation of the viral genome.

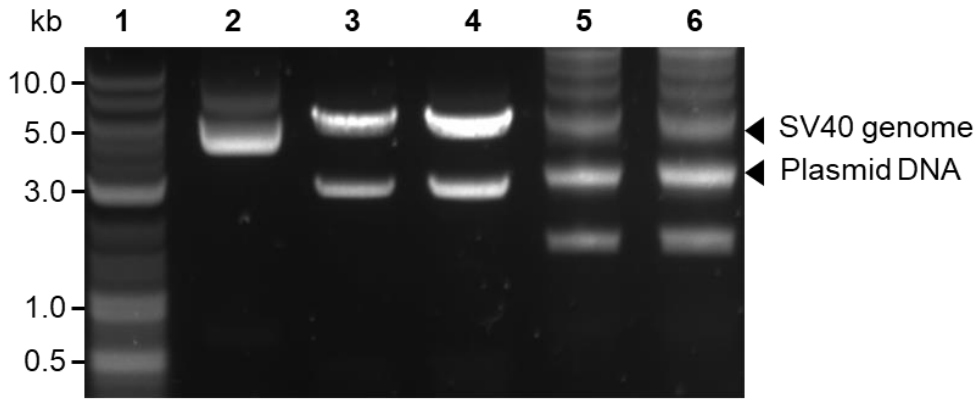

Lane	
1	1 kb Plus DNA Ladder (0.1-10 kb)
2	pUC-SV40
3-4	Digestion products
5-6	Ligation products

Figure 3.5 SV40 genome preparation for cell transfections. Digestion and ligation products, generated in two independent reactions, were analysed on a 0.7% agarose gel run for 40 minutes at 100 V. Each lane was loaded with 500 ng DNA. An image of the gel was taken during 2 seconds of UV exposure and is representative of at least three independent experiments.

3.2.2.2 Transfection of SV40 genome into Vero cells

SV40 propagation required the transfection of 4 µg circularised SV40 genome into two flasks cultured with Vero cells. Transfected cell cultures were incubated for a period of 7 days, at the end of which cultures were sampled and harvested. Cells were scrapped into their media, forming cell suspensions which were then sonicated, clarified and stored as viral stock (Figure 3.6A).

Total protein found in cellular lysates and media was assessed by SDS-PAGE and Western blot for the presence of late viral proteins, as markers for intracellular and extracellular SV40. Capsid proteins VP1, VP2 and VP3 were detected in both samples of SV40-transfected cell lysates (Figure 3.6B). GAPDH served as a loading control for proteins derived from cell lysates. Thirty µL of media from each flask were analysed for the presence of VP1 and its detection suggested that SV40 virions were secreted into the media of transfected cells (Figure 3.6C). Detection of viral antigens both in cells and their supernatants indicated successful cell transfections, leading to SV40 replication within Vero cells and subsequent virion secretion.

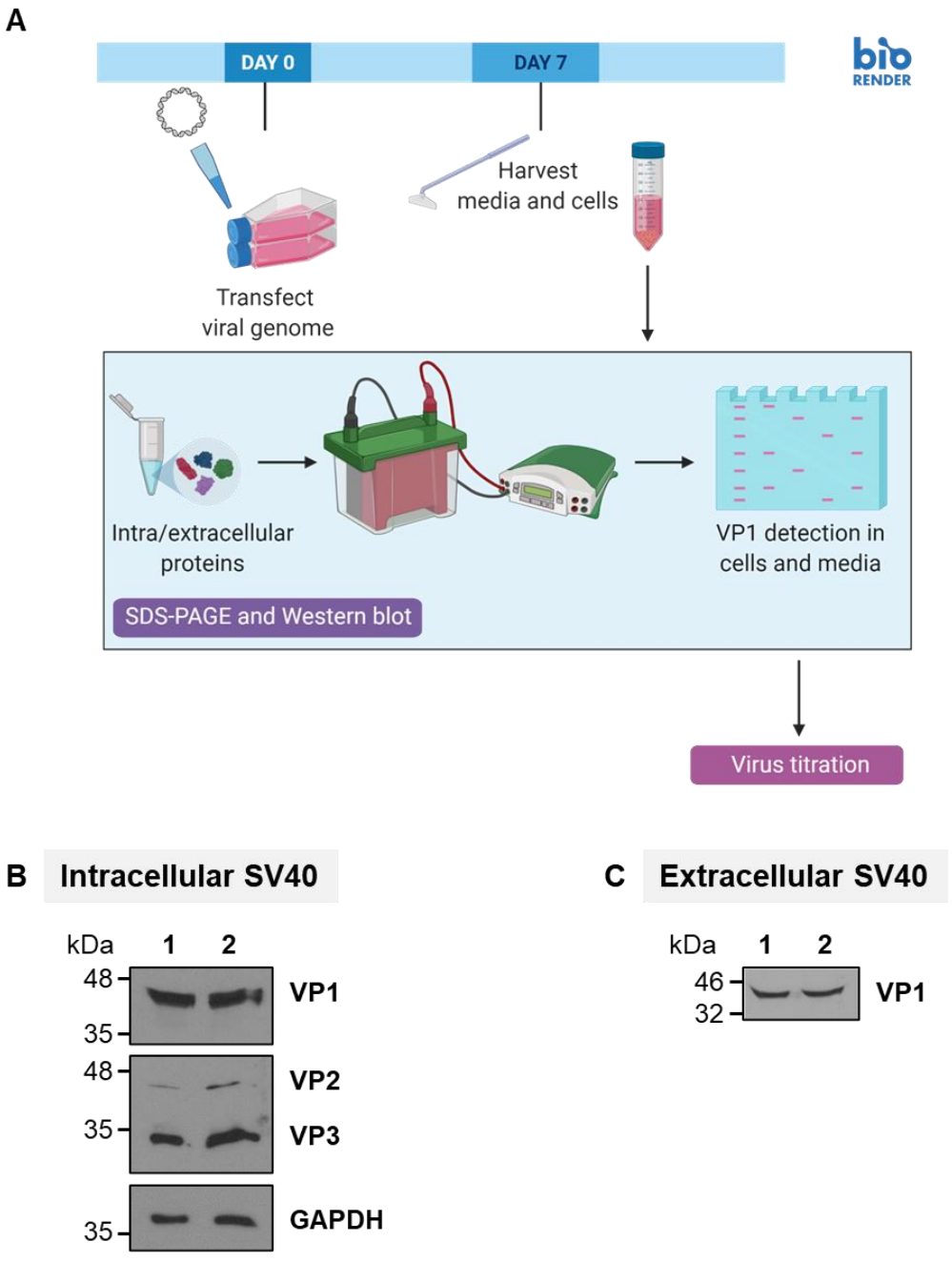

Figure 3.6 SV40 propagation in Vero cells. A) Schematic of SV40 stock production. Vero cells are transfected with SV40 viral genome and harvested at 7 days post-transfection. Samples are taken from cells and their media to be analysed by SDS-PAGE and Western blot techniques for the presence of viral antigens. B) Western blots of transfected cell lysates were probed with antibodies against VP1 and VP2/3 to detect intracellular SV40. GAPDH acted as a loading control. C) A Western blot of media from transfected cells was probed with an antibody against VP1 to detect secreted SV40. Representative blots are shown from at least three independent experiments.

3.2.2.3 Titration of crude SV40 stocks

To confirm the infectivity of the crude stock and determine the SV40 titre, an FFA was performed as described previously (section 3.2.1.4). Two-fold dilutions of SV40 stock were made across a 96-well plate cultured with Vero cells. Virus was allowed to infect cells for 2 hours, prior to removing any unbound virus and incubating with fresh media. Cells were fixed at 48 hours post-infection and labelled green for VP1, as a marker for infection.

The number of VP1-positive, infected cells per well decreased with each fold dilution (Figure 3.7A). Values for infectious units per mL were calculated for each dilution and the titre was averaged to 1 x 10^6 IU/mL for this specific batch of SV40 (Figure 3.7B). Data is representative of other FFAs performed on SV40 stocks during this study.

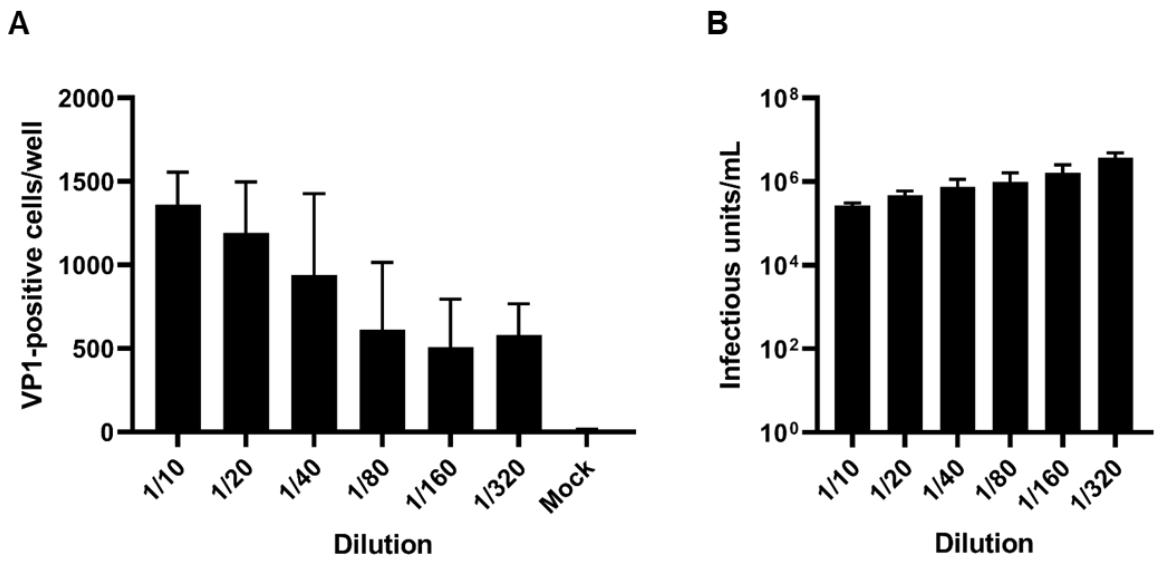

Figure 3.7 Infectious titre determination of SV40 viral stock. Vero cells were infected with two-fold serial dilutions of crude SV40 stock for 2 hours. At 48 hpi cells were labelled green for VP1 protein and imaged using IncuCyte® ZOOM. A) The number of VP1-positive, infected cells per well was extrapolated by the software for each dilution performed. Mock: Mock-infected cells. B) The virus titre was determined by averaging the infectious units per mL calculated for each dilution. Error bars represent the mean ± SD of three technical repeats from a single representative experiment.

3.2.2.4 Profile of SV40 infection in Vero cells

As optimisation of the screening assay was to be performed with SV40 infections, it was crucial to identify a time-point at which to assess polyomavirus infection. Therefore, we next sought to characterise the profile of the SV40 life cycle in Vero cells. Cells were infected with SV40 at an MOI of 1.0 for 2 hours and harvested at the indicated time-points following infection. Lysates and media were collected from each time-point. Western blot analysis of lysates was performed to probe for early and late viral proteins (Figure 3.7A). The earliest time-point at which large T-antigen (LT-Ag) is detected is 24 hours post-infection, while VP1 is first detected at 36 hours post-infection. Using the virus-containing media from the time-course assay, naïve Vero cells were infected in an FFA to investigate the release of infectious progeny (Figure 3.7B). While some infectious progeny was released at 36 hours post-infection, there was a steep increase in infectious units per mL at 48 hours post-infection. At the 48 hour time-point, early and late proteins were produced to detectable levels and infectious progeny was released into media, indicating that this time-point was an appropriate starting point for the screening assay.

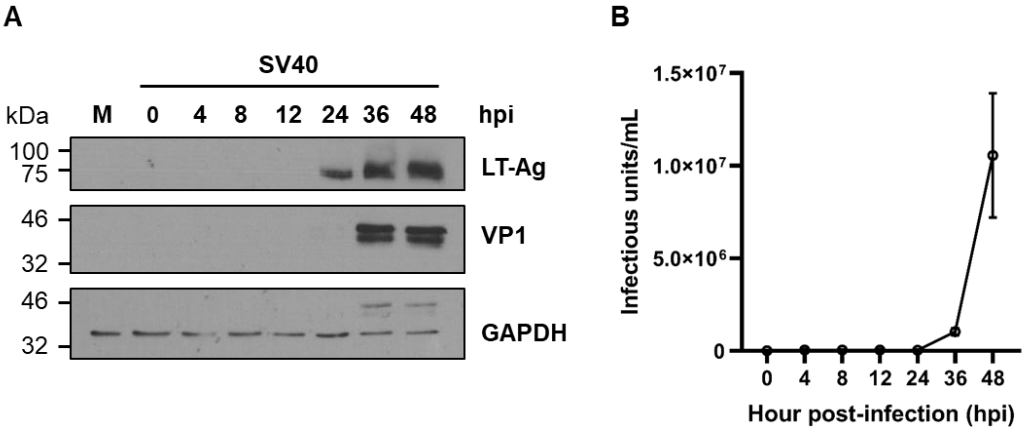

Figure 3.8 Detection of viral antigens and infectious progeny during the SV40 life cycle. Vero cells were infected with SV40 at MOI 1.0 for 2 hours and harvested at the indicated time-points following infection. Cells and media were collected from each time-point. A) Western blots of lysates probed for LT-Ag, VP1 and GAPDH. Representative blots are shown from three independent experiments. M: Mock-infected cells. B) The collected media was used to infect naïve Vero cells in an FFA to determine the IU/mL at the end of each time-point. Error bars represent the mean ± SD of three technical repeats from a single representative experiment.

3.2.3 Response of BKPyV infection to cytokine stimulation

3.2.3.1 Interferon gamma (IFN-γ) treatment of infected RPTE cells

The importance of cell-mediated immunity in controlling BKPyV persistent infection has been validated in several clinical reports. Since the presence of anti-BKPyV antibodies does not prevent the virus from replicating uncontrollably and causing PVAN, Abend *et al.* (2007) hypothesised that another aspect of the immune system may be involved in regulating persistent infection.

To recapitulate what Abend and colleagues (2007) have shown, we first infected primary RPTE cells with BKPyV at an MOI of 0.1. Infected cells were treated with 50 U/mL IFN-γ at 4 hours post-infection. Parallel treatment with 40 µg/mL of the nucleotide analogue cidofovir served as a control for the inhibition of BKPyV replication (Bernhoff *et al.*, 2008). At 72 hours post-infection, cells were harvested and total cell protein was collected. Lysates were analysed for VP1 by Western blot, indicating that VP1 levels were significantly decreased upon treatment with IFN-γ, compared to untreated cells (UNTR) (Figure 3.9A-B). A dose-dependent decrease in VP1 levels was observed at 72 hours post-infection when infected cells were treated with varying concentrations of IFN-γ (Figure 3.9C-D).

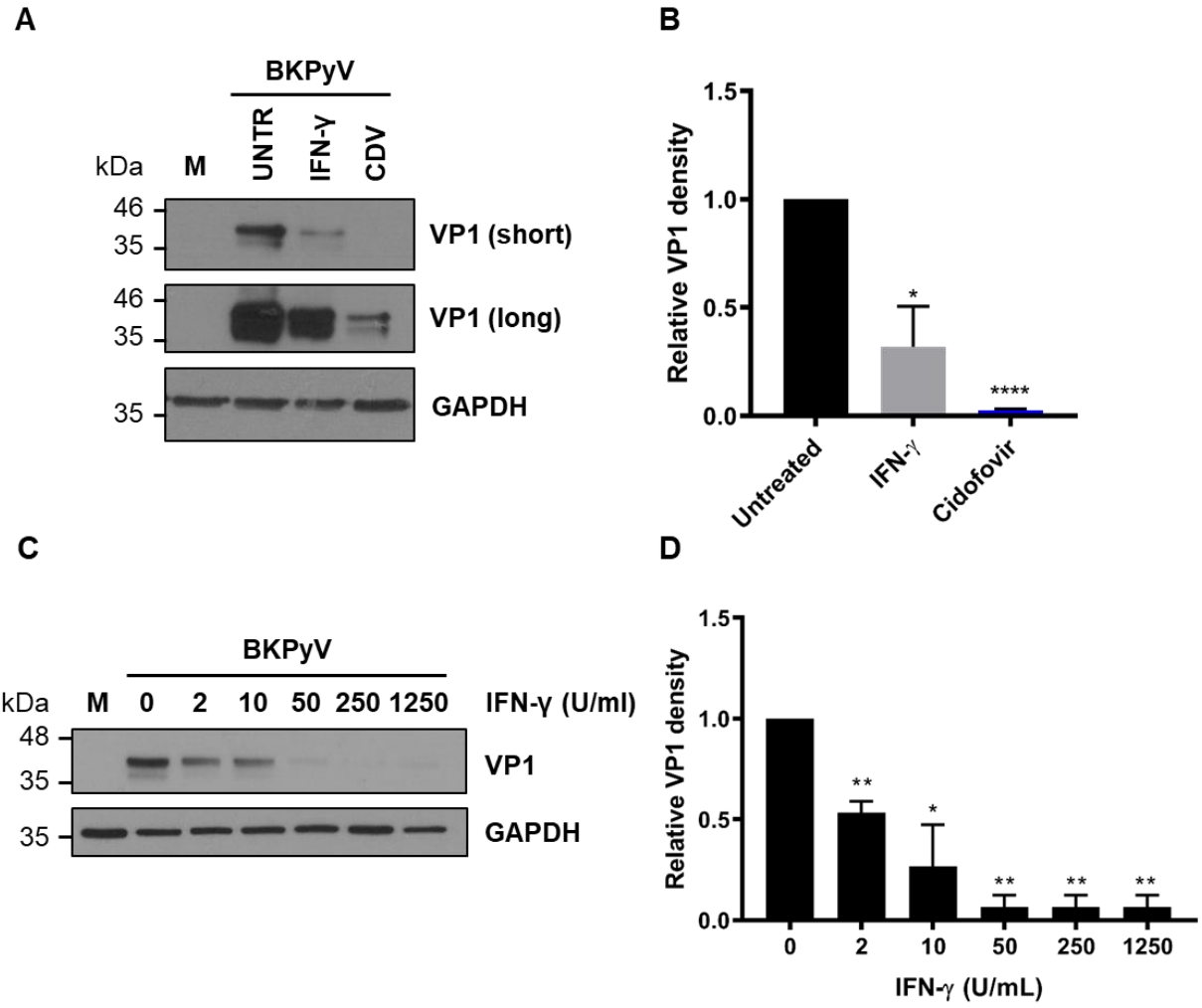

Figure 3.9 IFN-γ inhibition of BKPyV VP1 production in RPTE cells. RPTE cells were infected with BKPyV at MOI 0.1 and treated with IFN-γ at 4 hpi. Cells were harvested at 72 hpi and VP1 levels were assessed by Western blot. A) Representative Western blot of infected cells treated with 50 U/mL IFN-γ or left untreated (UNTR). Treatment with 40 µg/mL cidofovir (CDV) served as a control for the inhibition of BKPyV replication. B) Densitometry analysis from A. C) Representative Western blot of infected cells treated with varying concentrations of IFN-γ. D) Densitometry analysis from C. Values were calculated relative to untreated cells and represent the mean ± SD from three independent experiments (n=3). M: Mock-infected cells. * P≤0.05, ** P≤0.01, *** P≤0.001, **** P≤0.0001 (Welch's t-test).

3.2.3.2 Interferon alpha (IFN-α) treatment of infected RPTE cells

Furthermore, we examined the effect of IFN-α as a representative cytokine of the type I family of interferons. Primary RPTE cells were infected with BKPyV at an MOI of 0.1, followed by treatment with 50 ng/mL IFN-α after 4 hours. At 72 hours post-infection, cells were harvested and lysates were probed for VP1 protein in a Western blot. Cidofovir treatment of infected cells was performed as a control for inhibition of viral infection. VP1 levels were reduced dramatically by IFN-α (Figure 3.10A-B). Infected RPTE cells were then treated with varying concentrations of IFN-α at 4 hours post-infection. At 72 hours post-infection, cells were harvested and processed as described previously. Figure 3.10C-D demonstrates that IFN-α exhibited a dose-dependent inhibition of VP1 protein.

Together, these observations are in support of BKPyV infection being sensitive to both type I and II interferons. Type I interferons tend to be produced early on by infected cells upon viral invasion to activate the innate immune response. Type II interferons are predominantly produced by NK cells during this antiviral response to promote immunity against invading pathogens (Lee and Ashkar, 2018). By pursuing the events occurring early on during the antiviral response, we hypothesised that the IFN-susceptibility of BKPyV may be, in part, due to ISG activity. ISGs are induced following IFN signalling to bring about a cellular state ready to combat infection. The putative role of ISGs during BKPyV infection was further investigated with a gain-of-function screening assay.

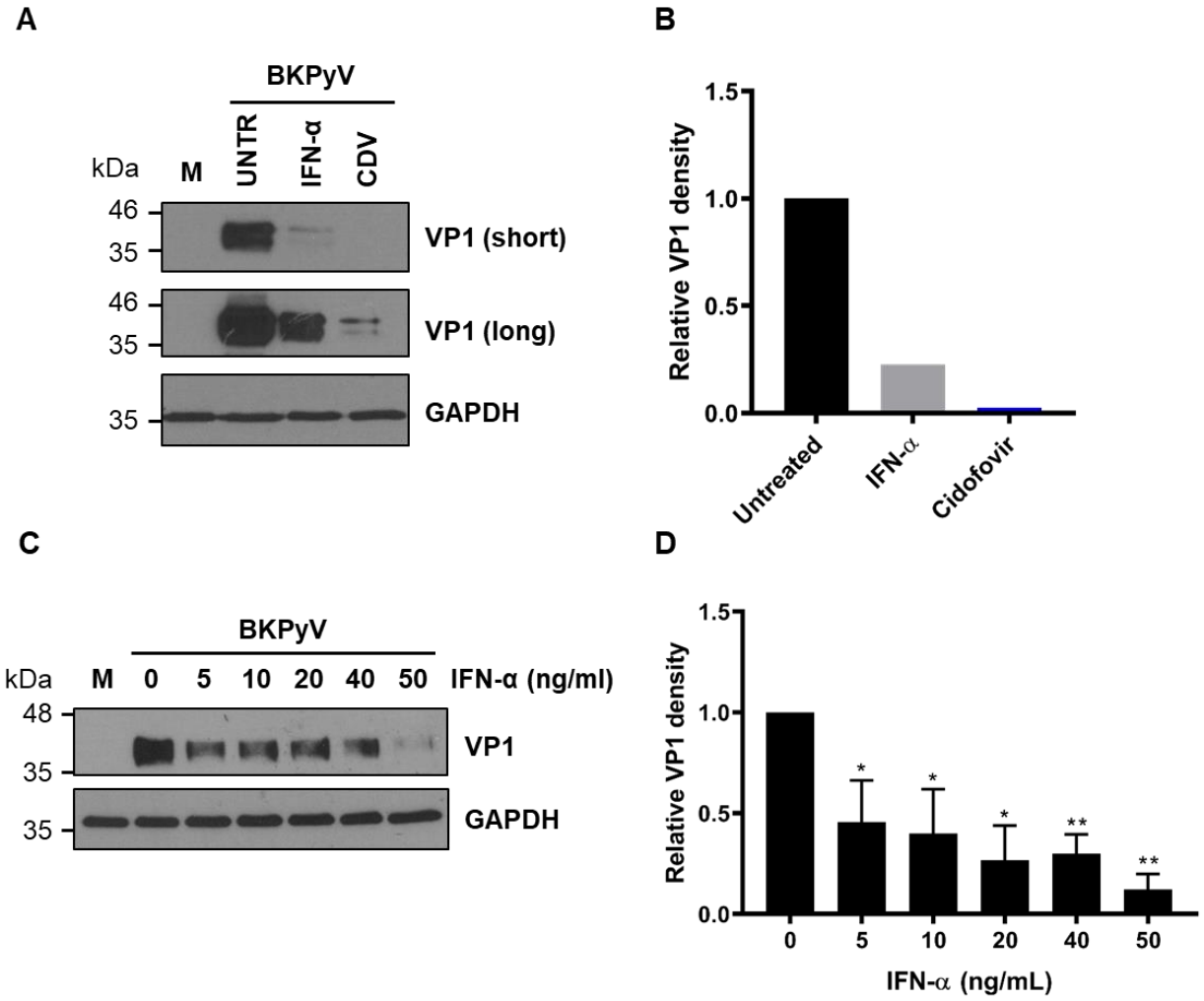

Figure 3.10 BKPyV VP1 production is inhibited in IFN-α-treated RPTE cells. RPTE cells were infected with BKPyV at MOI 0.1 and treated with IFN-α at 4 hpi. Cells were harvested at 72 hpi and VP1 levels were assessed by Western blot. A) Representative blot of infected cells treated with 50 ng/mL IFN-α or left untreated (UNTR). Treatment with 40 µg/mL cidofovir (CDV) served as a control for the inhibition of BKPyV replication. B) Densitometry analysis from A. Values were calculated relative to untreated cells and represent the mean of two independent experiments (n=2). C) Representative blot of infected cells treated with varying concentrations of IFN-α. D) Densitometry analysis from C. Values were calculated relative to untreated cells and represent the mean ± SD from three independent experiments (n=3). M: Mock-infected cells. * P≤0.05, ** P≤0.01, *** P≤0.001 (Welch's t-test).

3.2.4 Interferon-stimulated gene (ISG) screening

3.2.4.1 IRF1 inhibition of Chikungunya virus infection

One of the first steps in setting up the screening assay in our laboratory facilities was to assess whether previously-published data could be recapitulated. Thus, Vero cells were transduced overnight with lentiviruses overexpressing the interferon regulatory factor 1 (IRF1). Concurrent expression of TagRFP served as a marker for transduction (Figure 3.11A). At 48 hours post-transduction (hpt), cells were infected with Chikungunya virus (CHIKV) at MOI 10. At 18 hours post-infection, cells were collected and fixed in 4% paraformaldehyde, prior to flow cytometry analysis (Figure 3.11B).

The recombinant CHIKV used in this study had ZsGreen inserted into the non-structural protein 3 (nsP3). NsP3 plays an essential role during viral replication, forming part of the replicase complex (Götte, Liu and McInerney, 2018). Thus, green fluorescence emitted by the ZsGreen-nsP3 fusion was taken as a measure of CHIKV replication. ZsGreen-positive cells within the ISG-expressing ‘red’ cell population were quantified and viral replication was compared to control cells (Figure 3.11C-D). Control cells were transduced with lentiviruses which do not deliver the sequence for an ISG, however, they do deliver the TagRFP sequence. In the face of IRF1 overexpression, CHIKV replication was inhibited by 63% (Figure 3.11D).

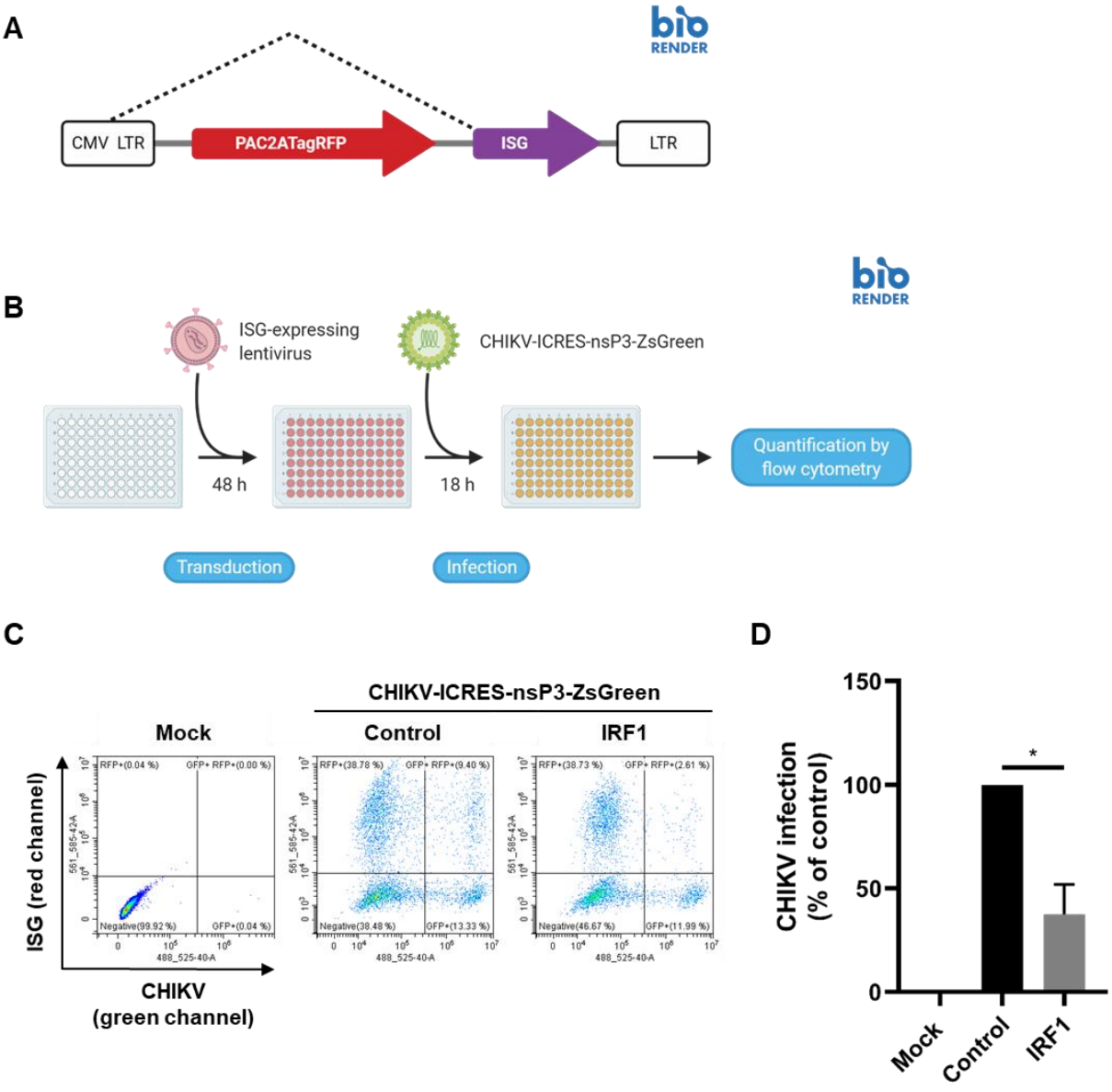

Figure 3.11 CHIKV inhibition by IRF1 overexpression. A) Schematic of the bicistronic lentiviral construct carrying sequences for TagRFP and the ISG of interest. The dotted line denotes mRNA splicing. CMV: human cytomegalovirus immediate-early promoter; PAC: puromycin resistance gene; 2A: ribosomal 'skipping' peptide; LTR: HIV-1 long terminal repeat. B) Schematic of the overexpression assay. Vero cells were transduced with IRF1- or control-expressing lentiviruses. At 48 hpt, cells were infected with CHIKV at MOI 10. At 18 hpi, cells were processed for flow cytometry. A-B) Created with BioRender.com. C) Representative dot plots from un-transduced mock-infected (mock), control-transduced infected (control) and IRF1-transduced infected

Vero cells (IRF1). ‘Red’ transduced, ‘green’ infected cells represent the population of interest. D) CHIKV infection, measured as the percentage of ZsGreen-positive cells within ISG-expressing ‘red’ cells, was normalised to that of control cells. Data represent the mean ± SD from three independent experiments (n=3). Mock: Mock-transduced, mock-infected cells. * P≤0.05, ** P≤0.01, *** P≤0.001 (Welch’s t-test).

3.2.4.2 Screening the ISG panel against polyomavirus infection

Conducting the primary screen against BKPyV infection, required optimisation of the assay within our facilities. To achieve this, a sample of the lentivirus-expressed ISG panel was screened for the inhibition or enhancement of SV40 infection in Vero cells. SV40 is propagated rapidly in cell cultures compared to BKPyV stock generation. As SV40 is a related non-human primate polyomavirus, we reasoned that SV40 infections were to be employed while optimising the flow cytometry-based screening assay with the same reagents to be used for BKPyV infections.

Vero cells seeded in a 6-well plate format were transduced for 48 hours and infected with SV40 polyomavirus for another 48 hours. At the end of the incubation period, cells were detached for fixation and processed for intracellular VP1 staining. VP1 was used as a marker to assess polyomavirus infectivity in the presence of individual ISGs (Figure 3.12A).

Cells transduced with IRF1-expressing lentiviruses demonstrated a significant reduction of 50% in SV40 infection compared to control cells (Figure 3.12B). Other ISGs, for example ZC3HAV1, may have had an inhibitory effect against SV40 infection, however, the decrease did not appear to be significant in this assay.

Once it was established that each step of the assay could successfully be performed and infection could be quantified through indirect staining of cells passed through the flow cytometer, the assay was performed with BKPyV infections at MOI of 0.1 at the same time-point. The complete ISG collection available to us was screened in a 96-well plate format. A few ISGs (EIF2AK2, NFIL3, UBA7) produced inconclusive results accompanied by large error bars, however, some ISGs demonstrated a statistically significant reduction in BKPyV infection (Figure 3.12C). EXT1, HPSE, IRF1, MDA5 and ZC3HAV1 overexpression significantly inhibited infection. Interestingly, TRIM56 overexpression led to a significant enhancement of infection. Table 3.1 lists the ISGs screened through this method for their effects in BKPyV infection.

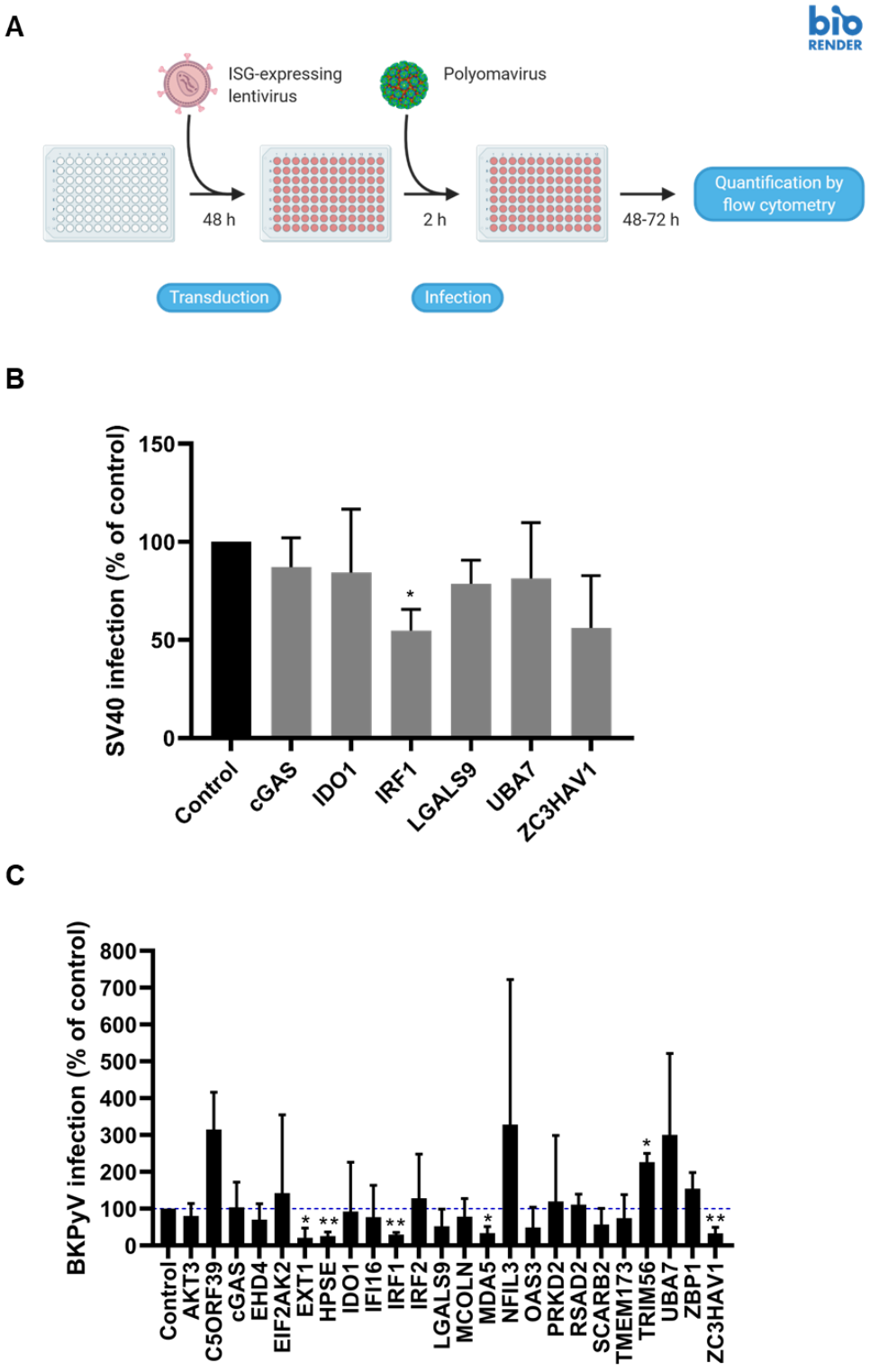

Figure 3.12 ISGs were screened for their effects on polyomavirus infection. A) Schematic of the screening process. ISGs are delivered to Vero cells through overnight transduction and allowed to be overexpressed for 48 h. Vero cells are then infected with polyomavirus at MOI of 0.1 for 2 h. At 48 hpi, cells are fixed, labelled green for VP1 and analysed by flow cytometry. B) A few

of the ISGs were tested against SV40 infection to facilitate optimisation of the screen. The percentage of infected ‘green’ cells within the ISG-expressing ‘red’ population was quantified by flow cytometry and normalised to control cells. C) The complete panel of ISGs was screened against BKPyV infection. The percentage of infected ‘green’ cells within the ISG-expressing ‘red’ population was quantified by flow cytometry and normalised to control cells. The blue dotted line represents infection in transduced cells (Control) which do not overexpress an ISG. Data show mean ± SD from three independent experiments (n=3). * P≤0.05, ** P≤0.01, *** P≤0.001 (Welch’s t-test).

Table 3.1 The ISG panel. For each ISG, its abbreviation, product name and reported functions in viral infections are listed below. A reference is given for defined ISG functions in viral infections. The percentage of BKPyV infection was calculated relative to infection within control cells, as described for Figure 3.12. ISGs are listed in alphabetical order according to the gene name.

ISG	Name	Function	Reference	% infection
AKT3	AKT serine/threonine kinase 3	Unknown		67.6
C5ORF39	Annexin A2 receptor	Unknown		244.8
cGAS	Cyclic GMP-AMP synthase	DNA sensor	Schoggins *et al.* (2014)	96.2
EHD4	EH domain-containing 4	Unknown		61.7
EIF2AK2	Eukaryotic translation initiation factor 2 alpha kinase 2	Targets EIF2A	Gal-Ben-Ari *et al.* (2019)	116.1
EXT1	Exostosin glycosyltransferase 1	Unknown		33.1
HPSE	Heparanase	Unknown		25.6
IDO1	Indoleamine-pyrrole 2,3-dioxygenase	Nutrient depletion	Kane *et al.* (2016)	75.1
IFI16	Interferon gamma inducible protein 16	DNA sensor	Unterholzner *et al.* (2010)	61.4
IRF1	Interferon regulatory factor 1	IFN/ISG inducer	Schoggins and Rice (2011)	25.2
IRF2	Interferon regulatory factor 2	Negative regulator	M. M. H. Li *et al.* (2016)	98.5

141

ISG	Name	Function	Reference	% infection
LGALS9	Lectin, galactoside-binding, soluble, 9	Unknown		42.1
MCOLN	Mucolipin	Viral entry	Rinkenberger and Schoggins (2018)	65.1
MDA5	Melanoma differentiation-associated protein 5	RNA sensor	Dias Junior *et al.* (2019)	36.0
NFIL3	Nuclear factor, interleukin 3 regulated	Unknown		246.4
OAS3	2'-5'-oligoadenylate synthetase 3	RNAse L activator	Y. Li *et al.* (2016)	38.6
PRKD2	Protein kinase D2	Negative regulator	Zheng *et al.* (2011)	94.1
RSAD2	Radical S-adenosyl methionine domain containing 2	Egress/signalling	Wang *et al.* (2007)	83.8
SCARB2	Scavenger receptor class B member 2	Unknown		65.0
TMEM173 (STING)	Transmembrane protein 173 (Stimulator of interferon genes)	Downstream mediator	Liu *et al.* (2016)	68.9
TRIM56	Tripartite motif containing 56	RNA-binding protein	Yang *et al.* (2019)	182.8
UBA7	Ubiquitin-like modifier activating enzyme 7	Protein ISGylation	Zhang and Zhang (2011)	233.8
ZBP1	Z-DNA binding protein	DNA sensor	Takaoka *et al.* (2007)	123.2
ZC3HAV1	Zinc-finger CCCH-type, antiviral 1	Targets viral RNA	Zhu *et al.* (2011)	35.2

142

3.2.5 Expression of anti-BKPyV candidates in IFN-treated RPTE cells

Following the screening of 24 ISGs against BKPyV infection, we selected two candidates which showed the most significant anti-BKPyV activity in the screening approach; IRF1 and HPSE. Both candidates were further examined in the following two chapters to elucidate their role in BKPyV infection.

Before each candidate was assessed further, we investigated whether the two genes are upregulated upon IFN stimulation in our primary cell culture system. Primary RPTE cells were treated with 50 ng/mL IFN-α or 50 U/mL IFN-γ for 24 hours and total RNA was extracted as previously described (section 2.16). Messenger RNA expression levels were evaluated by qRT-PCR and normalised to mock-treated cells.

Upon treatment with IFN-α, significant upregulation was observed for both IRF1 and HPSE expression (Figure 3.13A-B). Similarly, IFN-γ treatment of RPTE cells led to a substantial upregulation of both IRF1 and HPSE mRNA, compared to the mock treatment of cells (Figure 3.13C-D).

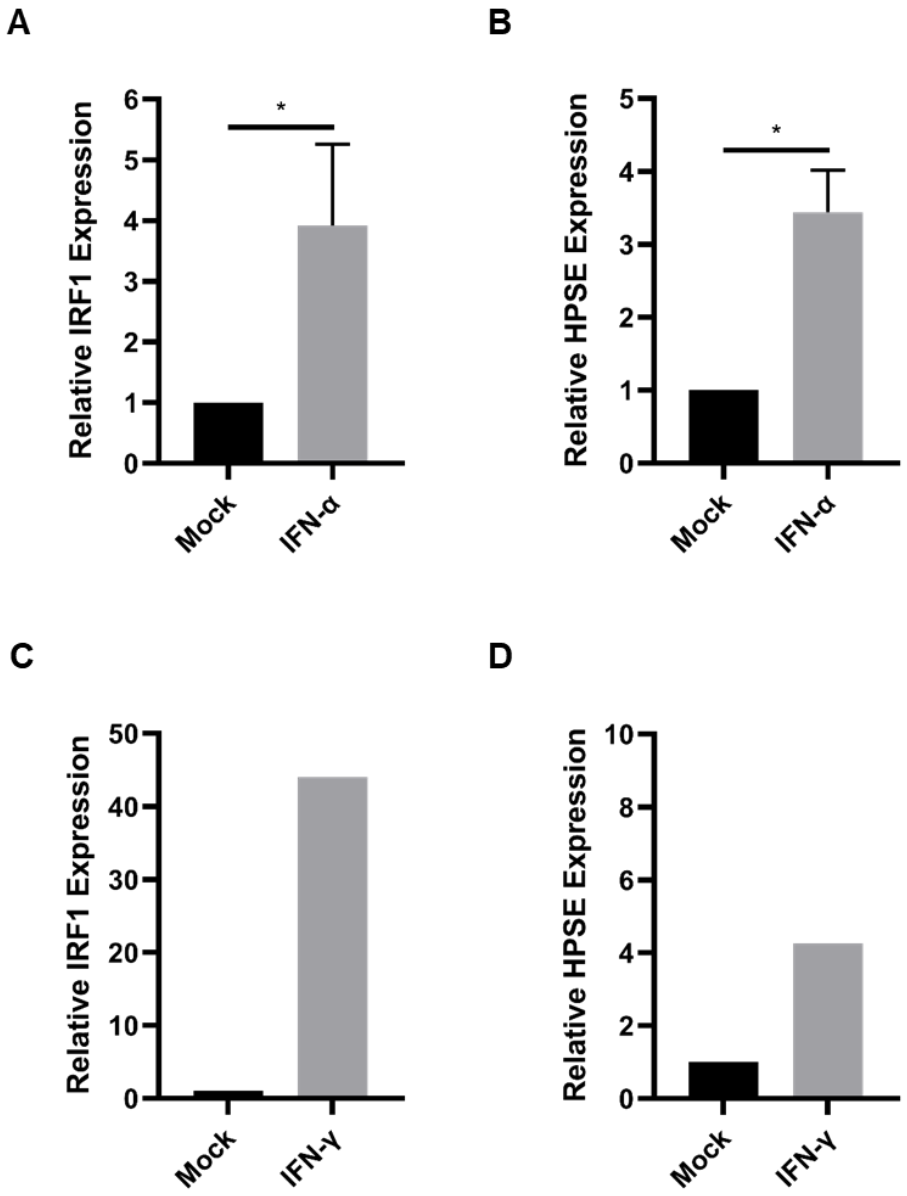

Figure 3.13 IFN upregulates IRF1 and HPSE expression in primary cells. A-B) RPTE cells were treated with 50 ng/mL IFN-α for 24 h. Total RNA was extracted for RT-qPCR analysis of IRF1 and HPSE expression. Samples were normalised against U6 mRNA levels and data is presented relative to mock treatments. Error bars represent the mean ± SD from three independent experiments (n=3). C-D) RPTE cells were treated with 50 U/mL IFN-γ for 24 h. Total RNA was extracted for RT-qPCR analysis of IRF1 and HPSE expression. Samples were normalised against U6 mRNA levels and data is presented relative to mock treatments. Data represent the mean of two independent experiments (n=2). Mock: Mock-treated cells. * P≤0.05, ** P≤0.01, *** P≤0.001 (Welch's t-test).

3.3 Discussion

3.3.1 Generation of polyomavirus stocks

In this chapter, we have demonstrated the process involved in generating purified stocks of BKPyV, which were required throughout this study for infection assays. Episomal BK polyomavirus DNA was first transfected in primary RPTE cells. Fourteen days following transfection, viral lysates were formed by scraping cells in the presence of cell culture medium and freeze-thawing these cell suspensions. To achieve high viral titres, naïve RPTE cells were infected with the resulting viral lysate for further replication rounds and harvested after 14 days of infections. Viral lysates were then formed and BKPyV was purified from these through ultracentrifugation, using a sucrose cushion and CsCl gradients.

BKPyV strains, including Dunlop, which contain a rearranged form of the NCCR are capable of efficient propagation in a variety of different cell types. Continuous lines of monkey kidneys cells, such as Vero and CV-1 cell lines, support productive BKPyV infection (Eash *et al.*, 2004; Bennett *et al.*, 2013). While many studies describe the use of non-human primate cells – particularly Vero cells – for producing cell culture-derived infectious BKPyV, cells of human origin appear to be a more appropriate choice.

BKPyV replicates more efficiently in human cells (Knowles, 2001). Human embryonic kidney (HEK) cultures have been commonly used for *in vitro* BKPyV propagation. A distinctive cytopathic effect (CPE) is exhibited in HEK cells following a relatively short incubation time with BKPyV, thus, facilitating the monitoring of viral replication (Knowles, 2001; Kane *et al.*, 2020). Of note, HEK-293TT cells represent a convenient cell culture system for growing archetype BKPyV due to overexpression of LT-Ag in this cell type (Broekema and Imperiale, 2012).

The shift in using primary cells for generating BKPyV accompanied the establishment of a model system for studying the viral life cycle as it may occur within its host. Low *et al.* (2004) first described that primary RPTE cells supported BKPyV growth, while arguing for the use of these cells in studying BKPyV lytic infection. The protocol discussed herein is based on the work by

Low and colleagues (2004) and an outline of the process is presented by Moriyama and Sorokin (2009).

Similar to other primary cells cultured *in vitro*, RPTE cells enter telomere-dependent replicative senescence following serial passaging (Wieser *et al.*, 2008). To overcome passage limitation and associated cost, immortalised RPTE cell lines were generated in two independent studies through stable expression of the catalytic subunit of telomerase; human telomerase reverse transcriptase (hTERT) (Wieser *et al.*, 2008; Zhao and Imperiale, 2019). Due to time constraints in our study, it was not possible to use hTERT-expressing RPTE (RPTE-hTERT) cells for BKPyV production.

SV40 propagation in permissive Vero cells (Clayson *et al.*, 1989) followed the same principles as BKPyV propagation, with a shorter incubation period for SV40. To establish a timeline for SV40 infection for the screening assay, we performed temporal analysis of early and late SV40 protein expression and virion release following infection of Vero cells. We have shown that LT-Ag and VP1 proteins are detected by Western blot as early as 24 and 36 hours post-infection, respectively. Furthermore, infectious virions are released in the media after 36 hours of infection. Our findings are in agreement with SV40 protein and progeny detection in infected BS-C-1 cells (Daniels, Rusan, Wilbuer, *et al.*, 2006). The BK polyomavirus protein expression profile was previously described both in literature (Low *et al.*, 2004) and within our group.

3.3.2 Titration of polyomavirus stocks

Titration of viral stock involved an FFA coupled to an automated imaging and analysis system. The protocol followed for determining the infectious titre of polyomaviruses was adapted from Stewart *et al.* (2015), as described in Panou *et al.* (2018). Stewart and colleagues (2015) reported a reliable, high-throughput method in calculating Hepatitis C infectious titres using the IncuCyte® ZOOM instrument and related software to count infected cells.

To determine the viral titre, samples from BKPyV and SV40 stocks were serially diluted two-fold into the existing media of permissive cells. Following a total incubation time of two days, indirect immunofluorescent staining of cells was conducted for the major capsid protein, VP1. Quantification of infected cells was achieved through automated detection of VP1 as a fluorescent signal within infected nuclei.

Interestingly, higher viral titres were noted for SV40 after 7 days of propagation compared to those of BKPyV following a month of propagation in cell culture. Discrepancies in starting materials may not account for this observation as an equal amount of viral DNA was transfected in the respective permissive cell lines. Although there are many uncontrolled variables in this comparison, it may serve to highlight the slow propagation of BKPyV in cell culture.

A variety of virus quantification techniques have been reported for polyomaviruses. Quantitative PCR measures viral load through quantification of viral genomes (Bechert *et al.*, 2010), while the haemagglutination assay (HA) relies on the ability of BKPyV to agglutinate type O erythrocytes in suspension (Portolani *et al.*, 1974; Dugan *et al.*, 2008). Nucleic acid- and protein-based assays are useful techniques, however, they fail to distinguish between non-infectious and infectious virus in a sample (Baer and Kehn-Hall, 2014). In contrast, an important advantage of infectivity assays is the quantification of infectious virions only.

To determine viral infectivity, the widely used plaque assay relies on cell lysis upon co-culture of cells with a lytic virus, leading to plaque formation. Manual counting of plaques is labour-intensive and is associated with variability amongst analysts. Such limitations have recently encouraged assay optimisation (Masci *et al.*, 2019). The plaque assay is, however, limited in its

use for BKPyV titration, as this polyomavirus forms poorly defined plaques in most cell types. Furthermore, due to the slow growth of BKPyV, the plaque assay can often proceed for up to 3 weeks before detectible plaques form (Seehafer *et al.*, 1978).

The FFA is an improved method to the plaque assay, which employs indirect immunofluorescent staining of viral antigens acting as infection markers. Infections for BKPyV titration using an FFA have traditionally been performed for 4-5 days using anti-large T-antigen antibodies (Abend *et al.*, 2007; Moriyama and Sorokin, 2009). Manual counting of infected cells by fluorescence microscopy is time-consuming and can be associated with human bias (Kang and Shin, 2012). Panou *et al.* (2018) adapted the FFA for polyomaviruses, decreasing the incubation time after infection to 2 days and offering an automated solution for counting infected cells using the IncuCyte® ZOOM system. Furthermore, less dilutions of viral stock were required than a $TCID_{50}$ assay which requires an endpoint dilution (Stewart *et al.*, 2015), overall representing a rapid, reproducible and cost-effective method for BKPyV titration.

Flow cytometry in conjunction with titration assays has been described for SV40 stock quantification (Drayman *et al.*, 2010). While the same principles of indirect immunofluorescence apply as in an FFA, preparation of cells for flow cytometry is a lengthy process in comparison to imaging plates using the IncuCyte® ZOOM device. Automated imaging and analysis with IncuCyte® ZOOM comprises a multi-functional tool in our research as this method can be adapted to study the effect of host factors on virus infectivity.

3.3.3 BKPyV susceptibility to interferon action

Humoral and cellular immunity are both involved in the defence against BKPyV infection. While up to 90% of healthy adults carry BKPyV-specific antibodies (Hirsch and Steiger, 2003), humoral immunity alone cannot contain BKPyV-associated disease. In a prospective study of 78 renal transplant patients, seropositivity prior to transplantation did not protect from progression to PVAN (Hirsch *et al.*, 2002; Comoli *et al.*, 2004). Furthermore, BKPyV-specific cytotoxic T lymphocytes (CTLs) fail to destroy all infected cells and, as a result, even immunocompetent individuals experience periodic shedding of the virus (Chen *et al.*, 2006). Such clinical observations raised the question on the importance of cell-mediated immunity in regulating BKPyV infection and persistence.

Infection by the closely related JC polyomavirus is restricted by a type I interferon response, orchestrated by IFN-stimulated genes (Assetta *et al.*, 2016). Furthermore, the antiviral state is reportedly activated by various polyomavirus T-antigens in mouse embryonic fibroblasts (MEFs). SV40, JCPyV and BKPyV large T-antigens induce ISG expression, a process which requires STAT1 activation through an intact retinoblastoma protein binding motif in LT-Ag (Giacobbi *et al.*, 2015). These findings prompted us to investigate the interplay between BKPyV infection and the interferon system.

As the main site of viral replication is within the renal system, primary RPTE cells are a useful tool for recapitulating the natural host cell environment encountered by BKPyV. Therefore, RPTE cells have recently been established as a powerful *in vitro* model for studying the viral life cycle (Barth *et al.*, 2016). Importantly, due to the absence of immune cells in cell culture, elements of the immune system can be individually introduced to examine their role in BKPyV infection (Abend *et al.,* 2007). Using RPTE cells, we have demonstrated the susceptibility of BKPyV infection to IFN-α and -γ in our investigation into the antiviral response against BKPyV. During application of either cytokine to primary kidney cell cultures, VP1 protein levels were substantially reduced, and became undetectable at specific cytokine concentrations. Additional data generated within our laboratory group, provided evidence of viral transcript inhibition by IFN-α. A knock-down, similar to the reduction in protein levels, was observed for LT-Ag and VP1 mRNA levels. Overall, our findings suggest a role for IFN-α in regulating BKPyV infection in RPTE cells.

Our observations for IFN inhibition of BKPyV infection are in agreement with published data by Abend *et al.* (2007). Their work focused on characterising the inhibitory effect of IFN-γ on BKPyV infection in RPTE cells. IFN-γ impeded BKPyV replication kinetics through inhibition of viral protein and infectious progeny production. Furthermore, they provided evidence of IFN-γ targeting viral transcript expression as reduced LT-Ag transcript levels were observed in treated cells. The IFN-γ-mediated inhibition occurred independent of BKPyV MOI and regardless of the three strains used in the investigation. Furthermore, RPTE cells are capable of IFN-α, IFN-β and IFN-γ expression as revealed by transcriptome profiling of BKPyV-infected RPTE cells (Assetta *et al.*, 2016).

An important consideration in our studies is cell-type specific immunity, which may influence BKPyV infection and persistence. Recent investigations have made way in expanding our limited knowledge of BKPyV immunity on a molecular level in RPTE cells. Evidence suggests that BKPyV-inoculated RPTE cells are unable to mount an efficient innate immune response against BKPyV as CXCL10 and DAI expression remained overall unchanged. Furthermore, RPTE cells were capable of eliciting a robust antiviral response against Influenza A, HSV-1 and CMV, but not BKPyV (de Kort *et al.*, 2017). Microarray analysis, conducted by Abend *et al.* (2010), further support a lack of antiviral immune response during the early and late stages of infection. Minimal transcriptional changes were observed related to the inflammatory response. An *et al.* (2019) compared the antiviral response in infected lung vascular endothelial cells (LVECs) and RPTE cells. LVECs respond to BKPyV infection by producing IFN-β, as evaluated by a Luminex assay at 3 and 5 days post-infection. IRF3 and STAT1 were activated and genes involved in type I IFN signalling were upregulated at 3 days post-infection (An *et al.*, 2019). These observations were not noted for RPTE cells. Specifically, there was an absence of STAT1-Y701 nuclear localisation following BKPyV inoculation and limited ISGs were induced, in agreement with previous studies (An *et al.*, 2019).

Clearly, cellular defences encountered by the virus may vary by cell type. For this reason, results from our screen were validated in both Vero and RPTE cells. Their effects were compared to determine the importance of different host factors in regulating BKPyV infection depending on cellular environment.

3.3.4 Identification of ISG 'hits' influencing BKPyV infection

Herein, we have adapted and conducted a screen of ISGs against BKPyV infection. Firstly, we recapitulated to a certain extent the previously-reported IRF1 inhibition of CHIKV replication using the cell-based overexpression assay. Schoggins *et al.* (2011) demonstrated a near complete inhibition of CHIKV-GFP replication by IRF1 in their initial large-scale ISG screen. In comparison, our screen revealed a relatively moderate reduction of 63% in CHIKV replication, which was more reminiscent of the inhibition level observed in the confirmation assay (Schoggins *et al.*, 2011). The use of different recombinant Chikungunya viruses in our respective experiments or infections performed in $STAT^{-/-}$ fibroblasts by Schoggins *et al.* (2011) may contribute to this discrepant finding. Nonetheless, detection of the inhibitory effect within our laboratory was crucial in performing the next step in our screening approach.

Investigating the effect of selected ISGs against SV40 infection was primarily aimed at setting up the assay in our laboratory. Importantly, *in* vitro studies have demonstrated the induction of an antiviral state by SV40 through ISG expression. Global changes in cellular gene expression were analysed in MEFs abortively infected with SV40 or stable MEF cell lines expressing SV40 LT-Ag. The observed surge in ISGs, including ISG56, OAS, RSAD2, IFI27 and MX1 upregulation, was attributed to various domains of SV40 LT-Ag (Rathi *et al.*, 2010) and was not restricted to MEFs (Forero *et al.*, 2014). The majority of ISGs screened against SV40 in our study had little to no significant impact on viral infection. This may reflect ISG products functioning in a cell-type-specific manner or the inability of certain ISGs in impeding SV40 infection. The small, nonetheless, significant reduction of SV40 infection by IRF1 is further discussed in section 4.2.5.

Lastly, 24 ISGs were examined for their ability to modulate BKPyV infection in Vero cells. Defective in their IFNA and IFNB1 genes and unable to produce type I interferon (Desmyter *et al.*, 1968; Emeny and Morgan, 1979; Prescott *et al.*, 2010), Vero cells represent an appropriate cell line for the screening assay (Feng *et al.*, 2018). Individual immune components were introduced in these cells and their direct activities towards BKPyV were examined. Overexpression of several gene products was sufficient to confer resistance to BKPyV infection, including EXT1, HPSE, IRF1, MDA5 and ZC3HAV1. The exostosin (EXT) family

of genes encodes glycosyltransferase proteins which reside in the Golgi apparatus. EXT1 and EXT2 form a hetero-oligomeric complex responsible for heparan sulphate (HS) biosynthesis (Busse *et al.*, 2007). The role of HS chains in infection is discussed with reference to the inhibitory effect of the heparanase (HPSE) enzyme on BKPyV infection in Chapter 5. The potent inhibitory effect observed upon IRF1 overexpression is the subject of discussion in Chapter 4.

The observed inhibitory effects by some ISGs against BKPyV infection are intriguing, given that several studies provide evidence of a lack of an antiviral immune response at the main site of infection and persistence (Caller *et al.*, 2019). ISG expression profiling has been performed for BKPyV-infected RPTE cells at 3, 6 and 9 days after initial infection. Oligoadenylate synthetase 3 (OAS3) transcript levels were one of four genes found to be overexpressed at 6 days post-infection (Assetta *et al.*, 2016). A 2.7 $\log_2$ ratio of BKPyV-infected cells to mock cells was also recorded for OAS3 upregulation at the earlier time-point of 48 hours post-infection (An *et al.*, 2019). Our screening assay did not seem to corroborate these findings. OAS3 is involved in the activation of RNase L, an antiviral enzyme which restricts viral replication and spread by degrading viral and cellular RNAs. Upon infection with diverse RNA and DNA viruses, OAS3 was the only OAS isoform to produce 2′,5′-oligoadenylate (2-5A) for RNase L activation in response to viral dsRNA recognition (Y. Li *et al.*, 2016).

Melanoma differentiation-associated protein 5 (MDA5) is a dsRNA-binding helicase which is expressed to a low abundance in resting RPTE cells (de Kort *et al.*, 2017). Heutinck, Rowshani, *et al.* (2012) demonstrated an increased expression of the dsRNA sensors Toll-like receptor 3 (TLR3), melanoma differentiation-associated gene 5 (MDA5) and retinoic acid-inducible gene-I (RIG-I) in kidney transplant biopsies with active BKPyV infection. Previously, expression of serpinB9 in human RPTE cells was linked to activation of these three RNA sensors, which may protect the cells from granzyme B-mediated apoptosis (Heutinck, Kassies, *et al.*, 2012). Activation of dsRNA sensors in RPTE cells favoured the production of pro-inflammatory TNF-α and antiviral IFN-β cytokines. Furthermore, dsRNA receptor signalling sensitised cells to CD95-mediated apoptosis. Heutinck, Rowshani, *et al.* (2012) speculated that this type of a pro-apoptotic response may facilitate preservation of tubular integrity and function.

The antiviral activities of zinc-finger CCCH-type, antiviral 1 (ZC3HAV1) protein are directed against a diverse range of viruses (Hatziioannou and Bieniasz, 2011). ZC3HAV1 prevents cytosolic accumulation of viral mRNAs by directly binding to the ZC3HAV responsive element (ZRE) in viral mRNAs (Guo *et al.*, 2006). The reported viral mRNA target of ZC3HAV1 proteins may explain the increasing studies into the restriction of RNA viruses by ZC3HAV1. Upon binding its target, ZC3HAV1 recruits the cellular RNA degradation machinery to promote RNA decay. A role for KHNYN has been proposed as a co-factor for ZC3HAV1 and TRIM25 in degrading HIV-1 CpG-containing RNA, but is dispensable for other ZC3HAV1-sensitive RNA viruses (Ficarelli *et al.*, 2019). Importantly, ZC3HAV1 belongs to the set of ISGs induced upon SV40 abortive infection or LT-Ag ectopic expression in MEFs (Rathi *et al.*, 2010). We also observed a small, albeit, non-significant decrease in SV40 infection in Vero cells. In the face of polyomavirus infection, including SV40 and BKPyV, ZC3HAV1 may be targeting an RNA intermediate in the viral life cycle which may be crucial for establishing successful infection. Of note is a significant inhibition of SV40 infection and progeny production seen in our preliminary data where ZC3HAV1 was overexpressed in HEK-293 cells.

In contrast to our findings, tripartite motif-56 (TRIM56) exhibits antiviral functions against RNA viruses, such as inhibiting the late stages of HIV-1 replication. In their study, Kane *et al.* (2016) described a STING-independent TRIM56 antiviral activity which likely enhances cellular sensitivity to IFN-α. Furthermore, TRIM56 is noted as a Zika virus restriction factor with its E3 ligase activity crucial for viral suppression (Yang *et al.*, 2019). Our data from TRIM56-overexpressing BKPyV-inoculated cells suggested enhancement of infection by this specific ISG. The C-terminal region of TRIM56 exhibits sequence homology to NHL repeats of TRIM-NHL proteins, involved in microRNA (miRNA) regulation (B. Liu *et al.*, 2016). Perhaps the enhancing activity seen in our screen could be explained through additional TRIM56 functionalities against different viral species; one that may be targeting miRNAs involved in regulating BKPyV mRNA expression.

Of importance, LGALS9 and RSAD2 are downregulated 2 and 3 days post-infection with BKPyV in RPTE cells and LVECs, respectively (An *et al.*, 2019). Neither ISG produced a significant effect to either end in our screen.

To provide support for the role of type I IFN in modulating BKPyV infection, we evaluated the gene expression levels of IRF1 and HPSE in IFN-α-treated primary RPTE cells. We compared our findings with the ISG expression levels in IFN-γ-stimulated cells, to reveal significant increases in both IRF1 and HPSE gene expression induced by IFN-α. Furthermore, treatment of RPTE cells with IFN-γ also raised the expression of the two ISGs assessed.

Investigations into the transcriptional and proteomic changes observed upon BKPyV infection of RPTE cells have provided valuable information in elucidating the interaction of BKPyV with cellular innate immunity pathways (Abend *et al.*, 2010; Justice *et al.*, 2015; Caller *et al.*, 2019; An *et al.*, 2019). To supplement our understanding of this relationship, we overexpressed ISGs and screened them for their ability to affect BKPyV infection in Vero cells. A gain-of-function screen may be a useful method for determining interactions between host factors and polyomaviruses, which may otherwise not be detected in RPTE cells. Furthermore, such an approach may ascribe novel functions to ISGs and facilitate investigations of the underlying molecular mechanism. The assay adapted herein, could be further improved with the use of a recombinant virus to express a fluorescent-tagged protein, eliminating the need for immunofluorescent staining of VP1 and increasing experimental output. An investigation into developing infectious recombinant BKPyV identified stability issues when exogenous sequences were fused to the VP2 or agnoprotein ORFs. The loss of inserted sequences was observed after infectious passage in cell culture (Husseiny and Lacey, 2011).

Chapter 4

The antiviral activity of IRF1 in BKPyV infection

4.1 Introduction

4.1.1 The IRF family of transcription factors

The interferon regulatory factor (IRF) family is a group of transcription factors (TFs) which, in mammals, consists of nine members (Taniguchi *et al.*, 2001). One of the main functions of IRF family members is the generation of innate and adaptive immune responses to invading pathogens where, as transcription factors, they can regulate the expression of a diverse set of gene targets. In addition to playing pivotal roles in immunity, several IRFs regulate the cell cycle and apoptosis, differentiation and oncogenesis (Tamura *et al.*, 2008; Ikushima *et al.*, 2013).

All IRF family members have a common structural characteristic located at the N-terminus; they possess a DNA-binding domain (DBD) (Figure 4.1). The DBD is composed of approximately 120 amino acids and contains five well-conserved tryptophan repeats, resembling the DBD of Myb transcription factors (Yanai *et al.*, 2012; Veals *et al.*, 1992). A helix-turn-helix structure formed by the DBD recognises a DNA region characterised by the consensus sequence 5′-AANNGAAA-3′ (recognised bases are underlined, N indicates any base) (Fujii *et al.*, 1999). This sequence is known as the IFN-stimulated response element (ISRE; also known as IRF-E) because of its discovery within promoters of genes induced by type I IFN signalling events (Levy *et al.*, 1988). ISREs are found in various promoters, including genes encoding type I IFN, genes involved in immunity or other cellular processes (Honda and Taniguchi, 2006).

Within the C-terminal region of all IRFs except IRF1 and IRF2, a second conserved domain, termed IRF-association domain 1 (IAD1), has been identified (Sharf *et al.*, 1997). In its place, IRF1 and IRF2 share a common IAD2. IADs are involved in mediating homomeric or heteromeric interactions with members of the IRF family, other transcriptional factors or co-factors. Therefore, these association modules may dictate whether the resulting transcriptional complex functions as an activator or repressor of transcription, and which sequences the complex is able to bind to (Meraro *et al.*, 1999).

Notably, some viruses encode viral IRFs (vIRFs). For example, Kaposi's sarcoma-associated herpesvirus (KSHV) expresses four vIRFs (vIRF1 to vIRF4), three of which have been mechanistically studied, to antagonise IFN-mediated immune responses (Lee *et al.*, 2009). KSHV vIRFs have a homologous N-terminus to that of cellular IRFs, although the lack in a series of tryptophan residues within their DBD indicated that these vIRFs may not be able to bind DNA directly (Tamura *et al.*, 2008). In support of this notion, vIRF1 represses IRF1-mediated transcriptional activity by an unknown mechanism which does not involve competing with IRF1 for DNA binding. In fact, truncated vIRF1 lacking the DBD maintains its inhibitory action over cellular IRF1 (Zimring *et al.*, 1998; Lee *et al.*, 2012). The evolution of viral IRFs as countermeasures to cellular IRFs highlights the important role of these TFs in regulating the immune response to viral infection.

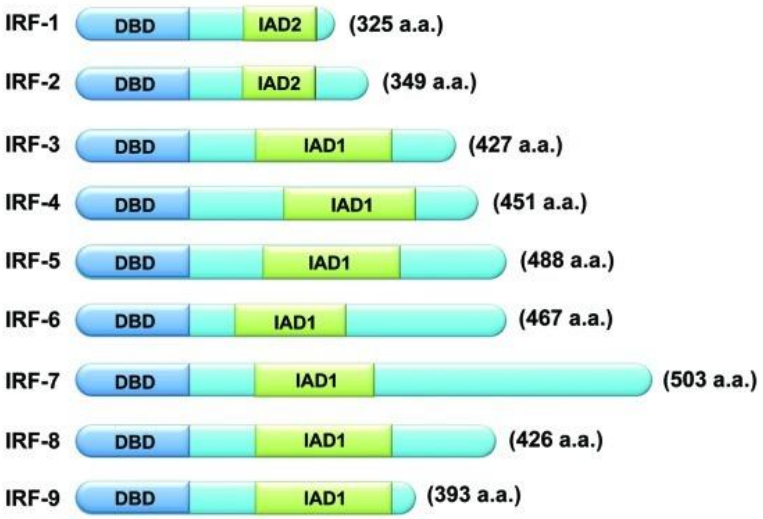

Figure 4.1 Schematic illustration of human IRF family members. The nine human IRF family members (IRF1 to IRF9) share two major structural similarities: the N-terminal DNA-binding domain (DBD) and the C-terminal IRF-association domain (IAD). The DBD mediates interaction with the IFN-stimulated response element (ISRE). Some members contain an IAD1, while IRF1 and IRF2 share IAD2; a structurally distinct region to IAD1. Length is reported in amino acid residues. Image adapted from Yanai *et al.* (2012).

4.1.2 IRF1 as a broadly-acting antiviral factor

IRF1 was the first member of the IRF family of proteins to be discovered as a regulator of the human interferon-β (IFN-β) gene (Miyamoto *et al.*, 1988). Apart from its pivotal role in regulating innate and adaptive immune responses, IRF1 also functions as a tumour suppressor and is involved in immune cell development (Tanaka *et al.*, 1994; Tamura *et al.*, 2008). It is constitutively expressed at low levels in various tissues, including kidneys, and is a short-lived protein with a half-life of approximately 30 minutes (Habuka *et al.*, 2014; Uhlen *et al.*, 2015; Watanabe *et al.*, 1991). Transcription of IRF1 is enhanced upon stimulation by various cytokines (IFN-α/β/γ, TNF-α, IL-1, IL-6), by viral infection and upon induction of the DNA damage response (DDR) (Rettino and Clarke, 2013).

Human IRF1 protein comprises of 325 amino acid residues (Santosh *et al.*, 2018). The amino acid segment 233–255 is responsible for mediating transactivation of target genes (Kim *et al.*, 2003). Sub-cellular localisation studies in HEK293T cells demonstrated that transfected IRF1 was predominantly localised to the nucleus (Negishi *et al.*, 2006). The use of IRF1 mutants mapped the nuclear localisation signal (NLS) to amino acids 117–141 (Schaper *et al.*, 1998). Furthermore, cytoplasmic IRF1 undergoes efficient nuclear translocation upon MyD88-dependent activation (Negishi *et al.*, 2006).

During our screen of the ISG panel, IRF1 exerted the most potent inhibition against BKPyV infection. Known as a broadly-acting antiviral factor, IRF1 restricts replication for a diverse set of viruses. RNA viruses, including flavi-, toga-, and retroviruses are targets of IRF1 antiviral activity (Schoggins *et al.*, 2011). DNA viruses are also suppressed by IRF1, although their restriction by ISGs has been studied to a lesser extent (Mboko *et al.*, 2014; Schoggins *et al.*, 2014). Despite its broad-spectrum inhibitory effect, the mechanism by which IRF1 mediates its antiviral functions is poorly elucidated. On the basis of its biology and its role in immunity, we chose to study IRF1 further as a plausible host factor in attenuating BKPyV infection. In this chapter, we aim to provide evidence, on a molecular level, to facilitate the delineation of the underlying IRF1-mediated mechanism of BKPyV restriction.

4.1.3 Chapter aims

In this chapter we seek to characterise the role of IRF1 as an antiviral factor in BKPyV infection. Cell lines with a stable expression of IRF1 are first established to conduct our assays with similar levels of IRF1 overexpression. We then validate the restriction of BKPyV infection in these stable cell lines at various time-points and investigate the impact of IRF1 on specific stages in the viral life cycle. To characterise the scope of inhibition by IRF1, we determine whether this inhibition is a conserved activity against the related polyomaviruses, SV40 and JCPyV. Lastly, we investigate whether the antiviral activities of IRF1 against BKPyV are active in our primary cell culture model.

4.2 Results

4.2.1 Generation of JCPyV stock

4.2.1.1 Infections of SVG-A cells with JCPyV commercial stock

JCPyV was propagated using a commercial stock of the Mad-4 strain to infect SVG-A cells. Upon a 2-week incubation period, cells were harvested in their media and viral lysates were prepared through three cycles of freeze-thaw. Samples obtained from infected cells and their media confirmed the presence of viral antigen in a Western blot (Figure 4.2). Bands of approximately 40 kDa, corresponding to VP1, were observed in samples of cellular lysate and confirmed the generation of intracellular JCPyV in both flasks. VP1 was also detected in the corresponding cell media, confirming the release of JCPyV virions.

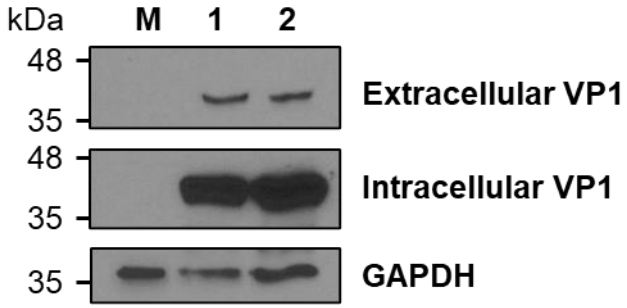

Figure 4.2 Infections of SVG-A cells with JCPyV Mad-4 commercial stock. SVG-A cell cultures were inoculated with JCPyV Mad-4 for 14 days, upon which infected cells and media were harvested as cell suspensions. SDS-PAGE and Western blot analysis was conducted on samples from media and lysates to detect extracellular and intracellular VP1, respectively. GAPDH acted as a loading control. Blots are representative of at least two independent experiments. M: Mock-infected media/cells, 1-2: JCPyV-infected media/cells.

4.2.1.2 Titration of crude JCPyV stocks

To confirm the generation of infectious JCPyV stock and determine its viral titre, crude virus was serially diluted two-fold in a 96-well plate seeded with Vero cells. After 2 hours of virus inoculation, cells were returned to their normal medium and incubated for a total of 48 hours. The monolayer was then fixed and stained for VP1 as an infection marker. The plate was imaged by IncuCyte® ZOOM and images were processed to calculate the viral titre as described previously (3.2.1.4). The number of VP1-positive Vero cells decreased with increasing dilution of the viral sample as expected (Figure 4.3A). Extracted data enabled the calculation of the infectious virus titre for each dilution made and is given in infectious units per mL (IU/mL) (Figure 4.3B). The average viral titre was calculated to 5 x 10^3 IU/mL for this specific JCPyV stock. Data presented here was obtained by titrating a sample from one batch of JCPyV and is representative of other FFAs performed during this study. The crude viral stock was used for cell infection assays without further purification.

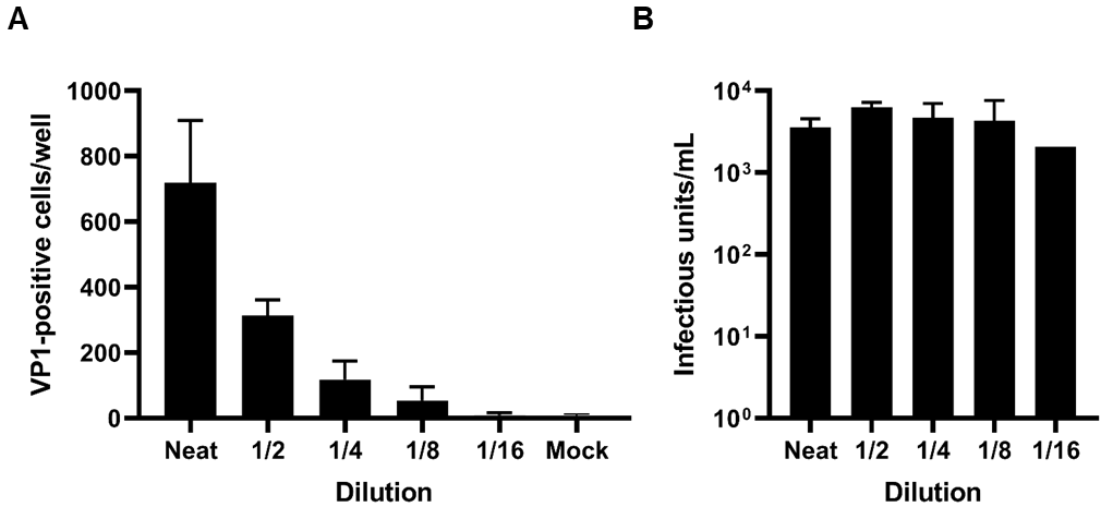

Figure 4.3 Titration of crude JCPyV stock. Vero cells were infected with a two-fold serial dilution of JCPyV for 2 h. Cells were fixed at 48 hpi, labelled green for VP1 protein and imaged using IncuCyte® ZOOM. A) The number of VP1-positive, infected cells per well for each dilution was extrapolated. Mock: Mock-infected cells. B) The virus titre was calculated by averaging the infectious units per mL of all dilutions made. Error bars represent the mean ± SD of three technical repeats from a single representative experiment.

4.2.2 Formation of Vero cell lines with stable expression of IRF1

To ensure a stable phenotype for IRF1 expression, we established Vero cell clones through transduction with a lentiviral vector encoding human IRF1. Selection of transduced cells occurred in antibiotic-containing medium until expansion of the polyclonal cell line was possible. A control cell line was established in the same manner, although the 'empty' SCRPSY lentiviral vector which transduced the control cells does not encode an ISG. The IRF1-overexpressing cell line and the control cell line are herein referred to as IRF1-Vero and Control-Vero, respectively.

The viability of Control-Vero and IRF1-Vero cells was assessed in an MTT assay (Figure 4.4A). No significant statistical differences between the viabilities of the Control-Vero and IRF1-Vero cell lines were observed. Importantly, the viability of Control-Vero cells did not differ from mock (untransduced) cells, indicating that the integrated lentiviral vector did not perturb normal cell growth. Treatment of cells with staurosporine for 18 hours prior to the MTT assay served as a control for cell death induction.

We then confirmed the expression of IRF1 in our stable cell line by RT-qPCR (Figure 4.4B). Total RNA was extracted from mock, Control-Vero and IRF1-Vero cell cultures. IRF1 transcript levels were evaluated to be significantly increased in IRF1-Vero cells compared to the control cell line.

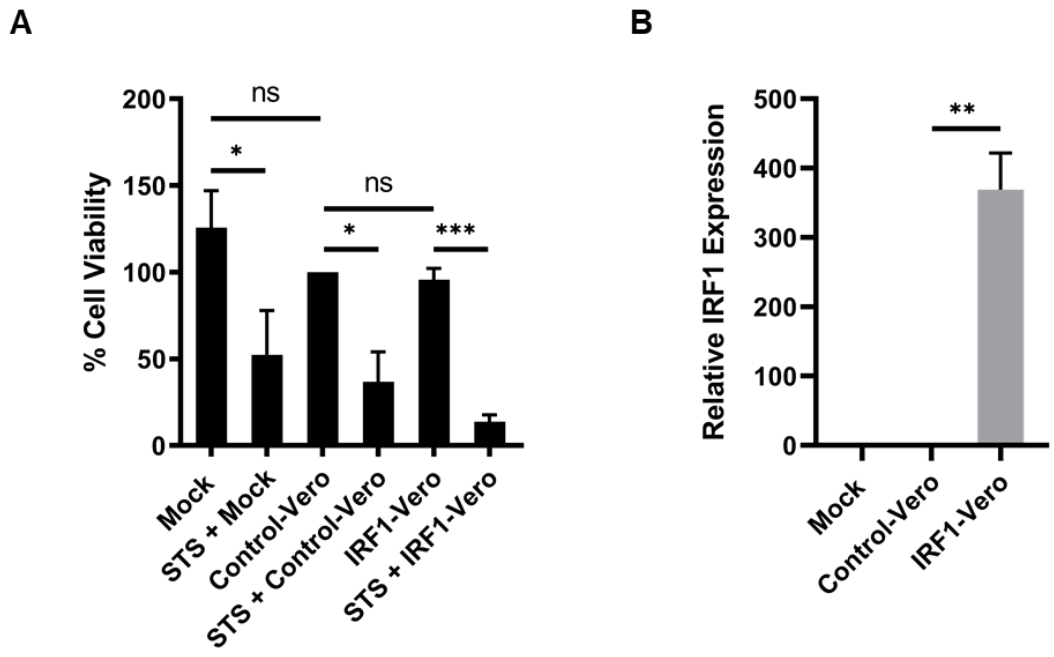

Figure 4.4 Establishment of an IRF1-expressing Vero cell line. A) The cell viabilities of mock (untransduced) Vero, Control-Vero and IRF1-Vero cells were evaluated by MTT assay. Cells were treated with 1 μM staurosporine (STS) for 18 hours as a control for the induction of cell death. B) Total RNA was extracted from mock Vero, Control-Vero and IRF1-Vero cells, and reverse transcribed to assess IRF1 transcript levels by RT-qPCR. Error bars represent the mean ± SD from three independent experiments (n=3). ns: not significant, * P≤0.05, ** P≤0.01, *** P≤0.001 (Welch's t-test).

4.2.3 Validation assay for the IRF1 antiviral effect against BKPyV

Once the IRF1-Vero cell line was established, we performed a validation assay for the antiviral activity of IRF1 against BKPyV infection to ensure the performance of our stable cell line. Cells with stable IRF1 expression were infected at MOI 0.1 for 2 hours, upon which cells were returned to normal medium. At 48 hours post-infection, cells were labelled for VP1 protein and processed for flow cytometry, as described previously in section 3.2.4.2 (Figure 4.5A-B). A significant reduction of approximately 76% was observed in VP1-positive cells within the IRF1-expressing cell population compared to the control cell line. As a comparison, in our screen using transduced cells there was an approximate 75% reduction of VP1-positive cells within the IRF1-expressing cells compared to their control. Therefore, the results from our validation assay using the stable cell lines were compatible with our data from the ISG screen.

Furthermore, cell lysates from side-by-side experiments of the flow cytometry assay, were probed for VP1 protein in a Western blot (Figure 4.5C-D). BKPyV-infected IRF1-Vero cells contained less VP1 protein in their lysates compared to BKPyV-infected Control-Vero cells. This reduction of VP1 protein levels in the presence of IRF1 overexpression was determined significant by densitometry analysis. Together our findings suggested that IRF1 suppresses the production of the major capsid protein, VP1, as determined by flow cytometry and Western blotting assays.

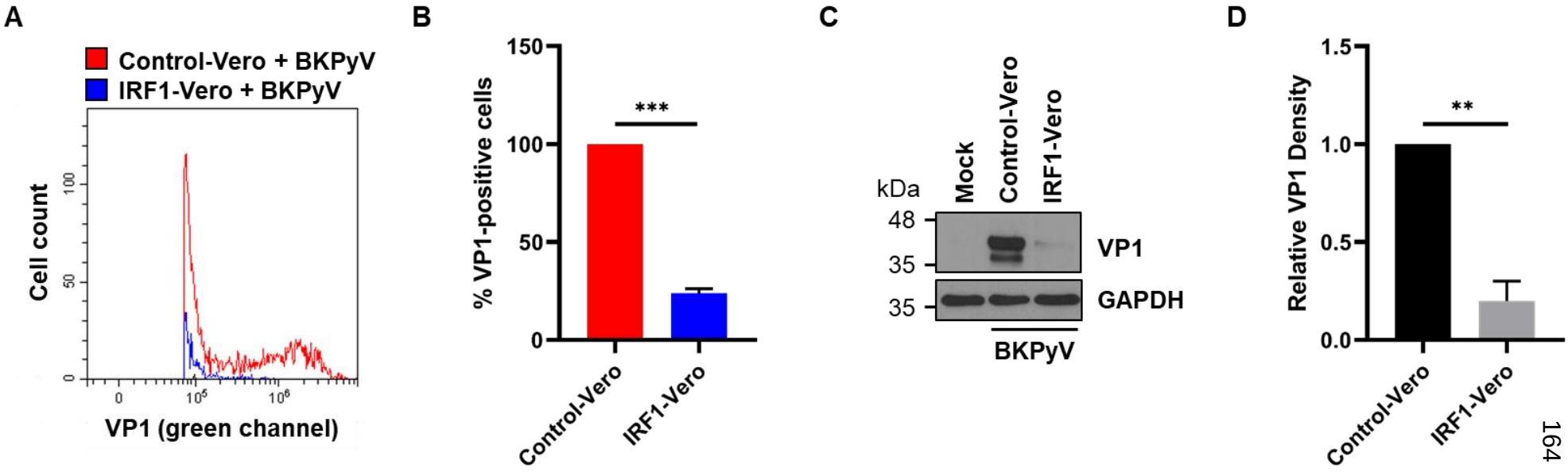

164

Figure 4.5 Confirmation of IRF1 suppression of BKPyV infection. Stable Vero cell lines were infected with BKPyV at MOI 0.1 for 2 h and processed at 48 hpi for flow cytometry (A-B) or SDS-PAGE followed by Western blot (C-D). A) Overlay of VP1-expression profiles of ISG-expressing Control-Vero and IRF1-Vero cells. B) The percentage of VP1-positive cells within IRF1-expressing cells was normalised to that of Control-Vero cells. C) Representative Western blots of mock-infected and BKPyV-infected cells. D) Densitometry analysis from C was performed using ImageJ and values were calculated relative to the control cell line. Error bars represent the mean ± SD from three independent experiments (n=3). * P≤0.05, ** P≤0.01, *** P≤0.001 (Welch's t-test).

4.2.4 IRF1-mediated inhibition of BKPyV life cycle stages

4.2.4.1 Time-course of BKPyV infection with exogenous IRF1 expression

Our investigation into IRF1 as a potential ISG against BKPyV infection first suggested that IRF1 overexpression suppressed the major viral protein, VP1. We wished to examine further the viral target within the BKPyV life cycle upon which IRF1 may be exerting its inhibitory effect. To this end, we first performed a time-course of infection assay to determine the optimal time-point of BKPyV inhibition by IRF1 (Figure 4.6). Control-Vero and IRF1-Vero cells were infected with BKPyV at MOI 0.1 and harvested between 0 and 96 hours post-infection. Western blot analysis of lysates probed for VP1 protein to represent late gene expression, revealed a gradual decline in VP1 levels in IRF1-Vero lysates. This reduction in viral protein levels was observed from 48 hours post-infection onwards. The peak of VP1 protein inhibition occurred at 72 hours post-infection. In both control-Vero and IRF1-Vero lysates, VP1 protein was first detected at 36 hours post-infection, indicating that there was no delay in the initiation of viral protein production. This finding suggested that IRF1 does not affect the kinetics of BKPyV replication.

Flow cytometry and Western blot data obtained at 72 hours post-infection was comparable to previously discussed findings at 48 hours post-infection (Figure 4.7). A slightly more potent inhibition of approximately 80% was evident by flow cytometry at the later time-point compared to 48 hours post-infection.

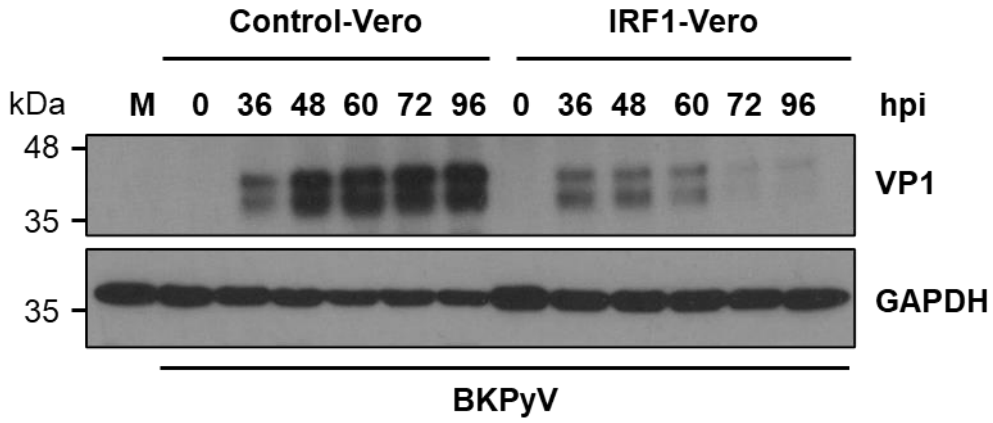

Figure 4.6 Time-course of BKPyV infection during IRF1 overexpression. BKPyV was incubated with Control-Vero and IRF1-Vero cells at MOI 0.1 during synchronised infections and cells were harvested over 4 days of infection. For 0 hpi, cells were harvested immediately after 1 hour of BKPyV adsorption. Cell lysates were resolved by SDS-PAGE and probed with anti-VP1 antibody. GAPDH served as the loading control. Blots are representative of three independent experiments (n=3). M: Mock-infected cells.

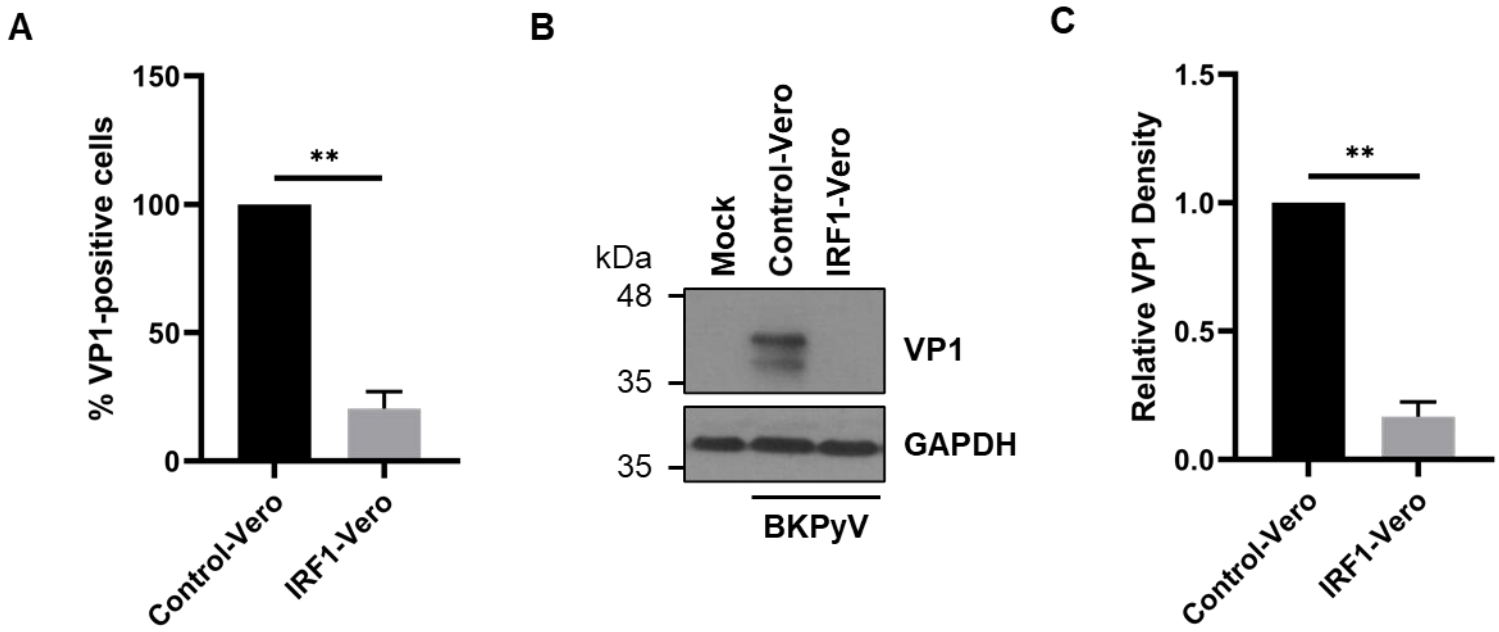

167

Figure 4.7 Potent suppression of VP1 protein levels by IRF1 at 72 hours post-infection. Control-Vero and IRF1-Vero cells were infected with BKPyV at MOI 0.1 for 2 h and processed at 72 hpi for flow cytometry (A) or lysates were resolved by SDS-PAGE and analysed by Western blot (B-C). A) The percentage of VP1-positive cells within IRF1-expressing cells was normalised to that of Control-Vero cells. B) Representative blots of mock-infected or BKPyV-infected cells probed with anti-VP1 and anti-GAPDH antibodies. C) Densitometry analysis from B was performed using ImageJ and values were normalised relative to the control cell line. Error bars represent the mean ± SD from three independent experiments (n=3). * P≤0.05, ** P≤0.01, *** P≤0.001 (Welch's t-test).

4.2.4.2 The release of infectious progeny virus is impaired by IRF1

To further examine the spectrum of the antiviral effect exerted by IRF1 on BKPyV infection, we assessed BKPyV virion release from Control-Vero and IRF1-Vero cells. Cells were inoculated with BKPyV at MOI 0.1 and infections occurred for 2 h. BKPyV-containing medium was collected at 72 hours post-infection and used to infect naïve Vero cells for 2 hours. At 48 hours post-infection, the cell monolayer was fixed, labelled for VP1 protein and processed for IncuCyte® ZOOM imaging (Figure 4.8A). The number of infected, VP1-positive cells in each well was extrapolated by the software and was used to calculate the percentage of VP1-positive cells in each condition relative to the control cell line. Significantly less naïve cells were infected by media collected from IRF1-Vero cells than by media collected from Control-Vero cells (Figure 4.8B). Our data therefore suggested that exogenous IRF1 expression restricts the release of infectious BKPyV progeny.

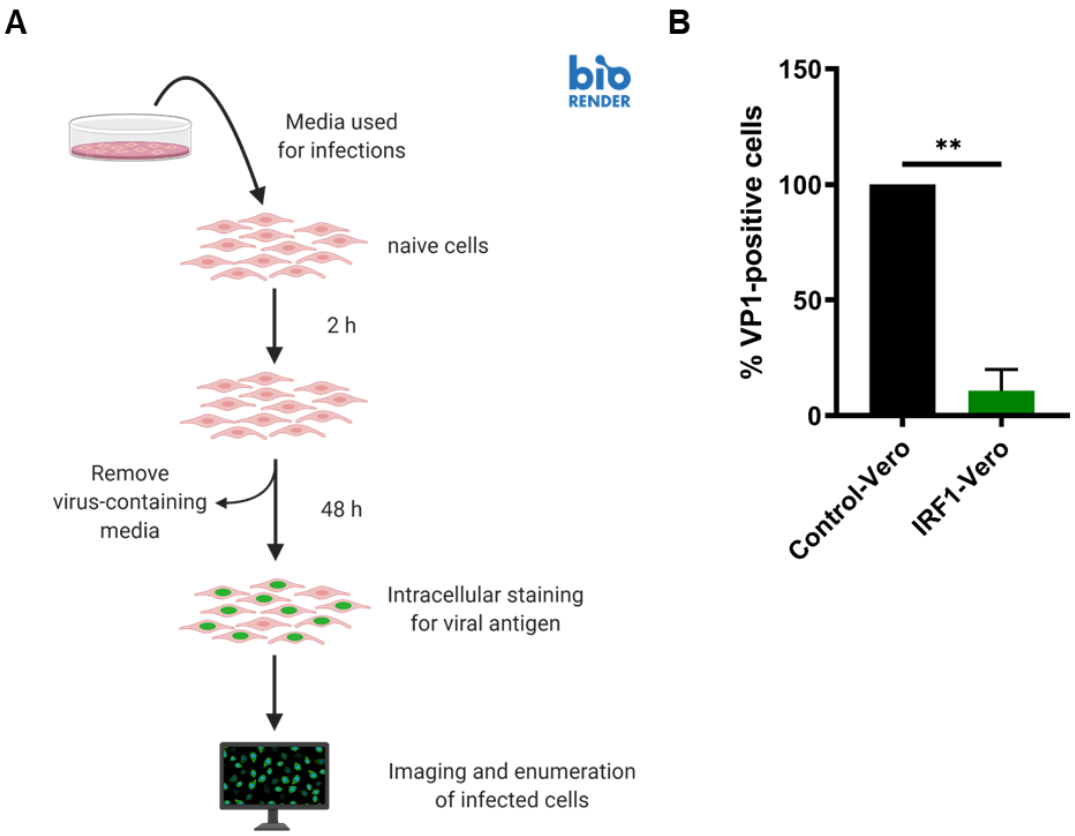

Figure 4.8 IRF1 restricts the release of infectious BKPyV virions. A) Schematic of the virion release assay. Naïve Vero cells were infected for 2 hours with BKPyV-containing medium collected from infected Control-Vero or IRF1-Vero cells. Cells were then incubated with normal medium, fixed after 48 hours of infection and labelled 'green' for VP1 protein. Imaging by the IncuCyte® ZOOM instrument enabled enumeration of 'green' VP1-positive cells. Created with BioRender.com. B) The percentage of infected, VP1-positive cells was calculated relative to the value obtained upon cell infection with media from Control-Vero cells. Error bars represent the mean ± SD from three independent experiments (n=3). * P≤0.05, ** P≤0.01, *** P≤0.001 (Welch's t-test).

4.2.4.3 IRF1 restricts BKPyV infection in an MOI-independent manner

To investigate whether the inhibitory effect of IRF1 is dependent on input virus levels, stable cell lines were infected with a ten-fold lower or higher MOI than previously used in our assays. Infected cells were harvested every 12 hours over a 72 hour period of infection for analysis of viral protein levels by Western blotting (Figure 4.9). LT-Ag and VP1 protein levels were overall inhibited by IRF1, regardless of the MOI used during infection. Importantly, LT-Ag was in fact undetectable in IRF1-Vero lysates at both MOIs throughout the experiment. Interestingly, we detected VP1 at 24 hours post-infection. This observation may be due, in part, to blot overexposure for viral antigen detection from a low MOI assay. At this particular time-point, detection of VP1 in our lysates may perhaps represent input virus instead of newly produced viral protein.

To provide further support for an MOI-independent IRF1-mediated inhibition of BKPyV infection, we assessed virus yields of infected cells over the 72 hour period of infection. BKPyV-containing medium collected from each time-point was titrated over naïve Vero cells and infections occurred over a 2 hour incubation period. At 48 hours post-infection, cells were labelled for VP1, imaged by IncuCyte® ZOOM and viral load was calculated as IU/mL as previously discussed. A similar pattern of increasing viral load was observed from Control-Vero cells until the end of the assay, regardless of the MOI (Figure 4.10A). The viral load from IRF1-Vero cells followed a similar trend for both MOIs, with a small reduction observed between the 60 and 72 hours post-infection time-points. By normalising the viral load of the end-point across our experiments, we observed there was no significant difference between viral loads obtained with MOI 0.01 or 1.0 when IRF1 was overexpressed (Figure 4.10B-C).

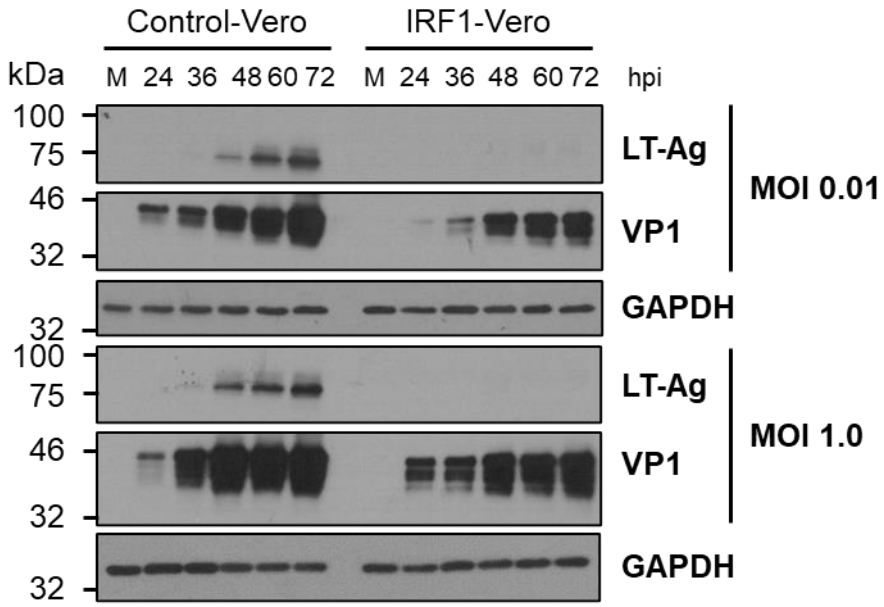

Figure 4.9 IRF1-mediated viral protein inhibition is independent of MOI. Synchronised infections of Control- and IRF1-Vero cells occurred with BKPyV at MOI 0.01 or 1.0. Total cell protein was harvested at the indicated time-point and analysed by Western blot for early (LT-Ag) and late (VP1) protein levels. GAPDH protein served as the loading control. Blots are representative of three independent experiments (n=3). M: Mock-infected cells.

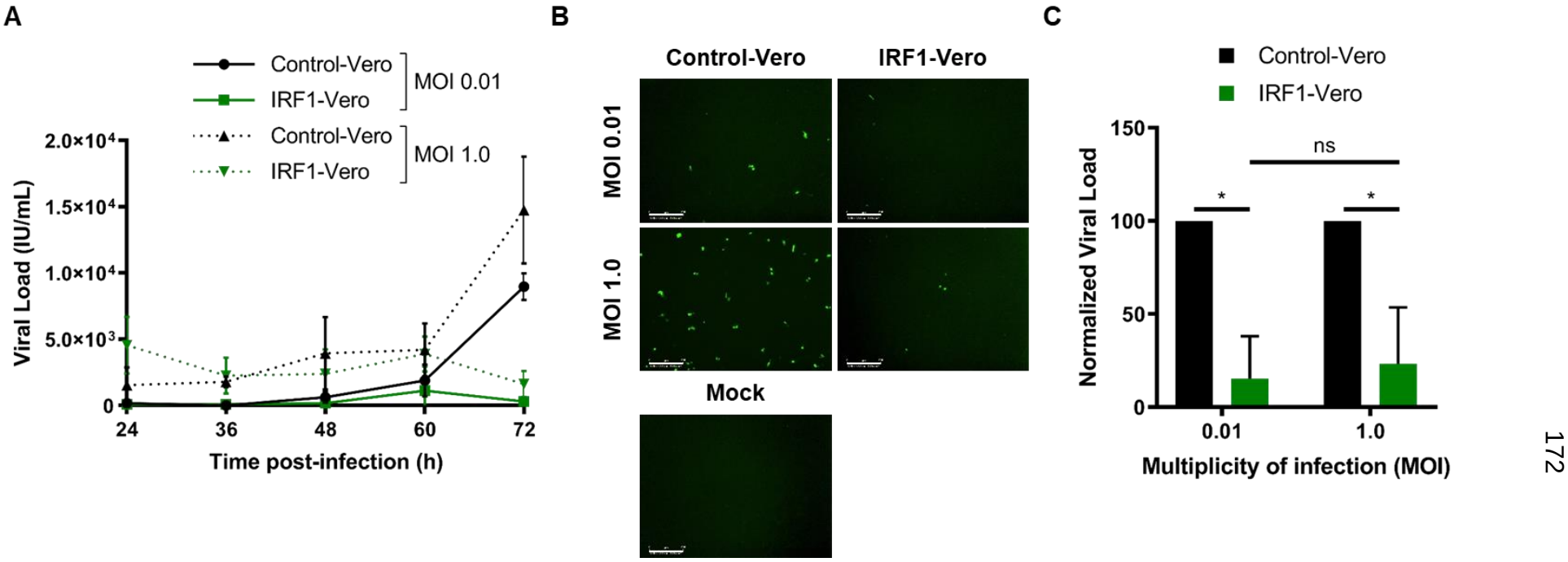

172

Figure 4.10 Restriction of infectious progeny release by IRF1 is independent of MOI. A-B) Media were collected over a period of 72 hours of infection from Control-Vero and IRF1-Vero cells infected at MOI 0.01 or 1.0. BKPyV-containing medium was titrated on naïve Vero cells for 2 h. At 48 hpi, cells were stained for VP1 protein and imaged. A) The viral load in infectious units per mL was calculated for each time-point from data extracted from IncuCyte® ZOOM images. Bars represent the mean ± SD of three technical repeats from a one representative experiment. B) Green fluorescence IncuCyte® ZOOM images from 72 hpi, where green represents VP1 staining. Scale bar: 300 µm. C) Viral load from 72 hpi was normalised to Control-Vero for each MOI used. Error bars represent the mean ± SD from three independent experiments (n=3). Mock: Mock-infected cells. ns: not significant, * P≤0.05, ** P≤0.01, *** P≤0.001 (Welch's t-test).

4.2.4.4 Viral genome replication is suppressed by IRF1

Our findings thus far supported IRF1-mediated inhibition of late viral protein levels and a subsequent defect in the release of infectious progeny. In addition, LT-Ag levels were undetectable upon enhanced IRF1 expression. We wished to investigate the impact of IRF1 on stages in the viral life cycle preceding late viral protein production and BKPyV progeny release.

We first investigated BKPyV replication in our Control-Vero cell line and compared it to viral replication occurring in normal Vero cells. Viral DNA was extracted at 72 hours post-infection and quantified by qPCR using specific primers against the BKPyV genome. The genome copy number per microgram (µg) of each sample was calculated by the qPCR software using a standard curve built into each repeat. There was no significant difference between the viral DNA levels of Vero and Control-Vero cells, suggesting that BKPyV replicates to similar levels in our stable control cell line as it does in normal Vero cells (Figure 4.11A).

To evaluate the effect of IRF1 on viral genome replication, total DNA was extracted from BKPyV-infected Control-Vero and IRF1-Vero cells at 72 hours post-infection. In addition, Control-Vero cells were treated with cidofovir as a control for the inhibition of BKPyV replication. A significant decrease in viral DNA levels was observed in IRF1-Vero cells compared to the levels in Control-Vero cells (Figure 4.11B). In addition, the levels of inhibition by IRF1 on BKPyV replication were comparable to cidofovir treatment. Together, our findings suggested that IRF1 impairs BKPyV infection on both protein and DNA levels.

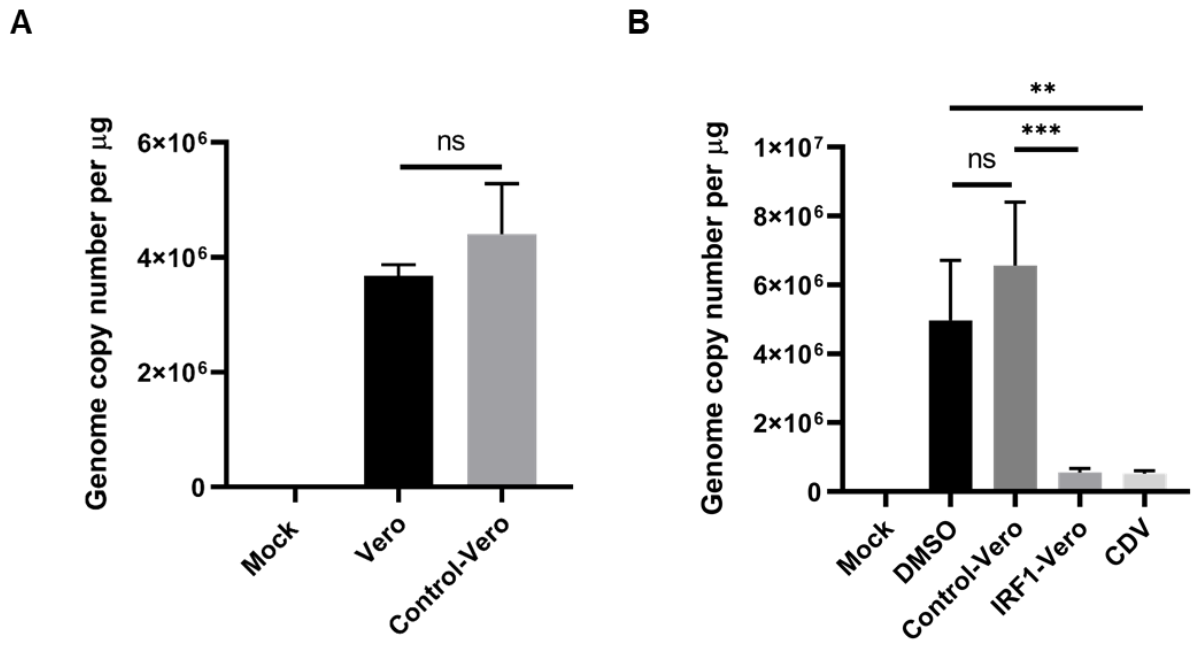

Figure 4.11 BKPyV DNA replication is blocked by IRF1 overexpression. BKPyV infection occurred at MOI 0.1 for 2 hours, upon which cells were returned to normal medium. At 72 hpi, total DNA was extracted from cells and analysed by qPCR to quantify viral DNA, given as genome copy number per microgram (µg). A) BKPyV-infected Vero or Control-Vero cells were assessed for viral genome copy numbers. B) BKPyV-infected IRF1-Vero and Control-Vero were evaluated for BKPyV genome copy numbers. Infected Control-Vero cells were treated with cidofovir (CDV), incubated with DMSO or left untreated. Error bars represent the mean ± SD from three independent experiments (n=3). Mock: Mock-infected cells. ns: not significant, * P≤0.05, ** P≤0.01, *** P≤0.001 (Welch's t-test).

4.2.4.5 Viral transcription is impeded by IRF1 overexpression

The function of IRF1 as a transcription factor and the intrinsic link between polyomavirus genome replication and viral gene expression, prompted us to examine the role of IRF1 in viral transcription.

To investigate the impact of IRF1 on viral gene expression, RT-qPCR analysis was conducted for early and late region transcripts. Total cell RNA was harvested at 72 hours post-infection from BKPyV-infected stable cell lines. RNA samples were analysed by RT-qPCR for LT-Ag and VP1 gene expression, representing early and late transcription, respectively. Overexpression of IRF1 resulted in a significant reduction in LT-Ag and VP1 transcript levels compared to control cells (Figure 4.12A-B). The inhibition of VP1 transcription concurs with VP1 protein level decrease in our previous experiments, further supporting viral gene transcription, as opposed to viral translation, as a target of IRF1.

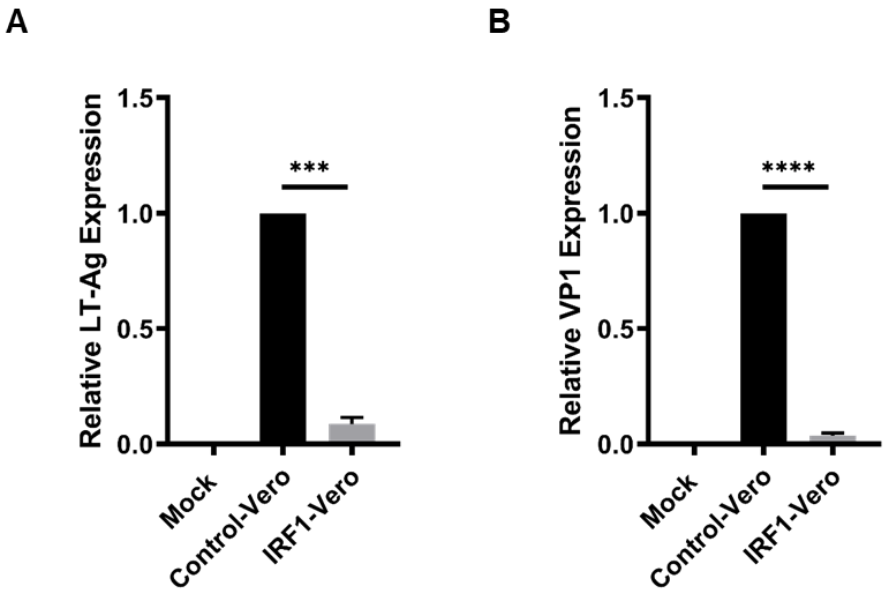

Figure 4.12 Viral transcription is inhibited by IRF1 overexpression. Control-Vero or IRF1-Vero cells were infected with BKPyV at MOI 0.1 for 2 h and harvested at 72 hpi. Total RNA was extracted for RT-qPCR analysis of viral early (A) and late (B) region gene expression. Samples were normalised against U6 mRNA levels. A) Gene expression of LT-Ag from the early region of the genome. B) Gene expression of VP1 from the late region of the genome. Data are presented relative to the control cell line and error bars represent the mean ± SD from three independent experiments (n=3). Mock: Mock-infected cells. * P≤0.05, ** P≤0.01, *** P≤0.001, **** P≤0.0001 (Welch's t-test).

4.2.5 IRF1 antiviral activity is conserved against some related polyomaviruses

IRF1 has previously demonstrated its inhibitory effect on a variety of virus species. To assess the magnitude of IRF1 protection against related polyomaviruses, we utilised the stable cell lines to evaluate the effect on the related human and primate polyomaviruses, JCPyV and SV40 respectively.

Control-Vero and IRF1-Vero cells were infected with SV40 at MOI 0.1 or JCPyV at MOI 0.07 for 2 hours. Total cell protein was harvested at 72 hours post-infection and resolved lysates were probed for viral antigens. The anti-LT-Ag and anti-VP1 antibodies used in this study are cross-reactive against related polyomaviruses, specifically JCPyV and SV40. Both SV40 LT-Ag and VP1 protein levels were significantly reduced by IRF1 (Figure 4.13A-C). In contrast, IRF1 overexpression had no significant effect on JCPyV VP1 protein levels (Figure 4.13D-E). We were unable to detect LT-Ag protein from JCPyV infection. These findings suggested that the magnitude of IRF1 protection was variable against different polyomavirus species.

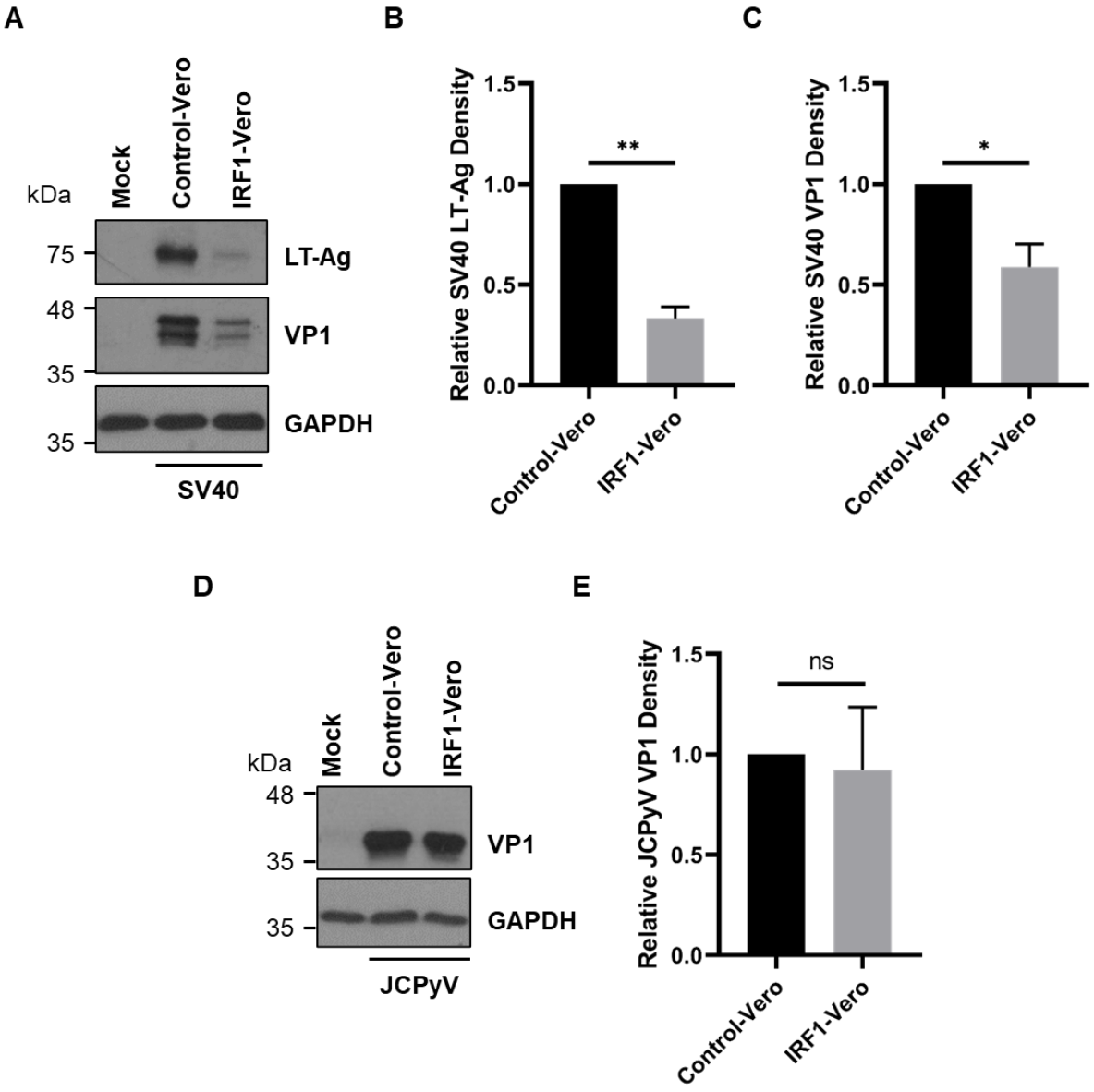

Figure 4.13 IRF1 restricts SV40 but not JCPyV infection. A) Control-Vero or IRF1-Vero cells were infected with SV40 at MOI 0.1 for 2 h. Lysates collected at 72 hpi were probed for LT-Ag, VP1 and GAPDH in representative Western blots. B-C) Densitometry analysis from A was performed using ImageJ. D) Control-Vero or IRF1-Vero cells were infected with JCPyV at MOI 0.07 for 2 h and harvested at 72 hpi. Representative Western blots of lysates probed for VP1 and GAPDH. GAPDH served as a loading control. E) Densitometry analysis from D. Values were calculated relative to the control cell line. Error bars represent the mean ± SD from three independent experiments (n=3). Mock: Mock-infected cells. ns: not significant, * P≤0.05, ** P≤0.01, *** P≤0.001 (Welch's t-test).

4.2.6 Exogenous IRF1 in RPTE cells restricts BKPyV infection

To determine whether the IRF1-mediated inhibitory effect against BKPyV is consistent in the primary cell culture system, we first transduced RPTE cells with IRF1-encoding (IRF1/RPTEC) or control (Control/RPTEC) lentiviruses. We monitored ISG expression by detecting the co-expressed TagRFP in images taken on IncuCyte® ZOOM (Figure 4.14).

At 72 hours post-transduction, RPTE cells were inoculated with BKPyV at MOI 0.01 or 1.0 for 2 hours. Cells were harvested 72 hours post-infection for analysis of viral protein levels by Western blotting. A significant decrease in LT-Ag and VP1 protein levels was observed upon IRF1 overexpression (Figure 4.15A-D). The inhibitory effect by IRF1 in RPTE cells was independent of the MOI used.

Furthermore, media from these cells was used in an FFA to determine the effect of exogenous IRF1 on progeny production from RPTE cells. Compared to control media, media from IRF1-transduced cells resulted in a significant reduction of 71% and 75% in infected cells for MOIs 0.01 and 1.0, respectively (Figure 4.16A-B). These results concur with data from our stable cell lines, where IRF1 inhibited viral gene expression and progeny production. Together, these data supported the notion of a conserved restriction of infection by IRF1 in primary RPTE cells and suggested that IRF1 may be acting in a similar manner to prevent the spread of BKPyV infection.

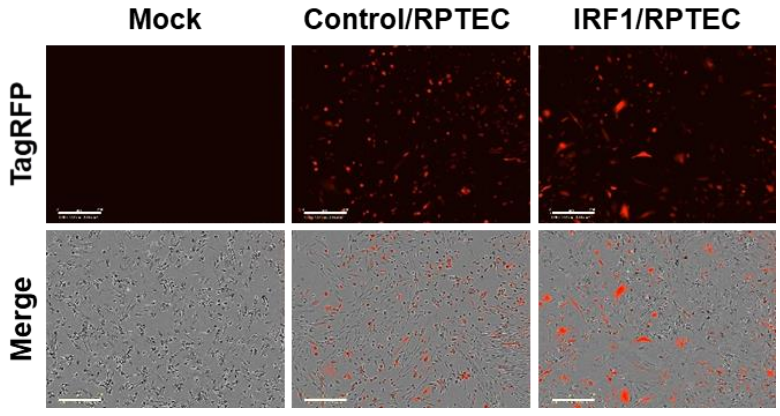

Figure 4.14 Confirmation of RPTE cell transduction. Red fluorescence images and images merged with phase contrast of mock-, control- (Control/RPTEC) or IRF1-transduced RPTE cells (IRF1/RPTEC) taken on IncuCyte® ZOOM at 72 hours post-transduction. Scale bar: 300 µm.

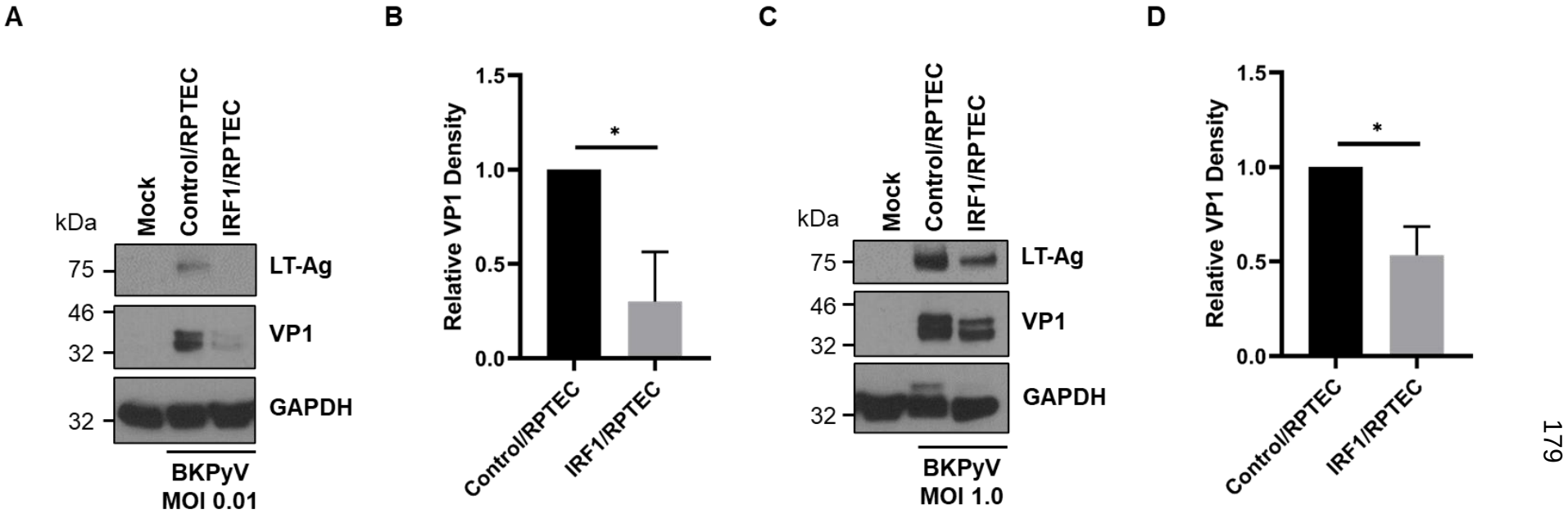

Figure 4.15 IRF1 inhibits viral protein production in RPTE cells independently of MOI. Control- (Control/RPTEC) and IRF1-transduced RPTE cells (IRF1/RPTEC) were infected for 2 h with BKPyV using different MOIs. Total cell protein was harvested at 72 hpi for analysis of LT-Ag and VP1 proteins by Western blotting. GAPDH served as a loading control. A) Representative Western blot of assay with an MOI 0.01. B) Densitometry analysis from A was performed using ImageJ. C) Representative Western blot of assay with an MOI 1.0. D) Densitometry analysis from C. Relative density was normalised to Control/RPTECs. Error bars represent the mean ± SD from three independent experiments (n=3). Mock: Mock-infected cells. * P≤0.05, ** P≤0.01, *** P≤0.001 (Welch's t-test).

179

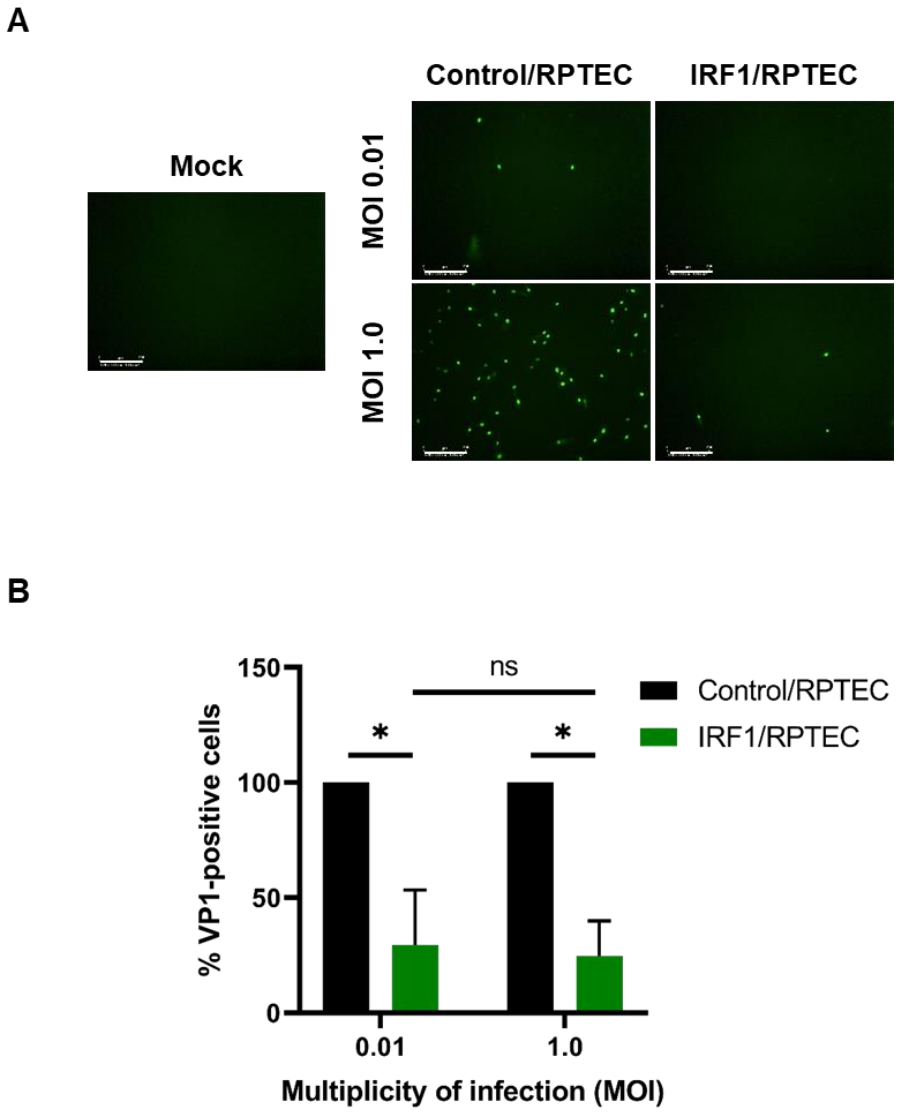

Figure 4.16 IRF1 suppresses infectious progeny release from RPTE cells in an MOI-independent manner. Media was collected at 72 hpi from control- (Control/RPTEC) and IRF1-transduced RPTE cells (IRF1/RPTEC) which were infected with two different MOIs. BKPyV-containing medium was used to infect naïve RPTE cells for 2 h. Cells were fixed 48 hpi and processed for IncuCyte® ZOOM imaging to detect VP1 produced in newly infected cells. A) Green fluorescence images from 72 hpi, where green represents VP1 staining, were extracted from the software. Scale bar: 300 µm. B) The percentage of infected, VP1-positive cells was calculated relative to the value obtained upon cell infection with media from control-transduced RPTE cells. Error bars represent the mean ± SD from three independent experiments (n=3). Mock: Mock-infected cells. ns: not significant, * P≤0.05, ** P≤0.01, *** P≤0.001 (Welch's t-test).

4.3 Discussion

4.3.1 Generation and titration of JCPyV stock

For the purpose of a comparison study between the IRF1 antiviral activities against BKPyV and the related human polyomavirus, JCPyV, the latter was propagated in SVG-A cells. Historically, JCPyV was propagated in PHFG cells. To overcome the inherent issues associated with cultivating PHFG cultures, Major *et al.* (1985) used an SV40 origin-defective mutant to transform human foetal glial cells, forming the SVG human astroglial cell line. To avoid any concerns regarding the recent discovery of SVG cell cultures contaminated with infectious BKPyV, we utilised a subclone of the original SVG cell line, termed SVG-A (Henriksen *et al.*, 2014).

JCPyV was grown in SVG-A cells for two weeks as described elsewhere (Assetta *et al.*, 2016). The JCPyV Mad-4 variant used in this study is commonly used as a lab strain and has been associated with PML (Gosert *et al.*, 2011). JCPyV Mad-4 contains a rearranged NCCR with a 19 nucleotide deletion, eliminating one of two TATA boxes found in the prototypical Mad-1 strain (Ferenczy *et al.*, 2012). Multiple TATA boxes do not confer a growth advantage and, in fact, variants such as Mad-4 grow better *in vitro* (Assetta and Atwood, 2017).

We assessed cell lysates and their culture media for the presence of JCPyV VP1 as a surrogate for successful viral propagation. VP1 was detected in both types of samples, suggesting late viral protein production and release of infectious progeny had taken place. Subsequent titration of our viral stock revealed a low JCPyV yield. Despite our efforts to increase the yield through multiple rounds of infection, this observation remained consistent and is in agreement with the reported challenge of generating sufficient amounts of JCPyV (Nukuzuma *et al.*, 1995).

4.3.2 Characterisation of IRF1-mediated anti-BKPyV activities

IRF1 was first discovered for its role in regulating type I IFN gene expression. Thereafter, it was demonstrated that IRF1 functions as a transcriptional activator downstream of IFN expression during *in vitro* and *in vivo* viral infection (Miyamoto *et al.*, 1988; Mboko *et al.*, 2014; Maloney *et al.*, 2012). Single gene studies have identified numerous target genes for IRF1, including the IFN-inducible genes GBP, iNOS, Caspase-1, Cox-2, CIITA, TAP1, and LMP2 (Tamura *et al.*, 2008). Furthermore, in IFN-γ treated cells IRF1 associates to MyD88 and, through TLR9 engagement, leads to transcriptional enhancement of IFN-β, iNOS, 1L-12p35 and IL-12p40 (Negishi *et al.*, 2006).

In the effort to characterise the inhibitory effect of IRF1 on BKPyV infection, we examined the timing of the effect on late viral protein production. We provided evidence of IRF1 overexpression leading to a reduction in the level of viral protein production, rather than a delay in the progression of infection. IRF1 exerted its most potent inhibitory effect on viral protein levels at 72 hours post-infection. In concurrence with a reduction in viral protein production, less infectious progeny was released from these cells at this specific time-point. Furthermore, our data supported that this inhibitory effect on viral protein and infectious virion production is not dependent on input virus levels. We, therefore, concluded that IRF1 is acting as a restriction factor against BKPyV infection.

Evidence of IRF1 as a broadly-acting restriction factor has been gathered by systematic screening of diverse viruses. Schoggins *et al.* (2011) demonstrated that IRF1 was amongst the four genes which inhibited Hepatitis C virus (HCV) infection in Huh-7.5 cells with z scores of less than -3.0. For IRF1, this corresponded to approximately 70% inhibition of HCV replication. In the same large-scale screen, IRF1 was also active against a second flavivirus, yellow fever virus (YFV), and reduced its replication down to 55.7% in Huh-7 cells. Togaviruses, CHIKV and Venezuelan equine encephalitis virus (VEEV), were potently inhibited by IRF1 by at least a 75% reduction in replication as indicated in confirmation assays. In addition, the broad-spectrum of IRF1 antiviral activities was further demonstrated against retroviruses, such as HIV-1 (Schoggins *et al.*, 2011).

IRF1 does not only act as an antiviral factor for RNA viruses; it is also protective against DNA viruses. In subsequent work, Schoggins *et al.* (2014) showed IRF1 reduced the infectivity of the poxvirus, vaccinia virus (VV), by 50% as determined in confirmation assays. An independent functional screen of 288 type I and II ISGs, revealed that IRF1 also targeted murine gammaherpesvirus 68 (MHV68) (Liu *et al.*, 2012). MHV68 infection of IRF1-deficient ($IRF1^{-/-}$) myeloid dendritic cells produced significantly increased progeny compared to wild-type cells (Schmitz *et al.*, 2007). The IRF1-driven antiviral signalling pathway was likewise operational in bone marrow-derived macrophages (BMDM). Furthermore, the protective effect of IRF1 was mirrored *in vivo* upon inoculation of wild-type mice which contained less viral progeny in their lungs compared to $IRF1^{-/-}$ mice. The contribution of the IRF1 signalling pathway in the antiviral immunity against MHV68 infection was characterised in primary murine BMDM. Mboko *et al.* (2014) showed that IRF1 transcription was enhanced by type I IFN signalling and IRF1 acted downstream of IFNAR to induce previously-identified MHV68-restricting ISGs (Liu *et al.*, 2012). In part, IRF1-mediated attenuation of MHV68 replication was attributed to cholesterol-25-hydroxylase (CH25H), an endoplasmic reticulum-associated enzyme. IRF1 was required for optimal CH25H expression which, in turn, interfered with late viral gene expression and DNA synthesis, therefore, inhibiting late stages of viral replication (Mboko *et al.*, 2014).

In this chapter we established stable expression of IRF1 in a Vero cell line, to ensure comparable ISG expression profiles across our assays by eliminating the transduction step. The use of cells which are defective in IFN-α/β production for our stable cell lines could also provide an environment whereby the effector mechanisms of IRF1 can be examined independently of type I IFN activity. Desmyter *et al.* (1968) provided evidence to support the defectiveness of Vero cells in producing IFN following inoculation with Newcastle disease virus (NDV). Cells did not secrete IFN, but held the ability to respond to exogenous IFN. Thereafter, Emeny and Morgan (1979) proposed that Vero cells sustained a genetic deletion or inactivation of the IFN gene. Subsequent work using DNA hybridisation analysis demonstrated that the entire type I IFN gene complex is ablated in both chromosome 12 copies, rendering Vero cells unable to engage

type I IFN signalling in response to infection (Diaz *et al.*, 1988; Osada *et al.*, 2014).

The complexity of an IRF1-mediated antiviral response was highlighted in an increasing number of studies showing that IRF1 can bypass IFN-mediated antiviral effects. IRF1 is capable of acting independently of IFN activity to induce cellular changes necessary to survive infection. Stirnweiss *et al.* (2010) demonstrated that IRF1 directly activated the promoter of murine viperin, a highly conserved antiviral ISG, upon VSV infection of MEFs. While VSV has the ability to block type I IFN function, IRF1-mediated enhancement of viperin allows suppression of VSV replication. Activation of the IRF1 pathway may represent a fail-safe mechanism by which the antiviral response is still triggered by cells when IFN signalling is circumvented by the virus. Adding to the intricate signalling of IRF1, acute MHV68 replication is restricted by IRF1 *in vivo* independently and in cooperation with type I IFN as assessed by lung viral titres (Mboko *et al.*, 2017).

Given the complexity of IRF1-mediated antiviral responses to other viruses, several hypotheses were considered regarding how IRF1 inhibits BKPyV infection in our overexpression system. Our initial findings demonstrated the inhibitory effect of IRF1 on the level of viral protein production and progeny release. Furthermore, IRF1 impeded BKPyV genome replication. To delineate whether this inhibitory effect occurs at the level of transcription or translation, we assessed the effect of IRF1 on viral transcript production. Increased IRF1 expression reduced transcription from early and late regions of the viral genome. Together, our findings suggest that IRF1 may intercept a life cycle stage prior to or during viral gene expression. With LT-Ag playing a central role in regulating viral replication and late gene expression, a plausible mechanism for IRF1-mediated restriction may be to target LT-Ag expression. Within the human genome, 345 unique genes exist with IRF1 binding sites within their promoter and/or 5'-UTR, which were identified using the refined 18 bp binding motif for IRF1 (Shi *et al.*, 2011). As a transcriptional activator, IRF1 may enhance one of these IRF1-regulated genes which, in turn, may suppress a viral target, such as LT-Ag. Further investigation could uncover any alterations to gene expression profiles in Vero cells, in the effort to identify any genes induced by IRF1 in the presence of BKPyV infection.

4.3.3 IRF1-mediated inhibition is conserved against SV40

SV40 transformation alters the gene expression of 800 genes as examined by microarray analysis in two different systems: SV40-transformed MEFs and enterocytes from transgenic mice (Cantalupo *et al.*, 2009). SV40 transformation of MEFs activates the IFN signalling pathway to induce ISG expression. In contrast, SV40-transformed enterocytes do not show an alteration in their pattern of ISG expression. While mouse genome-wide arrays revealed that the SV40 early region induced ISGs in a cell-type specific manner, a subsequent study in MEFs determined that SV40 LT-Ag was responsible for bringing about these changes in gene expression patterns (Cantalupo *et al.*, 2009; Rathi *et al.*, 2010). Assays with LT-Ag mutants demonstrated that the LXCXE motif of LT-Ag and interaction with p53 were both required for ISG upregulation. Giacobbi and colleagues (2015) further characterised the requirement of the LXCXE motif in the activation of STAT1 transcription factor for induction of the antiviral state.

LT-Ag-mediated ISG induction is also observed in immortalised and primary human fibroblasts (Forero *et al.*, 2014). ISG upregulation generated an antiviral state which protected human fibroblasts against vesicular stomatitis virus (VSV) infection. Knockdown experiments in immortalised human fibroblasts demonstrated that IRF1 was the link between SV40 LT-Ag and ISG expression. SV40 LT-Ag upregulated IRF1 and, subsequently, led to IFN-β expression which amplified ISG expression through IFNAR1. IRF1 induction by LT-Ag was mediated through the ATR kinase, revealing a mechanistic link between the induction of an antiviral IFN response and the DDR pathway (Forero *et al.*, 2014).

The small-scale screen performed in Chapter 3, identified a small, albeit, significant reduction in the percentage of SV40-infected cells during increased IRF1 expression in transduced cells. In this chapter, we demonstrated IRF1-mediated restriction of SV40 infection in IRF1-expressing Vero cell lines. IRF1 overexpression resulted in significant reductions in early and late viral protein levels as analysed by Western blotting. Our findings supported that IRF1 antiviral activity against BKPyV is also conserved against the related primate polyomavirus, SV40. We speculate that IRF1 may be restricting SV40 infection in our system by an alternative mechanism which is independent of type I IFN production. While in human fibroblasts, ISG induction is mediated by the DDR

and IFN production, in MEFs the interferon pathway is induced by LT-Ag without affecting IFN-α or IFN-β levels (Giacobbi *et al.*, 2015). To limit SV40 replication in Vero cells, IRF1 may be acting through a mechanism more similar to that occurring in MEFs in order to establish an antiviral state.

Data from our Western blot assay suggested there was no significant change in VP1 protein levels in JCPyV-infected IRF1-Vero cells. Transcriptome analysis of primary RPTE cells infected with JCPyV indicated that ISGs are robustly upregulated at 6 and 9 days post-infection (Assetta *et al.*, 2016). Amongst the enhanced ISGs were IRF7, ISG15, MX1, IFI6, RASD2, OAS1-3, IFITM2 and IFITM3. JCPyV-infected cells produced IFN-β to which JCPyV was sensitive, even at low physiologically relevant concentrations. Furthermore, Assetta and colleagues (2016) showed colocalisation of pSTAT1 and IRF9 in JCPyV-infected nuclei, which precedes ISG induction. In addition, induction of ISGs in MEFs was attributed to JCPyV LT-Ag, not sT-Ag (Giacobbi *et al.*, 2015). With literature indicating JCPyV sensitivity to the antiviral functions of ISGs, we expected an effect on JCPyV infection by IRF1 as a critical regulator of immune responses, which we did not detect. We cannot exclude the possibility of IRF1 exerting its effect on JCPyV infection in a cell type-specific manner and this could be further investigated in IRF1-transduced primary RPTE cells. Therefore, at the present time we conclude that the magnitude of protection by IRF1 in our stable cell line system included SV40 infection only.

4.3.4 IRF1-mediated restriction of BKPyV is not cell type-dependent

Exogenous IRF1 expression in primary RPTE cells resulted in the restriction of BKPyV infection. We have shown that protein production from the early and late regions decreased during overexpression of IRF1, as analysed by Western blotting. Both LT-Ag and VP1 protein levels were strongly inhibited by IRF1, regardless of the MOI used during the infection. The suppression of viral protein levels corresponded to a reduction in the release of infectious progeny virus by IRF1, as assessed by FFA. We, therefore, conclude that IRF1-mediated inhibition of BKPyV infection is not cell type-dependent.

Species-specific constrains of IRF1 antiviral function were unravelled in a report documenting the ability of IFN-γ pre-treated mouse and human fibroblasts to abrogate VV replication. IRF1 knockout experiments demonstrated the requirement for IRF1 in establishing an antiviral state in mouse, but not human, fibroblasts (Trilling *et al.*, 2009). However, evidence also exists in favour of IRF1 functioning independently of cell type to restrict other viral infections. For example, IRF1 strongly inhibits YFV in both Huh-7 cells and $STAT1^{-/-}$ fibroblasts (Schoggins *et al.*, 2011).

While the mechanism of infection by BKPyV varies in different cell types (Eash *et al.*, 2004; Zhao *et al.*, 2016), the antiviral programme induced by IRF1 seems to be conserved in both Vero and RPTE cells. This observation may further support IRF1 inducing an antiviral effector in order to have a post-nuclear entry effect. Furthermore, it is fundamental to consider what might occur *in vivo*. Several *in vitro* assays provided evidence of RPTE cells not eliciting a robust innate immune response against BKPyV infection, while other cell types are capable of combating the infection (An *et al.*, 2019). While we identified IRF1 as a restriction factor against BKPyV in both Vero and RPTE cells, the virus may possibly counteract or evade IRF1 antiviral activity *in vivo* by an uncharacterised mechanism which warrants further investigation. Knockout studies or the introduction of IRF1 following infection of primary cells, may define the importance of the IRF1 antiviral function in a physiologically relevant environment.

Chapter 5
The role of heparanase in BKPyV infection

5.1 Introduction

5.1.1 Heparan sulphate (HS) biosynthesis

Heparan sulphate (HS) is a sulphated glycosaminoglycan (GAG) polysaccharide made of repeating units of glucuronic acid (GlcUA)/iduronic acid (IdoUA) 1→4 linked to N-acetylated (GlcNAc) or N-sulphated (GlcNS) glucosamine (Rabenstein, 2002). HS is ubiquitously expressed on the cell surface of mammalian cells and in the extracellular matrix (ECM), in the form of heparan sulphate proteoglycans (HSPGs). HSPGs are comprised of at least one HS chain covalently linked to a transmembrane or secreted protein (Wu *et al.*, 2015).

HS biosynthesis occurs in the Golgi compartment, where most biosynthetic enzymes involved in the formation of HS chains are anchored to the Golgi membrane. Precursors are transported from the cytosol into the Golgi and the EXT1/EXT2 polymerase complex polymerises the disaccharide units which are linked to a core protein. Following HS chain formation, modification reactions take place, such as N-deacetylation/N-sulphation, epimerization and O-sulphation (Kreuger and Kjellén, 2012). The heterogeneity of HS chains produced by post-glycosylation modifications is important for the generation of protein-binding sites facilitating the interaction with various cytokines, chemokines and growth factors. Therefore, HS is involved in modulating a wide range of biological processes (McKenzie, 2007).

5.1.2 Heparanase (HPSE)

Heparanase (HPSE) is the principal enzyme involved in the breakdown of HS and is a member of the glycoside hydrolase 79 (GH79) family of carbohydrate-processing enzymes (Hulett *et al.*, 2000). Proteolytic activation of the 65 kDa HPSE pro-enzyme (proHPSE) by cathepsin L, gives rise to an N-terminal 8 kDa subunit and a C-terminal 50 kDa subunit. The liberated subunits form the non-covalent heterodimer of an active HPSE (Fairbanks *et al.*, 1999; Abboud-Jarrous *et al.*, 2008) (Figure 5.1A). The process of HPSE activation exposes an endo-acting binding cleft, where the enzyme recognizes low-sulphation sites in

its substrate and catalyses the hydrolysis of internal GlcUA(β1→4)GlcNS linkages (Wilson *et al.*, 2014; Wu *et al.*, 2015) (Figure 5.1B-C). Degradation by HPSE forms fragments of HS which are 10-20 sugar residues long (Peterson and Liu, 2010). Electron microscopy and co-localisation studies have confirmed that HPSE resides in late endosomes and lysosomes where it processes internalised HSPGs (Goldshmidt *et al.*, 2002). In addition, HPSE exerts its extracellular activity by trafficking to the cell surface or by being released into the ECM where it degrades HS moieties (Nadav *et al.*, 2002).

HPSE is a multi-functional protein with important roles in both normal and pathophysiological processes including cell motility, proliferation, angiogenesis, wound healing, inflammation and metastasis (Elkin *et al.*, 2001; Vlodavsky *et al.*, 2018). Accordingly, HPSE has been targeted by anti-cancer therapies. This strategy has seen the development of oligosaccharide-like HS mimetics and small-molecular inhibitors against HPSE (Coombe and Gandhi, 2019).

More recently, HPSE has been implicated in viral pathogenesis. In many instances, HS chains of HSPGs serve as cell surface receptors or co-receptors to facilitate attachment of viruses onto the cell surface. As the only enzyme known to degrade HS in mammals, the potential contribution of HPSE in the viral invasion of cells has generated interest (Thakkar *et al.*, 2017). The role of HPSE in BKPyV infection is the subject under study in this chapter.

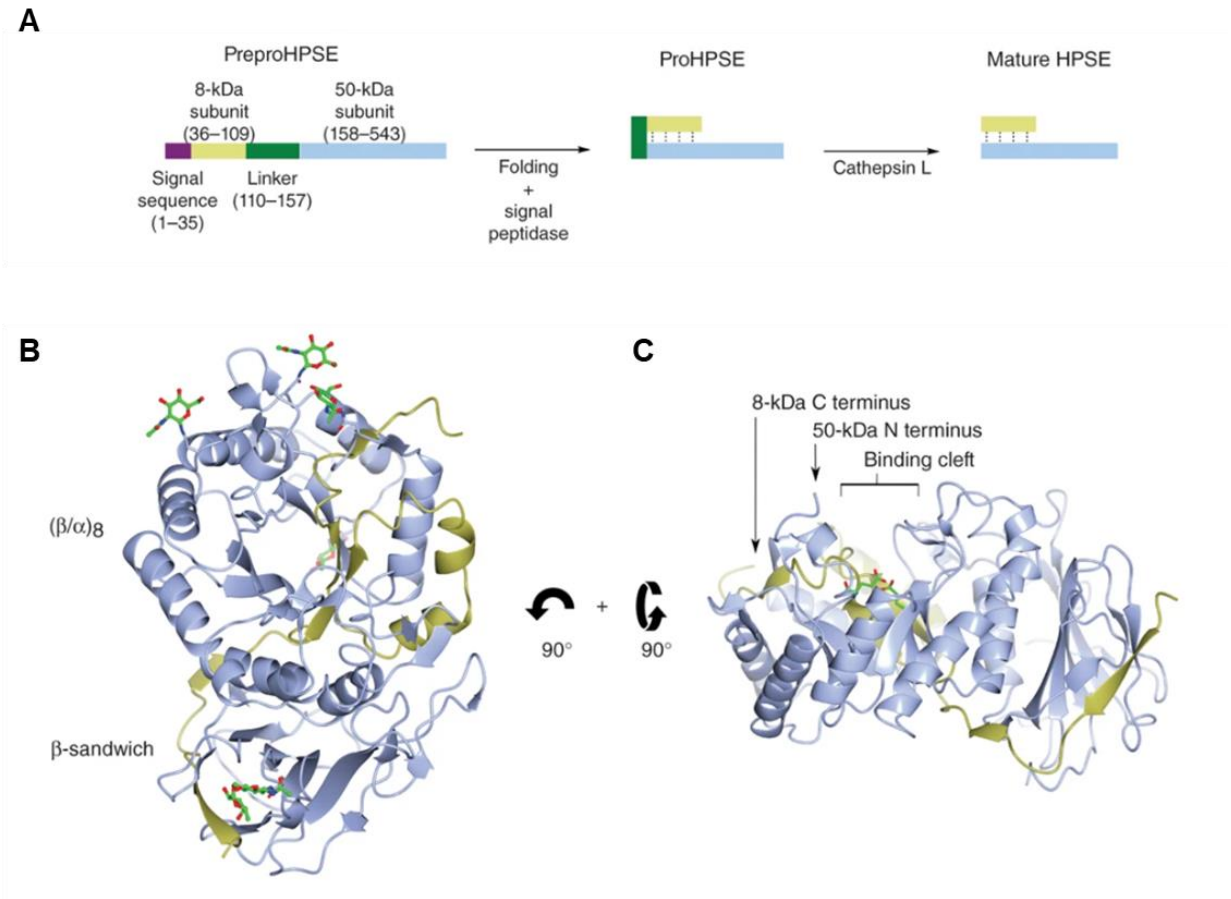

Figure 5.1 The three dimensional structure of human HPSE. A) Schematic representation of HPSE biogenesis. B) HPSE is comprised of a $(\beta/\alpha)_8$ domain and a smaller β-sandwich domain. The 8 kDa and 50 kDa subunits are coloured yellow and blue, respectively, and both contribute to the two domains of HPSE. Five of six sites of N-glycosylation are depicted in green. C) Side view of HPSE illustrating the binding cleft within the $(\beta/\alpha)_8$ domain and catalytic residues are shown in green. Adapted from Wu *et al.* (2015).

5.1.3 Chapter aims

In this chapter we address the potential antiviral role of HPSE against BKPyV infection and, to this end, establish a Vero cell line with stable HPSE expression. We attempt to define the mechanism by which HPSE may be restricting infection and begin by evaluating its effect on various stages in the viral life cycle. We block HPSE activity to demonstrate that BKPyV infection can be rescued upon specific inhibition of the enzyme. We then assess whether the antiviral activity of HPSE is conserved against the related polyomaviruses, JCPyV and SV40. Finally, we evaluate the role of HPSE during BKPyV infection in primary cells.

5.2 Results

5.2.1 Establishing an HPSE-expressing Vero cell line

To investigate the role of HPSE during polyomavirus infection, we established a Vero cell line with stable HPSE expression for our assays. The Vero cell line with HPSE overexpression is, herein, referred to as HPSE-Vero. Both HPSE-Vero and the control cell line (Control-Vero) were formed as described in section 4.2.2.

Prior to commencing our virologic assays, an MTT assay assessed the cell viability of Control-Vero and HPSE-Vero cell lines (Figure 5.2A). Cells were treated with staurosporine for 18 hours prior to the assay as a control for cell death induction. There was no significant difference between the viabilities of Control-Vero and HPSE-Vero cells, suggesting that HPSE overexpression does not perturb normal cell growth.

Furthermore, the expression of HPSE was confirmed by qRT-PCR in the stable cell line (Figure 5.2B). Total RNA was extracted from mock, Control-Vero and HPSE-Vero cell cultures. HPSE transcript levels were evaluated to be significantly enhanced in HPSE-Vero cells compared to the control cell line.

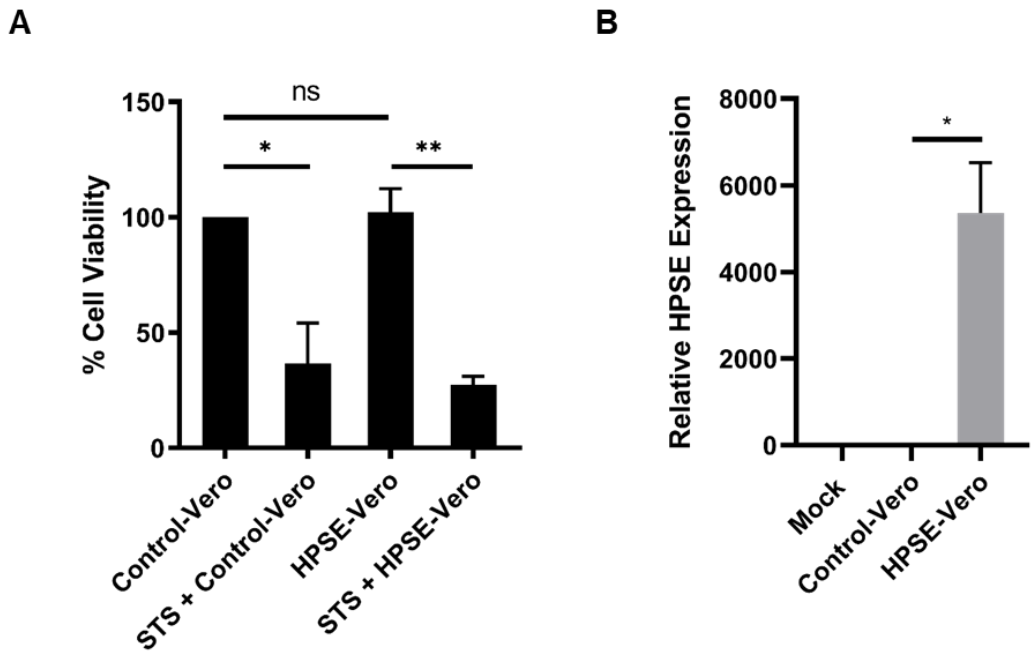

Figure 5.2 Establishment of a Vero cell line with stable HPSE expression. A) The cell viabilities of Control-Vero and HPSE-Vero cell lines were evaluated by MTT assay. As a control for the induction of cell death, cells were treated with 1 μM staurosporine (STS) for 18 hours prior to the assay. B) Total RNA was extracted from mock (untransduced) Vero, Control-Vero and HPSE-Vero cells, and reverse transcribed to assess HPSE transcript levels by RT-qPCR. Error bars represent the mean ± SD from three independent experiments (n=3). ns: not significant, * P≤0.05, ** P≤0.01, *** P≤0.001 (Welch's t-test).

5.2.2 Validation assay for BKPyV inhibition by HPSE

Upon formation of the HPSE-Vero cell line, we assessed whether the antiviral activity of HPSE observed in our ISG screen was still restrictive against BKPyV infection. Cells with stable HPSE expression were infected at MOI 0.1 for 2 hours and then returned to normal medium. At 48 hours post-infection, cells were processed for SDS-PAGE and probed for VP1 protein in a Western blot (Figure 5.3A). BKPyV-infected HPSE-Vero cells demonstrated fainter bands corresponding to VP1, compared to infected Control-Vero cells. Densitometry analysis determined that this reduction in VP1 protein levels during HPSE overexpression was statistically significant when compared to VP1 levels in the control cell line (Figure 5.3B). Our results from the validation assay using stable cell lines corroborated the results from the screen using cell transductions. Together, our data suggested that HPSE restricts the production of the major capsid protein, VP1.

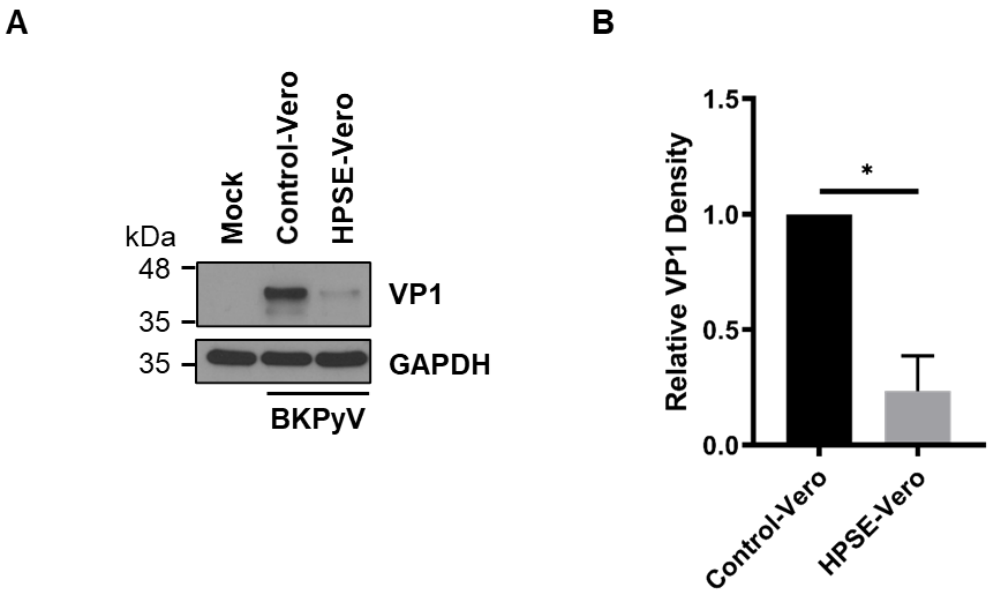

Figure 5.3 HPSE inhibits BKPyV VP1 protein production. Control-Vero and HPSE-Vero cells were infected with BKPyV at MOI 0.1 for 2 h and harvested at 48 hpi. Lysates were analysed by SDS-PAGE followed by Western blotting, probing for VP1 and GAPDH. A) Representative Western blots of mock-infected and BKPyV-infected cells. B) Densitometry analysis from A was performed using ImageJ software. Values were calculated relative to the control cell line and error bars represent the mean ± SD from three independent experiments (n=3). ns: not significant, * P≤0.05, ** P≤0.01, *** P≤0.001 (Welch's t-test).

5.2.3 HPSE-mediated antiviral effect is sustained for four days

To characterise further the HPSE-mediated inhibition of BKPyV infection, we investigated whether this effect can be sustained longer than the original time-point assessed (48 hours post-infection).

Control-Vero and HPSE-Vero were infected with BKPyV at MOI 0.1 for 2 hours, followed by removal of unbound virus. Cells were harvested every 24 hours post-infection for four days, starting at 48 hours post-infection. To evaluate the impact of HPSE at various time-points of infection, cells were fixed and labelled green for VP1 protein as a marker for infection. Infected, VP1-positive cells were then enumerated through IncuCyte® ZOOM imaging and analysed. The percentage of VP1-positive HPSE-Vero cells was significantly reduced at all three time-points compared to the percentages of Control-Vero cells (Figure 5.4A-B).

Furthermore, we resolved cell lysates collected at 72 hours post-infection by SDS-PAGE and probed these for VP1 protein in a Western blot (Figure 5.4C-D). VP1 protein levels were significantly decreased in HPSE-Vero cells compared to the control cell line, as determined through densitometry analysis. Our results suggested that the inhibitory effect exhibited by HPSE against BKPyV infection is sustained for at least four days, while the virus in not able to circumvent the antiviral activity during this period.

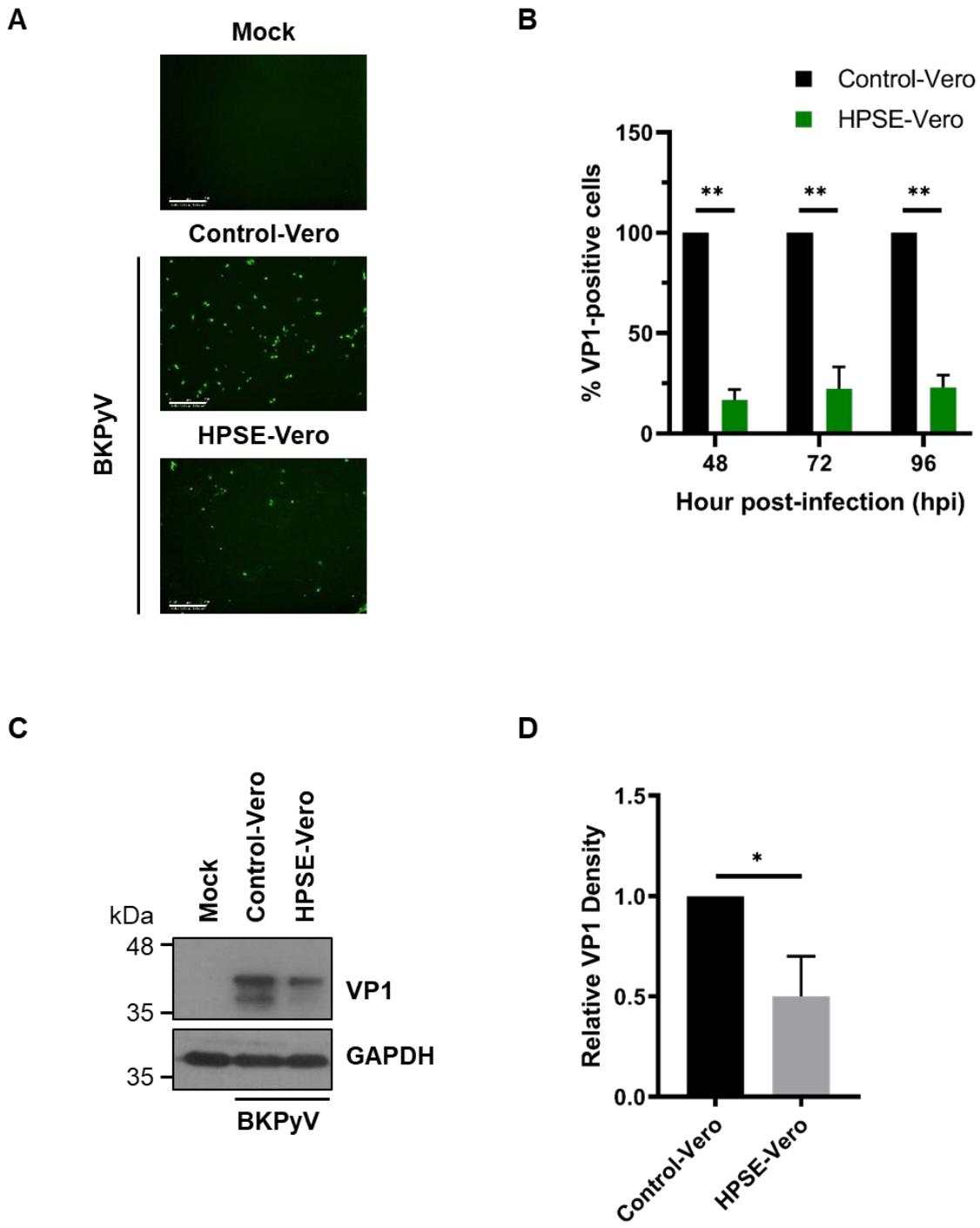

Figure 5.4. HPSE restriction of BKPyV infection is maintained for at least four days following infection. Control-Vero and HPSE-Vero cells were infected with BKPyV at MOI 0.1 for 2 h and harvested at 48, 72 and 96 hpi. Cells were processed for IncuCyte® ZOOM imaging (A-B) or lysates were analysed by SDS-PAGE and Western blot (C-D). A) Green fluorescence images from 72 hpi were extracted from the IncuCyte® ZOOM software, with green representing VP1 staining. Scale bar: 300 µm. B) The percentage of infected, VP1-positive cells was calculated relative to the value obtained upon cell

infection of Control-Vero cells at each time-point. C) Representative Western blots of mock-infected or BKPyV-infected cells harvested at 72 hpi and probed with anti-VP1 and anti-GAPDH antibodies. D) Densitometry analysis from C was performed using ImageJ software. Values were normalised relative to the control cell line and error bars represent the mean ± SD from three independent experiments (n=3). Mock: Mock-infected cells. * P≤0.05, ** P≤0.01, *** P≤0.001 (Welch's t-test).

5.2.4 HPSE inhibits viral genome replication and transcription

Our previous results supported HPSE-mediated restriction of the major capsid protein VP1, with inhibition sustained for at least four days post-infection. We wished to further assess the impact of HPSE on the stages of the BKPyV life cycle preceding late viral protein production, such as viral DNA replication and gene transcription.

To assess the effect of HPSE overexpression on viral DNA replication, Control-Vero and HPSE-Vero cells were infected with BKPyV at MOI 0.1 for 2 hours. As a control for the inhibition of viral DNA replication, Control-Vero cells were treated with cidofovir upon removal of virus-containing inoculum. Total DNA was extracted from cells at 72 hours post-infection and viral DNA was quantified by qPCR as described in section 4.2.4.4. A significant reduction in viral DNA levels was observed in HPSE-Vero cells compared to Control-Vero cells (Figure 5.5). Our findings, thus far, supported the notion of HPSE restricting BKPyV infection on both protein and DNA levels.

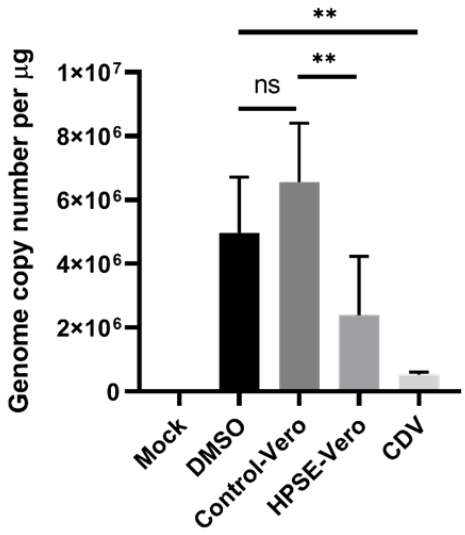

Figure 5.5 HPSE suppresses BKPyV genome replication. Control-Vero and HPSE-Vero cells were infected with BKPyV at MOI 0.1 for 2 hours. Upon removal of unbound virus, Control-Vero cells were treated with cidofovir (CDV), incubated with DMSO or left untreated. Total DNA was extracted from cells at 72 hpi and analysed by qPCR to quantify viral DNA, given as genome copy number per microgram (µg). Error bars represent the mean ± SD from three independent experiments (n=3). Mock: Mock-infected cells. ns: not significant, * P≤0.05, ** P≤0.01, *** P≤0.001 (Welch's t-test).

We then evaluated the impact of HPSE overexpression on viral gene transcription. BKPyV-infected cells were harvested at 72 hours post-infection and processed for total RNA isolation. Samples were analysed by RT-qPCR to determine LT-Ag and VP1 transcript levels representing early and late region gene expression, respectively. HPSE-Vero cells exhibited significantly reduced levels of LT-Ag compared to Control-Vero cells, indicating that HPSE inhibits early viral gene transcription (Figure 5.6A). As a result, viral genome replication is hindered and VP1 transcription is significantly impaired, ultimately leading to a reduction in VP1 protein levels (Figure 5.6B).

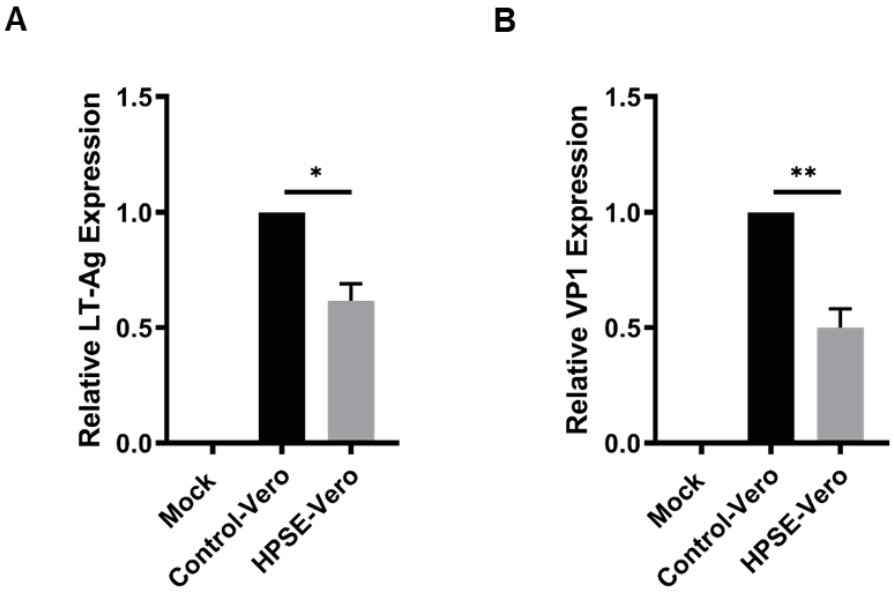

Figure 5.6 Early and late viral transcription is inhibited by HPSE. Control-Vero and HPSE-Vero cells were infected with BKPyV at MOI 0.1 for 2 h and harvested at 72 hpi. Total RNA was extracted for RT-qPCR analysis of viral transcripts. Samples were normalised against U6 mRNA levels. A) Gene expression of LT-Ag from the early region of the viral genome. B) Gene expression of VP1 from the late region of the viral genome. Data are presented relative to the control cell line and error bars represent the mean ± SD from three independent experiments (n=3). Mock: Mock-infected cells. * P≤0.05, ** P≤0.01, *** P≤0.001 (Welch's t-test).

5.2.5 HPSE overexpression prevents BKPyV trafficking to the ER

Our findings, thus far, suggested that HPSE affects a life cycle stage which involves or precedes early viral gene expression. To further define the stage during which HPSE acts to impair BKPyV infection, we considered its effect on the processes involved in virion intracellular trafficking which precede nuclear entry; a requisite for polyomavirus gene expression and replication. Between 6 and 12 hours post-infection, BKPyV virions transit to the ER where, upon interaction with host chaperones, their previously hidden VP2/VP3 minor capsid proteins become exposed (Moriyama and Sorokin, 2008; Rainey-Barger *et al.*, 2007).

To determine if HPSE overexpression interferes with the ability of BKPyV virions to transit to the ER, stable cell lines were incubated with BKPyV at MOI 0.5 during synchronous infections. Following virus removal, cells were treated with 25 mM NH_4Cl as a control to prevent intracellular trafficking or left untreated (Eash *et al.*, 2004). VP2/VP3 exposure was evaluated at 10 hours post-infection by immunofluorescent imaging, using a polyclonal antibody able to recognise both VP2 and VP3. VP2/VP3 puncta were visible mainly in the perinuclear area of infected Control-Vero and HPSE-Vero cells (Figure 5.7A). As expected, NH_4Cl-treated cells demonstrated few or no VP2/VP3 puncta.

Quantification of mean fluorescence intensity (MFI) supported that HPSE overexpression resulted in a substantial reduction of MFI from VP2/VP3 puncta compared to puncta observed in Control-Vero cells (Figure 5.7B). Our findings indicated that HPSE overexpression prevents the exposure of minor capsid proteins and, therefore, must be interfering with BKPyV entry into the ER.

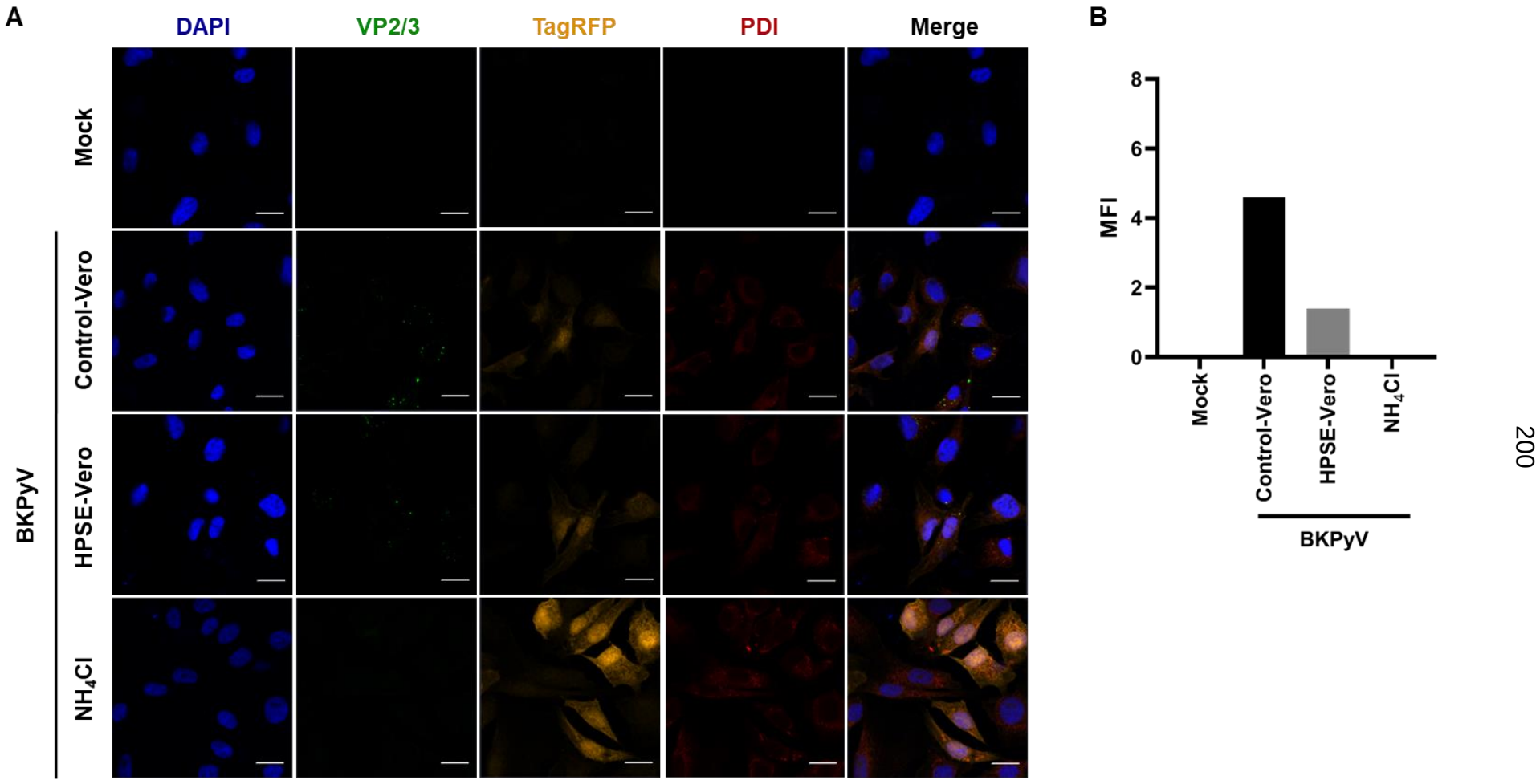

200

Figure 5.7 HPSE interferes with the exposure of minor capsid proteins. Control-Vero and HPSE-Vero cells were incubated with BKPyV at MOI 0.5 during synchronous infections. Control-Vero cells were treated with NH_4Cl to inhibit BKPyV intracellular trafficking,

or left untreated. At 10 hours post-infection, cells were fixed and immunostained with a polyclonal antibody against both VP2 and VP3. Cells were also incubated with an antibody against protein disulphide isomerase (PDI) to detect the endoplasmic reticulum (ER). TagRFP fluorescence was visualised to indicate stable cells. Nuclei were stained with DAPI. Immunofluorescence imaging was performed on a ZEISS LSM 700 confocal microscope and images were analysed using ZEN Black software. A) Representative microscopy images of the VP2/3 exposure assay. Scale bar: 15 µm. B) Quantification of VP2/3 puncta exemplified in A was performed using ImageJ software and is represented as mean fluorescence intensity (MFI). Data represents the mean of two independent experiments (n=2). Mock: Mock-infected cells.

201

5.2.6 BKPyV virion binding is restricted by HPSE

The contribution of HPSE in remodelling the cell surface and ECM through HS cleavage, and its emerging role in viral pathogenesis prompted us to examine its impact on virion attachment to the cell surface. For this purpose, we labelled purified BKPyV with Alexa Fluor® 488 dye and labelled virus is, henceforth, termed AF488-BKPyV.

To investigate virion binding, cells were incubated with AF488-BKPyV at MOI 0.2 for 1 hour at 4°C (Dugan *et al.*, 2008). Cells were then fixed and the amount of AF488-BKPyV bound to host cells was examined immediately by flow cytometry. No significant discrepancies were observed in the ability of AF488-BKPyV to bind to normal Vero cells or the control cell line (Figure 5.8A). The percentage of AF488-BKPyV bound to cells was significantly decreased when HPSE was overexpressed compared to that bound to Control-Vero cells (Figure 5.8B-C). Taken together, data from our overexpression approach demonstrated that BKPyV infection is targeted by HPSE at an early stage in the viral life cycle, most likely during virion attachment, to restrict infection.

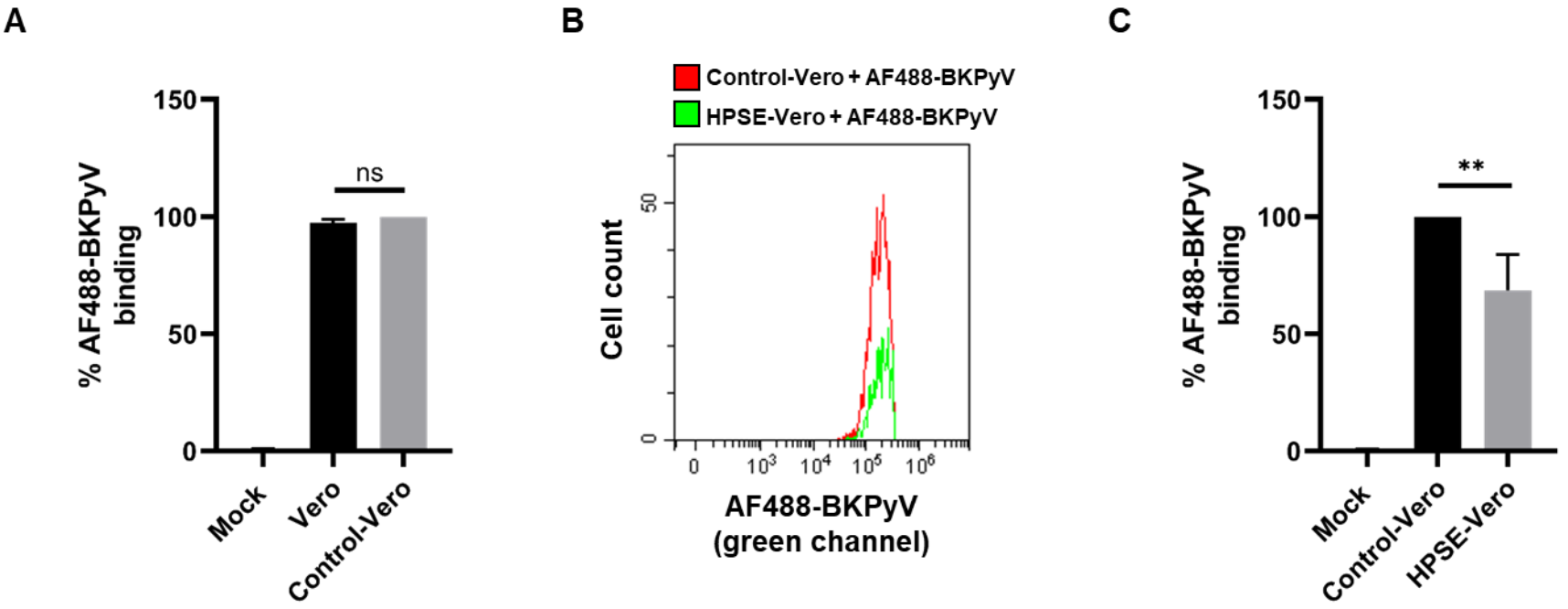

Figure 5.8 Viral binding is reduced by exogenous HPSE expression. Vero, Control-Vero and HPSE-Vero cells were incubated in suspension with AF488-BKPyV at MOI 0.2 for 1 hour at 4°C. Cells were fixed and viral binding was evaluated by flow cytometry. A) The percentage of virion binding on host cells was calculated relative to the control cell line. B) Overlay of green fluorescence intensities from ISG-expressing cells. C) The percentage of virion binding on host cells was calculated relative to the control cell line. Error bars represent the mean ± SD from three independent experiments (n=3). Mock: Mock-infected cells. ns: not significant, * P≤0.05, ** P≤0.01, *** P≤0.001 (Welch's t-test).

203

5.2.7 Pharmacological inhibition of HPSE may rescue infection

To investigate the importance of the enzymatic activity of HPSE in restricting BKPyV infection, we utilised a commercially available small-molecule HPSE specific inhibitor, OGT 2115. OGT 2115 blocks the enzymatic function of HPSE without significantly altering its expression (Courtney *et al.*, 2005; Goodall *et al.*, 2014).

We first evaluated the effect of OGT 2115 on cell viability. Control-Vero and HPSE-Vero cells were treated with varying concentrations of OGT 2115 for 48 hours, followed by an MTT assay (Figure 5.9A). Most concentrations of OGT 2115 resulted in a 25%, or higher, reduction in cell viability for either or both stable cell lines. Therefore, we chose 10 μM OGT 2115 for the treatment of cells in our rescue of infection assay, as this concentration did not substantially affect cell viability.

To examine if inhibition of HPSE rescues BKPyV infection, we first pre-treated cells with OGT 2115 for 24 hours. Cells were then infected with BKPyV for 2 hours in the presence of the inhibitor and harvested 72 hours post-infection. As expected, VP1 protein levels were decreased in DMSO-treated, HPSE-Vero cells compared to control cells (Figure 5.9B). In contrast, OGT 2115 treatment of HPSE-Vero cells resulted in an increase of VP1 protein levels compared to their DMSO-treated counterparts. The level of VP1 protein in OGT 2115-treated HPSE-Vero cells was comparable to that of Control-Vero cells. As this rescue of infection assay could only be conducted once during this study, independent repeats are required for a definitive conclusion. With the data currently available, we suggest that inhibiting the enzymatic activity of HPSE enables the restoration of BKPyV infection to a similar level observed in the absence of exogenous HPSE.

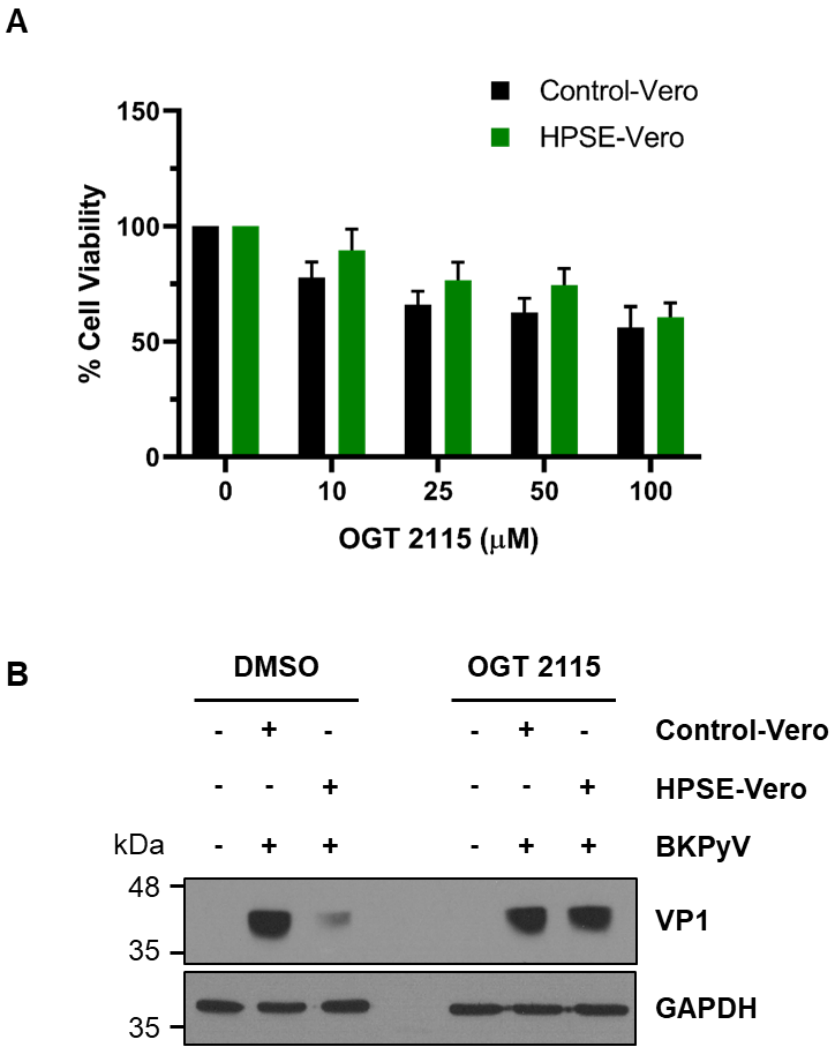

Figure 5.9 Pharmacological inhibition of HPSE restores VP1 levels. A) Control-Vero and HPSE-Vero cells were treated with different concentrations (μM) of OGT 2115 for 48 h. Cell viability was determined in technical triplicates by MTT assay. Data show mean ± SD from three technical repeats of one independent experiment (n=1). B) Control-Vero and HPSE-Vero cells were pre-treated with 10 μM OGT 2115 for 24 h and infected with BKPyV for 2 hours. OGT 2115 treatment was continued throughout the assay. Lysates collected at 72 hpi were resolved by SDS-PAGE and probed for VP1 in a Western blot. GAPDH served as a loading control. Blots shown are from one independent experiment (n=1).

5.2.8 HPSE antiviral activities against related polyomaviruses

To demonstrate whether the HPSE-mediated antiviral effect is conserved against related polyomaviruses or limited to BKPyV only, we evaluated the effect of HPSE on SV40 and JCPyV.

Stable cells were infected for 2 hours with SV40 at MOI 0.1 or JCPyV at MOI 0.07. At 72 hours post-infection, total cell protein was collected and resolved lysates were analysed by Western blot for the detection of VP1 protein. A significant reduction in SV40 VP1 protein levels was observed in HPSE-Vero cells compared to VP1 levels from Control-Vero cells (Figure 5.10A-B). A smaller, albeit, significant decrease was observed in VP1 protein levels from JCPyV-infected HPSE-Vero cells compared to their control (Figure 5.10C-D). Our results, therefore, suggested that HPSE-mediated inhibition of infection is conserved amongst the related polyomavirus species, BKPyV, JCPyV and SV40.

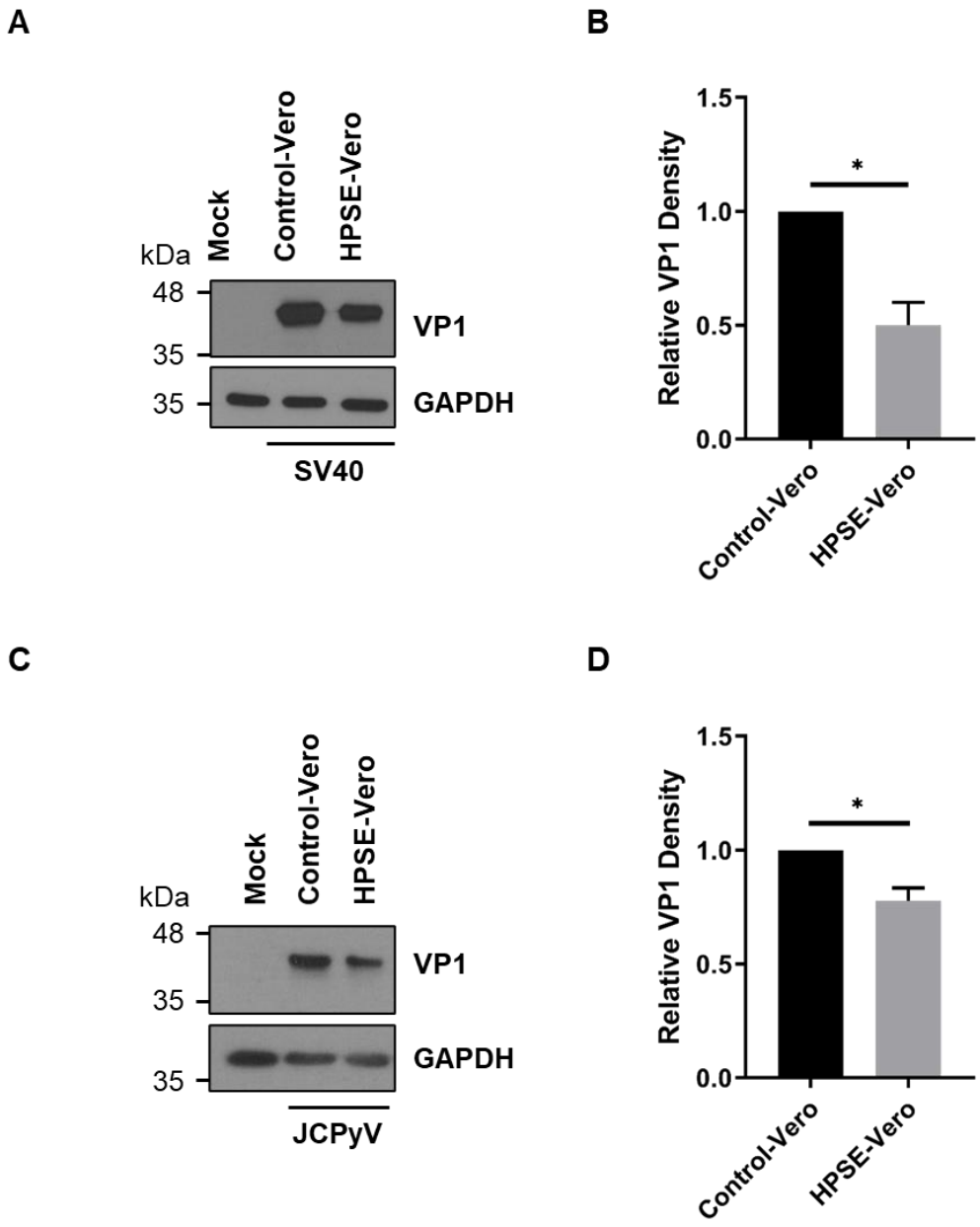

Figure 5.10 HPSE decreases VP1 protein levels in SV40 and JCPyV infections. A) Control-Vero and HPSE-Vero cells were infected with SV40 at MOI 0.1 for 2 h. Representative Western blots are shown of lysates from 72 hpi, probed for VP1 and GAPDH. B) Densitometry analysis from A was performed using ImageJ software. C) Cells were infected with JCPyV at MOI 0.07 for 2 h and harvested at 72 hpi. Representative Western blots of lysates probed for VP1 and GAPDH. D) Densitometry analysis from C. Error bars represent the mean ± SD from three independent experiments (n=3). Mock: Mock-infected cells. * P≤0.05, ** P≤0.01, *** P≤0.001 (Welch's t-test).

5.2.9 Exogenous HPSE does not affect infection of primary cells

To ascertain the role of HPSE during BKPyV infection of primary cells, RPTE cells were transduced with a HPSE-encoding (HPSE/RPTEC) or control (Control/RPTEC) lentivirus. As described previously in section 4.2.6, HPSE expression was monitored through detection of the co-expressed TagRFP in transduced cells (Figure 5.11).

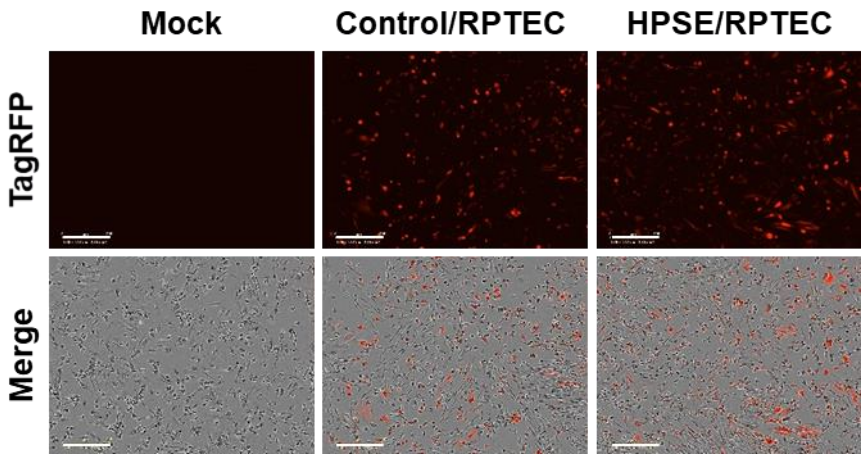

Figure 5.11 Confirmation of TagRFP-expression in transduced RPTE cells. IncuCyte® ZOOM images of red fluorescence (TagRFP) and phase contrast merged with red fluorescence of mock-, control- (Control/RPTEC) or HPSE-transduced RPTE cells (HPSE/RPTEC) taken at 72 hpi. Scale bar: 300 µm.

To examine the effect of HPSE on BKPyV infection in our primary cell culture system, RPTE cells were infected with BKPyV at MOI 1.0 for 2 hours and any unbound virus was removed before cells were incubated in normal medium. At 72 hours post-infection, cells were harvested and processed for flow cytometry by immunostaining for VP1 protein. The percentage of HPSE-transduced cells which were positive for VP1 and, thus, infected did not differ significantly from control cells (Figure 5.12A-B). We confirmed the absence of an effect from HPSE on VP1 protein levels by Western blotting, followed by densitometry analysis (Figure 5.12C-D). No significant change was observed in the levels of VP1 protein in HPSE/RPTECs compared to Control/RPTECs.

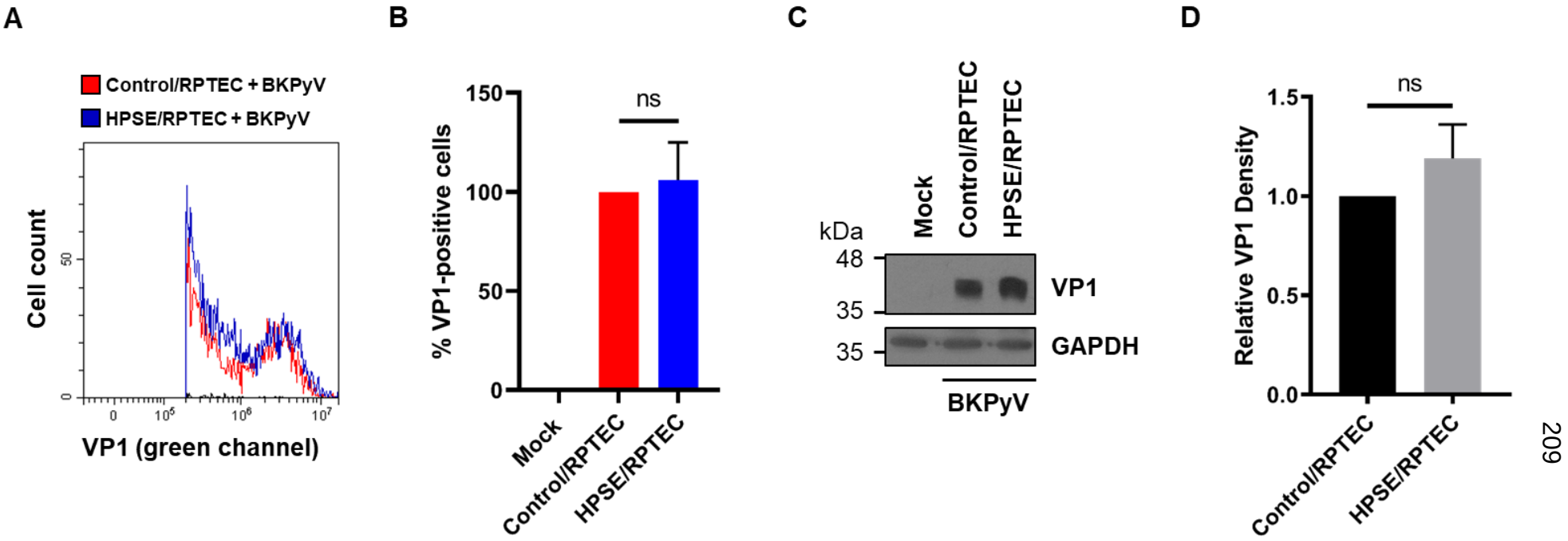

Figure 5.12 HPSE does not interfere with VP1 protein production in primary cells. Control-transduced RPTE cells (Control/RPTEC) or HPSE-transduced RPTE cells (HPSE/RPTEC) were infected with BKPyV at MOI 1.0 for 2 h. Cells were processed at 72 hpi for flow cytometry (A-B) or SDS-PAGE followed by Western blotting (C-D). A) Overlay of green (infected) fluorescence intensities from transduced RPTE cells. B) The percentage of VP1-positive, transduced cells was calculated relative to Control/RPTECs. C) Representative blots of lysates probed with anti-VP1 and anti-GAPDH antibodies. D) Densitometry analysis from C was performed with ImageJ software. Relative density was normalised to Control/RPTECs. Error bars represent the mean ± SD from three independent experiments (n=3). Mock: Mock-infected cells. ns: not significant, * P≤0.05, ** P≤0.01, *** P≤0.001 (Welch's t-test).

Furthermore, media collected from infected cells at 72 hours post-infection was used in an FFA to assess the impact of exogenously expressed HPSE on infectious progeny release. The higher MOI used during infections of primary cells enabled a better performance of the virion release assay. The percentage of VP1-positive cells did not differ significantly between HPSE/RPTEC- and Control/RPTEC-derived media (Figure 5.13). Taken together, primary cell data supported that HPSE overexpression does not interfere with BKPyV infection in RPTE cells. These findings contrast our observations in Vero cells, perhaps, reflecting a cell type-specific antiviral function of HPSE.

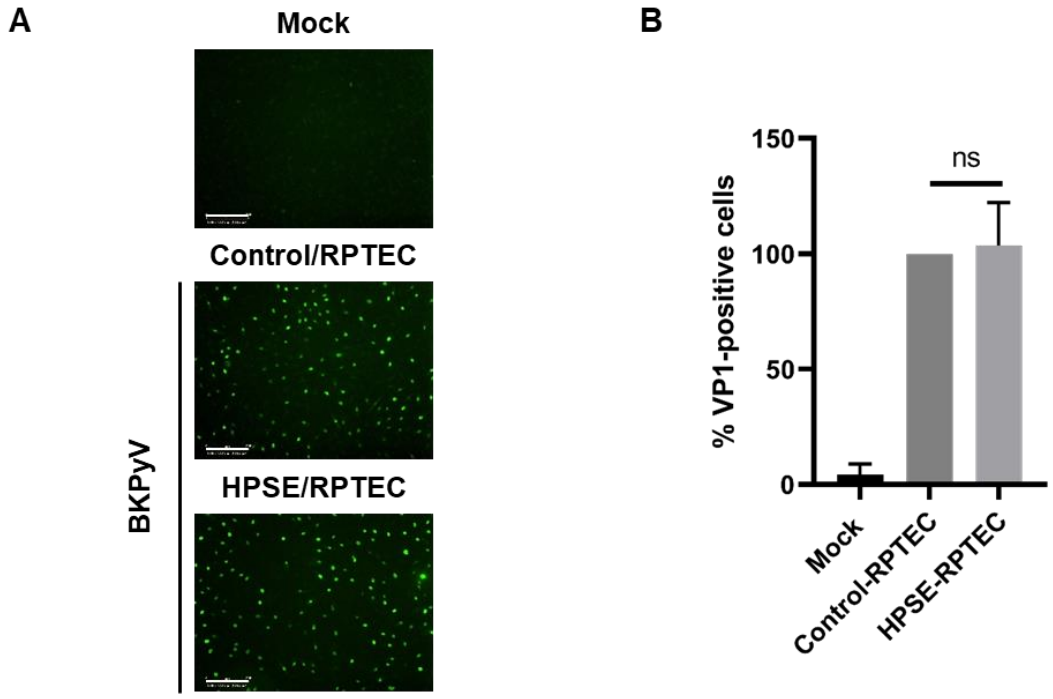

Figure 5.13 HPSE does not affect infectious progeny release from RPTE cells. Control-transduced RPTE cells (Control/RPTEC) or HPSE-transduced RPTE cells (HPSE/RPTEC) were incubated with BKPyV at MOI 1.0 for 2 h. At 72 hours post-infection, media was collected from cells and used to infect naïve RPTE cells for 2 h. Cells were fixed at 48 hpi and processed for IncuCyte® ZOOM imaging for VP1 detection. A) Green fluorescence images, where green represents VP1 immunostaining, were extracted from the software. Scale bar: 300 µm. B) The percentage of infected, VP1-positive cells was calculated relative to the value obtained upon cell infection with media from control-transduced RPTE cells. Error bars represent the mean ± SD from four independent experiments (n=4). Mock: Mock-infected cells. ns: not significant, * P≤0.05, ** P≤0.01, *** P≤0.001 (Welch's t-test).

5.3 Discussion

5.3.1 Exogenous HPSE restricts BKPyV infection by inhibiting entry

In this chapter, we validated HPSE-mediated inhibition of BKPyV infection in a cell line with stable HPSE expression and showed that our results were in agreement with the ISG screening approach in Chapter 3. We determined that BKPyV remains sensitive to HPSE and does not circumvent its antiviral activity during, at least, the first four days of infection. Initially, we identified the inhibitory effect of HPSE by observing lower levels of the major capsid protein VP1 by Western blot analysis. Through qPCR analysis of viral genome copy number, we have shown that HPSE also reduced viral genome production. Transcription of both early and late region viral genes was restricted by HPSE and the decrease in LT-Ag transcript levels correlated with the observed impairment in viral replication.

Our findings, thus far, were indicative of HPSE targeting a viral life cycle stage which either takes place in the nucleus or precedes nuclear entry. To investigate the impact on an earlier stage of infection we evaluated entry into the ER by assessing VP2/VP3 exposure through immunofluorescence imaging. A reduction in minor capsid exposure in cells overexpressing HPSE, indicated impairment of BKPyV trafficking to the ER. Consequently, the ability of virus to attach to cells was investigated to determine if the inability of BKPyV to transit to the ER was as a result of a pre-entry or post-entry effect of exogenous HPSE. The culmination of data from overexpression assays suggested that HPSE impairs an early stage of BKPyV infection by preventing virion attachment to the cell surface.

Attachment to a target cell surface is the first determinant of viral infection. Polyomaviruses bind to their receptors to activate signalling pathways which facilitate crucial steps in viral entry. Inhibition of these pathways is detrimental to infection. For example, SV40 binding to CV-1 cells initiates a signalling pathway necessary for SV40 entry and its inhibition by the tyrosine kinase inhibitor, genistein, blocks infection (Dangoria *et al.*, 1996). Genistein also prevents JCPyV entry into SVG-A cells by targeting ligand-inducible clathrin-dependent endocytosis (Querbes *et al.*, 2004). Furthermore, MPyV infection of MEFs requires the PI3K and FAK/Src pathways for endocytosis and virion trafficking,

respectively (O'Hara and Garcea, 2016). Liu *et al.* (2016) have reported that MCPyV infection of human dermal fibroblasts requires activation of WNT/β-catenin signalling and the MAP kinase pathway.

HS chains of HSPGs function as cell surface receptors or co-receptors for certain enveloped viruses, thus, playing critical a role in the mechanism of infection. Herpes simplex virus type-1 (HSV-1) interacts with HS moieties through the envelope glycoproteins gB and gC on the cell surface. Entry is initiated when a third HSV-1 envelope glycoprotein, gD, triggers fusion with the host cell upon interacting with 3-O-sulphated glucosamine residues of HS chains (O'Donnell and Shukla, 2008). Heparin, a molecule structurally similar to HS which only occurs in mast cells, is capable of inhibiting HSV-1 binding to cells (WuDunn and Spear, 1989).

The role of GAGs during the invasion of cells by non-enveloped viruses has also been investigated. It has been proposed that GAGs serve as co-receptors for MCPyV (O'Hara *et al.*, 2014). Schowalter *et al.* (2011) reported that MCPyV pseudovirion binding to cultured cells depends on the presence of cell surface GAGs, 'likely in the form of HS'. Their observation was confirmed using native MCPyV in 293-4T cells treated with bacterial heparinase I/III to enzymatically remove cell surface HS. Furthermore, non-sialylated GAGs serve as receptors for both wild-type and PML mutant JCV strains (Geoghegan *et al.*, 2017). Using JCPyV and BKPyV pseudovirions, the authors demonstrated that infectious entry of either virus into a range of cells was partially blocked upon application of exogenous heparin. The authors concluded that JCPyV and BKPyV relies, at least in part, on GAG-mediated attachment for entry. GAG dependency for SV40 infectious entry was reported in the same study using pseudovirions.

Structural analysis following on-grid binding of heparin to purified BKPyV virions, revealed density between the capsomeres and at the top of each capsomer pore (Hurdiss *et al.*, 2018). The site where GAG molecules are thought to bind between the pentamers is positively charged, as are other GAG binding sites observed in viruses, such as in adeno-associated virus-2 (O'Donnell *et al.*, 2009). One possible interpretation is GAGs binding in the VP1 pore to interact with VP2/VP3 found beneath it, in order to modulate cellular attachment or entry (Hurdiss *et al.*, 2018). Such interactions between GAGs and minor capsid proteins have also been postulated for the L2 minor protein of

HPV16 (Guan *et al.*, 2017). Furthermore, Schowalter and Buck, (2013) utilised BKPyV VP1-only pseudovirions to show that a lack of VP2/VP3 renders the pseudovirus less efficient in transducing different cell types. This observation may, in part, be explained as the lack of VP2/3 resulting to a decline in affinity for GAGs (Hurdiss *et al.*, 2018).

Given the integral role of HPSE in HS degradation, HPSE can modulate the life cycle of many pathogenic viruses, such as HSV, dengue virus, HPV, hepatitis B virus and hepatitis C virus (Thakkar *et al.*, 2017). We previously discussed the requirement of HS as a docking site for HSV-1. In fact, HS expression increases during the initial stages of HSV-1 infection, followed by a dramatic decline in HS during the later stages of infection (Bacsa *et al.*, 2011). At these later stages of infection, infected cell protein 34.5 upregulates the host-derived HPSE through NF-κB-mediated transcription (Hadigal *et al.*, 2015; Agelidis *et al.*, 2017). Active HPSE then translocates to the cell surface to cleave HS chains and prevent the interaction of newly formed viral progeny with HS during egress. Similarly, HPSE contributes to HSV-2 egress and spread (Hopkins *et al.*, 2018). Agelidis *et al.* (2017) reported on how HPSE drives HSV-1 pathogenesis in a mouse model of corneal epithelium. The study provided evidence of HPSE inhibiting type I interferon signalling and promoting pro-inflammatory cytokine production during HSV-1 infection of human corneal epithelial cells.

HPSE activity also contributes to the regulation of HPV infectivity. HPV particles attach to human keratinocyte (HK) host cells by, most commonly, binding to HS chains of HSPGs (Giroglou *et al.*, 2001). By inhibiting HPSE and matrix metalloproteinases (MMPs), Surviladze *et al.* (2015) demonstrated a decrease in HPV16 pseudovirions released from the ECM. As a result, there was a loss of viral uptake and infection of human keratinocytes. The authors proposed that HPSE facilitates the release of ECM-attached HPV16 particles by cleaving the HS chains of HSPGs found in complex with the particles. In a previous report, cell-attached HPV16 was shown to be released from the cell surface in a similar manner (Surviladze *et al.*, 2012). Studies of head and neck squamous cell carcinoma (HNSCC) cell lines have revealed that the HPV E6 gene drives HPSE upregulation, possibly by alleviating the p53-dependent inhibition of the HPSE promoter (Hirshoren *et al.*, 2014). As a result, HPSE contributes to the aggressive phenotype of HPV-positive HNSCC by enabling the release of

bioactive factors, such as growth factors, cytokines and chemokines, which are bound to HS moieties (Thakkar *et al.*, 2017).

Herein, we utilised an overexpression approach to investigate the mechanism through which HPSE may be regulating BKPyV infection. At present time, we speculate that by overexpressing HPSE there is a loss of HS moieties which, in turn, impedes virion attachment to the Vero cell surface, thereby, impairing the first step required for the initiation of infection. To strengthen our argument, the loss of HS from the cell surface could be monitored by immunofluorescence staining prior to and during infection. In addition, exogenous HPSE can be introduced following infection to evaluate its effect on the release of infectious progeny. HPSE-dependent HS turnover may represent yet another example of a normal cellular process commandeered by a virus to gain entry into the host cell, or HPSE may be working to defend the cell. Given the previously discussed examples of HPSE contribution to viral infection, the former argument may be favoured; however it is imperative for further investigative work to take place before we reach a definitive conclusion. For example, endogenous HPSE expression must be investigated in cells infected under normal conditions. This may also help in identifying any viral factors involved in potentially modulating HPSE expression. To determine whether BKPyV can manipulate HPSE expression, luciferase assays could be performed by transfecting the HPSE promoter together with individual viral components.

In our investigation, we attempted to restore BKPyV infectivity by inhibiting HPSE activity with OGT 2115. Similar levels of infection were observed for treated HPSE-Vero cells and control cells in a single independent experiment. Our observation suggested that inhibition of HPSE may restore cell surface HS to enable optimal virion attachment, further supporting a role for HS during BKPyV infection of Vero cells. Several HPSE inhibitors are being assessed in clinical trials as anti-cancer agents, however, none are currently being evaluated for the treatment of viral infections (Coombe and Gandhi, 2019; Thakkar *et al.*, 2017). OGT 2115 is a synthetic substrate which inhibits HPSE activity and has been used in *ex vivo* treatment of porcine corneas to arrest viral spread and associated pathologies during the later stages of HSV-1 infection (Courtney *et al.*, 2005; Agelidis *et al.*, 2017). Inhibition of HPSE activity impaired the release of newly produced HSV-1 progeny from the parental cell. Upon

confirming our own observation with OGT 2115 treatment and further assessing the effect of endogenous HPSE inhibition, the use of HPSE mutants can provide further proof for the role of its enzymatic activity in restricting infection. Alternatively, it may provide insights into the importance of non-enzymatic functions during infection.

In this study, we provided evidence which suggests that HPSE also targets related polyomaviruses. Through analysis of VP1 protein levels by Western blotting, we determined that HPSE is able to restrict the production of the major capsid protein of two related polyomaviruses, SV40 and JCPyV. Notably, both SV40 and JCPyV entry was reported to partially rely on GAG-mediated binding (Geoghegan *et al.*, 2017), which may explain why loss of HS through HPSE activity led to inhibition of infection by either virus. Our investigation into the spectrum of HPSE antiviral activities could be further explored by assessing the ability of SV40 and JCPyV to bind cells overexpressing HPSE.

Furthermore, it is important to consider the potential role of the EXT1 protein on BKPyV infection, which is part of the heterodimeric complex forming the major polymerase in HS biosynthesis. Busse *et al.* (2007) reported of EXT1 overexpression resulting in HS chain elongation in HEK-293 cells. Although knockdown of EXT1 expression by small interfering RNAs (siRNAs) was shown to impair filoviral entry (O'Hearn *et al.*, 2015), we observed a reduction in infectivity upon EXT1 upregulation by overexpression (3.2.4.2). While our observations require validation in the stable cell line system, discrepant results may be explained as EXT1 having a different effect on various viruses or that HS chain elongation may sterically hinder BKPyV from optimally binding to the target cell.

5.3.2 HPSE may not be important for primary cell infection

Data collected in stable Vero cell lines provided some insight into the importance of cell surface HS in polyomavirus infection, by focusing on its enzymatic breakdown by HPSE. Conversely, no effect was exerted by HPSE on BKPyV infection of primary cells, as evidenced by flow cytometry, Western blotting and immunofluorescence imaging. Further investigation is required to fully ascertain the importance of HPSE and, by extension, HS moieties during BKPyV infection of RPTE cells. Assays to determine if and where exogenous HPSE is active in primary cells may facilitate our understanding of this discrepant finding.

It is important to note that when BKPyV pseudovirions were allowed to transduce A549 cells in the presence of soluble GAGs, their ability to bind cells was unaffected (Schowalter *et al.*, 2011). In later studies, non-sialylated GAGs were determined to be important for BKPyV entry into ART, SFT or HEK-293TT cells (Geoghegan *et al.*, 2017). Therefore, one possible explanation for our results may be that a requirement for HS moieties differs depending on the cell type targeted by BKPyV. It is possible that BKPyV has evolved an alternative mechanism to facilitate its entry into RPTE cells.

Summary and Conclusion

BK polyomavirus (BKPyV) is an emerging pathogen in the immunosuppressed population. While in healthy individuals it causes a subclinical primary infection, patients with weakened immune responses are at risk of developing severe clinical complications due to BKPyV infection (Costa and Cavallo, 2012). One of the main BKPyV-associated diseases is a form of interstitial nephritis, termed polyomavirus-associated nephropathy (PVAN), which manifests in renal transplant patients (Boothpur and Brennan, 2010). With the number of kidney transplants increasing each year and the lack of specific antiviral treatment for BKPyV infection, the mainstay of PVAN management continues to rely on reducing immunosuppression (Black *et al.*, 2018; Saleh *et al.*, 2020). However, this approach ultimately poses a significant threat to allograft survival.

While host immunity influences the outcome of infection, there is limited information regarding the interaction of the innate immune response with BKPyV (Reploeg *et al.*, 2001). Innate immunity plays a vital role in protecting cells against invading pathogens, with the interferon (IFN) system upregulating IFN-stimulated genes (ISGs) to establish an antiviral state in cells (Randall and Goodbourn, 2008). Human renal proximal tubule epithelial (RPTE) cells, which represent the main site of infection and persistence, express IFN-α, IFN-β and IFN-γ upon infection (Assetta *et al.*, 2016). Notably, BKPyV is sensitive to the actions of interferons following treatment of RPTE cells (Abend *et al.*, 2007).

Herein, both IFN-α and IFN-γ treatment of BKPyV-infected RPTE cells resulted in reduced levels of late viral protein. In agreement with our observations, Abend *et al.* (2007) published on the inhibitory effect of IFN-γ on BKPyV gene expression and infectious progeny production in RPTE cells. The susceptibility of BKPyV infection to the actions of interferon along with reports of the virus evading host immune recognition, prompted us to investigate to what extent BKPyV may be engaging the antiviral response (de Kort *et al.*, 2017). Understanding the relationship between BKPyV infection and innate immunity in greater detail will expand our insight into how innate immune mediators, such as ISGs, are involved in the BKPyV life cycle and may allow assignment of novel functions to ISGs. Moreover, it may aid in the identification of potential therapeutic targets for treating associated diseases. Therefore, our aim centred

on identifying IFN effectors and elucidating their role in potentially modulating BKPyV infection.

Our study adapted and conducted a gain-of-function screening assay based on flow cytometry to assess the effect of individual ISGs on polyomavirus infection (Schoggins *et al.*, 2011). Optimisation of this assay was also aimed at delivering a high-throughput ISG screening protocol for polyomaviruses. Viral replication was quantified in Vero cells overexpressing individual ISGs with VP1 protein production used as an infection marker. A panel of 24 ISGs was screened against BKPyV infection in Vero cells to allow examination of the type I IFN-independent functions of these gene products. Several hits were identified for their ability to significantly modulate BKPyV replication, including the interferon regulatory factor 1 (IRF1) and heparanase (HPSE).

The ISG screen was succeeded by a more detailed investigation of the two aforementioned ISGs as candidate antiviral factors for BKPyV infection. To this end, we established stable cell lines expressing each ISG to validate its effect by assessing its impact on viral gene expression, viral genome replication or viral infectivity. Our findings suggest that IRF1, a broadly-acting antiviral factor, targets a stage in the BKPyV life cycle prior to or during viral gene expression (Schoggins *et al.*, 2011, 2014; Liu *et al.*, 2012). As a transcriptional activator, IRF1 may potentially enhance target genes to, ultimately, function as antiviral factors suppressing viral gene expression. Further investigation is required to establish a post-nuclear entry effect by IRF1 and to uncover any changes in host gene expression profiles.

IRF1-mediated inhibition of infection appears to be conserved against the primate polyomavirus, SV40. This antiviral effect could not be demonstrated against the human polyomavirus, JCPyV, in Vero cells. Further investigation is required to determine if anti-JCPyV activity is exerted by IRF1 in a cell-type dependent manner. On the contrary, evidence suggests that restriction of BKPyV infection is not dependent on cell type, as demonstrated in RPTE cells overexpressing IRF1. While exogenous IRF1 is capable of suppressing BKPyV infection in a physiologically relevant cell type, an important consideration is the role of endogenous IRF1 and whether the virus counteracts or evades IRF1-mediated inhibition *in vivo*. Several studies report little or complete absence of immune surveillance in BKPyV-infected RPTE cells (Abend *et al.*, 2010; Assetta

et al., 2016; de Kort *et al.*, 2017; An *et al.*, 2019). One hypothesis may be that RPTE cells lack the sensing machinery required for BKPyV detection (An *et al.*, 2019). Therefore, these cells may not enhance IRF1 expression following infection, thereby, allowing the virus to evade an IRF1-mediated immune response. Alternatively, BKPyV may utilise a viral component to counteract the antiviral actions of IRF1 (Manzetti *et al.*, 2020). To further define the importance of this restriction factor, IRF1 can be introduced following infection or its expression can be knocked out in RPTE cells.

Heparanase (HPSE), the principal enzyme involved in the breakdown of heparan sulphate (HS), demonstrated the second most potent inhibitory effect against BKPyV replication in our screening assay. Time-course of infection assays established that BKPyV remains susceptible to HPSE-mediated restriction up to 4 days following infection. Our observations of reduced viral transcripts, protein and genome levels suggested that HPSE interferes with an early stage in the BKPyV life cycle. As HPSE prevented BKPyV transit to the ER, we explored its effect on virion binding to evaluate if it exerts a pre- or post-entry antiviral effect. Flow cytometry-based virion binding assays demonstrated that HPSE prevents BKPyV attachment to the cell surface of Vero cells.

We speculate that, through overexpression of HPSE which cleaves HS moieties on the cell surface, BKPyV attachment to Vero cells is impeded and, thus, the first step required for infection cannot occur optimally. Previous studies have implicated HS, which is a sulphated glycosaminoglycan (GAG) molecule, in functioning as a receptor or co-receptor for both enveloped and non-enveloped viruses (Thakkar *et al.*, 2017). Importantly, GAGs – likely in the form of HS – serve as attachment receptors for MCPyV (Schowalter *et al.*, 2011). Furthermore, density exists on the BKPyV virion which suggests that HS could possibly bind to the viral particle during the attachment step (Hurdiss *et al.*, 2018). Together with published data, our investigation into the effect of HPSE overexpression on BKPyV supports HS involvement in the infectious entry of the virus in Vero cells. To further support our argument, endogenous HPSE expression must be investigated in infected cells which may help in determining if BKPyV is manipulating this enzyme to favour infection.

Importantly, pharmacological inhibition of HPSE activity appears to restore BKPyV infection, however, this observation requires further validation.

Furthermore, HPSE mutants can provide proof for the role of its enzymatic activity in restricting infection or, alternatively, it may give insights into important non-enzymatic functions. Moreover, our experimental evidence suggested that HPSE not only targets BKPyV, but also suppresses the related polyomaviruses, SV40 and JCPyV. These results concur with previously published data of SV40 and JCPyV entry partially relying on GAG-mediated binding (Geoghegan *et al.*, 2017). This observation can be further explored by assessing the ability of SV40 and JCPyV to bind cells with exogenous HPSE and ascertain whether the mechanism of inhibition is the same as with BKPyV infection. Contrary to what occurs in Vero cells, our results suggest that the ability of HPSE to suppress BKPyV infection is not effective in RPTE cells. One possible explanation for this discrepant finding may be that the requirement for HS moieties by BKPyV is cell-type dependent (Schowalter *et al.*, 2011; Geoghegan *et al.*, 2017).

In conclusion, we have identified ISGs which elicit potent antiviral effects against BKPyV infection. We report IRF1 and HPSE as restrictive factors because overexpressing these genes suppresses infection in Vero cells. Exogenous IRF1 is also active against BKPyV in infected RPTE cells, demonstrating its cell type-independent antiviral function. Crucially, our results with HPSE indicate a role for cell surface HS during polyomavirus infection of Vero cells. Further investigation is warranted to delineate the role and mechanism of each ISG in order to inform studies investigating potential therapeutic interventions. Moreover, this screening assay can be utilised to study ISGs which may potentiate polyomavirus infection and, ultimately, could be targeted or used to comprehend differing outcomes of infection.

Bibliography

Abboud-Jarrous, G. *et al.* (2008) ‘Cathepsin L is responsible for processing and activation of proheparanase through multiple cleavages of a linker segment.’, *The Journal of Biological Chemistry*. American Society for Biochemistry and Molecular Biology, 283(26), pp. 18167–76. doi: 10.1074/jbc.M801327200.

Abend, J. R. *et al.* (2009) ‘A truncated T antigen expressed from an alternatively spliced BK virus early mRNA’, *Journal of General Virology*. Microbiology Society, 90(5), pp. 1238–1245. doi: 10.1099/vir.0.009159-0.

Abend, J. R., Jiang, M. and Imperiale, M. J. (2009) ‘BK Virus and Human Cancer: Innocent until Proven Guilty’, *Seminars in Cancer Biology*, 19(4), pp. 252–260. doi: 10.1016/j.semcancer.2009.02.004.

Abend, J. R., Low, J. A. and Imperiale, M. J. (2007) ‘Inhibitory effect of gamma interferon on BK virus gene expression and replication.’, *Journal of virology*. American Society for Microbiology (ASM), 81(1), pp. 272–279. doi: 10.1128/JVI.01571-06.

Abend, J. R., Low, J. A. and Imperiale, M. J. (2010) ‘Global effects of BKV infection on gene expression in human primary kidney epithelial cells’, *Virology*, 397(1), pp. 73–79. doi: 10.1016/j.virol.2009.10.047.

Acheson, N. H. (2011) ‘Polyomaviruses’, in *Fundamentals of Molecular Virology*. 2nd ed. John Wiley & Sons, Inc., pp. 247–262. doi: 10.1002/pauz.200790112.

Agelidis, A. M. *et al.* (2017) ‘Viral Activation of Heparanase Drives Pathogenesis of Herpes Simplex Virus-1’, *Cell Reports*, 20(2), pp. 439–450. doi: 10.1016/j.celrep.2017.06.041.

Agnihotri, S. P. *et al.* (2014) ‘A fatal case of JC virus meningitis presenting with hydrocephalus in a human immunodeficiency virus-seronegative patient’, *Annals of Neurology*, 76(1), pp. 140–147. doi: 10.1002/ana.24192.

Ahuja, D., Sáenz-Robles, M. T. and Pipas, J. M. (2005) ‘SV40 large T antigen targets multiple cellular pathways to elicit cellular transformation’, *Oncogene*. Nature Publishing Group, pp. 7729–7745. doi: 10.1038/sj.onc.1209046.

Akira, S. and Takeda, K. (2004) ‘Toll-like receptor signalling’, *Nature Reviews*

Immunology. Nature Publishing Group, pp. 499–511. doi: 10.1038/nri1391.

Akira, S., Uematsu, S. and Takeuchi, O. (2006) 'Pathogen Recognition and Innate Immunity', *Cell*, 124, pp. 783–801. doi: 10.1016/j.cell.2006.02.015.

Allander, T. *et al.* (2007) 'Identification of a Third Human Polyomavirus', *Journal of Virology*. American Society for Microbiology, 81(8), pp. 4130–4136. doi: 10.1128/jvi.00028-07.

Ambalathingal, G. R. *et al.* (2017) 'BK Polyomavirus: Clinical Aspects, Immune Regulation, and Emerging Therapies', *Clinical Microbiology Reviews*, 30(2). doi: 10.1128/CMR.00074-16.

An, P. *et al.* (2019) 'Human polyomavirus BKV infection of endothelial cells results in interferon pathway induction and persistence', *PLoS Pathogens*. doi: 10.1371/journal.ppat.1007505.

An, P., Sáenz Robles, M. T. and Pipas, J. M. (2012) 'Large T Antigens of Polyomaviruses: Amazing Molecular Machines', *Annual Review of Microbiology*. Annual Reviews, 66(1), pp. 213–236. doi: 10.1146/annurev-micro-092611-150154.

Anders, H.-J., Lichtnekert, J. and Allam, R. (2010) 'Interferon-α and -β in kidney inflammation', *Kidney International*. Elsevier, 77(10), pp. 848–854. doi: 10.1038/KI.2010.71.

Andrei, G. *et al.* (1997) 'Activities of Various Compounds against Murine and Primate Polyomaviruses', *Antimicrobial Agents and Chemotherapy*, 41(3), pp. 587–593.

Andrews, C. A. *et al.* (1988) 'A Serological Investigation of BK Virus and JC Virus Infections in Recipients of Renal Allografts', *The Journal of Infectious Diseases*, 158(1), pp. 176–181.

Aoki, T. *et al.* (2009) 'Identification of the neuroblastoma-amplified gene product as a component of the syntaxin 18 complex implicated in Golgi-to-endoplasmic reticulum retrograde transport', *Molecular Biology of the Cell*. American Society for Cell Biology, 20(11), pp. 2639–2649. doi: 10.1091/mbc.E08-11-1104.

Arasaki, K. *et al.* (2006) 'RINT-1 Regulates the Localization and Entry of ZW10 to the Syntaxin 18 Complex', *Molecular Biology of the Cell*, 17, pp. 2780–2788. doi: 10.1091/mbc.E05-10.

Ashok, A. and Atwood, W. J. (2003) ‘Contrasting roles of endosomal pH and the cytoskeleton in infection of human glial cells by JC virus and simian virus 40.’, *Journal of virology*, 77(2), pp. 1347–1356. doi: 10.1128/JVI.77.2.1347-1356.2003.

Assetta, B. *et al.* (2013) ‘5-HT2 Receptors Facilitate JC Polyomavirus Entry’, *Journal of Virology*, 87(24), pp. 13490–13498. doi: 10.1128/JVI.02252-13.

Assetta, B. *et al.* (2016) ‘JC Polyomavirus Infection of Primary Human Renal Epithelial Cells Is Controlled by a Type I IFN-Induced Response.’, *mBio*. American Society for Microbiology, 7(4), pp. e00903-16. doi: 10.1128/mBio.00903-16.

Assetta, B. and Atwood, W. J. (2017) ‘The biology of JC polyomavirus’, *Biological Chemistry*, 398(8), pp. 839–855.

Åström, K.-E., Mancall, E. L. and Richardson Jr, E. P. (1958) ‘Progressive Multifocal Leuko-Encephalopathy. A Hitherto Unrecognized Complication Of Chronic Lymphatic Leukaemia And Hodgkin’s Disease’, *Brain*, 81, pp. 93–111.

Atencio, I. A. *et al.* (1993) ‘Adult Mouse Kidneys Become Permissive to Acute Polyomavirus Infection and Reactivate Persistent Infections in Response to Cellular Damage and Regeneration’, *Journal of Virology*, 67(3), pp. 1424–1432.

Atencio, I. A. and Villarreal, L. P. (1994) ‘Polyomavirus Replicates in Differentiating but Not in Proliferating Tubules of Adult Mouse Polycystic Kidneys’, *Virology*, 201(1), pp. 26–35. doi: 10.1006/viro.1994.1262.

Atwood, W. J. and Norkin, L. C. (1989) ‘Class I major histocompatibility proteins as cell surface receptors for simian virus 40.’, *Journal of Virology*. American Society for Microbiology, 63(10), pp. 4474–4477. doi: 10.1128/jvi.63.10.4474-4477.1989.

Babakir-Mina, M. *et al.* (2013) ‘The human polyomaviruses KI and WU: virological background and clinical implications’, *APMIS*. John Wiley & Sons, Ltd, 121(8), pp. 746–754. doi: 10.1111/apm.12091.

Bacia, K., Schwille, P. and Kurzchalia, T. (2005) ‘Sterol structure determines the separation of phases and the curvature of the liquid-ordered phase in model membranes’, *PNAS*, 102(9), pp. 3272–3277.

Bacsa, S. *et al.* (2011) ‘Syndecan-1 and syndecan-2 play key roles in herpes

simplex virus type-1 infection', *Journal of General Virology*, 92, pp. 733–743. doi: 10.1099/vir.0.027052-0.

Baer, A. and Kehn-Hall, K. (2014) 'Viral concentration determination through plaque assays: Using traditional and novel overlay systems', *Journal of Visualized Experiments*. Journal of Visualized Experiments, (93). doi: 10.3791/52065.

Banks, P. D. *et al.* (2016) 'Recent Insights and Advances in the Management of Merkel Cell Carcinoma', *Journal of Oncology Practice*. American Society of Clinical Oncology (ASCO), 12(7), pp. 637–646. doi: 10.1200/jop.2016.013367.

Barker, C. F. and Markmann, J. F. (2013) 'Historical overview of transplantation', *Cold Spring Harbor Perspectives in Medicine*. Cold Spring Harbor Laboratory Press, 3(4), p. a014977. doi: 10.1101/cshperspect.a014977.

Barth, H. *et al.* (2016) 'In Vitro and In Vivo Models for the Study of Human Polyomavirus Infection.', *Viruses*. Multidisciplinary Digital Publishing Institute (MDPI), 8(10). doi: 10.3390/v8100292.

Bauman, Y. *et al.* (2011) 'Identical miRNA of the Human JC and BK Polyoma Viruses Targets the Stress-Induced Ligand ULBP3 to Escape Immune Elimination', *Cell Host & Microbe*, 9, pp. 93–102. doi: 10.1016/j.chom.2011.01.008.

Bechert, C. J. *et al.* (2010) 'Monitoring of BK Viral Load in Renal Allograft Recipients by Real-Time PCR Assays', *American Journal of Clinical Pathology*. Oxford Academic, 133(2), pp. 242–250. doi: 10.1309/AJCP63VDFCKCRUUL.

Beckervordersandforth, J. *et al.* (2016) 'Frequent detection of human polyomavirus 6 in keratoacanthomas', *Diagnostic Pathology*. BioMed Central Ltd., 11(1), p. 58. doi: 10.1186/s13000-016-0509-z.

Beimler, J., Sommerer, C. and Zeier, M. (2007) 'The influence of immunosuppression on the development of BK virus nephropathy-does it matter?', *Nephrology Dialysis Transplantation*, 22(Suppl 8), pp. viii66–viii71. doi: 10.1093/ndt/gfm646.

Bennett, S. M. *et al.* (2015) 'Role of a nuclear localization signal on the minor capsid Proteins VP2 and VP3 in BKPyV nuclear entry', *Virology*. Academic Press, 474, pp. 110–116. doi: 10.1016/J.VIROL.2014.10.013.

Bennett, S. M., Broekema, N. M. and Imperiale, M. J. (2012) ‘BK polyomavirus: Emerging pathogen’, *Microbes and Infection*, 14(9), pp. 672–683. doi: 10.1016/j.micinf.2012.02.002.

Bennett, S. M., Jiang, M. and Imperiale, M. J. (2013) ‘Role of cell-type-specific endoplasmic reticulum-associated degradation in polyomavirus trafficking.’, *Journal of virology*. American Society for Microbiology Journals, 87(16), pp. 8843–52. doi: 10.1128/JVI.00664-13.

Berger, J. R. and Concha, M. (1995) ‘Progressive multifocal leukoencephalopathy: the evolution of a disease once considered rare.’, *Journal of neurovirology*, pp. 5–18. doi: 10.3109/13550289509111006.

Bernhoff, E. *et al.* (2008) ‘Cidofovir inhibits polyomavirus BK replication in human renal tubular cells downstream of viral early gene expression’, *American Journal of Transplantation*, 8(7), pp. 1413–1422. doi: 10.1111/j.1600-6143.2008.02269.x.

Bernhoff, E. *et al.* (2010) ‘Leflunomide Inhibition of BK Virus Replication in Renal Tubular Epithelial Cells’, *Journal of Virology*. American Society for Microbiology, 84(4), pp. 2150–2156. doi: 10.1128/jvi.01737-09.

Berrios, C. *et al.* (2015) ‘Malawi Polyomavirus Is a Prevalent Human Virus That Interacts with Known Tumor Suppressors’, *Journal of Virology*. American Society for Microbiology, 89(1), pp. 857–862. doi: 10.1128/jvi.02328-14.

Bethge, T. *et al.* (2015) ‘Sp1 Sites in the Noncoding Control Region of BK Polyomavirus Are Key Regulators of Bidirectional Viral Early and Late Gene Expression’, *Journal of Virology*. American Society for Microbiology, 89(6), pp. 3396–3411. doi: 10.1128/jvi.03625-14.

Bhattacharjee, S. and Chattaraj, S. (2017) ‘Entry, infection, replication, and egress of human polyomaviruses: an update’, *Canadian Journal of Microbiology*, 63, pp. 193–211. doi: 10.1139/cjm-2016-0519.

Binggeli, S. *et al.* (2007) ‘Polyomavirus BK-specific cellular immune response to VP1 and large T-antigen in kidney transplant recipients’, *American Journal of Transplantation*. Am J Transplant, 7(5), pp. 1131–1139. doi: 10.1111/j.1600-6143.2007.01754.x.

Black, C. K. *et al.* (2018) ‘Solid organ transplantation in the 21st century’,

Annals of Translational Medicine. AME Publishing Company, 6(20), pp. 409–409. doi: 10.21037/atm.2018.09.68.

Bofill-Mas, S. *et al.* (2001) 'Potential Transmission of Human Polyomaviruses through the Gastrointestinal Tract after Exposure to Virions or Viral DNA', *Journal of Virology*. American Society for Microbiology, 75(21), pp. 10290–10299. doi: 10.1128/jvi.75.21.10290-10299.2001.

Bogdanovic, G. *et al.* (2004) 'Association between a High BK Virus Load in Urine Samples of Patients with Graft-Versus-Host Disease and Development of Hemorrhagic Cystitis after Hematopoietic Stem Cell Transplantation', *Journal of Clinical Microbiology*, 42(11), pp. 5394–5396. doi: 10.1128/JCM.42.11.5394-5396.2004.

Bohl, D. L. *et al.* (2008) 'BK virus antibody titers and intensity of infections after renal transplantation', *Journal of Clinical Virology*. NIH Public Access, 43(2), pp. 184–189. doi: 10.1016/j.jcv.2008.06.009.

Bohl, D. L. and Brennan, D. C. (2007) 'BK Virus Nephropathy and Kidney Transplantation', *Clinical Journal of the American Society of Nephrology*, 2, pp. 36–46. doi: 10.2215/CJN.00920207.

Boldorini, R. *et al.* (2010) 'BK virus sequences in specimens from aborted fetuses', *Journal of Medical Virology*. John Wiley & Sons, Ltd, 82(12), pp. 2127–2132. doi: 10.1002/jmv.21923.

Boothpur, R. and Brennan, D. C. (2010) 'Human Polyoma Viruses and Disease with Emphasis on Clinical BK and JC', *Journal of Clinical Virology*, 47, pp. 306–312. doi: 10.1016/j.jcv.2009.12.006.

Bouley, S. J. *et al.* (2014) 'Host cell autophagy promotes BK virus infection', *Virology*. Academic Press Inc., 456–457(1), pp. 87–95. doi: 10.1016/j.virol.2014.03.009.

Briggs, J. P., Kriz, W. and Schnermann, J. B. (2014) 'Overview of Kidney Function and Structure', in Gilbert, S. J. and Weiner, D. E. (eds) *National Kidney Foundation's Primer on Kidney Diseases*. Sixth. Philadelphia: Elsevier, pp. 2–18.

Broekema, N. M. and Imperiale, M. J. (2012) 'Efficient propagation of archetype BK and JC polyomaviruses', *Virology*, 422(2), pp. 235–241. doi:

10.1016/j.virol.2011.10.026.

Broekema, N. M. and Imperiale, M. J. (2013) ‘miRNA regulation of BK polyomavirus replication during early infection’, *PNAS*, 110(20), pp. 8200–8205. doi: 10.1073/pnas.1301907110.

Brown, P., Tsai, T. and Gajdusek, D. (1975) ‘Seroepidemiology of human papovaviruses. Discovery of virgin populations and some unusual patterns of antibody prevalence among remote peoples of the world.’, *American Journal of Epidemiology*, 102(4), pp. 331–340.

Buck, C. B. *et al.* (2012) ‘Complete Genome Sequence of a Tenth Human Polyomavirus’, *Journal of Virology*, 86(19), pp. 10887–10887. doi: 10.1128/jvi.01690-12.

Buck, C. B. *et al.* (2016) ‘The Ancient Evolutionary History of Polyomaviruses’, *PLOS Pathogens*, 12(4), p. e1005574. doi: 10.1371/journal.ppat.1005574.

Busse, M. *et al.* (2007) ‘Contribution of EXT1, EXT2, and EXTL3 to heparan sulfate chain elongation’, *Journal of Biological Chemistry*, 282(45), pp. 32802–32810. doi: 10.1074/jbc.M703560200.

Butin-Israeli, V. *et al.* (2011) ‘Simian virus 40 induces lamin A/C fluctuations and nuclear envelope deformation during cell entry’, *Nucleus*, 2(4), pp. 320–330. doi: 10.4161/nucl.2.4.16371.

Caller, L. G. *et al.* (2019) ‘Temporal proteomic analysis of BK polyomavirus infection reveals virus-induced G2 arrest and highly effective evasion of innate immune sensing.’, *Journal of virology*, 93(16), pp. e00595-19. doi: 10.1128/JVI.00595-19.

Camargo, J. F. *et al.* (2016) ‘The use of brincidofovir for the treatment of mixed dsDNA viral infection’, *Journal of Clinical Virology*, 83, pp. 1–4. doi: 10.1016/j.jcv.2016.07.021.

Campbell, K. S. *et al.* (1997) ‘DnaJ/hsp40 chaperone domain of SV40 large T antigen promotes efhclent viral DNA replication’, *Genes & Development*, 11, pp. 1098–1110.

Cantalupo, P. G. *et al.* (2009) ‘Cell-type specific regulation of gene expression by simian virus 40 T antigens’, *Virology*, 386(1), pp. 183–191. doi: 10.1016/j.virol.2008.12.038.

Carr, M. *et al.* (2017) ‘Discovery of African bat polyomaviruses and infrequent recombination in the large T antigen in the Polyomaviridae’, *Journal of General Virology*, 98, pp. 726–738. doi: 10.1099/jgv.0.000737.

Carroll, R. G. (2007) ‘Renal System and Urinary Tract’, in *Elsevier’s Integrated Physiology*. Elsevier, pp. 117–137. doi: 10.1016/b978-0-323-04318-2.50017-0.

Carter, J. J. *et al.* (2009) ‘Association of Merkel Cell Polyomavirus-Specific Antibodies With Merkel Cell Carcinoma’, *Journal of the National Cancer Institute*, 101(21), pp. 1510–22. doi: 10.1093/jnci/djp332.

Caruso, M. *et al.* (2003) ‘Role of sialic acid-containing molecules and the α4β1 integrin receptor in the early steps of polyomavirus infection’, *Journal of General Virology*, 84(11), pp. 2927–2936. doi: 10.1099/vir.0.19369-0.

Chadda, R. *et al.* (2007) ‘Cholesterol-sensitive Cdc42 activation regulates actin polymerization for endocytosis via the GEEC pathway’, *Traffic*, 8(6), pp. 702–717. doi: 10.1111/j.1600-0854.2007.00565.x.

Chapagain, M. L. *et al.* (2007) ‘Polyomavirus JC infects human brain microvascular endothelial cells independent of serotonin receptor 2A’, *Virology*. Academic Press, 364(1), pp. 55–63. doi: 10.1016/j.virol.2007.02.018.

Chaplin, D. D. (2010) ‘Overview of the immune response’, *Journal of Allergy and Clinical Immunology*. NIH Public Access, 125(2 Suppl. 2), p. S3. doi: 10.1016/j.jaci.2009.12.980.

Chen, P.-L. *et al.* (2011) ‘Phosphorylation of Ser-80 of VP1 and Ser-254 of VP2 is essential for human BK virus propagation in tissue culture’, *Journal of General Virology*, 92, pp. 2637–2645. doi: 10.1099/vir.0.033282-0.

Chen, X. S., Stehle, T. and Harrison, S. C. (1998) ‘Interaction of polyomavirus internal protein VP2 with the major capsid protein VP1 and implications for participation of VP2 in viral entry’, *The EMBO Journal*, 17(12), pp. 3233–3240.

Chen, Y. *et al.* (2006) ‘Interplay of Cellular and Humoral Immune Responses against BK Virus in Kidney Transplant Recipients with Polyomavirus Nephropathy’, *Journal of Virology*, 80(7), pp. 3495–3505. doi: 10.1128/jvi.80.7.3495-3505.2006.

Cheon, H. *et al.* (2013) ‘IFNβ-dependent increases in STAT1, STAT2, and IRF9 mediate resistance to viruses and DNA damage’, *The EMBO Journal*, 32(20),

pp. 2751–2763. doi: 10.1038/emboj.2013.203.

Cho, U. S. *et al.* (2007) ‘Structural Basis of PP2A Inhibition by Small t Antigen’, *PLoS Biology*, 5(8), p. e202. doi: 10.1371/journal.pbio.

Chong, S. *et al.* (2019) ‘BK virus: Current understanding of pathogenicity and clinical disease in transplantation’, *Reviews in Medical Virology*, 29(4), p. e2044. doi: 10.1002/rmv.2044.

Chromy, L. R., Pipas, J. M. and Garcea, R. L. (2003) ‘Chaperone-mediated in vitro assembly of Polyomavirus capsids’, *PNAS*, 100(18), pp. 10477–10482.

Clayson, E. T., Brando, L. V and Compans, R. W. (1989) ‘Release of simian virus 40 virions from epithelial cells is polarized and occurs without cell lysis.’, *Journal of Virology*, 63(5), pp. 2278–2288. doi: 10.1128/jvi.63.5.2278-2288.1989.

De Clercq, E. (2007) ‘Acyclic nucleoside phosphonates: Past, present and future. Bridging chemistry to HIV, HBV, HCV, HPV, adeno-, herpes-, and poxvirus infections: The phosphonate bridge’, *Biochemical Pharmacology*. Elsevier Inc., 73(7), pp. 911–922. doi: 10.1016/j.bcp.2006.09.014.

Coleman, D. V *et al.* (1978) ‘Human polyomavirus (BK) infection and ureteric stenosis in renal allograft recipients’, *Journal of Clinical Pathology*, 31, pp. 338–347. doi: 10.1136/jcp.31.4.338.

Coleman, D. V *et al.* (1983) ‘Human polyomavirus in pregnancy. A model for the study of defence mechanisms to virus reactivation’, *Clinical and Experimental Immunology*, 53, pp. 289–296.

Comoli, P. *et al.* (2004) ‘Polyomavirus BK-Specific Immunity after Kidney Transplantation’, *Transplantation*, 78(8), pp. 1229–1232. doi: 10.1097/01.TP.0000137932.44791.D3.

Comoli, P. *et al.* (2013) ‘Immunity to Polyomavirus BK Infection: Immune Monitoring to Regulate the Balance between Risk of BKV Nephropathy and Induction of Alloimmunity’, *Clinical and Developmental Immunology*. doi: 10.1155/2013/256923.

Coombe, D. R. and Gandhi, N. S. (2019) ‘Heparanase: A Challenging Cancer Drug Target’, *Frontiers in Oncology*. Frontiers Media S.A., p. 1316. doi: 10.3389/fonc.2019.01316.

Costa, C. and Cavallo, R. (2012) ‘Polyomavirus-associated nephropathy’, *World Journal of Transplantation*, 2(6), pp. 84–94. doi: 10.5500/wjt.v2.i6.84.

Courtney, S. M. *et al.* (2005) ‘Furanyl-1,3-thiazol-2-yl and benzoxazol-5-yl acetic acid derivatives: novel classes of heparanase inhibitor’, *Bioorganic & Medicinal Chemistry Letters*. Pergamon, 15, pp. 2295–2299. doi: 10.1016/J.BMCL.2005.03.014.

Cubitt, C. L. (2006) ‘Molecular Genetics of the BK Virus’, in Ahsan, N. (ed.) *Polyomaviruses and Human Diseases. Advances in Experimental Medicine and Biology*. Springer, New York, NY, pp. 85–95. doi: 10.1007/0-387-32957-9_6.

Daha, M. R. and Van Kooten, C. (2000) ‘Is the proximal tubular cell a proinflammatory cell?’, *Nephrology Dialysis Transplantation*, 15(Suppl 6), pp. 41–43.

Dalianis, T. and Hirsch, H. H. (2013) ‘Human polyomaviruses in disease and cancer’, *Virology*, 437(2), pp. 63–72. doi: 10.1016/j.virol.2012.12.015.

Damm, E.-M. *et al.* (2005) ‘Clathrin-and caveolin-1-independent endocytosis: entry of simian virus 40 into cells devoid of caveolae’, *The Journal of Cell Biology*, 168(3), pp. 477–488. doi: 10.1083/jcb.200407113.

Dangoria, N. S. *et al.* (1996) ‘Extracellular simian virus 40 induces an ERK/MAP kinase-independent signalling pathway that activates primary response genes and promotes virus entry’, *Journal of General Virology*, 77, pp. 2173–2182.

Daniels, R., Rusan, N. M., Wilbuer, A.-K., *et al.* (2006) ‘Simian Virus 40 Late Proteins Possess Lytic Properties That Render Them Capable of Permeabilizing Cellular Membranes’, *Journal of Virology*, 80(13), pp. 6575–6587. doi: 10.1128/JVI.00347-06.

Daniels, R., Rusan, N. M., Wadsworth, P., *et al.* (2006) ‘SV40 VP2 and VP3 Insertion into ER Membranes Is Controlled by the Capsid Protein VP1: Implications for DNA Translocation out of the ER’, *Molecular Cell*. Cell Press, 24(6), pp. 955–966. doi: 10.1016/j.molcel.2006.11.001.

Darbinyan, A. *et al.* (2004) ‘Role of JC Virus Agnoprotein in DNA Repair’, *Journal of Virology*. American Society for Microbiology, 78(16), pp. 8593–8600. doi: 10.1128/jvi.78.16.8593-8600.2004.

Darbinyan, A. *et al.* (2013) ‘Polyomavirus JC infection inhibits differentiation of

oligodendrocyte progenitor cells', *Journal of Neuroscience Research*. NIH Public Access, 91(1), pp. 116–127. doi: 10.1002/jnr.23135.

Deb, S. *et al.* (1987) 'The T-antigen-binding domain of the simian virus 40 core origin of replication.', *Journal of Virology*. American Society for Microbiology, 61(7), pp. 2143–2149. doi: 10.1128/jvi.61.7.2143-2149.1987.

Decaprio, J. A. and Garcea, R. L. (2013) 'A cornucopia of human polyomaviruses', *Nature Reviews Microbiology*. Nature Publishing Group, pp. 264–276. doi: 10.1038/nrmicro2992.

Dejgaard, S. Y. *et al.* (2008) 'Rab18 and Rab43 have key roles in ER-Golgi trafficking', *Journal of Cell Science*. The Company of Biologists Ltd, 121(16), pp. 2768–2781. doi: 10.1242/jcs.021808.

Dekeyser, M. *et al.* (2015) 'Polyomavirus-specific cellular immunity: From BK-virus-specific cellular immunity to BK-virus-associated nephropathy?', *Frontiers in Immunology*. Frontiers Media S.A. doi: 10.3389/fimmu.2015.00307.

Desmyter, J., Melnick, J. L. and Rawls, W. E. (1968) 'Defectiveness of Interferon Production and of Rubella Virus Interference in a Line of African Green Monkey Kidney Cells (Vero)', *Journal of Virology*. American Society for Microbiology, 2(10), pp. 955–961. doi: 10.1128/jvi.2.10.955-961.1968.

Deyerle, K. L., Sajjadi, F. G. and Subramani, S. (1989) 'Analysis of Origin of DNA Replication of Human Papovavirus BK', *Journal of Virology*, 63(1), pp. 356–365.

Dias Junior, A. G., Sampaio, N. G. and Rehwinkel, J. (2019) 'A Balancing Act: MDA5 in Antiviral Immunity and Autoinflammation', *Trends in Microbiology*. Elsevier Ltd, pp. 75–85. doi: 10.1016/j.tim.2018.08.007.

Diaz, M. O. *et al.* (1988) 'Homozygous deletion of the α- and β1-interferon genes in human leukemia and derived cell lines', *Proceedings of the National Academy of Sciences of the United States of America*. National Academy of Sciences, 85(14), pp. 5259–5263. doi: 10.1073/pnas.85.14.5259.

Doherty, G. J. and Mcmahon, H. T. (2009) 'Mechanisms of Endocytosis', *Annual Review of Biochemistry*, 78, pp. 857–902. doi: 10.1146/annurev.biochem.78.081307.110540.

Dolei, A. *et al.* (2000) 'Polyomavirus persistence in lymphocytes : prevalence in

lymphocytes from blood donors and healthy personnel of a blood transfusion centre', *Journal of General Virology*, 81, pp. 1967–1973.

Dornreiter, I. *et al.* (1992) 'Interaction of DNA polymerase alpha-primase with cellular replication protein A and SV40 T antigen.', *The EMBO Journal*. Wiley, 11(2), pp. 769–776. doi: 10.1002/j.1460-2075.1992.tb05110.x.

Dörries, K. (2001) 'Latent and Persistent Polyomavirus Infection', in Khalili, K. and Stoner, G. L. (eds) *Human Polyomaviruses*. New York, USA: John Wiley & Sons, Inc., pp. 197–235. doi: 10.1002/0471221945.ch10.

Drab, M. *et al.* (2001) 'Loss of caveolae, vascular dysfunction, and pulmonary defects in caveolin-1 gene-disrupted mice', *Science*. American Association for the Advancement of Science, 293(5539), pp. 2449–2452. doi: 10.1126/science.1062688.

Drachenberg, C. B. *et al.* (2003) 'BK Polyoma Virus Allograft Nephropathy: Ultrastructural Features from Viral Cell Entry to Lysis', *American Journal of Transplantation*. John Wiley & Sons, Ltd (10.1111), 3(11), pp. 1383–1392. doi: 10.1046/j.1600-6135.2003.00237.x.

Drachenberg, C. B. *et al.* (2004) 'Histological Patterns of Polyomavirus Nephropathy: Correlation with Graft Outcome and Viral Load', *American Journal of Transplantation*, 4, pp. 2082–2092. doi: 10.1046/j.1600-6143.2004.00603.x.

Drachenberg, C. B. and Papadimitriou, J. C. (2006) 'Polyomavirus-associated nephropathy: Update in diagnosis', *Transplant Infectious Disease*. Transpl Infect Dis, pp. 68–75. doi: 10.1111/j.1399-3062.2006.00154.x.

Drayman, N. *et al.* (2010) 'Rapid method for SV40 titration', *Journal of Virological Methods*. Elsevier, 164(1–2), pp. 145–147. doi: 10.1016/j.jviromet.2009.12.003.

Dropulic, L. K. and Jones, R. J. (2008) 'Polyomavirus BK infection in blood and marrow transplant recipients', *Bone Marrow Transplantation*. NIH Public Access, 41, pp. 11–18. doi: 10.1038/sj.bmt.1705886.

Dugan, A. S. *et al.* (2007) 'Identification of Amino Acid Residues in BK Virus VP1 That Are Critical for Viability and Growth', *Journal of Virology*. American Society for Microbiology, 81(21), pp. 11798–11808. doi: 10.1128/jvi.01316-07.

Dugan, A. S. *et al.* (2008) 'Human alpha-defensins inhibit BK virus infection by

aggregating virions and blocking binding to host cells.', *The Journal of biological chemistry*. American Society for Biochemistry and Molecular Biology, 283(45), pp. 31125–32. doi: 10.1074/jbc.M805902200.

Dugan, A. S., Eash, S. and Atwood, W. J. (2005) 'An N-Linked Glycoprotein with α(2,3)-Linked Sialic Acid Is a Receptor for BK Virus', *Journal of Virology*. American Society for Microbiology, 79(22), pp. 14442–14445. doi: 10.1128/jvi.79.22.14442-14445.2005.

Eash, S. and Atwood, W. J. (2005) 'Involvement of Cytoskeletal Components in BK Virus Infectious Entry', *Journal of Virology*, 79(18), pp. 11734–11741. doi: 10.1128/JVI.79.18.11734-11741.2005.

Eash, S., Querbes, W. and Atwood, W. J. (2004) 'Infection of vero cells by BK virus is dependent on caveolae', *Journal of virology*. American Society for Microbiology Journals, 78(21), pp. 11583–90. doi: 10.1128/JVI.78.21.11583-11590.2004.

Elkin, M. *et al.* (2001) 'Heparanase as mediator of angiogenesis: mode of action', *The FASEB Journal*, pp. 1661–1663. doi: 10.1096/fj.00-0895fje.

Ellgaard, L., Sevier, C. S. and Bulleid, N. J. (2018) 'How Are Proteins Reduced in the Endoplasmic Reticulum?', *Trends in Biochemical Sciences*. Elsevier Ltd, pp. 32–43. doi: 10.1016/j.tibs.2017.10.006.

Ellman, M. *et al.* (1984) 'Localization of the Simian Virus 40 Small t Antigen in the Nucleus and Cytoplasm of Monkey and Mouse Cells', *Journal of Virology*, pp. 623–628.

Emeny, J. M. and Morgan, M. J. (1979) 'Regulation of the interferon system: Evidence that vero cells have a genetic defect in interferon production', *Journal of General Virology*. Microbiology Society, 43(1), pp. 247–252. doi: 10.1099/0022-1317-43-1-247.

Engel, S. *et al.* (2011) 'Role of Endosomes in Simian Virus 40 Entry and Infection', *Journal of Virology*. American Society for Microbiology, 85(9), pp. 4198–4211. doi: 10.1128/jvi.02179-10.

Erard, V. *et al.* (2004) 'BK Virus Infection in Hematopoietic Stem Cell Transplant Recipients: Frequency, Risk Factors, and Association with Postengraftment Hemorrhagic Cystitis', *Clinical Infectious Diseases*, 39, pp. 1861–5.

Erickson, K. D., Garcea, R. L. and Tsai, B. (2009) ‘Ganglioside GT1b Is a Putative Host Cell Receptor for the Merkel Cell Polyomavirus’, *Journal of Virology*. American Society for Microbiology, 83(19), pp. 10275–10279. doi: 10.1128/jvi.00949-09.

Evans, G. L. *et al.* (2015) ‘Anion homeostasis is important for non-lytic release of BK polyomavirus from infected cells’, *Open Biology*, 5, p. 150041. doi: 10.1098/rsob.150041.

Ewers, H. *et al.* (2010) ‘GM1 structure determines SV40-induced membrane invagination and infection’, *Nature Cell Biology*. Nature Publishing Group, 12(1), pp. 11–18. doi: 10.1038/ncb1999.

Fairbanks, M. B. *et al.* (1999) ‘Processing of the Human Heparanase Precursor and Evidence That the Active Enzyme Is a Heterodimer*’, *The Journal of Biological Chemistry*, 274(42), pp. 29587–29590.

Fang, C. Y. *et al.* (2010) ‘Global analysis of modifications of the human BK virus structural proteins by LC-MS/MS’, *Virology*. Academic Press, 402(1), pp. 164–176. doi: 10.1016/j.virol.2010.03.029.

Fang, C. Y. *et al.* (2015) ‘Global profiling of histone modifications in the polyomavirus BK virion minichromosome’, *Virology*. Academic Press Inc., 483, pp. 1–12. doi: 10.1016/j.virol.2015.04.009.

Farasati, N. A. *et al.* (2005) ‘Effect of Leflunomide and Cidofovir on Replication of BK Virus in an In Vitro Culture System’, *Transplantation*, 79(1), pp. 116–118. doi: 10.1097/01.TP.0000149338.97084.5F.

Fay, N. and Panté, N. (2015) ‘Nuclear entry of DNA viruses’, *Frontiers in Microbiology*. Frontiers Media S.A., p. 467. doi: 10.3389/fmicb.2015.00467.

Feng, H. *et al.* (2008) ‘Clonal integration of a polyomavirus in human Merkel cell carcinoma’, *Science*. American Association for the Advancement of Science, 319, pp. 1096–1100. doi: 10.1126/science.1152586.

Feng, J. *et al.* (2018) ‘Interferon-Stimulated Gene (ISG)-Expression Screening Reveals the Specific Antibunyaviral Activity of ISG20’, *Journal of Virology*, 92(13), pp. e02140-2157. doi: 10.1128/JVI.

Ferenczy, M. W. *et al.* (2012) ‘Molecular biology, epidemiology, and pathogenesis of progressive multifocal leukoencephalopathy, the JC virus-

induced demyelinating disease of the human brain', *Clinical Microbiology Reviews*. American Society for Microbiology Journals, pp. 471–506. doi: 10.1128/CMR.05031-11.

Ficarelli, M. *et al.* (2019) 'KHNYN is essential for the zinc finger antiviral protein (ZAP) to restrict HIV-1 containing clustered CpG dinucleotides', *eLife*, 8, p. e46767. doi: 10.7554/eLife.46767.001.

Fogazzi, G. B., Cantu, M. and Saglimbeni, L. (2001) '`Decoy cells' in the urine due to polyomavirus BK infection: easily seen by phase-contrast microscopy', *Nephrology Dialysis Transplantation*, 16, pp. 1496–1498.

Forero, A. *et al.* (2014) 'Simian Virus 40 Large T Antigen Induces IFN-Stimulated Genes through ATR Kinase', *The Journal of Immunology*. The American Association of Immunologists, 192(12), pp. 5933–5942. doi: 10.4049/jimmunol.1303470.

Fujii, Y. *et al.* (1999) 'Crystal structure of an IRF-DNA complex reveals novel DNA recognition and cooperative binding to a tandem repeat of core sequences', *The EMBO Journal*, 18(18), pp. 5028–5041.

Gaboriaud, P. *et al.* (2018) 'Age-specific seroprevalence of human polyomavirus 12 and Saint Louis and New Jersey polyomaviruses'. doi: 10.1038/s41426-018-0026-0.

Gal-Ben-Ari, S. *et al.* (2019) 'PKR: A kinase to remember', *Frontiers in Molecular Neuroscience*. Frontiers Media S.A., p. 480. doi: 10.3389/fnmol.2018.00480.

Galan, A., Rauch, C. A. and Otis, C. N. (2005) 'Fatal BK polyoma viral pneumonia associated with immunosuppression', *Human Pathology*. W.B. Saunders, 36(9), pp. 1031–1034. doi: 10.1016/j.humpath.2005.07.001.

Gambarino, S. *et al.* (2011) 'Genotyping of Polyomavirus BK by Real Time PCR for VP1 Gene', *Molecular Biotechnology*. Humana Press Inc, 49(2), pp. 151–158. doi: 10.1007/s12033-011-9386-6.

Garcea, R. L. and Imperiale, M. J. (2003) 'Simian virus 40 infection of humans.', *Journal of virology*. American Society for Microbiology, 77(9), pp. 5039–45. doi: 10.1128/JVI.77.9.5039-5045.2003.

Garcea, R. L., Salunket, D. M. and D Caspart, D. L. (1987) 'Site-directed

mutation affecting polyomavirus capsid self-assembly in vitro', *Nature*, 329(3), pp. 86–87.

Gardner, S. D. *et al.* (1971) 'New Human Papovavirus (B.K.) isolated from urine after renal transplantation', *The Lancet*. Elsevier, pp. 1253–1257. doi: 10.1016/S0140-6736(71)91776-4.

Gardner, S. D. (1973) 'Prevalence in England of Antibody to Human Polyomavirus (B.K.)', *British Medical Journal*, 1(5845), pp. 77–78. doi: 10.1136/bmj.1.5845.77.

Gariano, G. R. *et al.* (2008) 'The Intracellular DNA Sensor IFI16 Gene Acts as Restriction Factor for Human Cytomegalovirus Replication', *PLoS Pathogens*, 8(1), p. e1002498. doi: 10.1371/journal.ppat.1002498.

Gaynor, A. M. *et al.* (2007) 'Identification of a novel polyomavirus from patients with acute respiratory tract infections', *PLoS Pathogens*. Public Library of Science, 3(5), pp. 0595–0604. doi: 10.1371/journal.ppat.0030064.

Gedvilaite, A. *et al.* (2017) 'Novel polyomaviruses in shrews (Soricidae) with close similarity to human polyomavirus 12', *Journal of General Virology*, 98, pp. 3060–3067. doi: 10.1099/jgv.0.000948.

Geiger, R. *et al.* (2011) 'BAP31 and BiP are essential for dislocation of SV40 from the endoplasmic reticulum to the cytosol', *Nature Cell Biology*. Nature Publishing Group, 13(11), pp. 1305–1314. doi: 10.1038/ncb2339.

Geoghegan, E. M. *et al.* (2017) 'Infectious Entry and Neutralization of Pathogenic JC Polyomaviruses', *Cell Reports*. Cell Press, 21(5), pp. 1169–1179. doi: 10.1016/J.CELREP.2017.10.027.

Gerits, N. *et al.* (2011) 'Agnoprotein of polyomavirus BK interacts with proliferating cell nuclear antigen and inhibits DNA replication', *Virology Journal*, 12(7). doi: 10.1186/s12985-014-0220-1.

Gerits, N. and Moens, U. (2012) 'Agnoprotein of mammalian polyomaviruses', *Virology*. Elsevier, 432(2), pp. 316–326. doi: 10.1016/j.virol.2012.05.024.

Gheit, T. *et al.* (2017) 'Isolation and characterization of a novel putative human polyomavirus', *Virology*. Academic Press Inc., 506, pp. 45–54. doi: 10.1016/j.virol.2017.03.007.

Giacobbi, N. S. *et al.* (2015) 'Polyomavirus T antigens activate an antiviral

state', *Virology*. Academic Press, 476, pp. 377–385. doi: 10.1016/J.VIROL.2014.12.032.

Gilbert, J. and Benjamin, T. (2004) 'Uptake Pathway of Polyomavirus via Ganglioside GD1a', *Journal of Virology*. American Society for Microbiology, 78(22), pp. 12259–12267. doi: 10.1128/jvi.78.22.12259-12267.2004.

Gillingham, A. K. *et al.* (2014) 'Developmental Cell Resource Toward a Comprehensive Map of the Effectors of Rab GTPases', *Developmental Cell*, 31, pp. 358–373. doi: 10.1016/j.devcel.2014.10.007.

Gillock, E. T. *et al.* (1997) 'Polyomavirus Major Capsid Protein VP1 Is Capable of Packaging Cellular DNA When Expressed in the Baculovirus System', *Journal of Virology*, 71(4), pp. 2857–2865.

Ginevri, F. *et al.* (2003) 'Polyomavirus BK infection in pediatric kidney-allograft recipients: a single-center analysis of incidence, risk factors, and novel therapeutic approaches', *Transplantation*, 75(8), pp. 1266–1270. doi: 10.1097/01.TP.0000061767.32870.72.

Ginevri, F. *et al.* (2007) 'Prospective monitoring of polyomavirus BK replication and impact of pre-emptive intervention in pediatric kidney recipients', *American Journal of Transplantation*. John Wiley & Sons, Ltd, 7(12), pp. 2727–2735. doi: 10.1111/j.1600-6143.2007.01984.x.

Girardi, A. J. *et al.* (1962) 'Developinent of Tumors in Hamsters Inoculated in the Neonatal Period with Vacuolating Virus, SV40', *Proceedings of the Society for Experimental Biology and Medicine*. Williams & Wilkins Co, 109(3), pp. 649–660.

Giroglou, T. *et al.* (2001) 'Human Papillomavirus Infection Requires Cell Surface Heparan Sulfate', *Journal of Virology*. American Society for Microbiology, 75(3), pp. 1565–1570. doi: 10.1128/jvi.75.3.1565-1570.2001.

Gizzi, A. S. *et al.* (2018) 'A naturally occurring antiviral ribonucleotide encoded by the human genome.', *Nature*. NIH Public Access, 558(7711), pp. 610–614. doi: 10.1038/s41586-018-0238-4.

Glebov, O. O., Bright, N. A. and Nichols, B. J. (2006) 'Flotillin-1 defines a clathrin-independent endocytic pathway in mammalian cells', *Nature Cell Biology*, 8(1). doi: 10.1038/ncb1342.

Goldshmidt, O. *et al.* (2002) ‘Human heparanase is localized within lysosomes in a stable form’, *Experimental Cell Research*. Academic Press, 281(1), pp. 50–62. doi: 10.1006/excr.2002.5651.

Good, P. J., Welch, R. C., Barkan, A., *et al.* (1988) ‘Both VP2 and VP3 Are Synthesized from Each of the Alternatively Spliced Late 19S RNA Species of Simian Virus 40’, *Journal of Virology*, 62(3), pp. 944–953.

Good, Peter J, Welch, Renee C, Ryu, W.-S., *et al.* (1988) ‘The Late Spliced 19S and 16S RNAs of Simian Virus 40 Can Be Synthesized from a Common Pool of Transcripts’, *Journal of Virology*, 62(2), pp. 563–571.

Goodall, K. J. *et al.* (2014) ‘Soluble Heparan Sulfate Fragments Generated by Heparanase Trigger the Release of Pro-Inflammatory Cytokines through TLR-4’. doi: 10.1371/journal.pone.0109596.

Goodwin, E. C. *et al.* (2011) ‘BiP and Multiple DNAJ Molecular Chaperones in the Endoplasmic Reticulum Are Required for Efficient Simian Virus 40 Infection’, *mBio*, 2(3), pp. e00101-11. doi: 10.1128/mBio.00101-11.

Gosert, R. *et al.* (2008) ‘Polyomavirus BK with rearranged noncoding control region emerge in vivo in renal transplant patients and increase viral replication and cytopathology’, *Journal of Experimental Medicine*. The Rockefeller University Press, 205(4), pp. 841–852. doi: 10.1084/jem.20072097.

Gosert, R. *et al.* (2011) ‘CMX001 (1-O-hexadecyloxypropyl-cidofovir) inhibits polyomavirus jc replication in human brain progenitor-derived astrocytes’, *Antimicrobial Agents and Chemotherapy*. American Society for Microbiology Journals, 55(5), pp. 2129–2136. doi: 10.1128/AAC.00046-11.

Gossai, A. *et al.* (2016) ‘Seroepidemiology of Human Polyomaviruses in a US Population’, *American Journal of Epidemiology*, 183(1), pp. 61–69. doi: 10.1093/aje/kwv155.

Götte, B., Liu, L. and McInerney, G. M. (2018) ‘The enigmatic alphavirus non-structural protein 3 (nsP3) revealing its secrets at last’, *Viruses*. MDPI AG. doi: 10.3390/v10030105.

Goudsmit, J. *et al.* (1982) ‘The role of BK virus in acute respiratory tract disease and the presence of BKV DNA in tonsils’, *Journal of Medical Virology*, 10(2), pp. 91–99. doi: 10.1002/jmv.1890100203.

Grass, D. S. and Manley, J. L. (1987) ‘Selective Translation Initiation on Bicistronic Simian Virus 40 Late mRNA’, *Journal of Virology*, 61(7), pp. 2331–2335.

Grinde, B., Gayorfar, M. and Rinaldo, C. H. (2007) ‘Impact of a polyomavirus (BKV) infection on mRNA expression in human endothelial cells’, *Virus Research*. Elsevier, 123(1), pp. 86–94. doi: 10.1016/j.virusres.2006.08.005.

Gross, L. (1953) ‘A Filterable Agent, Recovered from Ak Leukemic Extracts, Causing Salivary Gland Carcinomas in C3H Mice’, *Proceedings of the Society for Experimental Biology and Medicine*, 83(2), pp. 414–421.

Gruda, M. C. *et al.* (1993) ‘Transcriptional Activation by Simian Virus 40 Large T Antigen: Interactions with Multiple Components of the Transcription Complex’, *Molecular and Cellular Biology*, pp. 961–969.

Gu, R. *et al.* (2009) ‘Gene regulation by sense-antisense overlap of polyadenylation signals’, *RNA*, 15, pp. 1154–1163. doi: 10.1261/rna.1608909.

Guan, J. *et al.* (2017) ‘Cryoelectron Microscopy Maps of Human Papillomavirus 16 Reveal L2 Densities and Heparin Binding Site’, *Structure*. Cell Press, 25(2), pp. 253–263. doi: 10.1016/j.str.2016.12.001.

Guasch, A. *et al.* (2010) ‘Assessment of Efficacy and Safety of FK778 in Comparison With Standard Care in Renal Transplant Recipients With Untreated BK Nephropathy’, *Transplantation*, 90(8), p. 1. doi: 10.1097/TP.0b013e3181f2c94b.

Guo, X. *et al.* (2006) ‘The zinc-finger antiviral protein recruits the RNA processing exosome to degrade the target mRNA’, *PNAS*, 104(1), pp. 151–156.

Gupta, G. *et al.* (2018) ‘Treatment for presumed BK polyomavirus nephropathy and risk of urinary tract cancers among kidney transplant recipients in the United States’, *American Journal of Transplantation*. Blackwell Publishing Ltd, 18(1), pp. 245–252. doi: 10.1111/ajt.14530.

Habuka, M. *et al.* (2014) ‘The Kidney Transcriptome and Proteome Defined by Transcriptomics and Antibody-Based Profiling’, *PLoS ONE*. Edited by H. Mischak. Public Library of Science, 9(12), p. e116125. doi: 10.1371/journal.pone.0116125.

Hadigal, S. R. *et al.* (2015) ‘Heparanase is a host enzyme required for herpes

simplex virus-1 release from cells', *Nature Communications*. Nature Publishing Group, 6(1), p. 6985. doi: 10.1038/ncomms7985.

Handala, L. *et al.* (2020) 'BK Polyomavirus Hijacks Extracellular Vesicles for En Bloc Transmission', *Journal of Virology*, 94(6), pp. e01834-19. doi: 10.1128/JVI.01834-19.

Harada, H. *et al.* (1989) 'Structurally similar but functionally distinct factors, IRF-1 and IRF-2, bind to the same regulatory elements of IFN and IFN-inducible genes', *Cell*. Cell Press, 58(4), pp. 729–739. doi: 10.1016/0092-8674(89)90107-4.

Harari, A. *et al.* (2006) 'Functional signatures of protective antiviral T-cell immunity in human virus infections', *Immunological Reviews*, 211(1), pp. 236–254. doi: 10.1111/j.0105-2896.2006.00395.x.

Hariharan, S. *et al.* (2005) 'BK Virus-Specific Antibodies and BKV DNA in Renal Transplant Recipients with BKV Nephritis', *American Journal of Transplantation*, 5(11), pp. 2719–2724. doi: 10.1111/j.1600-6143.2005.01080.x.

Haririan, A. *et al.* (2002) 'Polyomavirus nephropathy in native kidneys of a solitary pancreas transplant recipient', *Transplantation*. Lippincott Williams and Wilkins, 73(8), pp. 1350–1353. doi: 10.1097/00007890-200204270-00030.

Harms, J. S. and Splitter, G. A. (1995) 'Interferon-γ Inhibits Transgene Expression Driven by SV40 or CMV Promoters but Augments Expression Driven by the Mammalian MHC I Promoter', *Human Gene Therapy*. Hum Gene Ther, 6(10), pp. 1291–1297. doi: 10.1089/hum.1995.6.10-1291.

Harris, K. F. *et al.* (1998) 'Novel Mechanisms of E2F Induction by BK Virus Large-T Antigen: Requirement of Both the pRb-Binding and the J Domains', *Molecular and Cellular Biology*, 18(3), pp. 1746–1756.

Harris, K. F., Christensen, J. B. and Imperiale, M. J. (1996) 'BK Virus Large T Antigen: Interactions with the Retinoblastoma Family of Tumor Suppressor Proteins and Effects on Cellular Growth Control', *Journal of Virology*, 70(4), pp. 2378–2386.

Hatziioannou, T. and Bieniasz, P. D. (2011) 'Antiretroviral restriction factors', *Current Opinion in Virology*. Elsevier B.V., pp. 526–532. doi: 10.1016/j.coviro.2011.10.007.

Hatzinger, M. *et al.* (2016) ‘The history of kidney transplantation’, *Urologe* . Springer Verlag, 55(10), pp. 1353–1359. doi: 10.1007/s00120-016-0205-3.

Hedquist, B. G. *et al.* (1999) ‘Identification of BK virus in a patient with acquired immune deficiency syndrome and bilateral atypical retinitis’, *Ophthalmology*. Elsevier Inc., 106(1), pp. 129–132. doi: 10.1016/S0161-6420(99)90014-3.

Helle, F. *et al.* (2017) ‘Biology of the BKPyV: An Update.’, *Viruses*. Multidisciplinary Digital Publishing Institute (MDPI), 9(11), p. 327. doi: 10.3390/v9110327.

Hemmi, H. *et al.* (2000) ‘A Toll-like receptor recognizes bacterial DNA’, *Nature*, 408, pp. 740–745.

Henriksen, S. *et al.* (2014) ‘The Human Fetal Glial Cell Line SVG p12 Contains Infectious BK Polyomavirus’, *Journal of Virology*. American Society for Microbiology, 88(13), pp. 7556–7568. doi: 10.1128/jvi.00696-14.

Henriksen, S. *et al.* (2016) ‘The Presumed Polyomavirus Viroporin VP4 of Simian Virus 40 or Human BK Polyomavirus Is Not Required for Viral Progeny Release’, *Journal of Virology*. American Society for Microbiology, 90(22), pp. 10398–10413. doi: 10.1128/jvi.01326-16.

Heritage, J., Chesters, P. M. and McCance, D. J. (1981) ‘The persistence of papovavirus BK DNA sequences in normal human renal tissue’, *Journal of Medical Virology*, 8, pp. 143–150. doi: 10.1002/jmv.1890080208.

Heutinck, K. M., Kassies, J., *et al.* (2012) ‘SerpinB9 expression in human renal tubular epithelial cells is induced by triggering of the viral dsRNA sensors TLR3, MDA5 and RIG-I’, *Nephrol Dial Transplant*, 27, pp. 2746–2754. doi: 10.1093/ndt/gfr690.

Heutinck, K. M., Rowshani, A. T., *et al.* (2012) ‘Viral double-stranded RNA sensors induce antiviral, pro-inflammatory, and pro-apoptotic responses in human renal tubular epithelial cells’, *Kidney International*, 82, pp. 664–675. doi: 10.1038/ki.2012.206.

Hirsch, H. H. *et al.* (2002) ‘Prospective Study of Polyomavirus Type BK Replication and Nephropathy in Renal-Transplant Recipients’, *The New England Journal of Medicine*, 347(7), pp. 488–496.

Hirsch, H. H. *et al.* (2006) ‘Polyomavirus-associated nephropathy in renal

transplantation: Critical issues of screening and management', in Ahsan, N. (ed.) *Polyomaviruses and Human Diseases*. New York, NY: Springer, pp. 160–173. doi: 10.1007/0-387-32957-9_11.

Hirsch, H. H. *et al.* (2014) 'European perspective on human polyomavirus infection, replication and disease in solid organ transplantation', *European Society of Clinical Infectious Diseases*, 20, pp. 74–88. doi: 10.1111/1469-0691.12538.

Hirsch, H. H. *et al.* (2016) 'BK Polyomavirus Replication in Renal Tubular Epithelial Cells Is Inhibited by Sirolimus, but Activated by Tacrolimus Through a Pathway Involving FKBP-12', *American Journal of Transplantation*. Blackwell Publishing Ltd, 16(3), pp. 821–832. doi: 10.1111/ajt.13541.

Hirsch, H. H. and Steiger, J. (2003) 'Polyomavirus BK', *Lancet Infectious Diseases*, 3, pp. 611–23. doi: 10.1016/S1473-3099(03)00770-9.

Hirshoren, N. *et al.* (2014) 'Induction of heparanase by HPV E6 oncogene in head and neck squamous cell carcinoma', *Journal of Cellular and Molecular Medicine*, 18(1), pp. 181–186. doi: 10.1111/jcmm.12179.

Ho, E. S. *et al.* (2000) 'Cytotoxicity of Antiviral Nucleotides Adefovir and Cidofovir Is Induced by the Expression of Human Renal Organic Anion Transporter 1', *Journal of the American Society of Nephrology*, 11, pp. 383–393.

Honda, K. and Taniguchi, T. (2006) 'IRFs: Master regulators of signalling by Toll-like receptors and cytosolic pattern-recognition receptors', *Nature Reviews Immunology*, pp. 644–658. doi: 10.1038/nri1900.

Hopkins, J. *et al.* (2018) 'Host Enzymes Heparanase and Cathepsin L Promote Herpes Simplex Virus 2 Release from Cells', *Journal of Virology*. American Society for Microbiology (ASM), 92(23). doi: 10.1128/JVI.01179-18.

Huang, G. *et al.* (2015) 'Factors influencing graft outcomes following diagnosis of polyomavirus -associated nephropathy after renal transplantation', *PLoS ONE*. Public Library of Science, 10(11). doi: 10.1371/journal.pone.0142460.

Hulett, M. D. *et al.* (2000) 'Identification of active-site residues of the pro-metastatic endoglycosidase heparanase', *Biochemistry*. American Chemical Society , 39(51), pp. 15659–15667. doi: 10.1021/bi002080p.

Humes, H. D. *et al.* (2002) ‘Metabolic replacement of kidney function in uremic animals with a bioartificial kidney containing human cells’, *American Journal of Kidney Diseases*. W.B. Saunders, 39(5), pp. 1078–1087. doi: 10.1053/ajkd.2002.32792.

Hurdiss, D. L. *et al.* (2016) ‘New Structural Insights into the Genome and Minor Capsid Proteins of BK Polyomavirus using Cryo-Electron Microscopy’, *Structure*, 24, pp. 528–536. doi: 10.1016/j.str.2016.02.008.

Hurdiss, D. L. *et al.* (2018) ‘The Structure of an Infectious Human Polyomavirus and Its Interactions with Cellular Receptors.’, *Structure*. Elsevier, 26(6), pp. 839-847.e3. doi: 10.1016/j.str.2018.03.019.

Husseiny, M. I. and Lacey, S. F. (2011) ‘Development of infectious recombinant BK virus’, *Virus Research*. Elsevier, 161(2), pp. 150–161. doi: 10.1016/J.VIRUSRES.2011.07.017.

IARC (2014) *Malaria and some Polyomaviruses (SV40, BK, JC, and Merkel cell viruses)*, *IARC Working Group on the Evaluation of Carcinogenic Risks to Humans*. Lyon, France.

Iinuma, T. *et al.* (2009) ‘Role of syntaxin 18 in the organization of endoplasmic reticulum subdomains’, *Journal of Cell Science*. The Company of Biologists Ltd, 122(10), pp. 1680–1690. doi: 10.1242/jcs.036103.

Ikushima, H., Negishi, H. and Taniguchi, T. (2013) ‘The IRF family transcription factors at the interface of innate and adaptive immune responses’, *Cold Spring Harbor Symposia on Quantitative Biology*. Cold Spring Harbor Laboratory Press, 78(1), pp. 105–116. doi: 10.1101/sqb.2013.78.020321.

Imperiale, M. J. and Jiang, M. (2016) ‘Polyomavirus Persistence’, *Annual Review of Virology*, 3(1), pp. 517–532. doi: 10.1146/annurev-virology-110615-042226.

Inoue, T. *et al.* (2015) ‘ERdj5 Reductase Cooperates with Protein Disulfide Isomerase To Promote Simian Virus 40 Endoplasmic Reticulum Membrane Translocation’, *Journal of Virology*. American Society for Microbiology, 89(17), pp. 8897–8908. doi: 10.1128/jvi.00941-15.

Inoue, T. and Tsai, B. (2015) ‘A Nucleotide Exchange Factor Promotes Endoplasmic Reticulum-to-Cytosol Membrane Penetration of the Nonenveloped

Virus Simian Virus 40', *Journal of Virology*. American Society for Microbiology, 89(8), pp. 4069–4079. doi: 10.1128/jvi.03552-14.

Isaacs, A. and Lindenmann, J. (1957) 'Virus interference. I. The interferon', *Proceedings of the Royal Society of London. Series B. Biological Sciences*, 147(927), pp. 258–67.

Ishii, N. *et al.* (1996) 'Analysis of a Nuclear Localization Signal of Simian Virus 40 Major Capsid Protein Vp1', *Journal of Virology*, 70(2), pp. 1317–1322.

Ivashkiv, L. B. and Donlin, L. T. (2014) 'Regulation of type I interferon responses', *Nature Reviews Immunology*. Nature Publishing Group, 14(1), pp. 36–49. doi: 10.1038/nri3581.

Jackson, J. A. *et al.* (2011) 'Urinary chemokines CXCL9 and CXCL10 are noninvasive markers of renal allograft rejection and BK viral infection', *American Journal of Transplantation*. Am J Transplant, 11, pp. 2228–2234. doi: 10.1111/j.1600-6143.2011.03680.x.

Janeway, Jr, C. A. *et al.* (2001) *Immunobiology*. 5th edn. New York: Garland Science.

Jeffers, L. K., Madden, V. and Webster-Cyriaque, J. (2009) 'BK virus has tropism for human salivary gland cells in vitro: Implications for transmission', *Virology*. Academic Press, 394(2), pp. 183–193. doi: 10.1016/j.virol.2009.07.022.

Jeffers, L. and Webster-Cyriaque, J. Y. (2011) 'Viruses and Salivary Gland Disease (SGD)', *Advances in Dental Research*. SAGE PublicationsSage CA: Los Angeles, CA, 23(1), pp. 79–83. doi: 10.1177/0022034510396882.

Jia, L. *et al.* (2018) 'Identification of potential key protein interaction networks of BK virus nephropathy in patients receiving kidney transplantation', *Scientific Reports*. Nature Publishing Group, 8(1), pp. 1–8. doi: 10.1038/s41598-018-23492-2.

Jiang, M. *et al.* (2009) 'Early events during BK virus entry and disassembly.', *Journal of virology*. American Society for Microbiology (ASM), 83(3), pp. 1350–8. doi: 10.1128/JVI.02169-08.

Jiang, M. *et al.* (2011) 'Functional Reorganization of Promyelocytic Leukemia Nuclear Bodies During BK Virus Infection', *mBio*. American Society for

Microbiology, 2(1), pp. e00281-10. doi: 10.1128/mBio.00281-10.

Jiang, M. *et al.* (2012) 'Roles of ATM and ATR-Mediated DNA Damage Responses during Lytic BK Polyomavirus Infection', *PLoS Pathogens*. Edited by J. Pipas. Public Library of Science, 8(8), p. e1002898. doi: 10.1371/journal.ppat.1002898.

Jin, L., Gibson, P. E., Knowles, W. A., *et al.* (1993) 'BK virus antigenic variants: Sequence analysis within the capsid VP1 epitope', *Journal of Medical Virology*, 39(1), pp. 50–56. doi: 10.1002/jmv.1890390110.

Jin, L., Gibson, P. E., Booth, J. C., *et al.* (1993) 'Genomic typing of BK virus in clinical specimens by direct sequencing of polymerase chain reaction products', *Journal of Medical Virology*, 41, pp. 11–17. doi: 10.1002/jmv.1890410104.

Johannessen, M. *et al.* (2008) 'Phosphorylation of human polyomavirus BK agnoprotein at Ser-11 is mediated by PKC and has an important regulative function', *Virology*. Academic Press, 379(1), pp. 97–109. doi: 10.1016/j.virol.2008.06.007.

Johannessen, M. *et al.* (2011) 'BKV Agnoprotein Interacts with α-Soluble N-Ethylmaleimide-Sensitive Fusion Attachment Protein, and Negatively Influences Transport of VSVG-EGFP', *PLoS ONE*. Edited by R. J. Geraghty. Public Library of Science, 6(9), p. e24489. doi: 10.1371/journal.pone.0024489.

Jouhi, L. *et al.* (2015) 'The Expression of Toll-like Receptors 2, 4, 5, 7 and 9 in Merkel Cell Carcinoma ', *Anticancer Research*, pp. 1843–1850.

Jouve, T., Rostaing, L. and Malvezzi, P. (2015) 'Place of mTOR inhibitors in management of BKV infection after kidney transplantation', *Journal of Nephropathology*. Maad Rayan Publishing Company, 5(1), pp. 1–7. doi: 10.15171/jnp.2016.01.

Justice, J. L. *et al.* (2015) 'Quantitative Proteomic Analysis of Enriched Nuclear Fractions from BK Polyomavirus-infected Primary Renal Proximal Tubule Epithelial Cells HHS Public Access', *J Proteome Res. J Proteome Res*, 14(10), pp. 4413–4424. doi: 10.1021/acs.jproteome.5b00737.

Kalderon, D. *et al.* (1984) *A Short Amino Acid Sequence Able to Specify Nuclear Location*, *Cell*.

Kalluri, H. V. and Hardinger, K. L. (2012) 'Current state of renal transplant

immunosuppression: Present and future', *World Journal of Transplantation*. Baishideng Publishing Group Inc., 2(4), pp. 51–68. doi: 10.5500/wjt.v2.i4.51.

Kamminga, S. *et al.* (2018) 'Seroprevalence of fourteen human polyomaviruses determined in blood donors', *PLoS ONE*, 13(10), p. e0206273. doi: 10.1371/journal.pone.0206273.

Kane, J. R. *et al.* (2020) 'A polyomavirus peptide binds to the capsid VP1 pore and has potent antiviral activity against BK and JC polyomaviruses', *eLife*, 9, p. e50722. doi: 10.7554/eLife.50722.

Kane, M. *et al.* (2016) 'Identification of Interferon-Stimulated Genes with Antiretroviral Activity', *Cell Host and Microbe*. The Authors, 20(3), pp. 392–405. doi: 10.1016/j.chom.2016.08.005.

Kang, W. and Shin, E.-C. (2012) 'Colorimetric Focus-Forming Assay with Automated Focus Counting by Image Analysis for Quantification of Infectious Hepatitis C Virions', *PLoS ONE*. Edited by G. Waris. Public Library of Science, 7(8), p. e43960. doi: 10.1371/journal.pone.0043960.

Kawai, T. and Akira, S. (2010) 'The role of pattern-recognition receptors in innate immunity: Update on toll-like receptors', *Nature Immunology*. Nature Publishing Group, pp. 373–384. doi: 10.1038/ni.1863.

Kean, J. M. *et al.* (2009) 'Seroepidemiology of Human Polyomaviruses', *PLoS Pathogens*. Edited by W. J. Atwood. Public Library of Science, 5(3), p. e1000363. doi: 10.1371/journal.ppat.1000363.

Kelley, W. L. and Georgopoulos, C. (1997) 'The T/t common exon of simian virus 40, JC, and BK polyomavirus T antigens can functionally replace the J-domain of the Escherichia coli DnaJ molecular chaperone', *PNAS*. National Academy of Sciences, 94(8), pp. 3679–3684. doi: 10.1073/pnas.94.8.3679.

Kenan, D. J. *et al.* (2017) 'BK Polyomavirus Genomic Integration and Large T Antigen Expression: Evolving Paradigms in Human Oncogenesis', *American Journal of Transplantation*. Blackwell Publishing Ltd, 17(6), pp. 1674–1680. doi: 10.1111/ajt.14191.

Khalil, M. A. M. *et al.* (2018) 'Fluoroquinolones and BK virus nephropathy: A myth or a reality', *Indian Journal of Nephrology*. Wolters Kluwer Medknow Publications, pp. 257–264. doi: 10.4103/ijn.IJN_251_17.

Kim, E. J. *et al.* (2003) ‘Functional dissection of the transactivation domain of interferon regulatory factor-1’, *Biochemical and Biophysical Research Communications*. Academic Press Inc., 304(2), pp. 253–259. doi: 10.1016/S0006-291X(03)00575-8.

Kimura, A. *et al.* (2012) ‘Interferon-γ is protective in cisplatin-induced renal injury by enhancing autophagic flux’, *Kidney International*. Nature Publishing Group, 82(10), pp. 1093–1104. doi: 10.1038/ki.2012.240.

Kirchhof, M. G. *et al.* (2014) ‘Trichodysplasia spinulosa: rare presentation of polyomavirus infection in immunocompromised patients.’, *Journal of cutaneous medicine and surgery*. Decker Intellectual Properties, 18(6), pp. 430–5. doi: 10.2310/7750.2014.13189.

Knight, E. and Korant, B. D. (1979) ‘Fibroblast interferon induces synthesis of four proteins in human fibroblast cells’, *Proceedings of the National Academy of Sciences of the United States of America*. Proc Natl Acad Sci U S A, 76(4), pp. 1824–1827. doi: 10.1073/pnas.76.4.1824.

Knowles, W. A. (2001) ‘Propagation and assay of BK virus’, *Methods in Molecular Biology*. Humana Press Inc., 165, pp. 19–31. doi: 10.1385/1-59259-117-5:19.

Knowles, W. A. (2002) ‘Serendipity—The Fortuitous Discovery of BK Virus’, in Khalili, K. and Stoner, G. L. (eds) *Human Polyomaviruses*. New York, USA: John Wiley & Sons, Inc., pp. 45–51. doi: 10.1002/0471221945.ch4.

Knowles, W. A. *et al.* (2003) ‘Population-based study of antibody to the human polyomaviruses BKV and JCV and the simian polyomavirus SV40’, *Journal of Medical Virology*, 71(1), pp. 115–123. doi: 10.1002/jmv.10450.

Knowles, W. A., Gibson, P. E. and Gardner, S. D. (1989) ‘Serological typing scheme for bk-like isolates of human polyomavirus’, *Journal of Medical Virology*, pp. 118–123. doi: 10.1002/jmv.1890280212.

Kooreman, N. G. *et al.* (2017) ‘Alloimmune Responses of Humanized Mice to Human Pluripotent Stem Cell Therapeutics’, *Cell Reports*. Cell Press, 20(8), pp. 1978–1990. doi: 10.1016/J.CELREP.2017.08.003.

Koralnik, I. J. *et al.* (2005) ‘JC virus granule cell neuronopathy: A novel clinical syndrome distinct from progressive multifocal leukoencephalopathy’, *Annals of*

Neurology, 57(4), pp. 576–580. doi: 10.1002/ana.20431.

de Kort, H. *et al.* (2017) ‘Primary Human Renal-Derived Tubular Epithelial Cells Fail to Recognize and Suppress BK Virus Infection.’, *Transplantation*, 101(8), pp. 1820–1829. doi: 10.1097/TP.0000000000001521.

Korup, S. *et al.* (2013) ‘Identification of a Novel Human Polyomavirus in Organs of the Gastrointestinal Tract’, *PLoS ONE*. Edited by J. Qiu. Public Library of Science, 8(3), p. e58021. doi: 10.1371/journal.pone.0058021.

Koshiba, T. *et al.* (2011) ‘Mitochondrial membrane potential is required for MAVS-mediated antiviral signaling’, *Science Signaling*. American Association for the Advancement of Science, 4(158), pp. ra7–ra7. doi: 10.1126/scisignal.2001147.

Kreuger, J. and Kjellén, L. (2012) ‘Heparan Sulfate Biosynthesis: Regulation and Variability’, *Journal of Histochemistry and Cytochemistry*. Histochemical Society, 60(12), pp. 898–907. doi: 10.1369/0022155412464972.

Lamaze, C. *et al.* (2001) ‘Interleukin 2 receptors and detergent-resistant membrane domains define a clathrin-independent endocytic pathway’, *Molecular Cell*. Cell Press, 7(3), pp. 661–671. doi: 10.1016/S1097-2765(01)00212-X.

Lanford, R. E. *et al.* (2006) ‘Genomic response to interferon-α in chimpanzees: Implications of rapid downregulation for hepatitis C kinetics’, *Hepatology*. John Wiley & Sons, Ltd, 43(5), pp. 961–972. doi: 10.1002/hep.21167.

Larner, A. C. *et al.* (1984) ‘Transcriptional induction of two genes in human cells by β interferon’, *Proceedings of the National Academy of Sciences of the United States of America*. Proc Natl Acad Sci U S A, 81(21 I), pp. 6733–6737. doi: 10.1073/pnas.81.21.6733.

Lavoie, J. N. *et al.* (1996) ‘Cyclin D1 expression is regulated positively by the p42/p44(MAPK) and negatively by the p38/HOG(MAPK) pathway’, *Journal of Biological Chemistry*. J Biol Chem, 271(34), pp. 20608–20616. doi: 10.1074/jbc.271.34.20608.

Lea, A. P. and Bryson, H. M. (1996) ‘Cidofovir’, *Drugs*. Springer International Publishing, pp. 225–230. doi: 10.2165/00003495-199652020-00006.

Lee, A. J. and Ashkar, A. A. (2018) ‘The dual nature of type I and type II

interferons', *Frontiers in Immunology*. Frontiers Media S.A., p. 2061. doi: 10.3389/fimmu.2018.02061.

Lee, H.-R. *et al.* (2009) 'Viral interferon regulatory factors', *Journal of Interferon and Cytokine Research*. Mary Ann Liebert, Inc., 29(9), pp. 621–627. doi: 10.1089/jir.2009.0067.

Lee, H.-R. *et al.* (2012) 'Modulation of immune system by Kaposi's sarcoma-associated herpesvirus: Lessons from viral evasion strategies', *Frontiers in Microbiology*. Frontiers Research Foundation, 3. doi: 10.3389/fmicb.2012.00044.

Leuenberger, D. *et al.* (2007) 'Human polyomavirus type 1 (BK virus) agnoprotein is abundantly expressed but immunologically ignored', *Clinical and Vaccine Immunology*. American Society for Microbiology (ASM), 14(8), pp. 959–968. doi: 10.1128/CVI.00123-07.

Leung, A. Y. H. *et al.* (2005) 'Ciprofloxacin Decreased Polyoma BK Virus Load in Patients Who Underwent Allogeneic Hematopoietic Stem Cell Transplantation', *Clinical Infectious Diseases*, 40(4), pp. 528–537.

Levican, J. *et al.* (2018) 'Role of BK human polyomavirus in cancer', *Infectious agents and cancer*. BioMed Central, 13, p. 12. doi: 10.1186/s13027-018-0182-9.

Levy, D. E. *et al.* (1988) 'Interferon-induced nuclear factors that bind a shared promoter element correlate with positive and negative transcriptional control.', *Genes & development*, 2(4), pp. 383–393. doi: 10.1101/gad.2.4.383.

Li, M. M. H. *et al.* (2016) 'Interferon regulatory factor 2 protects mice from lethal viral neuroinvasion', *Journal of Experimental Medicine*. Rockefeller University Press, 213(13), pp. 2931–2947. doi: 10.1084/jem.20160303.

Li, M. M. H., MacDonald, M. R. and Rice, C. M. (2015) 'To translate, or not to translate: Viral and host mRNA regulation by interferon-stimulated genes', *Trends in Cell Biology*. Elsevier Ltd, 25(6), pp. 320–329. doi: 10.1016/j.tcb.2015.02.001.

Li, Y. *et al.* (2016) 'Activation of RNase L is dependent on OAS3 expression during infection with diverse human viruses', *Proceedings of the National Academy of Sciences of the United States of America*. National Academy of

Sciences, 113(8), pp. 2241–2246. doi: 10.1073/pnas.1519657113.

Liacini, A. *et al.* (2010) ‘Anti-BK virus mechanisms of sirolimus and leflunomide alone and in combination: Toward a new therapy for BK virus infection’, *Transplantation*. Transplantation, 90(12), pp. 1450–1457. doi: 10.1097/TP.0b013e3182007be2.

Liddington, R. C. *et al.* (1991) ‘Structure of simian virus 40 at 3.8-A resolution’, *Nature*, 354, pp. 278–284.

Liebl, D. *et al.* (2006) ‘Mouse Polyomavirus Enters Early Endosomes, Requires Their Acidic pH for Productive Infection, and Meets Transferrin Cargo in Rab11-Positive Endosomes’, *Journal of Virology*. American Society for Microbiology, 80(9), pp. 4610–4622. doi: 10.1128/jvi.80.9.4610-4622.2006.

Lilley, B. N. *et al.* (2006) ‘Murine Polyomavirus Requires the Endoplasmic Reticulum Protein Derlin-2 To Initiate Infection’, *Journal of Virology*, 80(17), pp. 8739–8744. doi: 10.1128/JVI.00791-06.

Lim, E. S. *et al.* (2013) ‘Discovery of STL polyomavirus, a polyomavirus of ancestral recombinant origin that encodes a unique T antigen by alternative splicing’, *Virology*. Academic Press, 436(2), pp. 295–303. doi: 10.1016/j.virol.2012.12.005.

Lim, E. S. *et al.* (2014) ‘Common exposure to STL polyomavirus during childhood’, *Emerging Infectious Diseases*. Centers for Disease Control and Prevention (CDC), 20(9), pp. 1559–1561. doi: 10.3201/eid2009.140561.

Liptak, P., Kemeny, E. and Ivanyi, B. (2006) ‘Primer: histopathology of polyomavirus-associated nephropathy in renal allografts’, *Nature Reviews Nephrology*, 2(11), pp. 631–636. doi: 10.1038/ncpneph0319.

Liu, B. *et al.* (2016) ‘The C-Terminal Tail of TRIM56 Dictates Antiviral Restriction of Influenza A and B Viruses by Impeding Viral RNA Synthesis’, *Journal of Virology*. American Society for Microbiology, 90(9), pp. 4369–4382. doi: 10.1128/jvi.03172-15.

Liu, S.-Y. *et al.* (2012) ‘Systematic identification of type I and type II interferon-induced antiviral factors’, *PNAS*, 109(11), pp. 4239–4244. doi: 10.1073/pnas.1114981109.

Liu, W. *et al.* (2016) ‘Identifying the Target Cells and Mechanisms of Merkel Cell

Polyomavirus Infection', *Cell Host and Microbe*. Cell Press, 19(6), pp. 775–787. doi: 10.1016/j.chom.2016.04.024.

Liu, Y. *et al.* (2016) 'RIG-I-Mediated STING Upregulation Restricts Herpes Simplex Virus 1 Infection', *Journal of Virology*. American Society for Microbiology, 90(20), pp. 9406–9419. doi: 10.1128/jvi.00748-16.

Livak, K. J. and Schmittgen, T. D. (2001) 'Analysis of relative gene expression data using real-time quantitative PCR and the 2-ΔΔCT method', *Methods*. Academic Press Inc., 25(4), pp. 402–408. doi: 10.1006/meth.2001.1262.

Low, J. *et al.* (2004) 'BKV and SV40 infection of human kidney tubular epithelial cells in vitro', *Virology*. Academic Press, 323(2), pp. 182–188. doi: 10.1016/J.VIROL.2004.03.027.

Low, J. A. *et al.* (2006) 'Identification of Gangliosides GD1b and GT1b as Receptors for BK Virus', *Journal of Virology*, 80(3), pp. 1361–1366. doi: 10.1128/JVI.80.3.1361-1366.2006.

Maggiore, U. *et al.* (2010) 'Increased viral load after intravenous immunoglobulin therapy for BK virus-associated nephropathy', *Transplant Infectious Disease*. Blackwell Publishing Inc., pp. 470–472. doi: 10.1111/j.1399-3062.2010.00512.x.

Maginnis, M. S. *et al.* (2010) 'Role of N-Linked Glycosylation of the 5-HT 2A Receptor in JC Virus Infection', *Journal of Virology*, 84(19), pp. 9677–9684. doi: 10.1128/JVI.00978-10.

Maginnis, M. S. (2018) 'Virus–Receptor Interactions: The Key to Cellular Invasion', *Journal of Molecular Biology*. Academic Press, pp. 2590–2611. doi: 10.1016/j.jmb.2018.06.024.

Maginnis, M. S. and Atwood, W. J. (2009) 'JC Virus: An oncogenic virus in animals and humans?', *Seminars in Cancer Biology*. NIH Public Access, 19(4), pp. 261–269. doi: 10.1016/j.semcancer.2009.02.013.

Major, E. O. *et al.* (1985) 'Establishment of a line of human fetal glial cells that supports JC virus multiplication', *Proceedings of the National Academy of Sciences of the United States of America*, 82(4), pp. 1257–1261. doi: 10.1073/pnas.82.4.1257.

Major, E. O. (2010) 'Progressive Multifocal Leukoencephalopathy in Patients on

Immunomodulatory Therapies', *Annual Review of Medicine*, 61, pp. 35–47. doi: 10.1146/annurev.med.080708.082655.

Major, E. O. and Di Mayorca, G. (1973) 'Malignant transformation of BHK21 clone 13 cells by BK virus. A human papovavirus', *PNAS*. National Academy of Sciences, 70(11), pp. 3210–3212. doi: 10.1073/pnas.70.11.3210.

Major, E. O. and Neel, J. V (1998) 'The JC and BK human polyoma viruses appear to be recent introductions to some South American Indian tribes: There is no serological evidence of cross-reactivity with the simian polyoma virus SV40', *Genetics*, 95, pp. 15525–15530.

Maloney, N. S. *et al.* (2012) 'Essential Cell-Autonomous Role for Interferon (IFN) Regulatory Factor 1 in IFN- -Mediated Inhibition of Norovirus Replication in Macrophages', *Journal of Virology*. American Society for Microbiology, 86(23), pp. 12655–12664. doi: 10.1128/jvi.01564-12.

Mantyjarvi, R. A., Arstila, P. P. and Meurman, O. H. (1972) 'Hemagglutination by BK Virus, a Tentative New Member of the Papovavirus Group', *Infection and Immunity*, 6(5), pp. 824–828.

Manzetti, J. *et al.* (2020) 'BK Polyomavirus Evades Innate Immune Sensing by Disrupting the Mitochondrial Network and Promotes Mitophagy', *iScience*. Elsevier Inc., 23(7), p. 101257. doi: 10.1016/j.isci.2020.101257.

Marié, I., Durbin, J. E. and Levy, D. E. (1998) *Differential viral induction of distinct interferon-α genes by positive feedback through interferon regulatory factor-7*, *The EMBO Journal*.

Masci, A. L. *et al.* (2019) 'Integration of Fluorescence Detection and Image-Based Automated Counting Increases Speed, Sensitivity, and Robustness of Plaque Assays', *Molecular Therapy: Methods & Clinical Development*, 14, pp. 270–274. doi: 10.1016/j.omtm.2019.07.007.

Mboko, W. P. *et al.* (2014) 'Interferon regulatory factor 1 restricts gammaherpesvirus replication in primary immune cells.', *Journal of virology*. American Society for Microbiology (ASM), 88(12), pp. 6993–7004. doi: 10.1128/JVI.00638-14.

Mboko, W. P. *et al.* (2017) 'Interferon Regulatory Factor 1 and Type I Interferon Cooperate To Control Acute Gammaherpesvirus Infection.', *Journal of virology*.

American Society for Microbiology Journals, 91(1), pp. e01444-16. doi: 10.1128/JVI.01444-16.

McKenzie, E. A. (2007) 'Heparanase: A target for drug discovery in cancer and inflammation', *British Journal of Pharmacology*. Br J Pharmacol, pp. 1–14. doi: 10.1038/sj.bjp.0707182.

van der Meijden, E. *et al.* (2010) 'Discovery of a new human polyomavirus associated with Trichodysplasia Spinulosa in an immunocompromized patient', *PLoS Pathogens*, 6(7), p. e1001024. doi: 10.1371/journal.ppat.1001024.

van der Meijden, E. *et al.* (2013) 'Different Serologic Behavior of MCPyV, TSPyV, HPyV6, HPyV7 and HPyV9 Polyomaviruses Found on the Skin', *PLOS ONE*, 8(11), p. e81078. doi: 10.1371/journal.pone.0081078.

Meng, L. *et al.* (1999) 'Epoxomicin, a potent and selective proteasome inhibitor, exhibits in vivo antiinflammatory activity', *PNAS*. National Academy of Sciences, 96(18), pp. 10403–10408. doi: 10.1073/pnas.96.18.10403.

Meraro, D. *et al.* (1999) 'Lymphoid-Specific IFN Regulatory Factors Interactions Affect the Activity of Protein-Protein and DNA-Protein', *The Journal of Immunology*, 163, pp. 6468–6478.

Mercer, J., Schelhaas, M. and Helenius, A. (2010) 'Virus Entry by Endocytosis', *Annual Review of Biochemistry*, 79, pp. 803–33. doi: 10.1146/annurev-biochem-060208-104626.

Mettlen, M. *et al.* (2009) 'Dissecting dynamin's role in clathrin-mediated endocytosis', *Biochemical Society Transactions*, 37, pp. 1022–1026. doi: 10.1042/BST0371022.

Michalska, A. *et al.* (2018) 'A positive feedback amplifier circuit that regulates interferon (IFN)-stimulated gene expression and controls type I and type II IFN responses', *Frontiers in Immunology*. Frontiers Media S.A., 9. doi: 10.3389/fimmu.2018.01135.

Mishra, N. *et al.* (2014) 'Identification of a Novel Polyomavirus in a Pancreatic Transplant Recipient With Retinal Blindness and Vasculitic Myopathy'. doi: 10.1093/infdis/jiu250.

Miyamoto, M. *et al.* (1988) 'Regulated expression of a gene encoding a nuclear factor, IRF-1, that specifically binds to IFN-β gene regulatory elements', *Cell*,

54(6), pp. 903–913. doi: 10.1016/S0092-8674(88)91307-4.

Moens, U. *et al.* (1997) *Mechanisms of Transcriptional Regulation of Cellular Genes by SV40 Large T-and Small T-Antigens*, *Virus Genes*. Kluwer Academic Publishers.

Moens, U. *et al.* (2013) 'Serological cross-reactivity between human polyomaviruses', *Reviews in Medical Virology*, 23(4), pp. 250–264. doi: 10.1002/rmv.1747.

Moens, U., Krumbholz, A., *et al.* (2017) 'Biology, evolution, and medical importance of polyomaviruses: An update', *Infection, Genetics and Evolution*. Elsevier, 54, pp. 18–38. doi: 10.1016/J.MEEGID.2017.06.011.

Moens, U., Calvignac-Spencer, S., *et al.* (2017) 'ICTV Virus Taxonomy Profile: Polyomaviridae.', *The Journal of general virology*. Microbiology Society, 98, pp. 1159–1160. doi: 10.1099/jgv.0.000839.

Moens, U. and Van Ghelue, M. (2005) 'Polymorphism in the genome of non-passaged human polyomavirus BK: Implications for cell tropism and the pathological role of the virus', *Virology*. Academic Press, pp. 209–231. doi: 10.1016/j.virol.2004.10.021.

Moens, U. and Macdonald, A. (2019) 'Effect of the Large and Small T-Antigens of Human Polyomaviruses on Signaling Pathways', *International Journal of Molecular Sciences 2019, Vol. 20, Page 3914*. Multidisciplinary Digital Publishing Institute, 20(16), p. 3914. doi: 10.3390/IJMS20163914.

Mogensen, T. H. (2009) 'Pathogen Recognition and Inflammatory Signaling in Innate Immune Defenses', *Clinical Microbiology Reviews*, 22(2), pp. 240–273. doi: 10.1128/CMR.00046-08.

Molloy, E. S. and Calabrese, L. H. (2009) 'Progressive multifocal leukoencephalopathy: A national estimate of frequency in systemic lupus erythematosus and other rheumatic diseases', *Arthritis & Rheumatism*, 60(12), pp. 3761–3765. doi: 10.1002/art.24966.

Monaco, M. C. *et al.* (1998) 'Detection of JC virus DNA in human tonsil tissue: evidence for site of initial viral infection.', *Journal of Virology*. American Society for Microbiology (ASM), 72(12), pp. 9918–23.

Monini, P. *et al.* (1996) 'Latent BK virus infection and Kaposi's sarcoma

pathogenesis', *International Journal of Cancer*. John Wiley & Sons, Ltd, 66(6), pp. 717–722. doi: 10.1002/(SICI)1097-0215(19960611)66:6<717::AID-IJC1>3.0.CO;2-2.

Moreland, R. B. and Garcea, R. L. (1991) 'Characterization of a nuclear localization sequence in the polyomavirus capsid protein VP1', *Virology*. Academic Press, 185(1), pp. 513–518. doi: 10.1016/0042-6822(91)90811-O.

Moriyama, T. *et al.* (2007) 'Caveolar Endocytosis Is Critical for BK Virus Infection of Human Renal Proximal Tubular Epithelial Cells', *Journal of Virology*. American Society for Microbiology, 81(16), pp. 8552–8562. doi: 10.1128/jvi.00924-07.

Moriyama, T. and Sorokin, A. (2008) 'Intracellular trafficking pathway of BK Virus in human renal proximal tubular epithelial cells', *Virology*, 371(2), pp. 336–349. doi: 10.1016/j.virol.2007.09.030.

Moriyama, T. and Sorokin, A. (2009) 'BK virus (BKV): Infection, propagation, quantitation, purification, labeling, and analysis of cell entry', *Current Protocols in Cell Biology*, (SUPPL. 42), pp. 1–15. doi: 10.1002/0471143030.cb2602s42.

Morrissey, K. M. *et al.* (2013) 'Renal Transporters in Drug Development', *Annual Review of Pharmacology and Toxicology*, 53, pp. 503–29. doi: 10.1146/annurev-pharmtox-011112-140317.

Moscarelli, L. *et al.* (2013) 'Everolimus leads to a lower risk of BKV viremia than mycophenolic acid in de novo renal transplantation patients: a single-center experience', *Clinical Transplantation*. Blackwell Publishing Ltd, 27(4), pp. 546–554. doi: 10.1111/ctr.12151.

Mostafavi, S. *et al.* (2016) 'Parsing the Interferon Transcriptional Network and Its Disease Associations', *Cell*. Cell Press, 164(3), pp. 564–578. doi: 10.1016/j.cell.2015.12.032.

Mourez, T. *et al.* (2009) 'Polyomaviruses KI and WU in immunocompromised patients with respiratory disease', *Emerging Infectious Diseases*. Centers for Disease Control and Prevention (CDC), 15(1), pp. 107–109. doi: 10.3201/eid1501.080758.

Mueller, K. *et al.* (2011) 'BK-VP3 as a new target of cellular immunity in BK virus infection', *Transplantation*. Transplantation, 91(1), pp. 100–107. doi:

10.1097/TP.0b013e3181fe1335.

Mühlbacher, T. *et al.* (2019) ‘Low-dose cidofovir and conversion to mTOR-based immunosuppression in polyomavirus-associated nephropathy’, *Transplant Infectious Disease*. Blackwell Publishing Inc., 22, p. e13228. doi: 10.1111/tid.13228.

Myhre, M. R. *et al.* (2010) ‘Clinical polyomavirus BK variants with agnogene deletion are non-functional but rescued by trans-complementation’, *Virology*. Academic Press, 398(1), pp. 12–20. doi: 10.1016/j.virol.2009.11.029.

Nadav, L. *et al.* (2002) ‘Activation, processing and trafficking of extracellular heparanase by primary human fibroblast’, *Journal of Cell Science*, 115, pp. 2179–2187.

Nakamura, K., Hayashi, H. and Kubokawa, M. (2015) ‘Proinflammatory Cytokines and Potassium Channels in the Kidney’, *Mediators of Inflammation*. doi: 10.1155/2015/362768.

Negishi, H. *et al.* (2006) ‘Evidence for licensing of IFN-induced IFN regulatory factor 1 transcription factor by MyD88 in Toll-like receptor-dependent gene induction program’, *PNAS*, 103(41), pp. 15136–15141.

Neil, S. J. D., Zang, T. and Bieniasz, P. D. (2008) ‘Tetherin inhibits retrovirus release and is antagonized by HIV-1 Vpu’, *Nature*. Nature Publishing Group, 451(7177), pp. 425–430. doi: 10.1038/nature06553.

Nelson, C. D. S. *et al.* (2013) ‘A retrograde trafficking inhibitor of ricin and Shiga-like toxins inhibits infection of cells by human and monkey polyomaviruses.’, *mBio*. American Society for Microbiology, 4(6), pp. e00729-13. doi: 10.1128/mBio.00729-13.

Neu, U. *et al.* (2010) ‘Structure-function analysis of the human JC polyomavirus establishes the LSTc pentasaccharide as a functional receptor motif’, *Cell Host and Microbe*. Cell Press, 8(4), pp. 309–319. doi: 10.1016/j.chom.2010.09.004.

Neu, U. *et al.* (2013) ‘A Structure-Guided Mutation in the Major Capsid Protein Retargets BK Polyomavirus’, *PLoS Pathogens*, 9(10), p. e1003688. doi: 10.1371/journal.ppat.1003688.

Ng, S.-C. *et al.* (1985) ‘Simian Virus 40 Maturation in Cells Harboring Mutants Deleted in the Agnogene’, *The Journal of Biological Chemistry*, 260(2), pp.

1127–1132.

Nguyen, K. D. *et al.* (2017) ‘Human Polyomavirus 6 and 7 Are Associated with a Pruritic and Dyskeratotic Dermatosis’, *Journal of the American Academy of Dermatology*, 76(5), pp. 932–40. doi: 10.1016/j.jaad.2016.11.035.

Nickeleit, V. *et al.* (2018) ‘The Banff Working Group Classification of Definitive Polyomavirus Nephropathy: Morphologic Definitions and Clinical Correlations’, *Journal of the American Society of Nephrology*. American Society of Nephrology, 29(2), pp. 680–693. doi: 10.1681/ASN.2017050477.

Nicol, J. T. J. *et al.* (2012) ‘Seroprevalence and Cross-reactivity of Human Polyomavirus 9’, *Emerging Infectious Diseases*, 18(8), pp. 1329–32. doi: 10.3201/eid1808.111625.

Nicol, J. T. J. *et al.* (2013) ‘Age-specific seroprevalences of merkel cell polyomavirus, human polyomaviruses 6, 7, and 9, and trichodysplasia spinulosa-associated polyomavirus’, *Clinical and Vaccine Immunology*. American Society for Microbiology (ASM), 20(3), pp. 363–368. doi: 10.1128/CVI.00438-12.

Nilsson, J. *et al.* (2005) ‘Structure and Assembly of a T1 Virus-Like Particle in BK Polyomavirus’, *Journal of Virology*, 79(9), pp. 5337–5345. doi: 10.1128/JVI.79.9.5337-5345.2005.

Nims, R. W. and Plavsic, M. (2013) ‘Polyomavirus inactivation - A review’, *Biologicals*. Academic Press, 41(2), pp. 63–70. doi: 10.1016/j.biologicals.2012.09.011.

Norkin, L. C. *et al.* (2002) ‘Caveolar Endocytosis of Simian Virus 40 Is Followed by Brefeldin A-Sensitive Transport to the Endoplasmic Reticulum, Where the Virus Disassembles’, *Journal of Virology*. American Society for Microbiology, 76(10), pp. 5156–5166. doi: 10.1128/jvi.76.10.5156-5166.2002.

Nukuzuma, S. *et al.* (1995) ‘Establishment and characterization of a carrier cell culture producing high titres of polyoma JC virus’, *Journal of Medical Virology*, 47(4), pp. 370–377. doi: 10.1002/jmv.1890470413.

O’Donnell, C. D. and Shukla, D. (2008) ‘The Importance of Heparan Sulfate in Herpesvirus Infection’, *Virologica Sinica*, 23(6), pp. 383–393. doi: 10.1007/s12250-008-2992-1.

O'Donnell, J., Taylor, K. A. and Chapman, M. S. (2009) 'Adeno-associated virus-2 and its primary cellular receptor-Cryo-EM structure of a heparin complex', *Virology*. Academic Press, 385(2), pp. 434–443. doi: 10.1016/j.virol.2008.11.037.

O'Hara, S. D. and Garcea, R. L. (2016) 'Murine Polyomavirus Cell Surface Receptors Activate Distinct Signaling Pathways Required for Infection', *mBio*, 7(6), pp. e01836-16. doi: 10.1128/mBio.01836-16.

O'Hara, S. D., Stehle, T. and Garcea, R. (2014) 'Glycan receptors of the Polyomaviridae: Structure, function, and pathogenesis', *Current Opinion in Virology*. Elsevier B.V., pp. 73–78. doi: 10.1016/j.coviro.2014.05.004.

O'Hearn, A. *et al.* (2015) 'Role of EXT1 and Glycosaminoglycans in the Early Stage of Filovirus Entry', *Journal of Virology*. American Society for Microbiology, 89(10), pp. 5441–5449. doi: 10.1128/jvi.03689-14.

Okada, Y. *et al.* (2005) 'Dissociation of heterochromatin protein 1 from lamin B receptor induced by human polyomavirus agnoprotein: Role in nuclear egress of viral particles', *EMBO Reports*. EMBO Rep, 6(5), pp. 452–457. doi: 10.1038/sj.embor.7400406.

Ortiz, A. *et al.* (2005) 'Tubular Cell Apoptosis and Cidofovir-Induced Acute Renal Failure', *Antiviral Therapy*, 10(1), pp. 185–90.

Orzalli, M. H. *et al.* (2018) 'An Antiviral Branch of the IL-1 Signaling Pathway Restricts Immune-Evasive Virus Replication', *Molecular Cell*, 71, pp. 825-840.e5. doi: 10.1016/j.molcel.2018.07.009.

Osada, N. *et al.* (2014) 'The Genome Landscape of the African Green Monkey Kidney-Derived Vero Cell Line', *DNA Research*, 21, pp. 673–683. doi: 10.1093/dnares/dsu029.

Padgett, B. L. *et al.* (1971) 'Cultivation of papova-like virus from human brain with progressive multifocal leucoencephalopathy', *The Lancet*. Elsevier, pp. 1257–1260. doi: 10.1016/S0140-6736(71)91777-6.

Pamenter, M. E. *et al.* (2012) 'DIDS Prevents Ischemic Membrane Degradation in Cultured Hippocampal Neurons by Inhibiting Matrix Metalloproteinase Release', *PLoS ONE*. Edited by E. C. Tsilibary. Public Library of Science, 7(8), p. e43995. doi: 10.1371/journal.pone.0043995.

Panou, M.-M. *et al.* (2018) ‘Agnoprotein Is an Essential Egress Factor during BK Polyomavirus Infection’, *International Journal of Molecular Sciences*. Multidisciplinary Digital Publishing Institute, 19(3), p. 902. doi: 10.3390/ijms19030902.

Panou, M.-M. *et al.* (2020) ‘Glibenclamide inhibits BK polyomavirus infection in kidney cells through CFTR blockade’, *Antiviral Research*. Elsevier BV, 178, p. 104778. doi: 10.1016/j.antiviral.2020.104778.

Papadopoulou, A. *et al.* (2014) ‘Activity of broad-spectrum T-cells as treatment for AdV, EBV, CMV, BKV and HHV6 infections after HSCT’, *Science Translational Medicine*, 6(242). doi: 10.1126/scitranslmed.3008825.

Pastrana, D. V. (2020) ‘mSphere of Influence: It’s Not Me, It’s You—How Donor Factors Influence Kidney Transplant Outcomes’, *mSphere*. American Society for Microbiology, 5(1). doi: 10.1128/msphere.00964-19.

Pastrana, D. V *et al.* (2009) ‘Quantitation of Human Seroresponsiveness to Merkel Cell Polyomavirus’, *PLoS Pathog*, 5(9), p. 1000578. doi: 10.1371/journal.ppat.1000578.

Pastrana, D. V *et al.* (2012) ‘Neutralization Serotyping of BK Polyomavirus Infection in Kidney Transplant Recipients’, *PLoS Pathog*, 8(4), p. e1002650. doi: 10.1371/journal.ppat.1002650.

Pastrana, D. V *et al.* (2013) ‘BK Polyomavirus Genotypes Represent Distinct Serotypes with Distinct Entry Tropism’, *Journal of virology*. American Society for Microbiology Journals, 87(18), pp. 10105–13. doi: 10.1128/JVI.01189-13.

Pelkmans, L., Kartenbeck, J. and Helenius, A. (2001) ‘Caveolar endocytosis of simian virus 40 reveals a new two-step vesicular-transport pathway to the ER’, *Nature Cell Biology*. Nature Publishing Group, 3(5), pp. 473–483. doi: 10.1038/35074539.

Pello, O. M. *et al.* (2017) ‘BKV-specific T cells in the treatment of severe refractory haemorrhagic cystitis after HLA-haploidentical haematopoietic cell transplantation’, *European Journal of Haematology*. Blackwell Publishing Ltd, 98(6), pp. 632–634. doi: 10.1111/ejh.12848.

Pestka, S., Krause, C. D. and Walter, M. R. (2004) ‘Interferons, interferon-like cytokines, and their receptors’, *Immunological Reviews*, 202(1), pp. 8–32. doi:

10.1111/j.0105-2896.2004.00204.x.

Peterson, S. B. and Liu, J. (2010) ‘Unraveling the specificity of heparanase utilizing synthetic substrates’, *Journal of Biological Chemistry*, 285(19), pp. 14504–14513. doi: 10.1074/jbc.M110.104166.

Pho, M. T., Ashok, A. and Atwood, W. J. (2000) ‘JC Virus Enters Human Glial Cells by Clathrin-Dependent Receptor-Mediated Endocytosis’, *Journal of Virology*, 74(5), pp. 2288–2292.

Pietropaolo, V. *et al.* (1998) ‘Transplacental transmission of human polyomavirus BK’, *Journal of Medical Virology*. J Med Virol, 56(4), pp. 372–376. doi: 10.1002/(SICI)1096-9071(199812)56:4<372::AID-JMV14>3.0.CO;2-4.

Pipas, J. M. (2001) ‘Tumor Antigens Encoded by Simian Virus 40’, in *Encyclopedia of Genetics*. Elsevier, pp. 2078–2081. doi: 10.1006/rwgn.2001.1624.

Platanias, L. C. (2005) ‘Mechanisms of type-I- and type-II-interferon-mediated signalling’, *Nature Reviews Immunology*, pp. 375–386. doi: 10.1038/nri1604.

Popik, W. *et al.* (2019) ‘BK virus replication in the glomerular vascular unit: Implications for BK virus associated nephropathy’, *Viruses*. MDPI AG, 11(7). doi: 10.3390/v11070583.

Portolani, M. *et al.* (1974) *Prevalence in Italy of antibodies to a new human papovavirus (BK virus)*, *Journal of Medical Microbiology*.

Portolani, M., Barbanti-Brodano, G. and Placa, M. La (1975) ‘Malignant Transformation of Hamster Kidney Cells by BK Virus’, *Journal of Virology*, 15(2), pp. 420–422.

Prado, J. C. M. *et al.* (2018) ‘Human polyomaviruses and cancer: an overview.’, *Clinics*. Hospital das Clinicas da Faculdade de Medicina da Universidade de Sao Paulo, 73(Suppl 1), p. e558s. doi: 10.6061/clinics/2018/e558s.

Prescott, J. *et al.* (2010) ‘New World Hantaviruses Activate IFNl Production in Type I IFN-Deficient Vero E6 Cells’, *PLoS ONE*, 5(6), p. e11159. doi: 10.1371/journal.pone.0011159.

Purighalla, R. *et al.* (1995) ‘BK virus infection in a kidney allograft diagnosed by needle biopsy’, *American Journal of Kidney Diseases*, 26(4), pp. 671–673. doi: 10.1016/0272-6386(95)90608-8.

Querbes, W. *et al.* (2004) ‘A JC Virus-Induced Signal Is Required for Infection of Glial Cells by a Clathrin- and eps15-Dependent Pathway’, *Journal of Virology*. American Society for Microbiology, 78(1), pp. 250–256. doi: 10.1128/jvi.78.1.250-256.2004.

Querbes, W. *et al.* (2006) ‘Invasion of Host Cells by JC Virus Identifies a Novel Role for Caveolae in EndosomalSorting of Noncaveolar Ligands’, *Journal of Virology*. American Society for Microbiology, 80(19), pp. 9402–9413. doi: 10.1128/jvi.01086-06.

Rabenstein, D. L. (2002) ‘Heparin and heparan sulfate: Structure and function’, *Natural Product Reports*. The Royal Society of Chemistry, pp. 312–331. doi: 10.1039/b100916h.

Radhakrishna, H. and Donaldson, J. G. (1997) ‘ADP-Ribosylation Factor 6 Regulates a Novel Plasma Membrane Recycling Pathway’, *The Journal of Cell Biology*, 139(1), pp. 49–61.

Radhakrishnan, S. *et al.* (2003) ‘JC Virus-Induced Changes in Cellular Gene Expression in Primary Human Astrocytes’, *Journal of Virology*, 77(19), pp. 10638–10644. doi: 10.1128/JVI.77.19.10638-10644.2003.

Rainey-Barger, E. K., Magnuson, B. and Tsai, B. (2007) ‘A Chaperone-Activated Nonenveloped Virus Perforates the Physiologically Relevant Endoplasmic Reticulum Membrane’, *Journal of Virology*. American Society for Microbiology, 81(23), pp. 12996–13004. doi: 10.1128/jvi.01037-07.

Ramos, E. *et al.* (2002) ‘Clinical Course of Polyoma Virus Nephropathy in 67 Renal Transplant Patients’, *Journal of the American Society of Nephrology*, 13, pp. 2145–2151. doi: 10.1097/01.ASN.0000023435.07320.81.

Randall, R. E. and Goodbourn, S. (2008) ‘Interferons and viruses: An interplay between induction, signalling, antiviral responses and virus countermeasures’, *Journal of General Virology*. Microbiology Society, pp. 1–47. doi: 10.1099/vir.0.83391-0.

Randhawa, P. S. *et al.* (1999) ‘Human polyoma virus-associated interstitial nephritis in the allograft kidney’, *Transplantation*. Lippincott Williams and Wilkins, 67(1), pp. 103–109. doi: 10.1097/00007890-199901150-00018.

Randhawa, P. S. *et al.* (2002) ‘Quantitation of viral DNA in renal allograft tissue

from patients with BK virus nephropathy', *Transplantation*. Lippincott Williams and Wilkins, 74(4), pp. 485–488. doi: 10.1097/00007890-200208270-00009.

Randhawa, P. S. *et al.* (2010) 'Polyomavirus BK Neutralizing Activity in Human Immunoglobulin Preparations', *Transplantation*, 89(12), pp. 1462–1465.

Randhawa, P., Shapiro, R. and Vats, A. (2005) 'Quantitation of DNA of Polyomaviruses BK and JC in Human Kidneys', *The Journal of Infectious Diseases*, 192, pp. 504–9.

Rao, S. *et al.* (2011) 'WU and KI polyomavirus infections in pediatric hematology/oncology patients with acute respiratory tract illness', *Journal of Clinical Virology*. Elsevier, 52(1), pp. 28–32. doi: 10.1016/j.jcv.2011.05.024.

Rascovan, N. *et al.* (2016) 'Human Polyomavirus-6 Infecting Lymph Nodes of a Patient With an Angiolymphoid Hyperplasia With Eosinophilia or Kimura Disease'. doi: 10.1093/cid/ciw135.

Rathi, A. V. *et al.* (2010) 'Induction of interferon-stimulated genes by Simian virus 40 T antigens', *Virology*. Academic Press, 406(2), pp. 202–211. doi: 10.1016/j.virol.2010.07.018.

Ravindran, M. S. *et al.* (2015) 'A Non-enveloped Virus Hijacks Host Disaggregation Machinery to Translocate across the Endoplasmic Reticulum Membrane', *PLOS Pathogens*. Edited by J. T. Schiller. Public Library of Science, 11(8), p. e1005086. doi: 10.1371/journal.ppat.1005086.

Rayment, I. *et al.* (1982) 'Polyoma virus capsid structure at 22.5 A resolution', *Nature*. Cullen, J. L. Geo/. Soc. Am, 295, pp. 110–115.

Rennspiess, D. *et al.* (2015) 'Detection of human polyomavirus 7 in human thymic epithelial tumors', *Journal of Thoracic Oncology*. Lippincott Williams and Wilkins, 10(2), pp. 360–366. doi: 10.1097/JTO.0000000000000390.

Reploeg, M. D., Storch, G. A. and Clifford, D. B. (2001) 'BK Virus: A Clinical Review', *Clinical Infectious Diseases*, 33, pp. 191–202.

Rettino, A. and Clarke, N. M. (2013) 'Genome-wide Identification of IRF1 Binding Sites Reveals Extensive Occupancy at Cell Death Associated Genes', *Journal of Carcinogenesis & Mutagenesis*. OMICS Publishing Group. doi: 10.4172/2157-2518.s6-009.

Ribeiro, A. *et al.* (2012) 'Activation of innate immune defense mechanisms

contributes to polyomavirus BK-associated nephropathy', *Kidney International*. Nature Publishing Group, 81(1), pp. 100–111. doi: 10.1038/ki.2011.311.

Ribeiro, A. *et al.* (2016) 'BK virus infection activates the TNFα/TNF receptor system in Polyomavirus-associated nephropathy', *Molecular and Cellular Biochemistry*. Springer New York LLC, 411(1–2), pp. 191–199. doi: 10.1007/s11010-015-2581-1.

Richards, K. F. *et al.* (2015) 'Merkel cell polyomavirus T antigens promote cell proliferation and inflammatory cytokine gene expression', *Journal of General Virology*, 96, pp. 3532–44. doi: 10.1099/jgv.0.000287.

Richterová, Z. *et al.* (2001) 'Caveolae Are Involved in the Trafficking of Mouse Polyomavirus Virions and Artificial VP1 Pseudocapsids toward Cell Nuclei', *Journal of Virology*. American Society for Microbiology, 75(22), pp. 10880–10891. doi: 10.1128/jvi.75.22.10880-10891.2001.

Rinaldo, C. H. *et al.* (2010) '1-O-Hexadecyloxypropyl Cidofovir (CMX001) Effectively Inhibits Polyomavirus BK Replication in Primary Human Renal Tubular Epithelial Cells', *Antimicrobial Agents and Chemotherapy*, 54(11), pp. 4714–4722. doi: 10.1128/AAC.00974-10.

Rinaldo, C. H., Traavik, T. and Hey, A. (1998) 'The Agnogene of the Human Polyomavirus BK Is Expressed', *Journal of Virology*, 72(7), pp. 6233–6236.

Rinkenberger, N. and Schoggins, J. W. (2018) 'Mucolipin-2 cation channel increases trafficking efficiency of endocytosed viruses', *mBio*. American Society for Microbiology, 9(1), pp. e02314-17. doi: 10.1128/mBio.02314-17.

Robertson, A. G. *et al.* (2017) 'Comprehensive Molecular Characterization of Muscle-Invasive Bladder Cancer', *Cell*, 171, pp. 540–546. doi: 10.1016/j.cell.2017.09.007.

Rodriguez, R. U. (2019) 'Prospective Grant of an Exclusive Patent License: Virus-Like Particles Vaccines Against Human Polyomaviruses, BK Virus (BKV) and JC Virus (JCV)', *Federal Register*, 84(FR 2555).

Rotondo, J. C. *et al.* (2019) 'Association Between Simian Virus 40 and Human Tumors', *Frontiers in Oncology*. Frontiers Media S.A., p. 670. doi: 10.3389/fonc.2019.00670.

Rubio, D. *et al.* (2013) 'Crosstalk between the type 1 interferon and nuclear

factor kappa B pathways confers resistance to a lethal virus infection', *Cell Host and Microbe*. Cell Press, 13(6), pp. 701–710. doi: 10.1016/j.chom.2013.04.015.

Saleh, A. *et al.* (2020) 'Update on the Management of BK Virus Infection', *Experimental and Clinical Transplantation*. Exp Clin Transplant. doi: 10.6002/ect.2019.0254.

Salunke, D. M., Caspar, D. L. D. and Garcea, R. L. (1986) 'Self-assembly of purified polyomavirus capsid protein VP1', *Cell*. Cell Press, 46(6), pp. 895–904. doi: 10.1016/0092-8674(86)90071-1.

Samuel, C. E. (2001) 'Antiviral Actions of Interferons', *Clinical Microbiology Reviews*, 14(4), pp. 778–809. doi: 10.1128/CMR.14.4.778-809.2001.

Santosh, K. M. *et al.* (2018) 'Recombinant human interferon regulatory factor-1 (IRF-1) protein expression and solubilisation study in Escherichia coli', *Molecular Biology Reports*. Springer Netherlands, 45(5), pp. 1367–1374. doi: 10.1007/s11033-018-4298-1.

Saribas, A. S. *et al.* (2016) 'Emerging From the Unknown: Structural and Functional Features of Agnoprotein of Polyomaviruses', *Journal of Cellular Physiology*. Wiley-Liss Inc., pp. 2115–2127. doi: 10.1002/jcp.25329.

Sariyer, I. K. *et al.* (2012) 'Bag3-Induced Autophagy Is Associated with Degradation of JCV Oncoprotein, T-Ag', *PLoS ONE*. Edited by L. Zhang. Public Library of Science, 7(9), p. e45000. doi: 10.1371/journal.pone.0045000.

Sauerbrei, A. and Wutzler, A. P. (2008) 'Testing thermal resistance of viruses', *Archives of Virology*, 154, pp. 115–119. doi: 10.1007/s00705-008-0264-x.

Savona, M. R. *et al.* (2007) 'Low-dose cidofovir treatment of BK virus-associated hemorrhagic cystitis in recipients of hematopoietic stem cell transplant', *Bone Marrow Transplantation*. Nature Publishing Group, 39(12), pp. 783–787. doi: 10.1038/sj.bmt.1705678.

Sawinski, D. and Goral, S. (2015) 'BK virus infection: an update on diagnosis and treatment', *Nephrol ogy Dialysis Transplantation*, 30, pp. 209–217. doi: 10.1093/ndt/gfu023.

Schachtner, T. *et al.* (2011) 'BK virus-specific immunity kinetics: A predictor of recovery from polyomavirus BK-associated nephropathy', *American Journal of Transplantation*. Am J Transplant, 11(11), pp. 2443–2452. doi: 10.1111/j.1600-

6143.2011.03693.x.

Schaper, F. *et al.* (1998) *Functional domains of interferon regulatory factor I (IRF-1)*, *Biochemical Journal*.

Schelhaas, M. *et al.* (2007) 'Simian Virus 40 Depends on ER Protein Folding and Quality Control Factors for Entry into Host Cells', *Cell*, 131, pp. 516–529. doi: 10.1016/j.cell.2007.09.038.

Schmidt, T. *et al.* (2014) 'BK polyomavirus-specific cellular immune responses are age-dependent and strongly correlate with phases of virus replication', *American Journal of Transplantation*. Blackwell Publishing Ltd, 14(6), pp. 1334–1345. doi: 10.1111/ajt.12689.

Schmitt, C. *et al.* (2014) 'Donor origin of BKV replication after kidney transplantation', *Journal of Clinical Virology*. Elsevier, 59(2), pp. 120–125. doi: 10.1016/j.jcv.2013.11.009.

Schmitz, F. *et al.* (2007) 'Interferon-regulatory-factor 1 controls Toll-like receptor 9-mediated IFN-β production in myeloid dendritic cells', *European Journal of Immunology*, 37(2), pp. 315–327. doi: 10.1002/eji.200636767.

Schneider, W. M., Chevillotte, M. D. and Rice, C. M. (2014) 'Interferon-stimulated genes: A complex web of host defenses', *Annual Review of Immunology*. Annual Reviews Inc., pp. 513–545. doi: 10.1146/annurev-immunol-032713-120231.

Schoggins, J. W. *et al.* (2011) 'A diverse range of gene products are effectors of the type I interferon antiviral response', *Nature*, 472, pp. 481–485. doi: 10.1038/nature09907.

Schoggins, J. W. *et al.* (2014) 'Pan-viral specificity of IFN-induced genes reveals new roles for cGAS in innate immunity', *Nature*, 505. doi: 10.1038/nature12862.

Schoggins, J. W. (2019) 'Interferon-Stimulated Genes: What Do They All Do?', *Annual Review of Virology*, 6, pp. 567–584. doi: 10.1146/annurev-virology-092818.

Schoggins, J. W. and Rice, C. M. (2011) 'Interferon-stimulated genes and their antiviral effector functions', *Current Opinion in Virology*, 1, pp. 519–525. doi: 10.1016/j.coviro.2011.10.008.

Schold, J. D. *et al.* (2009) ‘Treatment for BK virus: incidence, risk factors and outcomes for kidney transplant recipients in the United States’, *Transplant International*, 22(6), pp. 626–634. doi: 10.1111/j.1432-2277.2009.00842.x.

Schowalter, R. M. *et al.* (2010) ‘Merkel cell polyomavirus and two previously unknown polyomaviruses are chronically shed from human skin’, *Cell Host and Microbe*. Cell Press, 7(6), pp. 509–515. doi: 10.1016/j.chom.2010.05.006.

Schowalter, R. M. and Buck, C. B. (2013) ‘The Merkel Cell Polyomavirus Minor Capsid Protein’, *PLoS Pathog*, 9(8), p. 1003558. doi: 10.1371/journal.ppat.1003558.

Schowalter, R. M., Pastrana, D. V. and Buck, C. B. (2011) ‘Glycosaminoglycans and Sialylated Glycans Sequentially Facilitate Merkel Cell Polyomavirus Infectious Entry’, *PLoS Pathogens*. Edited by M. Imperiale. Public Library of Science, 7(7), p. e1002161. doi: 10.1371/journal.ppat.1002161.

Schroder, K. *et al.* (2004) ‘Interferon-γ: an overview of signals, mechanisms and functions’, *Journal of Leukocyte Biology*. Wiley, 75(2), pp. 163–189. doi: 10.1189/jlb.0603252.

Scuda, N. *et al.* (2011) ‘A Novel Human Polyomavirus Closely Related to the African Green Monkey-Derived Lymphotropic Polyomavirus’, *Journal of Virology*. American Society for Microbiology, 85(9), pp. 4586–4590. doi: 10.1128/jvi.02602-10.

Seamone, M. E. *et al.* (2010) ‘MAP kinase activation increases BK polyomavirus replication and facilitates viral propagation in vitro’, *Journal of Virological Methods*. Elsevier, 170(1–2), pp. 21–29. doi: 10.1016/j.jviromet.2010.08.014.

Seehafer, J. *et al.* (1978) ‘Observations on the growth and plaque assay of BK virus in cultured human and monkey cells’, *Journal of General Virology*. Microbiology Society, 38(2), pp. 383–387. doi: 10.1099/0022-1317-38-2-383.

Seif, L., Khoury, G. and Dhar, R. (1979) *The Genome of Human Papovavirus BKV*, *Cell*.

Seo, G. J. *et al.* (2008) ‘Evolutionarily Conserved Function of a Viral MicroRNA’, *Journal of Virology*, 82(20), pp. 9823–9828. doi: 10.1128/JVI.01144-08.

Shah, K. and Nathanson, N. (1976) ‘Human Exposure to SV40: Review and

Comment', *American Journal of Epidemiology*, 103(1), pp. 1–12.

Shahzad, N. *et al.* (2013) 'The T Antigen Locus of Merkel Cell Polyomavirus Downregulates Human Toll-Like Receptor 9 Expression', *Journal of Virology*. American Society for Microbiology, 87(23), pp. 13009–13019. doi: 10.1128/jvi.01786-13.

Sharf, R. *et al.* (1997) 'Phosphorylation events modulate the ability of interferon consensus sequence binding protein to interact with interferon regulatory factors and to bind DNA', *Journal of Biological Chemistry*. American Society for Biochemistry and Molecular Biology, 272(15), pp. 9785–9792. doi: 10.1074/jbc.272.15.9785.

Shaw, A. E. *et al.* (2017) 'Fundamental properties of the mammalian innate immune system revealed by multispecies comparison of type I interferon responses', *PLOS Biology*. Edited by H. Malik. Public Library of Science, 15(12), p. e2004086. doi: 10.1371/journal.pbio.2004086.

Shein, H. M. and Enders, J. F. (1962) 'Transformation Induced by Simian Virus 40 in Human Renal Cell Cultures, I. Morphology and Growth Characteristics', *Proceedings of the National Academy of Sciences*. Proceedings of the National Academy of Sciences, 48(7), pp. 1164–1172. doi: 10.1073/pnas.48.7.1164.

Shi, L. *et al.* (2011) 'Genome-Wide Analysis of Interferon Regulatory Factor I Binding in Primary Human Monocytes', *Gene*, 487(1), pp. 21–28. doi: 10.1016/j.gene.2011.07.004.

Shuda, M. *et al.* (2008) 'T antigen mutations are a human tumor-specific signature for Merkel cell polyomavirus', *PNAS*, 105(42), pp. 16272–16277.

Siebrasse, E. A. *et al.* (2012) 'Identification of MW Polyomavirus, a Novel Polyomavirus in Human Stool', *Journal of Virology*. American Society for Microbiology, 86(19), pp. 10321–10326. doi: 10.1128/jvi.01210-12.

Sinibaldi, L. *et al.* (1987) 'Inhibition of BK Virus Haemagglutination by Gangliosides', *Journal of General Virology*, 68, pp. 879–883.

Skoczylas, C., Fahrbach, K. M. and Rundell, K. (2004) 'Cellular Targets of the SV40 Small-t Antigen in Human Cell Transformation', *Cell Cycle*, 3(5), pp. 606–610.

Smith, J. M. *et al.* (2004) 'Polyomavirus Nephropathy in Pediatric Kidney

Transplant Recipients', *American Journal of Transplantation*, 4(12), pp. 2109–2117. doi: 10.1111/j.1600-6143.2004.00629.x.

Smith, M. H., Ploegh, H. L. and Weissman, J. S. (2011) 'Road to Ruin: Targeting Proteins for Degradation in the Endoplasmic Reticulum', *Science*, 334, pp. 1086–1090. doi: 10.1126/science.1209126.

Solis, M. *et al.* (2018) 'Neutralizing Antibody-Mediated Response and Risk of BK Virus-Associated Nephropathy', *Journal of the American Society of Nephrology*, 29, pp. 326–334. doi: 10.1681/ASN.2017050532.

Song, T.-R. *et al.* (2016) 'Fluoroquinolone prophylaxis in preventing BK polyomavirus infection after renal transplant: A systematic review and meta-analysis', *The Kaohsiung Journal of Medical Sciences*. Elsevier (Singapore) Pte Ltd, 32(3), pp. 152–159. doi: 10.1016/j.kjms.2016.01.004.

Spence, J. S. *et al.* (2019) 'IFITM3 directly engages and shuttles incoming virus particles to lysosomes', *Nature Chemical Biology*. Nature Publishing Group, 15(3), pp. 259–268. doi: 10.1038/s41589-018-0213-2.

Šroller, V. *et al.* (2016) 'Seroprevalence rates of HPyV6, HPyV7, TSPyV, HPyV9, MWPyV and KIPyV polyomaviruses among the healthy blood donors', *Journal of Medical Virology*. John Wiley and Sons Inc., 88(7), pp. 1254–1261. doi: 10.1002/jmv.24440.

Stahl, H., Dröge, P. and Knippers, R. (1986) 'DNA helicase activity of SV40 large tumor antigen.', *The EMBO journal*. European Molecular Biology Organization, 5(8), pp. 1939–1944. doi: 10.1002/j.1460-2075.1986.tb04447.x.

Starrett, G. J. and Buck, C. B. (2019) 'The case for BK polyomavirus as a cause of bladder cancer', *Current Opinion in Virology*. Elsevier, 39, pp. 8–15. doi: 10.1016/J.COVIRO.2019.06.009.

Stehle, T. *et al.* (1994) 'Structure of murine polyomavirus complexed with an oligosaccharide receptor fragment', *Nature*. Nature, 369(6476), pp. 160–163. doi: 10.1038/369160a0.

Stehle, T. *et al.* (1996) 'The structure of simian virus 40 refined at 3.1 Å resolution', *Structure*. Cell Press, 4(2), pp. 165–182. doi: 10.1016/S0969-2126(96)00020-2.

Stehle, T. and Harrison, S. C. (1996) 'Crystal structures of murine polyomavirus

in complex with straight-chain and branched-chain sialyloligosaccharide receptor fragments', *Structure*, 4(2), pp. 183–194.

Stehle, T. and Harrison, S. C. (1997) 'High-resolution structure of a polyomavirus VP1-oligosaccharide complex: implications for assembly and receptor binding', *The EMBO Journal*, 16(16), pp. 5139–5148.

Stewart, H. *et al.* (2015) 'A novel method for the measurement of hepatitis C virus infectious titres using the IncuCyte ZOOM and its application to antiviral screening', *Journal of Virological Methods*. Elsevier, 218, pp. 59–65. doi: 10.1016/j.jviromet.2015.03.009.

Stewart, S. E. *et al.* (1957) 'The induction of neoplasms with a substance released from mouse tumors by tissue culture', *Virology*. Academic Press, 3(2), pp. 380–400. doi: 10.1016/0042-6822(57)90100-9.

Stirnweiss, A. *et al.* (2010) 'IFN Regulatory Factor-1 Bypasses IFN-Mediated Antiviral Effects through Viperin Gene Induction', *The Journal of Immunology*. The American Association of Immunologists, 184(9), pp. 5179–5185. doi: 10.4049/jimmunol.0902264.

Streuli, C. H. and Griffin, B. E. (1987) *Myristic acid is coupled to a structural protein of polyoma virus and SV40*, *Nature*.

Stroh, L. J. *et al.* (2014) 'Structure Analysis of the Major Capsid Proteins of Human Polyomaviruses 6 and 7 Reveals an Obstructed Sialic Acid Binding Site', *Journal of Virology*. American Society for Microbiology, 88(18), pp. 10831–10839. doi: 10.1128/jvi.01084-14.

Sullivan, C. S. *et al.* (2005) 'SV40-encoded microRNAs regulate viral gene expression and reduce susceptibility to cytotoxic T cells', *Nature*. Nature Publishing Group, 435(7042), pp. 682–686. doi: 10.1038/nature03576.

Sundsfjord, A. *et al.* (1994) 'Detection of BK Virus DNA in Nasopharyngeal Aspirates from Children with Respiratory Infections but Not in Saliva from Immunodeficient and Immunocompetent Adult Patients', *Journal of Clinical Microbiology*, 32(5), pp. 1390–1394.

Surviladze, Z., Dziduszko, A. and Ozbun, M. A. (2012) 'Essential Roles for Soluble Virion-Associated Heparan Sulfonated Proteoglycans and Growth Factors in Human Papillomavirus Infections', *PLOS Pathogens*, 8(2), p.

e1002519. doi: 10.1371/journal.ppat.1002519.

Surviladze, Z., Sterkand, R. T. and Ozbun, M. A. (2015) ‘Interaction of human papillomavirus type 16 particles with heparan sulfate and syndecan-1 molecules in the keratinocyte extracellular matrix plays an active role in infection’, *Journal of General Virology*. Microbiology Society, 96, pp. 2232–2241. doi: 10.1099/vir.0.000147.

Sutherland, C. L. *et al.* (2006) ‘ULBPs, human ligands of the NKG2D receptor, stimulate tumor immunity with enhancement by IL-15’, *Blood*. American Society of Hematology, 108(4), pp. 1313–1319. doi: 10.1182/blood-2005-11-011320.

Suzuki, T. *et al.* (2010) ‘The Human Polyoma JC Virus Agnoprotein Acts as a Viroporin’, *PLoS Pathogens*. Edited by M. J. Imperiale. Public Library of Science, 6(3), p. e1000801. doi: 10.1371/journal.ppat.1000801.

Sweet, B. H. and Hilleman, M. R. (1960) ‘The Vacuolating Virus, S.V.40’, *Experimental Biology and Medicine*. SAGE PublicationsSage UK: London, England, 105(2), pp. 420–427. doi: 10.3181/00379727-105-26128.

Takaoka, A. *et al.* (2007) ‘DAI (DLM-1/ZBP1) is a cytosolic DNA sensor and an activator of innate immune response’, *Nature*. Nature Publishing Group, 448(7152), pp. 501–505. doi: 10.1038/nature06013.

Takeuchi, O. and Akira, S. (2010) ‘Pattern Recognition Receptors and Inflammation’, *Cell*, 140, pp. 805–820. doi: 10.1016/j.cell.2010.01.022.

Tamura, T. *et al.* (2008) ‘The IRF Family Transcription Factors in Immunity and Oncogenesis’, *Annual Review of Immunology*, 26, pp. 535–84. doi: 10.1146/annurev.immunol.26.021607.090400.

Tanaka, N. *et al.* (1994) ‘Cellular commitment to oncogene-induced transformation or apoptosis is dependent on the transcription factor IRF-1’, *Cell*. Cell, 77(6), pp. 829–839. doi: 10.1016/0092-8674(94)90132-5.

Taniguchi, T. *et al.* (2001) ‘IRF family of transcription factors as regulators of host defense’, *Annual Review of Immunology*, 19, pp. 623–55.

Teunissen, E. A., De Raad, M. and Mastrobattista, E. (2013) ‘Production and biomedical applications of virus-like particles derived from polyomaviruses’, *Journal of Controlled Release*. Elsevier, pp. 305–321. doi: 10.1016/j.jconrel.2013.08.026.

Thakkar, N. *et al.* (2017) ‘Emerging Roles of Heparanase in Viral Pathogenesis.’, *Pathogens (Basel, Switzerland)*. Multidisciplinary Digital Publishing Institute (MDPI), 6(3). doi: 10.3390/pathogens6030043.

Thangaraju, S. *et al.* (2016) ‘Risk Factors for BK Polyoma Virus Treatment and Association of Treatment With Kidney Transplant Failure’, *Transplantation*. Lippincott Williams and Wilkins, 100(4), pp. 854–861. doi: 10.1097/TP.0000000000000890.

Tian, Y. C. *et al.* (2014) ‘Polyomavirus BK-encoded microRNA suppresses autoregulation of viral replication’, *Biochemical and Biophysical Research Communications*. Academic Press Inc., 447(3), pp. 543–549. doi: 10.1016/j.bbrc.2014.04.030.

Tikhanovich, I. *et al.* (2011) ‘Inhibition of Human BK Polyomavirus Replication by Small Noncoding RNAs Downloaded from’, *Journal of Virology*, 85(14), pp. 6930–6940. doi: 10.1128/JVI.00547-11.

Tikhanovich, I. and Nasheuer, H. P. (2010) ‘Host-Specific Replication of BK Virus DNA in Mouse Cell Extracts Is Independently Controlled by DNA Polymerase-Primase and Inhibitory Activities’, *Journal of Virology*, 84(13), pp. 6636–6644. doi: 10.1128/JVI.00527-10.

Tippin, T. K. *et al.* (2016) ‘Brincidofovir Is Not a Substrate for the Human Organic Anion Transporter 1: A Mechanistic Explanation for the Lack of Nephrotoxicity Observed in Clinical Studies’, *Therapeutic Drug Monitoring*, 38(6).

Tognon, M. *et al.* (2003) ‘Oncogenic transformation by BK virus and association with human tumors’, *Oncogene*. Nature Publishing Group, 22, pp. 5192–5200. doi: 10.1038/sj.onc.1206550.

Tognon, M. and Provenzano, M. (2015) ‘New insights on the association between the prostate cancer and the small DNA tumour virus, BK polyomavirus’, *Journal of Translational Medicine*. BioMed Central Ltd. doi: 10.1186/s12967-015-0754-z.

Tremolada, S. *et al.* (2010) ‘Polymorphisms of the BK virus subtypes and their influence on viral in vitro growth efficiency’, *Virus Research*. Elsevier, 149(2), pp. 190–196. doi: 10.1016/j.virusres.2010.01.017.

Trilling, M. *et al.* (2009) ‘Gamma Interferon-Induced Interferon Regulatory Factor 1-Dependent Antiviral Response Inhibits Vaccinia Virus Replication in Mouse but Not Human Fibroblasts’, *Journal of Virology*. American Society for Microbiology, 83(8), pp. 3684–3695. doi: 10.1128/jvi.02042-08.

Trydzenskaya, H. *et al.* (2011) ‘Novel Approach for Improved Assessment of Phenotypic and Functional Characteristics of BKV-Specific T-Cell Immunity’, *Transplantation*, 92(11), pp. 1269–1277. doi: 10.1097/TP.0b013e318234e0e5.

Tsai, B. *et al.* (2003) ‘Gangliosides Are Receptors for Murine Polyoma Virus and SV40’, *The EMBO Journal*, 22(17), pp. 4346–55.

Ugi, S. *et al.* (2004) ‘Protein Phosphatase 2A Negatively Regulates Insulin’s Metabolic Signaling Pathway by Inhibiting Akt (Protein Kinase B) Activity in 3T3-L1 Adipocytes’, *Molecular and Cellular Biology*. American Society for Microbiology, 24(19), pp. 8778–8789. doi: 10.1128/mcb.24.19.8778-8789.2004.

Uhlen, M. *et al.* (2015) ‘Tissue-based map of the human proteome’, *Science*. American Association for the Advancement of Science, 347(6220), pp. 1260419–1260419. doi: 10.1126/science.1260419.

Ungewickell, E. and Branton, D. (1981) ‘Assembly units of clathrin coats’, *Nature*, 289, pp. 420–422.

Unterholzner, L. *et al.* (2010) ‘IFI16 is an innate immune sensor for intracellular DNA’, *Nature Immunology*, 11(11). doi: 10.1038/ni.1932.

Unterstab, G. *et al.* (2010) ‘The polyomavirus BK agnoprotein co-localizes with lipid droplets’, *Virology*. Academic Press, 399(2), pp. 322–331. doi: 10.1016/j.virol.2010.01.011.

Vallbracht, A. *et al.* (1993) ‘Disseminated BK type polyomavirus infection in an AIDS patient associated with central nervous system disease’, *American Journal of Pathology*. American Society for Investigative Pathology, 143(1), pp. 29–39.

Del Valle, L. and Piña-Oviedo, S. (2019) ‘Human Polyomavirus JCPyV and Its Role in Progressive Multifocal Leukoencephalopathy and Oncogenesis’, *Frontiers in Oncology*. Frontiers Media S.A. doi: 10.3389/fonc.2019.00711.

Vanloock, M. S. *et al.* (2002) ‘SV40 Large T Antigen Hexamer Structure: Domain Organization and DNA-Induced Conformational Changes’, *Current*

Biology, 12, pp. 472–476.

Varella, R. B. *et al.* (2018) ‘BK polyomavirus genotypes Ia and Ib1 exhibit different biological properties in renal transplant recipients’, *Virus Research*. Elsevier, 243, pp. 65–68. doi: 10.1016/J.VIRUSRES.2017.10.018.

Varinou, L. *et al.* (2003) ‘Phosphorylation of the Stat1 Transactivation Domain Is Required for Full-Fledged IFN-γ-Dependent Innate Immunity’, *Immunity*. Cell Press, 19(6), pp. 793–802. doi: 10.1016/S1074-7613(03)00322-4.

Varki, A. *et al.* (2015) ‘Symbol Nomenclature for Graphical Representations of Glycans’, *Glycobiology*, 25(12), pp. 1323–24.

Veals, S. A. *et al.* (1992) *Subunit of an Alpha-Interferon-Responsive Transcription Factor Is Related to Interferon Regulatory Factor and Myb Families of DNA-Binding Proteins*, *Molecular and Cellular Biology*.

de Veer, M. J. *et al.* (2001) ‘Functional classification of interferon-stimulated genes identified using microarrays’, *Journal of Leukocyte Biology*, 69.

Verhalen, B. *et al.* (2015) ‘Viral DNA Replication-Dependent DNA Damage Response Activation during BK Polyomavirus Infection’, *Journal of Virology*. American Society for Microbiology, 89(9), pp. 5032–5039. doi: 10.1128/jvi.03650-14.

Verma, S. *et al.* (2006) ‘JC virus induces altered patterns of cellular gene expression: Interferon-inducible genes as major transcriptional targets’, *Virology*. Academic Press, 345(2), pp. 457–467. doi: 10.1016/j.virol.2005.10.012.

Viscidi, R. P. and Clayman, B. (2006) ‘Serological cross reactivity between polyomavirus capsids’, *Advances in Experimental Medicine and Biology*. Springer, New York, NY, pp. 73–84. doi: 10.1007/0-387-32957-9_5.

Viscount, H. B. *et al.* (2007) ‘Polyomavirus Polymerase Chain Reaction as a Surrogate Marker of Polyomavirus-Associated Nephropathy’, *Transplantation*, 84(3), pp. 340–345. doi: 10.1097/01.tp.0000275205.41078.51.

Vlodavsky, I. *et al.* (2018) ‘Opposing Functions of Heparanase-1 and Heparanase-2 in Cancer Progression’, *Trends in Biochemical Sciences*. Elsevier Ltd, pp. 18–31. doi: 10.1016/j.tibs.2017.10.007.

Vu, D. *et al.* (2015) ‘Efficacy of intravenous immunoglobulin in the treatment of

persistent BK viremia and BK virus nephropathy in renal transplant recipients', *Transplantation Proceedings*. Elsevier USA, 47(2), pp. 394–398. doi: 10.1016/j.transproceed.2015.01.012.

Walczak, C. P. *et al.* (2014) 'A Cytosolic Chaperone Complexes with Dynamic Membrane J-Proteins and Mobilizes a Nonenveloped Virus out of the Endoplasmic Reticulum', *PLoS Pathogens*. Public Library of Science, 10(3). doi: 10.1371/journal.ppat.1004007.

Walker, D. L. (2002) 'Progressive Multifocal Leukoencephalopathy: Cultivation and Characterization of the Etiologic Agent', in Khalili, K. and Stoner, G. L. (eds) *Human Polyomaviruses*. New York, USA: John Wiley & Sons, Inc., pp. 25–43. doi: 10.1002/0471221945.ch3.

Wang, Q., Li, A. and Ye, Y. (2008) 'Inhibition of p97-dependent protein degradation by Eeyarestatin I', *Journal of Biological Chemistry*. American Society for Biochemistry and Molecular Biology, 283(12), pp. 7445–7454. doi: 10.1074/jbc.M708347200.

Wang, W. *et al.* (2017) 'Transcriptional Regulation of Antiviral Interferon-Stimulated Genes', *Trends in Microbiology*. Elsevier Ltd, pp. 573–584. doi: 10.1016/j.tim.2017.01.001.

Wang, X., Hinson, E. R. and Cresswell, P. (2007) 'The Interferon-Inducible Protein Viperin Inhibits Influenza Virus Release by Perturbing Lipid Rafts', *Cell Host & Microbe*, 2, pp. 96–105. doi: 10.1016/j.chom.2007.06.009.

Watanabe, N. *et al.* (1991) 'Activation of IFN-β element by IRF-1 requires a post-translational event in addition to IRF-1 synthesis', *Nucleic Acids Research*, 19(16), pp. 4421–4428.

Weber, F. *et al.* (2006) 'Double-Stranded RNA Is Produced by Positive-Strand RNA Viruses and DNA Viruses but Not in Detectable Amounts by Negative-Strand RNA Viruses', *Journal of Virology*. American Society for Microbiology, 80(10), pp. 5059–5064. doi: 10.1128/jvi.80.10.5059-5064.2006.

Weikert, B. C. and Blumberg, E. A. (2008) 'Viral Infection after Renal Transplantation: Surveillance and Management', *Clinical Journal of the American Society of Nephrology*, 3(Supplement 2), pp. S76–S86. doi: 10.2215/CJN.02900707.

Wensveen, F. M., Jelenčić, V. and Polić, B. (2018) 'NKG2D: A master regulator of immune cell responsiveness', *Frontiers in Immunology*. Frontiers Media S.A., 9, p. 441. doi: 10.3389/fimmu.2018.00441.

Wieser, M. *et al.* (2008) 'hTERT alone immortalizes epithelial cells of renal proximal tubules without changing their functional characteristics', *American Journal of Physiology - Renal Physiology*. American Physiological Society, 295(5). doi: 10.1152/ajprenal.90405.2008.

Williamson, E. M. L. and Berger, J. R. (2017) 'Diagnosis and Treatment of Progressive Multifocal Leukoencephalopathy Associated with Multiple Sclerosis Therapies', *Neurotherapeutics*. Springer New York LLC, pp. 961–973. doi: 10.1007/s13311-017-0570-7.

Wilson, J. C. *et al.* (2014) '1H NMR spectroscopic studies establish that heparanase is a retaining glycosidase', *Biochemical and Biophysical Research Communications*. Academic Press, 443, pp. 185–188. doi: 10.1016/j.bbrc.2013.11.079.

Wollebo, H. S. *et al.* (2013) 'Epigenetic regulation of polyomavirus JC', *Virology Journal*. BioMed Central, 10, p. 264. doi: 10.1186/1743-422X-10-264.

Wu, J. K. and Harris, M. T. (2008) 'Use of Leflunomide in the Treatment of Polyomavirus BK-Associated Nephropathy', *The Annals of Pharmacotherapy*, 42, pp. 1679–1685. doi: 10.1345/aph.1L180.

Wu, L. *et al.* (2015) 'Structural characterization of human heparanase reveals insights into substrate recognition', *Nature Structural & Molecular Biology*. Nature Publishing Group, 22(12), pp. 1016–1022. doi: 10.1038/nsmb.3136.

Wu, X. *et al.* (2006) 'Proteasome inhibitors uncouple rhesus TRIM5α restriction of HIV-1 reverse transcription and infection', *Proceedings of the National Academy of Sciences of the United States of America*. National Academy of Sciences, 103(19), pp. 7465–7470. doi: 10.1073/pnas.0510483103.

WuDunn, D. and Spear, P. G. (1989) 'Initial Interaction of Herpes Simplex Virus with Cells Is Binding to Heparan Sulfate', *Journal of Virology*, 63(1), pp. 52–58.

Wüthrich, C. *et al.* (2009) 'Fulminant JC virus encephalopathy with productive infection of cortical pyramidal neurons', *Annals of Neurology*, 65(6), pp. 742–748. doi: 10.1002/ana.21619.

Yanai, H., Negishi, H. and Taniguchi, T. (2012) ‘The IRF family of transcription factors: Inception, impact and implications in oncogenesis’, *OncoImmunology*. Taylor & Francis, 1(8), pp. 1376–1386. doi: 10.4161/onci.22475.

Yang, D. *et al.* (2019) ‘The E3 ligase TRIM56 is a host restriction factor of Zika virus and depends on its RNA-binding activity but not miRNA regulation, for antiviral function’, *PLOS Neglected Tropical Diseases*. Edited by M. A. Rabaa. Public Library of Science, 13(6), p. e0007537. doi: 10.1371/journal.pntd.0007537.

Yokoyama, N. *et al.* (2007) ‘Mutational Analysis of the Carboxyl-terminal Region of the SV40 Major Capsid Protein VP1’, *The Japanese Biochemical Society*, 141(2), pp. 279–286. doi: 10.1093/jb/mvm038.

Yu, G. *et al.* (2012) ‘Discovery of a Novel Polyomavirus in Acute Diarrheal Samples from Children’, *PLoS ONE*, 7(11). doi: 10.1371/journal.pone.0049449.

Yu, R. K. *et al.* (2011) ‘Structures, biosynthesis, and functions of gangliosides - An overview’, *Journal of Oleo Science*. NIH Public Access, pp. 537–544. doi: 10.5650/jos.60.537.

Yu, Y. and Alwine, J. C. (2002) ‘Human Cytomegalovirus Major Immediate-Early Proteins and Simian Virus 40 Large T Antigen Can Inhibit Apoptosis through Activation of the Phosphatidylinositide 3′-OH Kinase Pathway and the Cellular Kinase Akt’, *Journal of Virology*. American Society for Microbiology, 76(8), pp. 3731–3738. doi: 10.1128/jvi.76.8.3731-3738.2002.

Yu, Y. and Alwine, J. C. (2008) ‘Interaction between Simian Virus 40 Large T Antigen and Insulin Receptor Substrate 1 Is Disrupted by the K1 Mutation, Resulting in the Loss of Large T Antigen-Mediated Phosphorylation of Akt’, *Journal of Virology*. American Society for Microbiology, 82(9), pp. 4521–4526. doi: 10.1128/jvi.02365-07.

Zcharia, E. *et al.* (2009) ‘Newly Generated Heparanase Knock-Out Mice Unravel Co-Regulation of Heparanase and Matrix Metalloproteinases’, *PLoS ONE*. Edited by S. Wölfl. Public Library of Science, 4(4), p. e5181. doi: 10.1371/journal.pone.0005181.

Zhang, D. and Zhang, D. E. (2011) ‘Interferon-stimulated gene 15 and the protein ISGylation system’, *Journal of Interferon and Cytokine Research*. Mary

Ann Liebert, Inc., pp. 119–130. doi: 10.1089/jir.2010.0110.

Zhang, H. *et al.* (2003) ‘The cytidine deaminase CEM15 induces hypermutation in newly synthesized HIV-1 DNA’, *Nature*. Nature Publishing Group, 424(6944), pp. 94–98. doi: 10.1038/nature01707.

Zhang, J. *et al.* (2016) ‘Intracellular Trafficking Network of Protein Nanocapsules: Endocytosis, Exocytosis and Autophagy’, *Theranostics*, 6(12), pp. 2099–2113. doi: 10.7150/thno.16587.

Zhao, H. *et al.* (2018) ‘LncRNA BDNF-AS inhibits proliferation, migration, invasion and EMT in oesophageal cancer cells by targeting miR-214’, *Journal of Cellular and Molecular Medicine*. Blackwell Publishing Inc., 22(8), pp. 3729–3739. doi: 10.1111/jcmm.13558.

Zhao, L. *et al.* (2016) ‘Caveolin- and clathrin-independent entry of BKPyV into primary human proximal tubule epithelial cells’, *Virology*. Academic Press Inc., 492, pp. 66–72. doi: 10.1016/j.virol.2016.02.007.

Zhao, L. and Imperiale, M. J. (2017) ‘Identification of Rab18 as an Essential Host Factor for BK Polyomavirus Infection Using a Whole-Genome RNA Interference Screen’, *mSphere*. American Society for Microbiology (ASM), 2(4). doi: 10.1128/MSPHEREDIRECT.00291-17.

Zhao, L. and Imperiale, M. J. (2019) ‘Establishing Renal Proximal Tubule Epithelial-Derived Cell Lines Expressing Human Telomerase Reverse Transcriptase for Studying BK Polyomavirus’, *Microbiology Resource Announcements*, 8(42), pp. e01129-19. doi: 10.1128/MRA.

Zheng, H. *et al.* (2011) ‘Ligand-Stimulated Downregulation of the Alpha Interferon Receptor: Role of Protein Kinase D2’, *Molecular and Cellular Biology*. American Society for Microbiology, 31(4), pp. 710–720. doi: 10.1128/mcb.01154-10.

Zhou, J. *et al.* (2018) ‘Type III Interferons in Viral Infection and Antiviral Immunity’, *Cellular Physiology and Biochemistry*. S. Karger AG, 51(1), pp. 173–185. doi: 10.1159/000495172.

Zhu, Y. *et al.* (2011) ‘Zinc-finger antiviral protein inhibits HIV-1 infection by selectively targeting multiply spliced viral mRNAs for degradation’, *Proceedings of the National Academy of Sciences of the United States of America*, 108(38),

pp. 15834–15839. doi: 10.1073/pnas.1101676108.

Zimring, J. C., Goodbourn, S. and Offermann, M. K. (1998) ‘Human Herpesvirus 8 Encodes an Interferon Regulatory Factor (IRF) Homolog That Represses IRF-1-Mediated Transcription’, *Journal of Virology*, 72(1), pp. 701–707. doi: 10.1128/jvi.72.1.701-707.1998.